Chapter 11: Weather and climate extreme events in a changing climate

Coordinating Lead Authors:
Sonia I. Seneviratne (Switzerland), Xuebin Zhang (Canada)

Lead Authors:
Muhammad Adnan (Pakistan), Wafae Badi (Morocco), Claudine Dereczynski (Brazil), Alejandro Di Luca (Australia/Argentina), Subimal Ghosh (India), Iskhaq Iskandar (Indonesia), James Kossin (USA), Sophie Lewis (Australia), Friederike Otto (UK/Germany), Izidine Pinto (Mozambique), Masaki Satoh (Japan), Sergio M. Vicente-Serrano (Spain), Michael Wehner (USA), Botao Zhou (China)

Contributing Authors:
Richard Allan (UK), Markus Donat (Germany/Spain), Robert Dunn (UK), Nathan Gillett (Canada), Peter Greve (Germany/Austria), LoftiHalimi (Algeria), Mathias Hauser (Switzerland), Megan Kirchmeier-Young (Canada/USA), Tim R. McVicar (Australia), Seung-Ki Min (Korea), Jonathan Spinoni (Italy), Ying Sun (China), Wim Thiery (Belgium), Claudia Tebaldi (USA/Italy), Seth Westra (Australia), Jakob Zscheischler (Germany/Switzerland)

Review Editors:
Johnny Chan (China), Asgeir Sorteberg (Norway), Carolina Vera (Argentina)

Chapter Scientists:
Mathias Hauser (Switzerland), Hui Wan (Canada)

Date of Draft: 29 April 2019

Note: TSU Compiled Version

Table of Contents

Executive Summary

This chapter provides assessments on observed and projected changes in weather and climate extremes, as well as on their attribution to human-induced greenhouse gas forcing. Changes in weather and climate extremes are of high relevance because of their impacts on human, managed and natural systems. As one of the three "regional chapters" of the AR6 WG1 report (together with Chapters 10 and 12), this chapter also focuses on regional changes in extremes. This is the first time that a chapter in a main IPCC assessment report focuses solely on weather and climate extremes, although a comprehensive assessment was provided as part of the IPCC Special Report on Extremes and disasters (IPCC SREX: IPCC, 2012). Changes in marine extremes, including marine heatwaves, are addressed in Chapter 9 {11.1; Cross-chapter Box 9.1 on marine extremes}

Methods and new data basis compared to AR5

Methods to assess weather and climate extremes and their changes under enhanced greenhouse gas (GHG) forcing were already well established at the time of the IPCC SREX (IPCC, 2012) and AR5 (IPCC, 2013) reports. However, there were several new methodological developments since then. In particular, there is more literature and higher confidence in the field of extreme event attribution. This is related to the quantification of human influence on the intensity and occurrence probability of a wider variety of extreme events, an overall higher maturity of the field, including the recognition of the dependence of attribution statements on "framing", i.e. the attribution question being addressed. In addition, there is now a broader body of literature on changes in extremes at regional and subregional scale, including results from regional climate model simulations and high-resolution/convection-permitting simulations, as well as more analyses based on remote sensing observations. There is also a substantial body of emerging literature on compound events and multi-variate extremes compared to the literature available for the SREX and AR5. Finally, there is also extensive new literature on the assessment of changes in climate extremes for low-emissions (e.g. 1.5°C and 2°C global warming) scenarios, following the 2015 Paris Agreement and the preparation of the IPCC Special Report on 1.5°C global warming (IPCC SR15:IPCC, 2018). {11.2, 11.8}

Observed and attributed changes in extremes and future projections at different levels of global warming

Human-induced global warming has reached 1°C approximately in 2017 compared to the pre-industrial period, i.e. 1850-1900 (IPCC SR15). Recent extreme event attribution studies related to observed events in the past decade provide a broad picture of the level of human influence on the magnitude and/or frequency of such events when anthropogenic global warming is close to or about 1°C {11.3,11.4,11.5,11.6,11.9}. Detection and attribution of changes in extremes are generally available after 1950 due to the lack of reliable data before this date. Detected and/or attributed trends from 1950 to the early 21st century correspond to a global warming of 0.5°C or larger (IPCC AR5; IPCC SR15). Detection of observed trends and associated attribution assessments provided in this executive summary are determined with respect to this time frame (typically 1950-2012), unless indicated otherwise. {11.1, 11.2}

Projected changes in climate extremes can be provided for different global warming levels. This chapter focuses on changes in climate extremes for global warming levels of 1.5°C, 2°C and 3°C (and in some analyses up to 4°C). The present (First-order draft, FOD) projections are mainly based on CMIP5 simulations, it is anticipated that projections based on CMIP6 simulations will be included in the second-order draft (SOD). The literature shows that there are substantial changes in the occurrence and/or intensity of weather and climate extremes for each +0.5°C of additional global warming, also consistent with the SR15, which implies additional risks for human and natural systems with increasing global warming levels (*high confidence*[1]). In general, details of emissions scenarios do not affect projected changes in extremes as a function of global warming, although there is *high confidence* that regional changes in aerosol or land use

[1]This chapter's assessment uses both likelihood and confidence language following the IPCC guidance document (Mastrandrea et al., 2010) on the treatment of uncertainty. The use of likelihood language ("*likely*", "*very likely*", "*virtually certain*") implies "*high confidence*" in the underlying assessment.

forcing affect regional changes in extremes (*high confidence*). {11.2; Tables 11.1 and 11.2}

Temperature extremes

It is *virtually certain* that there has been a global-scale increase in the number of warm days and nights. It is also *virtually certain* that there has been a global-scale decrease in the number of cold days and nights. It is *very likely* that there has been a global-scale increase in the intensity, duration, and in the number of heatwaves. These changes are identified in most land regions but in some regions, in particular in Africa, there is less certainty regarding these changes due to lack of data availablity (*high confidence*).{11.3, 11.9}

There is *high confidence* in the ability of climate models to simulate the sign of the observed recent changes in temperature extremes at regional to global scales, but *medium confidence* in their ability to reproduce more specific and in particular some quantitative characteristics of changes in temperature extremes. Observed trends in global and regional temperature extremes lie within the spread of simulated trends in CMIP5 (*high confidence*). CMIP6 simulations are not yet available for this assessment but will be assessed for the second-order draft (SOD). The ability of models to capture observed trends in temperature-related extremes depends on the extreme indices evaluated, the way indices are calculated within models, and the time frames and spatial domains considered (*high confidence*). {11.3}

It is *very likely* that anthropogenic increases in greenhouse gases have contributed to the increases in the likelihood and/or severity of observed hot extremes (annual, seasonal, daily, heatwaves) and the decreases in the frequency and/or severity of cold extremes on the global scale. Although effects of greenhouse gases are generally the dominant factor at the regional scale, they can be masked/counteracted or - in contrary – amplified in localized areas by natural variability or forcings, or other local human-induced factors. In particular, there is *medium confidence* that human-induced irrigation and crop expansion have attenuated summer hot extremes in some regions. There is also *medium confidence* that land cover changes have affected changes in hot extremes over the course of the 20th century. There is *high confidence* that trends in aerosol concentrations have also affected trends in hot extremes in some regions. Furthermore, some literature suggests that changes in atmospheric circulation patterns resulting from greenhouse-gas induced Arctic ice loss may have had an influence on mid-latitude weather, including an increased likelihood of cold extremes (such as frost days) in some locations in winter, but there is only *low confidence* in the underlying processes and the existence of a causal relationship. {11.3; Cross-chapter Box on Arctic climate hosted in Chapter 10}

It is *virtually certain* that increases in the frequency and severity of warm days and nights and decreases in the frequency and severity of cold days and nights would occur through the 21st century at the global and continental scales, and in nearly all inhabited regions[2], if global warming increases to +1.5°C or higher above preindustrial values. It is *virtually certain* that the length, frequency, and/or intensity of warm spells or heat waves (defined with respect to late 20th century conditions) will increase over most land areas. It is *very likely* that the number of hot days will increase in most land regions, with the highest increases in the tropics when hot days are defined using relative thresholds (e.g. 90th percentile of late 20th century conditions), for a global warming of +1.5°C and higher. All of these changes would become increasingly larger for each increment of 0.5°C of warming (*high confidence*). There is *high confidence* that the temperature extremes warm more strongly on land than global mean temperature does. This includes a warming of extreme hot daytime temperatures up to twice larger than global warming in mid-latitudes, i.e. about +3°C at +1.5°C global warming and about +8°C at +4°C global warming (*medium confidence*). The warming in extreme cold night-time temperatures in the Arctic and several northern high-latitude (and in some case mid-latitude) regions is about three times the warming of global mean temperature, i.e. about +4.5°C at +1.5°C global warming, and about +12°C at +4°C global warming (*medium confidence*). Increases in the magnitude of temperature extremes at higher global warming levels are approximately linear in most regions (*high confidence*), however, increases or decreases in the frequency of exceedance of given extreme thresholds (e.g. hot days or cold days) are non-linear with increasing global warming (*high confidence*). {11.3, 11.9}

[2] See Figure 1.16 in Chapter 1 for definition.

Heavy precipitation

There is *high confidence* that heavy precipitation has intensified in a majority of land regions with adequate observations. Due to the high spatial and temporal variability of precipitation, the level of confidence of the trends depends on the region. Changes in precipitation extremes are, in general, more complex and spatially more heterogeneous than changes in temperature extremes. The observed tendencies show particularly larger percentage increases in heavy precipitation in the northern high-latitudes in all seasons, as well as in the mid-latitudes in the cold season (*high confidence*). There have been regional increases in the frequency and/or in the intensity of heavy rainfall over: i) central Asia, most of South Asia, northwest Australia, northern Europe, Southeast South America, the Amazon region and most of the United States (*high confidence*) and ii) West and South Africa, Central Europe, eastern Mediterranean region, Mexico (*medium confidence*). Elsewhere, there is generally *low confidence* in observed trends in heavy precipitation due to data limitations. A few regions show *medium confidence* in decreases in heavy precipitation. {11.4; 11.9}

There is *high confidence* that anthropogenic influence has contributed to the observed intensification of heavy precipitation in land regions. Thermodynamic processes are the dominant driver for this response, but dynamic processes are also relevant (*high confidence*). There is an improved understanding of processes leading to extreme rainfall and their representation in climate models (*high confidence*). Moreover, climate models are being improved in resolution and some are now better able to capture certain classes of extreme storms, especially for shorter-lived events at regional scales (*high confidence*). {11.4, Box 11.1}

It is *likely* that observed upwards trends in heavy precipitation will continue under a global warming of +1.5°C or higher. A larger set of studies based on global and regional climate projections are becoming available and they will provide a more coherent picture of regional changes in extreme rainfall and snowfall with the associated uncertainties. {11.4}

There is *medium-to-high confidence* that heavy precipitation associated with tropical cyclones produce yet more precipitation at higher levels of global warming. {11.4, 11.7.1, 11.9}

Floods and water logging

Floods and water logging are affected by multiple factors including heavy rainfall (*high confidence*). Other factors include catchment characteristics, antecedent soil moisture, storm surges and tides and their link to sea level rise in coastal regions, human intervention such as dam operation, and/or changes in land use and land cover (*high confidence*). An increase in heavy rainfall does not necessarily result in an increase in flooding and such changes are greatly affected by the size of the catchment. Consideration of multiple complex hydrologic factors at multiple scales and resolutions results in significant uncertainties in both observed and projected trends in flooding. Such uncertainties are also being reflected in attribution studies related to flooding. For projections, there is *medium confidence* that an increase in global warming to 2°C compared to 1.5°C or present-day conditions would lead to a larger fraction of land area affected by flood hazard at global scale, as assessed in the IPCC SR15. There is *medium confidence* that further increases would occur at higher levels of global warming (i.e. >3°C or higher). {11.5}

Droughts

There are several definitions of droughts and these definitions may affect assessments regarding their changes under increased greenhouse gas forcing (*high confidence*). It is important to distinguish meteorological drought (precipitation deficits) from soil drought (lack of soil moisture, also termed “agricultural drought”, relevant for agriculture and ecosystems), hydrological drought (lack of streamflow), atmospheric dryness (lack of moisture in the air), and overall atmospheric evaporative demand (associated with potential evaporation). In addition, there is *medium confidence* that the relative importance of these drought measures may change under enhanced CO_2 concentrations due to physiological effects of the latter on plant transpiration. Anthropogenic influence on drought and water scarcity is complex, it includes climate influences, land use influences, and socio-economical influences (*high confidence*). {11.6}

There is *high confidence* that the occurrence of a drought event is driven by both dynamic and thermodynamic processes. There is *high confidence* that greenhouse gas forcing on thermodynamic processes affecting droughts is enhancing drought severity in some areas, but there is *low confidence* related to greenhouse gas forcing on global changes in circulation mechanisms that contribute to the occurrence of drought events. Drought complexity, and the fact that drought events are more long-lived than e.g. consecutive hot days or heavy precipitation days, makes it difficult to quantify the drought severity and to assess recent drought trends. There are also different drought types and a variety of associated impacts that make it difficult to give a complete overview of drought trends. There are also data availability problems, for instance for the quantification of different meteorological variables that affect drought but also the soil moisture availability, i.e. soil moisture/agricultural drought. There is *low confidence* in global drought changes, either driven by precipitation and/or atmospheric moisture deficits and associated evaporative demand, associated to soil moisture deficits, or lack of streamflow. There is *medium confidence* in global hydrological drought trends attributed to human emissions, given human activities related to water management (dams, irrigation), and land use changes, There is *low confidence* in a global attribution of trends in large drought events over the last decades. There is *medium confidence* that recent severe drought events affecting the Mediterranean-type climates, in particular in Southern Europe, have an attributable anthropogenic component. There is *medium confidence* that an increasing trend in the severity or likelihood of observed drought events in Southern Africa and Southern Europe is due to anthropogenic effects.There is *medium confidence* in the ability of models to reproduce drought trends, mostly at the regional scale. There are uncertainties related to global mechanisms but also to the internal variability of models and the General Circulation Models (GCMs) used. {11.6, Box 11.1}

Projected drought changes display large geographical variations, and hence “global-scale” drought is not well defined or meaningful. Thereby, there is *high confidence* that historical and projected changes in drought patterns cannot be fully encompassed with the catch phrase “dry-get-drier, wet-gets-wetter”, since many dry or wet regions display uncertain changes, and some humid regions display drying trends and/or are projected to become drier. There is *medium confidence* regarding an increased probability of higher drought frequency and/or severity in the Mediterranean, Southern Africa, Southern North America, Central America and Northeast Brazil under a global warming of 1.5°C, and in the probability of higher drought frequency and/or severity in these regions under a global warming of 2°C. The *confidence* is *medium* because there is agreement among climate models, but some uncertainties in drought representation in climate models, drought metrics used by the projections, and lack of observations in several regions. {11.6, Box 11.1}

Tropical cyclones

There is generally *low confidence* in the detection and attribution of any anthropogenic influence on historical tropical cyclone intensity (i.e. wind speed) in any basin or globally. This does not imply that no such trends exist, but rather that known data heterogeneities reduce confidence in their fidelity. An exception to this is in the North Atlantic where there is *medium confidence* that a reduction in aerosol forcing has contributed at least in part to the observed increase in tropical cyclone intensity since the 1970s. There is *low-to-medium confidence* that the poleward migration of the location of peak tropical cyclone intensity in the western North Pacific lies outside the range of natural variability. {11.7.1}

There is *medium-to-high confidence* that mean global tropical cyclone precipitation rates increase at least at Clausius-Clapeyron rate of 7% per °C and that average peak wind speed would increase at a rate of a few percent per °C at +1.5°C and higher levels of global warming. Attribution and projections studies find that extremely heavy tropical cyclone precipitation rates can also increase at rates substantially exceeding Clausius-Clapeyron scaling (*medium confidence*), possibly due to storm structural changes. In addition, there is evidence that tropical cyclone translation speed may be slowing, possibly enhancing precipitation totals during tropical cyclone events, but at present there is only *low confidence* in this signal.

Larger intensity increases are projected in stronger storms and there is *medium-to-high confidence* that the global proportion of very intense (Category 4-5) storms will increase under higher levels of global warming. There is *low confidence* regarding global projections of changes in the overall frequency of tropical cyclones. Most projections identify an average reduction of a few percent per °C, but recent literature showing projections of increased frequency has challenged this previous assessment. There is *low confidence* in projections of changes in tropical cyclones in individual ocean basins. {11.7.1}

Severe convective storms

Severe convective storms are mesoscale convective systems that are associated with severe events such as tornadoes, hail, heavy precipitation, strong winds, and lightning. Their characteristics have been viewed with new perspectives in recent years, such as related to convective aggregation, linear-shaped stationary systems, or warm rain processes. Because the definition of severe convective storms depends on the literature, it is not straightforward to provide a synthetic view. However, observations show a *medium confidence* regarding an intensification of severe convective storms in some regions *(medium agreement, medium evidence)*. For projections, there is *low evidence* on changes in severe convective storms with global warming because of limited availability of suitable climate and atmospheric simulations. {11.7.3}

Compound events

Compound events, or multi-variate extremes, can be very relevant for impacts. Importantly, the combination of two or more non-extreme events can lead to extreme impacts (*high confidence*). There is *high confidence* that some compound events, for instance co-occurrent heatwaves and droughts, are becoming more frequent under enhanced greenhouse gas forcing, and will continue to increase under higher levels of global warming. {11.8}

Regional changes in weather and climate extremes

In Africa, there is *medium to high confidence* in the increase in the number of warm days and nights and decrease in the number of cold days and night over North, West and South Africa since 1951. Heat waves have increased with *medium confidence* over Africa except Central and East Africa. These changes are expected to continue in the future with *medium to high confidence*. There is *low confidence* in observed change in heavy precipitation over the most part of the continent owing to lack of information. Positive trends in the intensity of extreme precipitation over West and South Africa have been observed with *medium confidence* which is projected to continue in the future (*medium to high confidence*). With respect to dryness, there is *medium confidence* in increase (decrease) of Consecutive Dry Days (CDD) over South Africa (West Africa). In the future, there is *medium to high confidence* in projected increase in dryness over the continent except in the Sahara, central and eastern Africa.

In Asia, there is *high confidence* in the increase of daily temperature extreme during the last decades over most part of Asian continent including the Himalaya and Tibetan Plateau. Observed precipitation extremes show an increasing trend with *high confidence* over most part of Asia. However, there is *medium confidence* in observed decrease in precipitation extreme in the central Tibetan Plateau, the south-western part of Pakistan, and a southwest–northeast belt from Southwest China to Northeast China. Projections of extreme precipitation show with *high confidence* a general wetting with increases of heavy precipitation in most parts of Asia.

In Australasia, there is *high confidence* that it is *very likely* that temperature extremes have increased over South and North Australia, New Zealand and western Pacific islands. There is *high confidence* that it is *extremely likely* that by the end of the century there will be a reduction in the number of cold temperature extremes and an increase in the number of warm temperature extremes in Australasia. There is *medium confidence* that heavy precipitation has increased in North Australia and low confidence that it has decreased in South Australia with important regional and seasonal variations. There is *low confidence* on trends over New Zealand where also important seasonal and spatial variations are observed. There is *low to medium confidence* that extreme precipitation will increase over Australia and New Zealand by the end of the 21st century. There is *low confidence* in a decrease in the frequency of tropical cyclones affecting the northern Australian region since 1982 and *medium confidence* that no changes have been observed in extreme extratropical cyclones over the east coast of Australia.

In Europe, there is *high confidence* in the increase of maximum temperatures and in the frequency of heat waves. There is also *high confidence* that human-induced climate change has contributed to the increase in the frequency and intensity of short-term heat waves. There is *high confidence* of projected increase in high temperature extremes over the whole continent. Regarding precipitation, there is *medium confidence* in the increase in extreme wet events which are also projected to continue into the future with *medium confidence*.

In South (Central) America, there is a *medium-to-high confidence* in an increase in the number of warm days and nights and decrease in the number of warm days and nights in the last decades, except over South East South America (SES) where hot extremes have decreased during austral summer. With *high confidence*, projected changes in temperature extreme indices show a widespread *extremely likely* warming over Central and South America by the end of the 21st century. Observations since 1950 suggest an overall increase in precipitation extremes (*medium confidence*) and a *likely* increase over South East South America with *high confidence*. There is *medium confidence* on projected increase in precipitation extremes over SES and *low confidence* on decrease over Central America and northern South America.

In North America, dominant changes in observed extremes include *very likely* increase (*high confidence*) in the number of warm days and nights and decrease in the number of cold days and nights, also over central North America and the eastern United States, albeit with changes smaller than elsewhere in North America. Projections in temperature extremes for the end of 21st century (*high confidence*), show that warm (cold) days and warm (cold) nights are *very likely* or *likely* to increase (decrease) in all regions. There is *medium confidence* in large increases in warm days and warm nights in summer particularly over the United States and in large decreases in cold days in Canada in fall and winter. There is *high confidence* that precipitation extremes have been increasing throughout North America, especially in the eastern half of the United States. There is *medium confidence* that droughts have become less frequent, less intense, or shorter in North America since 1950. Increases in both moderate and rare precipitation extremes in all regions of the United States have been projected. Increases in agricultural drought through North America and severe hydrological drought in the western United States are also projected.

Storylines, potential surprises, and low-probability high-impact events

Multi-decadal climate model projections and Earth System observations alone do not allow us to provide a fully comprehensive quantitative assessment of changing hazards from extreme weather across timescales (*high confidence*). However, by conditioning climate models on plausible but rare atmospheric states while forcing the models with different levels of warming, storylines of potential hazards including tipping-element-like behaviour can develop insights (*medium confidence*).

High-impact low-probability events remain a critical gap in our understanding of extremes (*high confidence*). This is particularly the case for events that lie outside of observed analogues and are difficult to explore (*high confidence*). However, storylines can be developed to assess events that do not appear in observations but can be conceived on the basis of them (i.e. with different combinations of observed patterns) and which could have potentially high impacts (*medium confidence*). Low-probability high-impact events can also be explored using statistical approaches and large-ensemble model experiments.

Knowledge gaps

There are some remaining areas associated with knowledge gaps in extremes research at present. Some topics are still unsufficiently investigated such has hail. Also, possible changes associated with global and regional tipping points (high-risks low probability events) are associated with *low confidence*, but cannot be excluded, especially at high global warming levels (>3°C). Finally, there are still remaining important observational gaps in several world’s regions, in particular in Africa.

11.1 Framing

11.1.1 Introduction to the chapter

This chapter provides assessments on changes in weather and climate extremes (collectively referred to as extremes) with a focus on the relevance to the Working Group II assessment. Here, we assess observed changes, their attribution to causes, and future projections. The occurrence of extremes in an environment with exposed and vulnerable human and natural systems can lead to disasters (IPCC, 2012). Changes in extremes result in changes in impacts not only as a direct consequence of changes in the magnitude and frequency of extremes (which are termed "hazards" in a risk framework, see also Chapter 12), but also through their influence on exposure and resilience.As such, extremes are an essential component assessed in IPCC reports. The Special Report on Managing the Risks of Extreme Events and Disasters to Advance Climate Change Adaptation (referred as SREX report, IPCC, 2012) provided a comprehensive assessment on changes in extremes and how exposure and vulnerability to extremes determine impacts and likelihood of disasters. The Chapter 3 of that report (Seneviratne et al., 2012a, hereafter also referred to as SREX Ch3) assessed physical aspect of extremes, and laid a foundation for the follow-up assessments of changes in extremes including the IPCC Working Group I 5th Assessment report (IPCC AR5; IPCC, 2013), and the recent IPCC special report on 1.5°C global warming(SR15,IPCC, 2018), and the upcoming IPCC special reports on climate change and land (SRCCL) and on oceans and the cryosphere(SROCC). These assessments are the starting point of the present assessment.

The AR5 WGI report assessed changes in extremes in various chapters, including observed changes (Hartmann et al., 2013), the evaluation of models' performance in simulating extremes (Flato et al., 2013), the detection and attribution of changes in extremes to causes (Bindoff et al., 2013), and long-term projections in extremes(Collins et al., 2013a). The assessments were of largescale in general. The AR6 WGI report dedicates this chapter to assess past and projected changes in extremes, as one of the three "regional chapters" of the WG1 report (along with Chapters 10 and 12). As such, while we assess changes in extremes from global and continental perspective to provide a large-scale context, this chapter also addresses changes in extremes from a regional perspective. The Chapter 3 of SREX has a similar role in that report, here we adapt the general approach used in SREX Ch3 regarding the chapter structure, and extremes assessed. This provides a traceability and basis of comparison to earlier assessments. Note that this chapter does not assess impacts, which are covered in the WGII report. Chapter 12 of this report takes up the assessments presented here and expand them as needed from the perspective of hazards, providing key handshake with the WGII report.

This chapter is structured as follows. This section (11.1) provides a general framing and introduction for the chapter, highlighting key aspects that underlie the confidence and uncertainty in the changes of extremes, and introducing some main elements of the chapter. Section 11.2 introduces methodological aspects of research on climate extremes. Sections 11.3 to 11.7 assess past changes and their attribution to causes, and projected future changes in extremes, for different categories of extremes, such as temperature extremes, heavy precipitation, floods and droughts, and storms in separate sections. Section 11.8 addresses compound events or multivariate extremes. Section 11.9 summarizes regional information on extremes by continents. Finally, Section 11.10 presents some assessment on high impact and low probability events. The chapter also entails several boxes and FAQs to more specific topics.

11.1.2 What is an extreme event?

The risk framework defined in the SREX report (IPCC, 2012) articulates clearly that the exposure and vulnerability to extremes determine impacts associated with a given hazard, for instance related to an extreme event, and that adaptation can reduce exposure and vulnerability and increase resilience resulting in reduced impacts to the same extremes. There is thus a distinction between weather and climate extremes ("hazards" in the risk framework) and extreme impacts, and there is not always a one-to-one correspondence between the two. Extreme impact can also result if very vulnerable human and natural systems are exposed to a weather and climate event that in itself may not be very extreme. Conversely, a weather and climate extreme event may not result in much impact if there is not a vulnerable system exposed to it (SREX Ch3). Yet there is no precise definition for weather and climate extremes. Building on the SREX report, the AR5 defined an extreme weather event as "an event that is rare at a particular place and time of year" and an extreme climate event as "a pattern of extreme weather that persists for some time, such as a season" (AR5 Glossary). These definitions are adopted here. The definitions of rare vary, depending on purposes. Many studies consider an event as extreme if the value of a variable exceeds (or lies below) an absolute threshold above (below) which an impact may occur, or as a relative threshold represented by a high (or low) percentile value. Such a percentile threshold corresponds to a low probability of occurrence (e.g. 1%, 5% or 10%) at either tail of distributions of climate variables (e.g. hot or cold for temperature extremes). There is no clear-cut distinction between an extreme weather event and an extreme climate event although usage implies that they are of different space and time scales in general. An extreme weather event has typically a weather scale (from minutes to days) while an extreme climate event has typically a climate scale (months or years). For simplicity, we collectively refer here to weather and climate extremes as "extremes" or "extreme events". The rarity of an event is relative to climatology which is always linked to space and time scales.

Interpretation of an analysis of extremes needs to be placed in proper context because, as highlighted above, there are different ways to define an extreme event (e.g. spatial and temporal dimensions, considered variables) and different questions to ask regarding how extremes have changed or are projected to change. For example, two sets of frequency of hot/warm days have been used in the literature. One set counts the number of days when maximum daily temperature is above a relative threshold defined as the 90^{th} or higher percentile of maximum daily temperature for the calendar day over a base period. An event based on such definition can occur during any time of the year and impact of such an event would differ depending on the season. The other set counts the number of days in which maximum daily temperature is above an absolute threshold such as 35°C, as exceedance of this temperature can sometimes cause health impact (however, these impacts may depend on location and whether ecosystems and the population are adapted / used to such temperatures). While both types of hot extreme indices have been used to assess the frequency of hot/warm events, they represent different events that occur in different time of year, possibly affected by different types of processes and mechanisms, and possibly also associated with different impacts.

Another example relates to the way questions are posed, such as change in the frequency for a given magnitude of extremes or change in the magnitude for a particular return period. Change in the probability of extreme temperatures is dependent on the rarity of the extreme event that is assessed, with a larger change in the probability associated with rarer event(e.g. Kharin et al., 2018). On the other hand, change in the magnitude represented by the return level of the extreme events may not be as sensitive to the rarity of the event. While the answers to the two different questions are related, their relevance to different audiences may differ. Conclusions regarding the respective contribution of greenhouse gas forcing to changes in magnitude vs frequency of extremes may also differ (Otto et al., 2012). Correspondingly the sensitivity of changes in extremes to increasing global warming is also dependent on the definition of considered extremes: In the case of temperature extremes, changes in magnitude have been shown to often depend linearly on global temperature (Seneviratne et al., 2016; Wartenburger et al., 2017), while changes in frequency tend to be non-linear and can e.g. be exponential for increasing global warming levels (Fischer and Knutti, 2015; Kharin et al., 2018).When similar damage occurs once a fixed threshold is exceeded, it is more important toask a question regarding changes in the frequency. On the other hand, if the impact of an event increases with the intensity of the event, it would be more relevant to examine changes in the magnitude. Finally, adaptation to climate change might change the relevant thresholds over time, although such aspects are still rarely integrated in the assessment of projected changes in extremes.

11.1.3 Extreme types addressed in this chapter

The types of extremes and phenomena assessed in this chapter include temperature and precipitation extremes, drought, floods,tropical cyclones and severe convective storms. In addition, we also consider compound events, i.e. bivariate or multi-variate extreme events. The considered extremes are included because of their relevance to impacts. Most of the considered extremes were also assessed in the SREX and AR5. However, compound events were not assessed in detail in past IPCC reports, although the SREX briefly addressed this topic (SREX Ch3). Marine extremes such as marine heat wave, extreme sea level, are assessed in Chapter 9 (Cross-chapter box 9.1) of this report rather than in this chapter.

Temperature and precipitation extremes studied in the literature are often based on extremes derived from daily values, such as annual maxima or minima of daily temperatures, annual counts of daily temperature above or below certain percentiles, duration of heatwaves based on daily temperature data, annual maximum one-day or 5-day precipitation events.Studies on events of longer time scales for both temperature or precipitation, or on sub-daily extremes are scarcer. This necessarily limits the assessment for such events, although there has been an increase in related literature since the AR5. When possible, extremes of time scale different from daily are assessed here. We assess drought and storms as phenomena in general, not limited by their extreme forms, because of their relevance to impacts. We also consider both precipitation and wind extremes associated with storms. Extreme phenomena in the atmosphere are of different spatial and temporal scales (von Storch, 2005). Tornadoes have a spatial scale of less than 100 meters and a temporal scale of only a few minutes. On the other hand, a drought can last for multiple years, affecting a whole continent. The level of complexity of the involved processes differs from one type of extreme to another, affecting our capability in detecting and attributing, and in projecting changes in the weather and climate extremes.

Multiple stressors can combine to yield more extreme hazards and/or exhaust the adaptative capacity of a system more quickly. For this reason, the occurrence of multiple (e.g. multivariate) extremes concurrently or in succession, or so-called “compound events” (SREX Ch3), can lead to impacts that are much larger than the sum of the impacts due to the occurrence of individual extremes alone. For the first time in an IPCC report changes in compound events are also assessed in some depth in this chapter, although literature in this area is still limited (Section 11.8).

As in the SR15 report(Hoegh-Guldberg et al., 2018, hereafter referred to as SR15 Ch3), the assessment of projected future changes is mainly given according to different levels of global warming. This is to provide traceability and comparison to the SR15 assessment, as well as for providing actionable information for decision makers because much of policy discussion and adaptation planning can be tied to the level of global warming. For example, regional changes in extremes and thus their impacts can be directly linked to global mitigation efforts. Additionally, there is also an advantage of separating uncertainty in future projection due to natural internal variability from other factors such as difference in model sensitivities and emission scenarios. However, some analyses related to specific emissions scenarios are also provided and will be expanded in the SOD based on CMIP6 simulations, this will provide easier comparsion with the AR5 assessment.

Tables 11.1 and 11.2 provide a synthesis on the assessments from this chapter for observed and attributed changes, and projected changes at different levels of global warming, respectively.

[START TABLE 11.1 HERE]

Table 11.1 Synthesis table on observed changes in extremes and contribution by human influences. Note that observed changes in marine extremes are assessed in the cross-chapter box 9.1 in Chapter 9.

[END TABLE 11.1 HERE]

[START TABLE 11.2 HERE]

Table 11.2 Synthesis table on projected changes in extremes. Note that projected changes in marine extremes are assessed in the cross-chapter box 9.1 in Chapter 9.

[END TABLE 11.2 HERE]

11.1.4 Effects of greenhouse gas and other external forcings on extremes

External forcings such as human emissions of greenhouse gases are the main drivers of the past and future changes in the climate. They are also the main drivers of the changes in extremes, at least globally, as extremes are an integral part of the climate system. The SREX, AR5 and SR15 reports assessed that there is evidence from observations that some extremes have changed since the mid 20th century, that some of the changes are a result of anthropogenic influences, and that some observed changes are projected to continue into the future while other changes are projected to emerge from natural climate variability under enhanced global warming (SREX Ch3, AR5 Ch10; see also 11.1.3).

At the global and continental scales and regional scale to some extent, much of the changes in extremes are a direct consequence of the enhanced radiative forcing, and the associated global warming and/or its resultant increase in the water-holding capacity of the atmosphere through the Clausius-Clapeyron relationship through thermodynamical processes (see Box 11.1 on Thermodynamical vs Dynamical processes).Widespread observed and projected increases in hot extremes and decreases in cold extremes are consistent with global and regional warming (Section 11.3). Increases in annual maximum daily maximum temperatures and in annual minimum temperatures scale robustly and generally linearly with global mean temperature change across different geographical regions and different emission scenarios (Seneviratne et al., 2016;Wartenburger et al., 2017;Kharin et al., 2018). The number of heatwave days and the length of heatwave seasons in various regions also scale well, but non-linearly (because of threshold effect) with global mean temperatures (Wartenburger et al., 2017; Sun et al., 2018a). Changes in annual maximum one-day precipitation are proportional to global mean temperature changes, at about 7% increase per 1°C temperature increase in the observations (Westra et al., 2013) and in future projections (Kharin et al., 2013) at the global scale, i.e. following the Clausius-Clapeyron relationship (Box 11.1). Extreme short-duration precipitation in North American also scale with global mean temperature (Li et al., 2018a;Prein et al., 2016b). At the local and regional scales, changes in extremes are also strongly modulated and controlled by regional forcings and feedback mechanisms (Section 11.1.6), whereby some regional forcings, e.g. associated with land use/albedo or aerosol emissions, can have non-local or some (non-homogeneous) global-scale effects (Persad and Caldeira, 2018;Seneviratne et al., 2018a). In general, there is *high confidence*in changes in extremes due to global-scale thermodynamical processes (i.e. mean global warming, mean moisterning of the air) as the processes are well understood, while those related to dynamical processes or regional and local forcing and processes, including regional and local thermodynamic processes, are much lower due to multiple factors (see two following sub-sections and Box 11.1).

[START BOX 11.1 HERE]

BOX 11.1: Thermodynamical vs dynamical processes affecting changes in extremes

Thermodynamics is “the branch of physical science that deals with the relations between heat and other forms of energy (such as mechanical, electrical, or chemical energy), and, by extension, of the relationships between all forms of energy” (Oxford English Dictionary, 2019). On the other hand, in physics, dynamics is “the branch of mechanics concerned with the motion of bodies under the action of forces”, while it may also refer more generally to “the branch of any science in which forces or changes are considered” (Oxford English Dictionary, 2019). Applied to climate science, this implies that thermodynamical changes refer to exchanges of energy, and dynamical changes to modifications associated with atmospheric motions. Because mechanical changes are ultimately associated with energy exchanges, and because atmospheric motion transports heat and moisture across the Earth, thermodynamical and dynamical processes are necessarily interconnected. But considering them separately has been shown to be particularly relevant in research on extreme weather and climate events, as it allows to disentangle separate processes contributing to the occurrence of climate extremes as a result of greenhouse forcing and internal climate variability (e.g. Shepherd, 2016).

Because greenhouse gases induce the trapping of heat within the Earth system, increases in their concentrations induce in a first step essential thermodynamical modifications of the climate, i.e. warming at the Earth's surface and in the atmosphere, enhanced heat storage in the oceans, melting of cryosphere, increased evaporation of the oceans and resulting changes in moisture content in the atmosphere. Regional-scale thermodynamical processes can also be of high importance. For instance, the Arctic amplification occurs largely due to thermodynamic changes that include the increase in surface absorption of solar radiation when snow and ice retreat (i.e, snow-ice albedo feedback; e.g. Hall and Qu, 2006), and this process is shown to strongly affect the temperature of cold extremes, leading to regional and seasonal warming rates in extremes three times larger than that of global mean warming (Section 11.3). As another example of regional thermodynamic processes, if soils dry as a result of increased incident radiation, and the warming of air (leading to higher atmospheric moisture demand on continents, Section 11.6), they may no longer sustain evapotranspiration (from soil surface and from plants), leading to enhanced sensible heat flux and thus a further heating of the air, resulting in a positive, i.e self-enhancing, feedback of temperature increases on continents (Seneviratne et al., 2010; Vogel et al., 2017). Greenhousegasesalso have a direct radiative forcing on regionaltemperatures on land due to physiologicalresponses of plants to enhanced CO2 (Lemordant et al., 2016; Swann et al., 2016; Section 11.6).

Overall there is high confidence in the relevance and sign of thermodynamical effects on temperature extremes, but there can be uncertainty regarding their magnitude and even sign of some regional thermodynamical feedbacks (e.g. Vogel et al., 2018). On the other hand, long-lasting heatwave events are generally associated with persistent perturbations of the atmospheric flow, which are an essential element of synoptic weather development, whereby there is only low confidence in possible effects of greenhouse gas forcing on changes in atmospheric circulation patterns, and in particular their persistence characteristics (Section 11.1.5).

Droughts are also the combined result of thermodynamic and dynamic processes (11.6). While greenhouse gas forcing on drought is strongly related to thermodynamic processes (through increased radiation, air temperature and atmospheric drying, which all increase evaporative demand), it is uncertain how changes in circulation patterns may affect drought occurrence (11.6). Thereby, there is high confidence that historical and projected changes in drought patterns cannot be fully encompassed with the catch phrase "dry-get-drier, wet-gets-wetter", since many dry or wet regions display uncertain changes, and some humid regions display drying trends and/or are projected to become drier (Greve et al., 2014; Byrne and O'Gorman, 2015). This highlights that thermodynamic processes cannot be understood alone from the Clausius-Clapeyron relationship, as in that case limited moisture supply on continents is a further explanation for this response, together with internal climate variability (Kumar et al., 2015).

A particularly fruitful use of the thermodynamics vs. dynamics decomposition framework has been made with respect to precipitation extremes (Byrne and O'Gorman, 2015; O'Gorman, 2015; Pfahl et al., 2017; Trenberth et al., 2015). Thereby, overall changes in precipitation extremes are separated according to dynamical and thermodynamical contributions to understand and quantify observed and future changes in precipitation extremes arising from anthropogenic influences (Byrne &O'Gorman, 2015; O'Gorman, 2015; Pfahl et al., 2017; Trenberth et al., 2015;Vautard et al., 2016; Yiou et al., 2017). Changes in water vapour under a warming climate have been shown in first approximation to be controlled by temperature changes through increases in ocean evaporation and in the water-holding capacity of the atmosphere (e.g., Trenberth, 1999). As a result, there is high confidence that water vapour content increases on the global scale roughly following the Clausius-Clapeyron (C-C) relation at a rate of approximately 7 % for every degree of surface warming near the Earth's surface (Held and Soden, 2006; O'Gorman and Schneider, 2009). Nonetheless, there are regional departures from this value in particular over continents, as atmospheric moisture over land is also strongly controlled by land evapotranspiration (van der Ent et al., 2010). Land evapotranspiration can be reduced under enhanced greenhouse gas concentrations, both as a result of enhanced soil drying and direct physiological effects of CO2 concentrations on plant transpiration. In a multi-model experiment, it was found that the regional thermodynamic effect of soil moisture drying on evapotranspiration leads to a projected mean decreased intensity of heavy precipitation events in several subtropical and mid-latitude regions in the warm season (Seneviratne et al., 2013). CMIP3 and CMIP5 models consistently project increases in global-scale atmospheric moisture close to the C-C relationship thus suggesting that the global thermodynamic contribution to relative humidity is overall well constrained and robust (high confidence). However, regional changes in thermodynamic processes affecting droughts display large model variations are only associated with medium confidence (Section 11.6). In particular, observed atmospheric drying in recent decades over land is not well captured in the CMIP5 multi-model ensemble (Douville and Plazzotta, 2017), with possible consequences for drought and heavy precipitation projections.

Regarding the dynamic contribution to heavy precipitation, atmospheric vertical motion results from a range of synoptic and subsynoptic phenomena including tropical cyclones, extratropical cyclones, fronts, mesoscale-convective systems and thunderstorms whose frequency and intensity are largely controlled by the large-scale circulation. There is medium confidence in current and future changes in these phenomena partly because changes in atmospheric circulation occur as an indirect effect of thermodynamic changes and because the circulation effects in synoptic and subsynoptic phenomena are usually complex due to the interplay between several large-scale drivers that often have opposing influences (e.g., Shaw et al., 2016). Therefore changes in the dynamical contributions are more uncertain and exhibit a low signal-to-noise ratio with large difference across models (Pfahl et al., 2017; Shepherd, 2014; Trenberth et al., 2015). In particular, contributions from changes in the dynamical term can either lead to increases or decreases of precipitation extremes and thus lead to smaller or even a reversal of thermodynamic climate changes (Nie et al., 2018; Norris et al., 2019; Otto et al., 2016; Pfahl et al., 2017; Tandon et al., 2018).

Employing different methodologies to disentangle the thermodynamic and dynamically driven part of extreme precipitation events attribution studies found that for winter storms in England changes in the thermodynamics and dynamics contributed to roughly half of the overall change each (Vautard et al. 2016; Yiou et al. 2017). On the other hand, attribution studies on summer rainfall in Europe indicate that changes in dynamics have the effect to reduce extreme precipitation that balances out the increases in extreme precipitation from the thermodynamic effects (Otto et al., 2015c; Schaller et al., 2014). Attributing the rainfall associated with tropical cyclones in the Atlantic suggests a stronger increase in the dynamic aspect of precipitation (Risser and Wehner, 2017; van der Wiel et al., 2017; van Oldenborgh et al., 2017). A dominant role of the dynamic contribution towards less rainfall was found in extreme summer rainfall in Australia (Grose et al., 2015).

Figure 1 shows an estimated decomposition of the fractional change (in % per degree of warming) in annual maximum precipitation day together with thermodynamic and dynamic contributions over the period 1950-2100 based on 22 CMIP5 models (Pfahl et al., 2017). The dynamical and thermodynamical terms were obtained by approximating the surface precipitation rate during an extreme event as the product of three terms: the efficiency, the vertical velocity (dynamical term) and the vertical derivative of the saturation specific humidity (thermodynamical term) as described by O'Gorman (2015). Precipitation extremes (Figure 1a) are projected to intensify with global warming over most of the globe with the exception of some subtropical areas where no changes or even decreases are observed. The thermodynamical contribution (Figure 1b) leads to increases everywhere and appears to be very robust across models (in every grid point at least 80% of the models agree on the sign of the change) and relatively homogeneous in space (mostly between 4 and 8% K^{-1}). The dynamic contribution (Figure 1c) varies greatly in space with large regions in the subtropics and extratropics showing substantial decreases and an area in the equatorial Pacific showing substantial increases. Most areas where changes are substantial also show high agreement across models but in transition areas and in middle and high latitudes agreement is quite poor, but the overall effect is also close to zero on average. In the subtropics and extratropics, negative contributions from the dynamical term have been linked with a decrease in the horizontal scale of the ascending motion related to increases in static stability (Tandon et al., 2018).

[START BOX 11.1, FIGURE 1 HERE]

Box 11.1, Figure 1: Multi-model mean fractional changes in thermodynamical scaling in which the vertical velocity ωe is kept constant (it is replaced with its mean value over the period 1950–2100). b, Difference between changes in full scaling and changes in thermodynamical scaling (full minus thermodynamic). Note that the maxima in the Pacific are above 60% K^{-1}. Stippling indicates that at least 80% of the models agree on the sign of signal. (From Pfahl et al., 2017)

[END BOX 11.1, FIGURE 1 HERE]

Extreme precipitation can also be enhanced by dynamical responses and feedbacks occurring within the storms resulting from the extra latent heat released from changes in the thermodynamic contribution (Lackmann, 2013; Marciano et al., 2015; Nie et al., 2018; Willison et al., 2013). The extra latent heat released within the storms has been shown to increase precipitation extremes by strengthening convective updrafts and the intensity of the cyclonic circulation. As these dynamical effects result from feedback processes within the storms and include convective processes, their proper representation might require models to have higher horizontal and vertical resolutions than that afforded by current global climate models and explicitly represent convective processes (i.e., Ban et al., 2015; Nie et al., 2018; Prein et al., 2015; Westra et al., 2014). Some studies performed using convection permitting simulations have suggested that the future intensification of precipitation extremes can depend on the duration of events with shorter-duration events showing higher scaling rates (e.g., Kendon et al., 2014), but other studies did not show differences (e.g., Ban et al., 2015).

In summary, both thermodynamical and dynamical processes contribute to the occurrence of climate extremes. Thermodynamical processes are generally more directly related to greenhouse gas forcing and thus better understood and generally more easily attributed to human-induced global warming. However, there remains large uncertainties and substantial model spread with respect to some regional-scale thermodynamic processes (e.g. snow-albedo temperature feedbacks or soil moisture-evapotranspiration-temperature/precipitation feedbacks). Dynamical processes are usually an indirect response to thermodynamical changes and also strongly affected by internal climate variability.Dynamical processes can be substantial and can either enhance or counteract the thermodynamical responses as in the case of precipitation extremes.

[END BOX 11.1 HERE]

11.1.5 Effects of large-scale circulation on changes in extremes

Atmospheric large-scale circulation patterns and associated atmospheric dynamics are important determinants of the regional climate and as such of the occurrence and severity of extremes (see also Box 11.1). We provide here more background on processes affecting large-scale circulation patterns. For example, the occurrence of the El Niño-Southern Oscillation (ENSO) influences precipitation regimes in many areas favoring droughts in some regions and heavy rains in others(BOX 11.3). The position and strengh of the Hadley circulation determine regions where tropical and extra-tropical cyclonesoccur with important consequences for the characteristics of extreme precipitation and winds. The circulation patterns associated with land-ocean heat contrast, which affect the monsoon circulations (Biasutti et al., 2018), lead to heavy precipitation along the coastal regions in East Asia (Freychet et al., 2015). As a result, changes in the spatial and/or temporal variability of atmospheric circulation in response to warming affect characteristics of weather systems such astropical cyclones (Sharmila and Walsh, 2018), storm tracks (Shaw et al., 2016), and atmospheric rivers (Waliser and Guan, 2017) (see also Section 11.7). Changes in weather systems in turn affect the frequency and intensity of extreme winds, extreme temperatures and extreme precipitation, on the backdrop of thermodynamic responses of extremes to warming. Aerosol forcing through changing pattern of the sea surface temperatures (SSTs) also affects circulation patterns and tropical cyclone activities (Takahashi et al., 2017).

Changes of most of various atmospheric large-scale circulation drivers are uncertain (Chapter 2, 3, 4, and 8). Among them, there is *medium confidence* that the Hadley circulation has expanded poleward(Chapter 3), which would affecttendencies for drought occurrence (see Section 11.6) and poleward shifts of tropical cyclones and storm tracks (see sections 11.7.1 and 11.7.2). While the projection of ENSO is uncertain (Chapter 4), it is relevant for projected global changes in extreme events because it is *very likely* that ENSO favour various extreme events in wide areas including droughts (Section 11.6 and Box 11.3) and tropical cyclones (see sections 11.7.1). A case study is provided for the intense ENSO in 2015/2016 in Box 11.3. However, given the uncertainty associated with changes in ENSO under a warming climate, there is only *low* *confidence* regarding possible greenhouse-gas induced changes in climate extremes associated with ENSO.

In summary, there is *high confidence* that large-scale atmospheric circulation patterns are important drivers for local and regional extremes, especiallyon interannual time scale, although there is overall*low confidence* about future changes in the strength of these patterns. There is also *low confidence* in projected responses of extremes due to changes in circulation.

11.1.6 Effects of regional-scale processes and forcings and feedbacks on changes in extremes

At the local and regional scales, changes in extremes are strongly modulated by regional and local feedbacks (Seneviratne et al., 2013;Miralles et al., 2014; Lorenz et al., 2016;Vogel et al., 2017), changes in large-scale circulation patterns (11.1.5), and regional forcings such as changes land use or aerosol concentrations(Hirsch et al., 2017, 2018; Seneviratne et al., 2018; Thiery et al., 2017;Wang et al., 2017f). It should be noted that these regional-scale forcing and feedbacks are often found to be asymmetric for temperature distributions, with generally higher effects for the hottest percentiles (Section 11.3).

Land use can affect regional extremes, in particular hot extremes, in several ways (*high confidence*). For instance, cropland intensification has been suggested to be responsible for a cooling of the highest temperature percentiles in the US Midwest (Mueller et al., 2016b). Similarly, irrigation has been shown to be responsible for a cooling of up to 1-2°C in many mid-latitude regions in present climate (Thiery et al., 2017), a process not represented in state-of-the-art Earth System Model simulations of the 5th or 6th phase of the Coupled Model Intercomparison Project (CMIP5, CMIP6). Changes in agricultural management associated with no-till farming, which lead to higher surface albedo after harvest (ca. +0.1) and reduced surface evaporation, may also asymmetrically cool hot days more than median days, with effects of ca. 1°C (Davin et al., 2014). In addition, the decrease soil evaporation may also mitigate the onset of drought (Wilhelm et al., 2015). Finally, deforestation has been shown to have substantially contributed to the warming of hot extremes in some mid-latitude regions over the course of the 20th century (Lejeune et al., 2018); it should be noted that this effect is often not well captured in Earth System Models (ESMs), because while observations show a cooling effect of forest cover compared to non-forest vegetation during daytime (Li et al., 2015), in particular in arid, temperature and tropical regions (Alkama and Cescatti, 2016), several models simulate a warming of daytime temperatures for regions with forest vs non-forest cover (Lejeune et al., 2017). Overall, the effects of land use forcing may be particularly relevant in the context of low-emissions scenarios, which include large land use modifications, for insance associated with the expansion of biofuels, or biofuels with carbon capture and storage (BECCS) or re-/afforestation to ensure negative emissions, as well as with the expansion of food production (e.g. Seneviratne et al., 2018b, Hirsch et al., 2018).

Aerosol forcing also has a strong regional footprint associated with regional emissions (*high confidence*). From the 1960s to 1980s approximately, enhanced aerosol loadings led to regional coolingsdue to decreases in global solar radiation (“global dimming”) which was followed by a phase of “global brightening” (Chapter 7; Wild et al., 2005). King et al. (2016a) show that aerosol-induced cooling delays the timing of the identification of a significant human contribution to record-breaking heat extremes in some regions. On the other hand, the decreased aerosol loading since the 1990s has led to an accelerated warming of hot extremes in some regions. Based on simulations with an ESM, Dong et al. (2017b) suggest that a substantial fraction of the warming of the yearly hottest days in Western Europe since the mid-1990s has been due to decreases in aerosol concentrations in the region. Dong et al. (2016) also identify non-local effects of decreases in aerosol concentrations in Western Europe, which they estimate played a dominant role in thewarming of hottest daytime temperatures in Northeast Asia since the mid-1990s, via induced coupled atmosphere-land surface and cloud feedbacks, rather than through a direct impact of anthropogenic aerosol changes on cloud condensation nuclei.

Beside regional forcings, also regional feedback mechanisms can substantially affect extremes (*high confidence*). This is the case with soil moisture feedbacks on hot extremes in several mid-latitude regions, which lead to a marked additional warming of hot extremes compared to mean global warming (Seneviratne et al., 2016), which is superimposed on the known land-sea contrast in mean warming (Vogel et al., 2017). In addition, there are also feedbacks between soil moisture content and precipitation occurrence, generally characterized by negative spatial feedbacks and positive local feedbacks (Taylor et al., 2012;Guillod et al., 2015). Climate model projections suggest that these feedbacks are relevant for projected changes in heavy precipitation (Seneviratne et al., 2013), however, there is evidence that climate models do not capture the correct sign of the soil moisture-precipitation feedbacks in several regions, in particular spatially and/or in some cases also temporally (Taylor et al., 2012;Moon et al., 2019). Locally the presence of lakes may amplify heavy precipitation associated with thunderstorms (Thiery et al., 2016). In high latitudes of the Northern Hemisphere, the snow- and ice-albedo feedback is projected to largely amplify temperature increases (e.g., Pithan and Mauritsen, 2014) although the effect in temperatures extremes is still unclear. It is also still unclear whether snow-albedo feedbacks on mountainous regions might have an effect on temperature and precipitation extremes (e.g., Gobiet et al., 2014), however they play an important role in projections of changes in high-latitude warming (Hall and Qu, 2006), and in particular changes in cold extremesin these regions (Section 11.3).

Finally, in some regions, weather and climate extremes may amplify one another. This is for instance the case between heatwaves and droughts, with high temperatures leading to drying tendencies on land because of increased evapotranspiration, and drier soil conditions leading later on to decreased evapotranspiration and higher sensible heat flux and hot temperatures (Seneviratne et al., 2013;Vogel et al., 2017;Zscheischler and Seneviratne, 2017;Miralles et al., 2014; see also Box 11.1 and Section 11.8).

In summary, there is *high confidence* that regional forcings and feedbacks, in particular associated with land use and aerosol forcings, and soil moisture-temperature, soil moisture-precipitation, and snow/ice-albedo-temperature feedbacks,play an important role in modulating regional changes in extremes. These can also lead to a higher warming of extremes compared to mean temperature (*high confidence*), and possibly some coolings in some regions (*medium confidence*). However, there is only *medium confidence* in the representation of the associated processes in state-of-the-art Earth System Models.

11.2 Data and Methods

11.2.1 Observations for extremes

The SREX and AR5 WGI reports (SREX Ch3, AR5 Ch2) discussed critical issues regarding the quality and availability of observed data and their relevance for the assessment of changes in extremes. Compared with mean climate, there are unique challenges and special data requirements when characterizing long-term changes in extremes. By definition, extremes are rare. This means that only the extremal portion of the distribution in the available observations are the most relevant when analyzing long-term changes in extremes. For example, while daily temperature are available for computing annual or seasonal mean temperatures, only a very small portion of the daily observations is relevant to characterize hottest temperature in a year. Because much of daily variability is averaged out when computing seasonal mean, summer mean temperature should have much smaller variability than the hottest day temperature has. As warming among different days in a season would not be drastically different, it follows that summer mean temperature should have larger signal to noise ratio than the hottest day temperature. Some climate extremes or phenomena such as drought have a large spatial and temporal scales, lasting several months to multiple years. Obviously, many years of data are required to obtain sufficient sample size to examine long-term trend. For these reasons, examining changes in extremes has stronger demand in data availability when compared with that for mean values, and their results can also be more uncertain due to smaller signal to noise ratio.

11.2.1.1 The ground-based instrumental record

The analysis of shorter duration extreme events, such as land and marine heatwaves, cold spells, flooding, tropical cyclones and extra tropical cyclones, often requires daily or sub-daily instrumental observations. In many regions, such observational records are short, stations may have not been uniformly maintained and/or their data are not openly available. Additionally, the networks' density with station data avaiable have decreased in recent years. The spatial coverage of extremes-relevant observed data is uneven, and there are large data gaps for various regions and countries (Donat et al., 2013a). While spatial coverage of daily data can be improved by integrating data sources, such as the International Surface Temperature Initiative (ISTI) databank that combines the Global Historical Climatology Network (GHCN)–Daily data sets with other historical data sources (Karl et al., 2015)the leve of improvment is still limited by the avaiability of underlying station observations.Some conutries only release the summary data discussed below, enabling broader spatial coverage for certain types of extreme weather analyses. The restriction of open release of original observations hinders the tracebility, however. Sub-daily observations of precipitation and temperature are more widely available than humidity (Willett et al., 2014) which necessary to calculate heat indices and other measures of human discomfort during heat waves. In-situ observations of soil moisture (Seneviratne et al., 2010;Dorigo et al., 2011), and to a lesser extent streamflow and runoff (Do et al., 2018), are limited as well, complicating the characterization of changes in drought and water logging statistics. Data inhomogeneity due to changes in siting, instruments, observation practice, is not always addressed, especially for precipitation data. Different quality control schemes may have also been used (Dunn et al., 2014). These introduces various sources of uncertainty, making trend analysis more uncertain. Station data have been used to produce gridded data products for different purposes including infilling data gaps and climate model evaluation. Different orders of operation have been used in producing such datasets. In one instance, daily values of station observations are gridded and various indices representing different aspects of extremes are thencomputed. In regions with high station density, the gridded values are closer to extremes of area mean. In regions with very limited station density, the gridded values are closer to point estimate of extremes. It follows that it can be difficult to interpret the extremes computed from gridded values due to different station density in different regions. In another case, the indices are computed first and then gridded. These gridded values are more representative for point estimate of extremes, subject to some spatial smoothing due to gridding. Because of spatial variability of the climate and different station densities in different regons, these two types of data products are not always comparable. And they are also not always directly comparable with extreme values derived from model simulations, which often represent extremes of area mean.

Agreement between different global and regional datasets varies, with between agreement for extreme temperatures than for extreme precipitation (Donat et al. 2014). While index-based data products provide a broader spatial coverage than raw variables, deterioration of networks over time is also reported, particularly for Africa and parts of South and Central America (Donat et al., 2013). These differences can be substantial enough to lead to very different conclusions about whether a specific precipitation event is actually extreme (Angélil et al., 2017).

Studies of long-term changes in extremes have used datasets of different lengthes with varying levels of data quality and homogeneity, and data may have also been processed differently prior to the analyses. All thses differences, along with strong demand on data avaiability which cannot always be met, make it difficult to synthesis those results. Consequently, quatitative assessment of long-term changes for some extremes can be difficult to produce.

11.2.1.2 The satellite-based instrumental record

Introduced in 1979, satellite remote sensing offers complementary data to in-situ measurements and the opportunity for more spatially homogeneous, albeit shorter temporal coverage. In some regions with sparse data coverage, they may provide the main source of information on observed changes. However, satellites do not observe the primary atmospheric state variables directly and orbiting satellites do not observe any given place at all times. Hence, their utility as a substitute for high-frequency (i.e. daily) ground-based observations is limited. For instance, Timmermans et al. (2019)analysed extreme daily and pentad precipitation and found little relationship between the timing of observed extreme precipitation in satellite and gridded station data products over the United States. [SOD PLACEHOLDER: WILL UPDATE THIS ASSESSMENT BASED ON WCRP GC SPECIAL ISSUE ON EXTREME PRECIPITATION FROM SATELLITES]. Satellite products provide useful insights on the interannual variability of drought conditions as well as on some emerging trends (e.g. Rodell et al., 2018), butthey are generally too short and too inhomogeneous to provide insights on long-term drought trends. [SOD PLACEHOLDER: WILL MENTION SATELLITES AS CONSTRAINTS FOR UNDERSTANDING MECHANISMS UNDERLYING EXTREMES, EG FEEDBACKS LEADING TO EXTREMES].

11.2.1.3 Reanalyses as a proxy observation for extremes.

While reanalyses products are often used as a proxy observations (Sillmann, et al. 2013), data homogeneity due to changes in the source data such as the addition of satellite data has been an important issue for assessing long-term changes. There is little evidence that they are of a high enough quality to provide a model evaluation metric for extreme precipitation as precipitation is not generally directly assimilated, although humidity and total column integrated water vapour is. Timmermans et al. (2018) found little tail dependence for extreme pentadal precipitation between the ERA-Interim and the gridded station data products over the United States. However, as the North American Regional Reanalysis (NARR) directly assimilates station precipitation data, they found that this measure of agreement to be high.

11.2.2 Statistical methods for trend detection

Various indices have been used to characterize different aspects of temperature and precipitation extremes (Alexander et al., 2006, Donat et al., 2013). They are of different statistical property, in particular, they may follow different probability distributions. Because it can be difficult to know the form of the underlying probability distribution, trend detection and estimation for these indices are often conducted with non-parametric method (Donat et al., 2013a). While the non-parametric method does have the advantage of being distribution free, this comes at the cost of reduced power in detecting a significant trend.

For values such as annual maximum one-day precipitation are known or assumed to follow the Generalized Extreme Value (GEV) distribution. In this case, the analysis is often conduced with fitting a non-stationary version of the GEV distribution to the data with time or other variables as co-variates (Katz, 2010). As the distribution is known (or assumed to be known), this method often has higher power of detecting a significant trend. When other variables such as global mean surface temperature is used, this method has been used in event attribution analyses (van Oldenborgh et al., 2017; Risser and Wehner, 2017), or to link changes in extremes with the global warming levels (Kharin et al., 2018).

11.2.3 Modelling and model evaluation for extremes

The ability of the various modelling approaches to simulate weather and climate extremes varies greatly, depending on their complexity and spatiotemporal scales. Some extremes are also affected by local feedbacks. Abnormally hot or cold seasons are often large enough in scale that the appropriate large scale meteorological patterns can be simulated well (Angélil et al., 2016, 2017;Stegall and Kunkel, 2017) at standard CMIP5/6 horizontal resolutions (~100km). Likewise, very wet seasons and droughts at regional scales can be adequately simulated by these models. The Atmosphere-Ocean coupled General Circulation Models (AOGCMs) and ESMs are usually able to represent some, although not all, aspects of synoptic scale phenomena such as heatwaves, cold snaps, extratropical cyclones and atmospheric blocking. However, depending on the phenomena and the specific region, biases can be important, generally larger for the magnitude/intensity of events than for their frequency of occurrence (e.g., Zappa et al., 2013b). For short duration events, AOGCM and ESM models fail to reproduce some key features of the observed distribution. This is the case even for high temperature extremes in well observed European regions (Kew et al., 2018; Min, et al. 2013; Sippel, et al., 2016) and in Asia. In particular minimum temperature extremes are less well represented (Seo et al., 2018).

Simulations of precipitation rates in extreme storms are generally too low at standard CMIP5 resolutions as the simulated gradients of temperature and moisture are too weak (Wehner et al., 2014). Dynamical downscaling of time slices of CMIP5/6 class AOGCM simulations allows for a better representation of some phenomena and more realistic surface forcings (e.g., topography and land-sea contrasts) often leading to more realistic simulation of extreme temperatures and precipitation (Di Luca et al., 2016a). Higher resolution model simulations systematically show more realistic representation of phenomena leading to extreme events including extratropical cyclones (Schaaf and Feser, 2018), tropical cyclones (Xue et al., 2013), atmospheric rivers (Whan and Zwiers, 2016), precipitation in complex orography areas (Prein et al., 2013). However, limited ensemble sizes reduce confidence in assessing the structural uncertainty in projected changes. Continental and regional scale atmospheric modelling at 4km or finer can resolve certain classes of short-term extreme events including convective storms (Ban et al., 2014; Kendon et al., 2017; Prein et al., 2017c, 2017a; Prein et al.,. 2017c). However, multi-decadal convection permitting simulations are not currently computational feasible, limiting their usefulness in evaluating changes in extremes.

11.2.4 Detection and attribution of extremes

The optimal fingerprint method has been traditionally used to detect and attribute changes in the climate to external forcings (section 3.2.1). This method requires the data to follow Gaussian distributions. While extreme values don't follow Gaussian distributions, they can be transferred such that the optimal fingerprint method can still be used. Kim et al., (2016)and Zhang et al., (2013)converted annual extrema to a "probability index" ranging from 0 to 1 using Generalized Extreme Value (GEV) distributions. Wen et al., (2013)and Wan et al., (2018) averaged extreme temperature over the space such that the averaged series follow Gaussian distribution. More recent studies have used non-stationary GEV distributions with model simulated responses as co-variates. This more appropriate statistical description of the non-stationary probability indices has allowed for detailed detection and attribution of regional trends in temperature extrema(Wang et al., 2017d). However, the method itself is not optimized.

11.2.5 Extreme event attribution

AR5 determined that there was an emerging consensus that the role of external drivers of climate change in specific extreme weather events could be quantified (10.6.2). It is noted that event attribution is still confined to particular case studies, often using a single model, and typically focussing on high-impact events for which the issue of human influence has already arisen.

However, since AR5, the number of studies on extreme event attribution has increased considerably (see series of supplements to the annual State of the Climate report (Herring et al., 2014, 2015, 2016, 2018, Peterson et al., 2012, 2013b) including the number of approaches to examining extreme events (described in Easterling et al., 2016; Otto, 2017; Stott et al., 2016). Two distinct but equivalent approaches to framing an event attribution study have been used to examine the role of external drivers of climate change in specific extreme weather events: likelihood- or magnitude-based. These approaches produce statements such as 'anthropogenic climate change made this event type twice as likely' or 'anthropogenic climate change made this event 15% more intense'. Jézéquel et al., (2018) and Otto et al., (2016)identifiedthat the framing of and conditions imposed on the attribution question can affect the sensitivity of an attribution statement.

In the risk-based approach, the change in probability of an event occurring due to large-scale warming is quantified by comparing the likelihood of its occurrence in a realistic present-day climate to its occurrence in a counterfactual "world that might have been" without anthropogenic climate change. There are a number of different analytical methods encompassed in the risk-based approach based on observations and statistical analysis (e.g. van Oldenborgh et al., 2012), optimal fingerprint method (Sun et al., 2014) regional climate and weather forecast models (e.g. Schaller et al., 2016), GCMs (Lewis and Karoly, 2013) and large ensembles of atmosphere-only GCMs (e.g. Lott et al., 2013). In contrast to the risk-based approach, the magnitude-based approach similarly compares the magnitude of an event of a fixed probability in the current climate with the magnitude of such an event in a climate without anthropogenic influence on the atmosphere. While these two framing approaches were developed independently, many recent analyses ask both the frequency and magnitude questions in a single framework.

A key component in any event attribution analysis is the level of conditioning on the state of the climate system. The occurrence of extreme events can depend strongly on state of the climate system including sea surface temperatures and sea ice concentrations. The extent of the human influence on an extreme event may depend on this state. In the least conditional approach, the combined effect of the overall warming and changes in the large scale atmospheric circulation are considered and often utilize fully coupled climate models (Sun et al., 2014). More conditional approaches involve prescribing certain aspects of the climate system. These range from prescribing the pattern of the surface ocean change at the time of the event (e.g. Hoerling et al., 2013, 2014), often using AMIP-style global models, to prescribing the large scale circulation of the atmosphere and using weather forecasting models or methods (e.g. Pall et al., 2017; Patricola et al., 2018;Wehner et al., 2018c). These highly conditional approaches have also been called “storylines” (Shepherd, 2016) and can be useful when applied to extreme events that are too rare to otherwise analyze. However, the imposed conditions limit an overall assessment of the anthropogenic influence on an event as the fixed aspects of the analysis may also have been affected by climate change. For instance, the specified initial conditions in the highly conditional hindcast attribution approach often applied to tropical cyclones (e.g. Patricola and Wehner, 2018; Takayabu et al., 2015) permit only a conditional statement about the magnitude of the storm if similar large scale meteorological patterns had occurred in a world without climate change thus precluding any attribution statement about the change in frequency.

This limitation of very conditional attribution studies highlights that there are two ways that climate change affects extreme events; locally through the influence of higher temperatures and moisture and non-locally through changes in the general circulation of the atmosphere. The overall influence of climate change on an extreme event is a combination of local thermodynamical and large-scale dynamical processes. These can be separated (Shepherd, 2016), although such analyses are very limited so far (Cheng et al., 2018).

The key sources of uncertainty in event attribution are the definition of the event and the uncertainty resulting from the framing and modelling approach. Observational uncertainties arise both in the estimating the magnitude of an event as well as its rarity (Angélil et al., 2017). Results of attribution studies can also be very sensitive to choice of climate variables. For example, a heat wave defined on temperature alone may yield different attribution results than a measure of heat stress (Sippel and Otto, 2014; Wehner et al., 2016). Attribution statements are also dependent on the spatial (Uhe et al., 2016) and temporal (Harrington, 2017) extent of event definitions, with large scale averages generally yielding higher attributable changes in magnitude or probability due to the smoothing out of the noise. In general, confidence in attribution statements for large-scale heat and lengthy extreme precipitation events have higher confidence than shorter and more localized events such as extreme storms.

The reliability of the representation of the event in question in the climate models used in the study is of utmost importance (Angélil et al., 2016; Herger et al., 2018) Very extreme events stress the capabilities of current generation models and is a factor in choosing a framing approach. The limited number of multi-model assessments of events and the lack of model evaluation has led to criticism of the emerging field of attribution science as a whole (Trenberth et al., 2015) and of individual studies (Angélil et al., 2017). While an overarching model evaluation framework for event attribution is currently not available, several ways of quantifying statistical uncertainty (Paciorek et al., 2018) and model evaluation (Lott and Stott, 2016; Philip et al., 2018a) have been employed. Paciorek et al. (2018) assessed a variety of advanced statistical methods to estimate standard error, making several recommendations for estimating risk ratio uncertainty (11.2.4). The ability to confidently attribute the human influence on extreme events depends on these uncertainties and limits the types of events that can be studied (National Academies of Sciences, Engineering, 2016).

Event attribution studies using a single method or a single model are assessed with low confidence unless they are assessments of events where several studies of the same type exist that thoroughly assessed the uncertainties involved.

11.2.6 Global warming levels and their connection to regional changes in extremes

The most important quantity used to characterize past and future climate change is the globally averaged mean surface temperature (GMST) relative to its pre-industrial level. On one hand, changes in GMST is linked linearly to global cumulative carbon emission. On the other hand, changes in regional climate including many types of extremes scale well with changes in GMST. For example, Sun et al., (2018a)found that increase in GMST has a linear relationship with the number of heatwave days, the length of heatwave season, and the annual hottest day temperature in China. The connections between global warming and regional changes in extremes, and between global warming and cumulative carbon emissions make it possible to link regional changes in extremes and thereby regional impacts of climate change to cumulative carbon emissions. Indeed, Seneviratne et al., (2016) showed that regional changes in annual maximum daytime temperature scale approximately linearly with cumulative CO_2 emissions. For these reasons and as assessed in SR15, many studies attempted to project regional changes in extreme according to global warming levels (e.g., Kharin et al., 2018).

Projection of future changes in extremes in relation to global warming levels has an important advantage in separating uncertainty due to natural internal variability of the climate system from uncertainty due to model structural errors and due to differences in emission scenarios. If the interest is in the projection of regional changes at certain global warming levels such as those defined by the Paris Agreement, projections based on time periods and emission scenarios would have unnecessarily larger uncertainty due to differences in model sensitivities. To take this advantage and to provide easy comparison with the SR15 assessment, assessment of future changes in this chapter are largely provided in relation to future global warming levels, including 1.5°C, 2°C, 3°C and 4°C above pre-industrial.

While regional changes of many types of extremes scale with global mean temperature linearly, irrespective to emission scenarios, effect of local forcing can distort such relation. In particular, emission scenario with the same radiative forcing can have different extreme precipitation response under different aerosol forcing. Another example is related to land use changes. Climate models are known to overestimate observed changes in annual maximum daily maximum temperature. Part of the overestimation may be due to the lack of representation of some land forcings, in particular crop intensification and irrigation (Mueller et al., 2016b;Thiery et al., 2017). As these local forcings are not represented and as their future changes are difficult to project, these can be significant caveats when using global warming scaling to project future changes for these regions.

The SR15 (SR15 Ch3) assessed different climate responses, including transient climate responses, short-term stabilization responses, and long-term equilibrium stabilization responses and their implications for future projections of different extremes. The use of different definition of responses can have profound effects on certain extremes such as sea level rise. This seems to be less a problem for extremes assessed in this chapter. For this reason, the assessment presented here is mainly based on transient responses.

11.3 Temperature extremes

11.3.1 Mechanisms and drivers

The SREX Ch3 and AR5 Ch10 concluded that greenhouse gas forcing is the dominant factorfor theincreases in warm extremes and a decrease in cold extremes, although many other factors also contribute to long-term changes and short-term variations in temperature extremes. These include land-atmosphere feedbacks, local and regional forcings such as land use change or changes in aerosol concentrations, and changes in large-scale circulations due to anthropogenic warming (Sections 11.1.5, 11.1.6).

The dominant driver of changes in temperature extremes is global warming associated with greenhouse gas forcing, and hence changes in regional extremes are observed over all land surfaces in the historical data record (11.3.2; 11.9), consistent with the observed global warming since that time period (Chapter 2). The magnitude of changes in extremes, e.g. the temperature of hottest days or coldest nights, are shown to increase more than GMST in several regions (e.g. Seneviratne et al., 2016, Wartenburger et al., 2017; IPCC SR15 Ch3). There are several reasons for this (11.1.4, 11.1.6, Box11.1): 1) the mean differential warming between land and ocean, with higher warming on land due to less potential for heat storage; 2) snow/ice-albedo-temperature feedbacks in high latitudes and mountainous regions, which lead to a high warming in regions/seasons with decreased snow/ice cover; 3) soil moisture-evapotranspiration-temperature feedbacks leading to an additional warming in dry seasons/locations on land (see also hereafter). In addition, the decrease of plant transpiration under enhanced CO_2 concentrations is a direct CO_2 forcing of land temperatures (warming due to lack of cooling), which contributes to higher warming on land (Lemordant et al., 2016). At the regional scale, changes in temperature extremes, in observations and CMIP5 models, tend to follow changes in local mean temperature, with little change in variability (Lewis and King, 2017; Li et al., 2018a), although most regions display changes in skewness towards the hotter part of the distribution (Donat and Alexander, 2012).

Warming at the global or regional scales may have a secondary impact on temperature-related extremes through large-scale circulation changes (Section 11.1.5). Extreme temperature events are associated with regional air mass excursions induced by circulation anomalies that are part of large-scale meteorological patterns (LSMPs) (North America: Grotjahn et al., 2016). This occurs directly through large-scale circulation that facilitates air mass excursions or alternatively the indirect modulation of variability, such as storm track behavior by blocking patterns. Quasi-stationary anticyclonic circulation anomalies or atmospheric blocking mechanisms are linked to extremes in many regions. Such large-scale circulation anomalies are also associated with temperature extremes in Australia (Parker et al., 2014), Europe (Schaller et al., 2018) and Asia (Ratnam et al., 2016). Mid-latitude planetary wave modulations affects short duration temperature extremes such as heatwaves (Perkins, 2015). Therefore, if circulation changes in response to warming, these changes would affect temperature extremes. As highlighted in Chapter 3, it is *likely* that there have been observational changes in storm tracks and blocking patterns, but there is *low confidence* in the attribution of these changes and the associated projections(Woollings et al., 2018,Chapters 4, 5). There is also *low confidence* in possible effects of Arctic warming on mid-latitude circulation (Section 11.1.5; Cross-chapter box 10.1). Hence, the literature is inconclusive at the moment regarding greenhouse gas effects on temperature extremes, that would be mediated through large-scale circulation changes.

Since AR5, the effect of multi-decadal climate variability on extremes has been examined and it is understood that aspects of global mean temperatures were decoupled from some characteristics of temperature extremes due to natural variabilities(Kamae et al., 2017b). The increase in temeperature extremes is detected during the hiatus period, that is the “slow down period” in 1998-2012 (Chapter 3) (Imada et al., 2017; Kamae et al., 2014; Seneviratne et al., 2014). . It is suggested that cold and warm extremes in mid-latitudes are associated with atmospheric circulation patterns including atmosphere-ocean coupled modes such as the Pacific Decadal Oscillation (PDO) and the Atlantic Multidecadal Oscillation (AMO) (Johnson et al., 2018; Kamae et al., 2014).

Feedback mechanisms, such as land-atmosphere feedbacks strongly modulate regional- and local-scale changes in temperature extremes (*high confidence*; Section 11.1.6; Seneviratne et al., 2013;Vogel et al., 2017;Donat et al., 2017). This effect is particularly notable in the mid-latitude regions where drying of soil moisture amplifies high temperatures (Douville et al., 2016; Whan et al., 2015). Douville et al., (2016)concluded based on a single-model study that drying-induced warming accounts for up to one third of the projected mean increase in daily maximum temperatures andabout half of the increase in the severity of heat waves over densely populated areas of the northern midlatitudesin the 21st century (*medium confidence*).Vogel et al., (2017)showed based on a multi-model study that the additional warming of hot extremes projected in several mid-latitude regions compared to mean global warming is due for the largest part to soil moisture-temperature feedbacks, i.e. the projected warming of land hot extremes would be roughly equivalent to global warming without this feedback mechanism. This soil moisture-temperature feedback was also shown to be relevant for present-day heatwaves based on observations and model simulations (Hirschi et al., 2011;Mueller and Seneviratne, 2012;Quesada et al., 2012;Miralles et al., 2014;Hauser et al., 2016).

Regional external forcings, such as land use changes or anthropogenic aerosols play an important role in the changes of temperature extreme at regional scale in several regions (*high confidence*), as highlighted in Section 11.1.6. Deforestation has been shown to have contributed about one third of the warming of hot extremes in some mid-latitude regions since pre-industrial time (Lejeune et al., 2018); there is *medium confidence* in these conclusions given the large spread of Earth System Models in representing the underlying processes, which requires model weighting based on observational evidence. Some aspects of agricultural management, including no-till farming, irrigation, and overall crop intensification are *likely* to cool hot temperature extremes, but these processes are generally not represented in the CMIP5 and on-going CMIP6 simulations (Section 11.1.6). On the other hand, it has been suggested that double cropping could have led to increased hot extremes in the inter-cropping season in part of China (Jeong et al., 2014). Rapid increases in summertime warming in western Europe and northeast Asia since the 1990s are also linked to a reduction in anthropogenic aerosols precursor emissions over Europe, which was a key factor in increases in temperature extremes (Tmax, Tmin, Txx, Tnx) in both regions (Dong et al., 2016, 2017) in addition to the effect of increased greenhouse gas forcing. This effect of aerosols on temperature-related extremes is also noted for declines in short-lived anthropogenic aerosol emissions over North America (Mascioli et al., 2016).

On local scale, the urban heat island effect also contributes to warming in cities, in addition to greenhouse gas forcing (e.g. RIZWAN et al., 2008;Imhoff et al., 2010; Peng et al., 2012;Zhao et al., 2014;Zhou et al., 2014b). These effects may be partially mitigated through the implementation of reflective surfaces or increased vegetation cover in cities, which could potentially reduce mean warming and hot extremes(Oleson et al., 2010;Li et al., 2014a;Seneviratne et al., 2018a).The urbanization may advance the timing of the onset of heat waves, and also make heat waves become more frequent, more intense and longer lasting (Herbel et al., 2018; Lin et al., 2018a; Luo and Lau, 2016). For the impacts of local land cover and land use change on temperature, is is*likely* that changes in agricultural land use in continental scale moderate hot temperature extremes in summer (Mueller and Seneviratne, 2014; Thiery et al., 2017).

Summary: There are multiple mechanisms underlying changes in extreme temperatures, with long-term changes being clearly attributable to greenhouse gas forcing and related to global warming. While the dominant driver of changes in temperature extremes is global warming (*high confidence*), in several regions amplified by soil moisture-evapotranspiration-temperature or snow/ice-albedo-temperature feedbacks (*high confidence*), the short-term behaviour of extremes can be modulated by natural variability or shorter-lived anthropogenic climate forcings, such as aerosols (*high confidence*). Also land use, either related to land cover change or agricultural management, can affect trends and short-term variations in extremes (*high confidence*). There is *high confidence* that changes in background global mean temperatures are the dominant driver of hot extremes, including through the strength of local- or regional-scale land-atmosphere feedbacks, or changes in circulation patterns. There is *high confidence* that in Asia and Europe, this effect has *likely* been enhanced by reductions in anthropogenic aerosols since the 1990s. There is *low confidence*in projections of characteristics of storm tracks, jets, and blockings, and their links to extreme temperatures in mid-latitudes.

11.3.2 Observed trends

The SREX Ch3 reported a*very likely* decrease in cold days and nights and increase in the number of warm days and nights at the global scale. Confidence in trends was assessed as regionally variable (*low to medium confidence*) due to either a lack of observations or varying signals in sub-regions.

Since the SREX and AR5, many regional-scale studies have examined trends in extremes of shorter-duration measures such as daily temperatures and ETCCDI indices in many locations, providing strengthened evidence for increased heat-related extremes. The magnitude of trends in temperature-related observed extremes varies depending on the region, spatial and temporal scales, and metric assessed. In particular, we note the importance of distinguishing trends in frequency and magnitude measures of temperature. Here we refer to percentile-based indices (e.g. TX90p) as frequency indicators and absolute measures (e.g. TXx) as magnitude indicators. Furthermore, as noted in 11.2, in most locations observational data is of a length that restricts the assessment of long-term trends in daily temperature extremes.

Alexander (2016) examined trends in temperature-related ETCCDI measures at the global scale over the period 1951-2014. Trends in the frequency of hottest days (TX90p) increased (from 10.5% days/year in 1951 to 15% days/ year in 2010), with larger decreases in the frequency of coldest nights (TN10p) (from 12% of nights in 1951 to about 6% of nights in 2014). Nearly all regions showed statistically significant decreases in TN10p, though trends in TX90p are variable with some decreases in the number of warm days in southern South America. An decrease in number of 5-day duration cold spells is also reported over nearly all land surface areas (Easterling et al., 2016). Consistent warming trends in temperature extremes globally and in most land areas over the past century are also found in a range of largely independent observations-based data sets(Donat et al., 2016b). Analysis of daily extremes and these indices demonstrate seasonal variations in trends in temperature-related extremes. Over the recent 1997-2010 period, a further increase in warm-season temperature extremes was determined over most land areas, despite constant or slight warming of global annual mean temperature (Seneviratne et al., 2014). Over that period, warm extreme trends were strongest in the warm season, with some cooling of warm extremes in the boreal winter recorded over a large fraction of the northern hemisphere mid- and high latitudes (see also Section 11.3.1).

Figure 11.1a shows the observed linear trend over 1951 to 2018 in the annual maximum daily maximum temperature (*TXx*) from the beta version of the HadEX3 dataset(Dunn et al., 2014). Figure 11.1b show this trend for the annual minimum daily minimum temperature (*TNn*). HadEX3 is a 2.5° latitude x 3.75 ° longitude gridded product obtained from the GHCN weather station data. Linear trends are calculated only for stations that have 66% of the daily data available over this 45-year period. Parts of South America, Asia, Australia and much of Africa are without adequate station measurements of daily temperature and are shown in grey.

[START FIGURE 11.1 HERE]

Figure 11.1: Linear trends over 1951-2018 in the annual maximum daily maximum temperature (TXx, 11.1a (left)) and the annual minimum daily minimum temperature (TNn, 11.1b (right)) from the beta version of the most recent HadEX3 data set. Units: °C/decade.

[END FIGURE 11.1 HERE]

Various studies report trends in particular regions or countries, with many regions displaying trends in temperature-related extremes consistent with global averages (for a detailed assessment see also Section 11.9).

In Australia, for example, HadEX2 observations show increase in the TXx, TNx, TXn, TNn, Tn90p and Tx90p, with decrease in Tn10p and Tx10p (Alexander and Arblaster, 2017). These changes also occur in the independent gridded AWAP datasets, although TNn values are lower and a decrease in TX10p is calculated. Similar results are observed in New Zealand with a positive trend in both the maximum and the minimum temperatures, in particular, in the autumn-winter seasons (Caloiero, 2017).

In Europe, an increase in the magnitude (e.g. value) and frequency (e.g. decrease in return time) of high maximum temperatures has been observed consistently across regions including in central (Christidis et al., 2015; Twardosz and Kossowska-Cezak, 2013) and southern Europe (Christidis et al., 2015; Croitoru and Piticar, 2013; El Kenawy et al., 2013; Fioravanti et al., 2016; Nastos and Kapsomenakis, 2015; Ruml et al., 2017). In Northern Europe, a strong increase in extreme winter warming events has been observed (Matthes et al., 2015; Vikhamar-Schuler et al., 2016).

In Africa, an increase in the frequency of warm days and nights, and a decrease in frequency of cold days and nights has been observed over almost the continent, where data are available (Donat et al., 2013b, 2014a; Filahi et al., 2016; Funk et al., 2016; Kruger and Sekele, 2013).

In Asia, changes in temperature extremes in China are consistent with warming since 1960, including, decreases in cold extremes and increases in warm extremes (Zhou et al., 2016). The warming in the coldest day and night is larger than the warmest day and night, respectively, which is concurrent with the coldest night larger than the coldest day and the warmest night larger than the warmest day. Changes in the number of the cold and warm nights are more substantial than the cold and warm days. Over the south Asian region (Bangladesh, India, Nepal, Pakistan and Sri Lanka), warm extremes have similarly become more common and cold extremes less common, although magnitude of warming varies (Sheikh et al., 2015).

In North America, there is substantial spatial and seasonal variation in trends in temperature extremes. Minimum temperatures display substantial warming across the continent, while there are more constrasted trends in the year maximum temperatures (Fig 11.1). In the US, some stations show a cooling in monthly maximum temperatures, although minimum temperatures show significant warming (Lee et al., 2014). The western United States, northern Midwest, and New England have experienced the largest increase in monthly temperatures. Grotjahn et al. (2015) examine changes in the US observed temperature over 1950–2007, calculating the change in 20-year return values (°C) of TXx, TXn, TNx and TNn. This provides further evidence that broadest region of warming occurs for the cold tail of minimum temperature, with cooling occurs in the upper tail of both daily maximum and minimum temperature in some parts of southeastern US. There is *medium confidence* that the lack of warming of hottest extremes is due to crop intensification, based on an analysis of Mueller et al., (2016b); Fig. 11.2; see also Sections 11.1.6 and 11.3.1). In addition, it is possible that irrigation also played a role in masking the warming of hot extremes in this region (Thiery et al., 2017).The spatial variation in trends across the US varies depending on the dataset, time period and temperature metric examined. For example, trends daily maximum temperature values greater than the 95th percentile over 1979–2014 in NLDAS-2 show that warm anomalies have generally increased, except for parts of the Intermountain West and the western Northern Plains in winter where a decreasing trend has occurred (Yu et al., 2018).

In South America, temperature-related extreme indices show spatially variable trends (Alexander, 2016; Donat et al., 2016b; Meseguer-Ruiz et al., 2018). For example, of 47 stations covering most of the Brazilian Amazon, minimum and maximum average annual temperatures show an increasing trend of approximately 0.04°C/year, with just a few stations recording no significant trends (Almeida et al., 2017). Extreme temperatures of 77 stations in Chile showed general warming trends but with particular differences depending on the behaviour of minimum temperaturesover the period of 1966 – 2015 (Meseguer-Ruiz et al., 2018). However, a decrease in TXx by about 0.3 °C/decade is reported over southeastern South America in HadEX2 over 1955–2005 (Wu and Polvani, 2017).

[START FIGURE 11.2 HERE]

Figure 11.2: Centennial trend towards cooler daily maximum temperatures during the summer in the US Midwest: a) 95th percentile Tx trends (C°/decade), b) 50th percentile Tx trend (°C/decade), c) 5th percentile Tx trend (°C/decade); d) peak rates of summer chlorophyll fluorescence, a measure of plant activity. (from (Mueller et al., 2016b).

[END FIGURE 11.2 HERE]

Trends in some measures of heatwaves are also observed at the globalscale. Globally averaged heatwave intensity, duration, and the number of heatwave days have increased from 1950-2011 (Perkins 2015). There are some regional differences in trends in characteristics of heatwave with significant increases reported in Europe and Australia, though decreases in Excess Heat Factor (EHF) are observed in South America in data derived from HadGHCND.

Trends in some locations are also sensitive to the time period examined, or the heatwave metric analysed. The majority of heatwave characteristics examined of China between 1961-2014 shows negative/positive trends of HW days before/after 1990 over the whole of China, which reflects rapid warming since 1990 (You et al., 2016) and *likely* possible effects from aerosol forcing (11.1.6, 11.3.1). In the UK, positive trends in numbers and lengths of heat waves were identified at most of 27 stations examined. However, for some stations in the south east of England, lengths of very long heat waves (over 10 days) had declined since the 1970s, whereas the lengths of shorter heat waves had increased (Sanderson et al., 2017b). Also recent evidence suggests with *medium confidence* (study based on multi-model evidence and observational constraints) that deforestation has contributed about 1/3 of warming of hot extremes in some mid-latitude regions, with strongest relative effects compared to greenhouse gas forcing up to ca. 1980 (Lejeune et al., 2018; see also 11.1.6, 11.3.1).

Studies since SREX and AR5 have also focused on trends in marine heatwaves. In water off eastern Tasmania, Australia, trends in six marine heatwave characteristics (duration, Maximum intensity, Cumulative intensity, Onset rate, Decline rate, Depth) were calculated over 1993-2015. Trends in marine heatwave frequency were positive in nearly every sub-region examined, and annual marine heatwave days and penetration depths indicate significant positive changes (Oliver et al., 2018a). Using satellite observations from 1982-2016, global mean trends in the maximum annual intensity and annual spatial extent of marine heatwaves were recorded (Frölicher et al., 2018). While marine heatwaves have been reported and examined off Alaska, Western Australia, and in the Mediterranean, no other systematic analyses have been conducted on marine heatwaves. More detailed assessments on changes in marine heatwaves and other marine extremes are provided in the Cross-Chapter Box 9.1.

Summary: It is *virtually certain* that there has been a global-scale increase in the number of warm days and nights. It is *virtually certain* that there has been a global-scale decrease in the number of cold days and nights. It is *very likely* these changes in both warm and cold extremes have also occurred over Europe, Australasia, and Asia, where data are available. It is *very likely* that there has been a global-scale increase in the intensity, duration, and the number of heatwave days. These trends occur in Europe, Asia and Australia. It is *likely* that marine heatwave frequency and intensity has increased at the global scale. There is *medium confidence* in trends in temperature-related extremes in southern Africa and South America due to reduced data availability and fewer studies. However, changes in both mean temperatures and extremes in these regions are consistent with those occurring over other land surface.

11.3.3 Model evaluation

AR5 assessed that CMIP5 models generally capture observed spatial distributions of the mean state during 1986-2005, and trends in the second half of the 20th century for indices of extreme temperature (AR5 WG1 9.5.4.1). The CMIP5 modelled trends were consistent with both reanalyses and station-based estimates, with ensemble simulations outperforming individual model realisations. CMIP5 multi-model ensembles also simulate present-day warm extremes (in terms of 20-year return values), reasonably well, with errors typically within a few degrees Celsius over most of the globe (AR5 WG1 9.5.4.1).

Since AR5, an increasing number of studies has been performed to evaluate the performance of CMIP5 models in simulating temperature extremes at regional scales and local scales. Validation of models depends on the metric assessed (e.g. change in mean or variability of extremes, spatial distribution, trends of past change), and no single metric is universally insightful about model performance.

Overall, the characteristics of changes in global-scale temperature extremes arecaptured by CMIP5 models, but with varying performance on regional scale, in some regions displaying a good representation of specific features but in some others also some quantitative biases (though good overall qualitative representation), either in terms of spatial features or trends over certain time periods.

Over East Asia, the CMIP5 GCM models are able to simulate the climatologically spatial distribution of the observed extreme temperature indices over China during 1986-2005, with the ensemble performing better than individual models and the ensemble simulated threshold indices better than percentile indices (Dong et al., 2015; Sun et al., 2016; Yang et al., 2014; Zhou et al., 2014). Over North America, CMIP5 model skill in capturing observed ETCCDI metrics over the period 1979-2005 was highest in spring, compared to winter, then summer and autumn (Grotjahn et al., 2016).

In terms of historical trends, the models' ability in capturing observed trends in temperature-related extremes depends on metric evaluated, the time period considered and how indices are calculated within models. Observed trends in global temperature extremes lie within the spread of simulated trends in CMIP5, with better consistency for the longer period considered. However, a systematic overestimation of the warming of hot extremes compared to local mean warming is identified in many land regions, in particular over Europe, North America, South America, and parts of Southern Africa, for a comparison between the late 20th/early 21st century (1981-2010) vs the mid-20th century (1951-1980) (Donat et al., 2017). This systematic bias is also consistent with an identification of overestimated mean June-July-August temperatures in many mid-latitude land regions in the CMIP5 GCMs, which also present a concomitant overestimation of dryness conditions (underestimated precipitation and evapotranspiration) in these regions (Mueller and Seneviratne, 2014). For the recent 15 years, there is a discrepancy between observed and simulated trends in global mean surface temperature due to the so-called hiatus (Fyfe et al., 2016; Karl et al., 2015; Santer et al., 2017), but this observation-model discrepancy does not generally extend to temperature extremes (Sillmann et al., 2014). The observed warming trends in hot extremes (TXx) during this time period are well represented in CMIP5 simulations(Sillmann et al., 2014). Trends in cold extremes (TNn) are less well represented in CMIP5 simulations, but the simulated trends are nevertheless consistent with observed trends globally and in many regions (Sillmann et al., 2014). Although the multi-model mean averaged over regions may be relatively small, the range of model differences in trends is large. The largest discrepancy between observed and simulated trends in cold extremes is found in the Northern mid-latitudes, where observed cold extremes indicate a coherent zonal band of cooling trend over the recent 15 years (Sillmann et al., 2014). This discrepancy may suggest the influence of interannual variability and spatial and temporal scale. Some external forcing components not fully represented in current climate models may also have contributed to the local cooling trends in cold extremes (England et al., 2014; Fyfe and Gillett, 2014; Meehl, Gerald A et al., 2013; Sillmann et al., 2014).

Regionally, over East Asia, the CMIP5 ensemble performs well in reproducing the observational trend of temperature extremes averaged over China during 1961-2005 (Dong et al., 2015). Over Australia, the multi-model mean performs better than individual models in capturing observed trends in ETCCDI temperature measures in gridded observational datasets, with some individual models showing stronger or weaker than observed trends in temperature indices (Alexander and Arblaster, 2017). Over Europe, North America, South America, and parts of Southern Africa, as mentioned, CMIP5 models simulate an accelerated warming rates in TXx relative to annual average warming rates, which appears inconsistent with observations except over Europe, which may be due to relevant terrestrial processes (Donat et al., 2017). In particular, the lack of representation of agricultural management, including crop intensification or irrigation (11.3.2) may explain some of these discrepancies.

[PLACEHOLDER FOR SOD: CMIP6 update for mean and trends]

AMIP or SST-forced simulations are also used to assess the characteristics of temperature-related extremes (e.g. trends, heatwaves etc.). The observed trends in temperature extremes are generally well captured by the SST-forced simulations although some regional features such as the lack of warming in daytime warm temperature extremes over South America are not reproduced in the model simulations (Dittus et al., 2018). The dynamics of heat-wave events over central-eastern China are well reproduced by the AMIP models. However, the AMIP models assessed tend to produce too-persistent heat-wave events (lasting more than 20 days). The bias in the duration of the events does not impact the reliability of the models' positive trends, which is mainly controlled by the changes in mean temperatures (Freychet et al., 2018; Wang et al., 2018a).

Several regional climate models (RCMs) have also been evaluated in terms of their performances in simulating the climatology of extremes in various CORDEX regions, especially in East Asia (Bucchignani et al., 2017; Gao et al., 2017; Hui et al., 2018; Ji and Kang, 2015; Niu et al., 2018; Park et al., 2016; Shi et al., 2017; Wang et al., 2018a; Yu et al., 2015; Zhu et al., 2018), Europe (Cardoso et al., 2019; Kotlarski et al., 2014; Ruti et al., 2016) and Africa (Diallo et al., 2015; Dosio et al., 2015). Compared to global climate models, RCM simulations show a substantial improvement in simulating temperature-related extremes, though this depends on topographical complexity. This improvement with resolution is noted in East Asia (Hui et al., 2018; Park et al., 2016; Shi et al., 2017). However, there are key cold deficiencies in temperature extremes over areas with complex topography (Niu et al., 2018). Over North America, 12 RCMs were evaluated over the ARCTIC-CORDEX region (Diaconescu et al., 2018). Models were able to simulate well climate indices related to mean air temperature and hot extremes over most of the Canadian Arctic, with the exception of the Yukon region where models displayed the largest biases related to topographic effects. Two RCMs were evaluated against observed extremes indices over North America over the period 1989–2009, with a cool bias in minimum temperature extremes in both RCMs shown (Whan and Zwiers, 2016). The most significant biases are found in TXx and TNn, with fewer differences in the simulation of TXn and TNx in central and western North America.

Summary: There is *high confidence* that climate models can represent the overall warming observed globally and in most regions, although the magnitude of the trends may differ. The ability of models to capture observed trends in temperature-related extremes depends on the metric evaluated, how indices are calculated within models, and the temporal and spatial periods considered (*high confidence*).

11.3.4 Detection and attribution, event attribution

The SREX Ch3 assessed that it is *likely* that anthropogenic influences have led to warming of extreme daily minimum and maximum temperatures at the global scale. AR5 concluded that human influence has *very likely* contributed to the observed changes in the frequency and intensity of daily temperature extremes on the global scale in the second half of the 20th century. These assessments are largely based on the analyses of changes in extreme daily temperatures, as studies on changes in temperature extremes of longer-time scale such as extreme monthly or seasonal temperatures were limited at the time of assessments.With regard to individual, or regionally- or locally-specific events, AR5 concluded that it is *likely* that human influence has substantially increased the probability of occurrence of heat waves in some locations, in addition to natural weather variability contributing to the overall magnitude of heatwave events.

There is more recentliterature on human influence onlong-term changes in frequency or intensity of global-sclae, continental-scale, and sometimes regional-scaleextreme temperatures of shorter duration. Focusing on measures of warmest days and warmest nights, Kim et al. (2016)compared changes in the HadEX2 datasets with those simulated by the CMIP5 models for 1951-2010using the optimal fingerprinting method. Results confirm previous HadEX/CMIP3-based results, where an anthropogenic signal is detected through optimal fingerprinting at global and continental scales.Wang et al., (2017e)fitted the observed daily extreme temperatures to generalized extreme value distribution with model simulated responses as predictors, their results are similar to those of Kim et al., (2016). Fischer and Knutti(2015) quantify that as much as 75% of the moderate daily hot extremes over land are attributable to anthropogenic warming. Wan et al. (2018)and Wen et al. (2013)separately attributed observed increases in extreme hot temperatures to anthropogenic influence in Canada and China, respectively. Anthropogenic signals are robustly detected in the changes in the mean of extreme daily temperatures at the global and continental scales. The detected anthropogenic signals are clearly separable from the response to natural forcing, and results are generally insensitive to the use of different model samples as well as different data availability. In general, climate models accurately simulate the observed changes in the warmest night-time temperatures, overestimated changes in the hottest day tempertures and underestimate the changes in the coldest temperatures (e.g., Dong et al., 2018; Kim et al., 2016). Some of the overestimation in the observed changes of hottest day tempertaure may be due to lack of representation of some land forcings, in particular crop intensification and irrigation (Mueller et al., 2016b;Thiery et al., 2017).

Long-term changes in various othertemperature-related indices, including the percentage of days when daily temperature is above its 90^{th} percentile or below its 10^{th} percentile in various regions have also been attributed to anthropogenic influence. Regions include Asia (Dong et al., 2018), Australia (Alexander and Arblaster, 2017), and Europe (Christidis and Stott, 2016). Studies also find attributable trends in multi-day heat indices such as Warm Spell Duration Index (WSDI). For example, Christidis et al. (2016) found a detectable increase in WSDI in Europe of the previous two decades. At the continental scale, anthropogenic increases in WSDI are detectable (Lu et al., 2018). Using an index that combines multiple ETCCDI indices (Combined Extreme Index, CEI), a clear anthropogenic signal is found in the trends in the maximum and minimum temperature index components for North America, Asia, Australia and Europe. While studies have described increasing trends in various heatwave metrics (HWD, HWA, EHF etc) in different global regions, few recent studies have explicitly attributed these changes and rather stated that observed trends are consistent with anthropogenic warming.

There are also studies examining the rate at which new high-temperature records are observed. Studies of monthly, seasonal and annual records in various regions (Bador et al., 2016; Kendon, 2014; Lewis and King, 2015) and globally (King, 2017) show an increase in hot record breaking. For global-scale records, an anthropogenic influence on rate of record-breaking was detected in CMIP5 simulations as far back as 1930s (King, 2017). Changes in anthropogenically attributable record breaking rates are noted to be largest over Northern Hemisphere land surfaces (Shiogama et al., 2016).

Long-term changes of cold extremes on various timescales have also been examined. King (2017) found a decreased likelihood in the occurrence of cold extremes due to anthropogenic forcings. Focusing on the rate of cold record-breaking, this study showed that it was harder to attribute cold extremes to a particular cause due to the rarity of the occurrence of new records. Christidis and Stott (2016) found that a human influence could be detected in cold nights on a global scale, but changes in the cold extremes were not detected in Europe, providing different results to SREX where *likely* decreases in cold nights were reported (Table 3-2). Furthermore, no attributable signal was detected for the cold indices FD and ID (frost and icing days). This study was based on simulations by two climate models, however Yin and Sun (2018) found clear evidence of an anthropogenic signal when multiple model simulations were used. In some key wheat-producing regions of southern Australian, increases in frost days or frost season length have been reported (Crimp et al., 2016; Dittus, Karoly, Lewis, & Alexander, 2014). The increase in frost days or season-length in southern (east and west) Australia is linked to decreases in rainfall, cloud-cover and subtropical ridge strength, despite an overall increase in regional mean temperatures (Dittus et al., 2014; Crimp et al., 2016).

There are a large number of studies focusing on extreme temperature events, using various extreme event attribution methods. Using a combination of observations and 30 realisations of a single model, Diffenbaugh et al. (2017) examined the anthropogenic contribution to observed changes in the hottest day and hottest month. Anthropogenic warming was found to have increased the severity and probability of the hottest month at >80% of the available observational area. Similarly, Christidis and Stott (2014) examined how anthropogenic forcings changed the odds of warm years, summers, or winters in a number of regions using an attribution framework where two different types of ensembles of simulations are generated with an atmospheric model to represent the actual climate and what the climate would have been in the absence of human influences. In all cases, warm events become more probable because of anthropogenic forcings. Mueller et al. (2016a) compared mean summer temperatures between observations and simulations for different regions and found anthropogenic influence in most of the land regions they analyzed. They infer large increases in the probability of historical hottest summers over many regions. Li et al. (2017) focused on the change of wet-bulb globe temperature (WBGT) that measures environmental conditions related to heat stress in northern hemispheric land areas. They estimate that the probability of summer mean WGBT exceeding the highest recorded value in the observational history has increased by a factor of at least 70 at regional scales due to anthropogenic influence. In most regions of the NH, the likelihood changes of extreme summer average WBGT were found to be about an order of magnitude larger than the likelihood changes of extreme hot summers estimated by surface air temperature. In addition to these generalised, global-scale approach, extreme event studies have found an attributable increase in the likelihood of hot annual and seasonal temperatures in many locations, including Australia (Knutson et al., 2014; Lewis and Karoly, 2014b), China (Sun et al., 2014) and Europe (King et al., 2015).

There have also been many extreme event attribution studies that have examined short duration temperature extremes (daily temperatures, temperature indices, heatwave metrics). Examples of these events from different regions are summarised in various annual Explaining Extreme Events supplements of the Bulletin of the American Meteorological Society (Herring et al., 2014, 2015, 2016, 2018; Peterson et al. 2012, 2013), including in the number of approaches to examining extreme events (described in Easterling et al., 2016; Otto, 2017; Stott et al., 2016). Several studies of recent events from 2016 onwards have determined an infinite risk ratio (FAR of 1), indicating that the occurance probability for such events is close to zero in model simulations without anthropogenic influences (see Herring et al., 2018). However, caution should be exercised in this intrepretation if rigorous uncertainty quantification techniques have not been applied (Paciorek et al. 2018).

Further studies have focused on the attributable signal in observed cold extreme events, producing complex results. Individual attribution studies on the extremely cold winter in Europe of 2011 find a decreasing likelihood (BAMS EEE 2012). On small spatial scales, the role of natural variability and dynamical responses to anthropogenic warming have been identified as important and have been examined in event attribution studies. Several studies of extreme cold conditions occurring in eastern US during 2014 and 2015 demonstrate that winter climate variability is decreasing due to anthropogenic influences and observed extreme cold spells are less probable due to climate change (Bellprat et al., 2016; Trenary et al., 2015, 2016; Wolter et al., 2015). These studies determined that extreme cold was caused largely by internal natural variability.A similar attributable reduction in likelihood of cold was found in the cold spring of 2013 occurring in the United Kingdom (Christidis et al., 2014) and eastern China in 2016 (Qian et al., 2018; Sun et al., 2018b).

The interpretation of difference in the results from temperature event attribution analyses need to be placed in proper context as different framing may lead to different results. The temperature event definition itself plays a crucial role in the attributable signal (Fischer and Knutti, 2015). Large-scale, longer duration events tend to have notably larger attributable risk ratios (Angélil et al., 2014, 2018; Harrington, 2017; Uhe et al., 2016), as the anthropogenic signal is large in comparison to natural variability. While uncertainty in the best estimates of risk ratio may be significant, the lower bounds can be quite insensitive to uncertainties in observations or model description thus increasing confidence in conservative attribution statements (Jeon et al, 2016). The relative strength of anthropogenic influences on temperature extremes is regionally variable, in part due to differences in changes in atmospheric circulation, land surface feedbacks and other external drivers like aerosols. For example, in the Mediterranean risk ratios of the order of a 100 have been found (Kew et al., accepted, BAMS 2018) whereas in the US changes are much less pronounced. This is probably an artifact of the land-surface feedback enhanced extreme 1930s temperatures that reduce the rarity of recent extremes, in addition to the definition of the events and framing of attribution analyses (e.g. spatial and temporal scales considered). In India, heatwave likelihoods are not changing (van Oldenborgh et al., 2018) or even decreasing in some parts while increasing in others (Wehner et al., 2016). In this region, short-lived aerosols or increase in irrigation may be masking the warming effect of greenhouse gases (Wehner et al., 2018c). More generally, irrigation and crop intensification have been shown to lead to a cooling in some regions, in particular in North America, Europe and India (Mueller et al., 2016b;Thiery et al., 2017; see also 11.1.6, 11.3.2) (*high confidence*), although these effects are not represented in the CMIP5 or CMIP6 GCMs. There is also evidence that several models represent the effects of deforestation on temperature extremes with a wrong sign (cooling instead of warming, Lejeune et al., 2017), although there is *medium confidence* that deforestation has contributed about 1/3 of the total warming of hot extremes in some mid-latitude regions since pre-industrial times (Lejeune et al., 2018). Despite all these differences, and larger uncertainties at regional scale, nearly all studies demonstrated that human influence has contributed to the increase in the frequency or magnitude of hot extremes and to decrease in the frequency or severity of cold extremes.

***Summary:* Since the AR5, evidence isincreasing for human influences on various temperature extremes. Long-term changes in various aspects of long and short-duration extreme temperatures, including intensity, frequency, duration and other relevant characteristics have been detected in observations and attributed to human influence at global and continental scales. Studies on the attribution of single extreme temperature events – which there were relatively few at the time of the AR5 assessment, point to human influence on recent extreme heat-related events – regardless of various methods, framing, definitions of events, and in different regions, all. We conclude that it is *virtually certain* that anthropogenic increases in greenhouse gases have caused increases in the likelihood and/or magnitude of observed heat extremes (annual, seasonal, daily, heatwaves) and**

decreases in the frequency and/or severity of cold extremes across nearly land areas. Although these changes are generally dominant at regional scale, they can be masked or counteracted, and in some cases amplified, in a few locations by natural variability or forcings, or other anthropogenic forcing factors. In particular, human-induced irrigation and crop expansion may have attenuated summer hot extremes in some regions, while deforestation may have contributed to the warming of hot extremes in some mid-latitude regions since pre-industrial time (*medium confidence*)

11.3.5 Projections

The AR5 concluded that it is *virtually certain* that there would be more frequent hot extremes and fewer cold temperature extremes at global scale and over most land areas in a future warmer climate and it is *very likely* that heat waves would occur with a higher frequency and duration. More recently, the SR15 Ch3 provided a more specific assessment regarding projected changes in hot extremes at 1.5°C vs 2°C global warming. It came to consistent conclusions, assessing that it is *very likely* that a global warming of 2°C versus 1.5°C would lead to more frequent and more intense hot extremes on land, as well as to longer warm spells, affecting many densely inhabited regions. It also assessed that it is *very likely* that the strongest increases in the frequency of hot extremes are projected for the rarest events, while cold extremes would become less intense and less frequent, and cold spells would be shorter.

The available studies since the AR5 and SR15 using either Global Climate Model (GCM) or Regional Climate Model (RCM)simulations provide more specific information on future projections of extreme temperatures and generally confirm the conclusions of the AR5 and SR15. Compared to AR5, important literature updates include projections of temperature-related extremes relative to mean changes in global warming, analyses of CMIP6 projections (still on-going and to be updated in the SOD), analyses of existing projections based on global mean stabilization targets, and examined new metrics. The forced response pattern of hot extremes in RCP8.5 simulations over the period 2006-2100 show the greatest intensification over mid-latitudinal land regions and overall warming of the hottest days that substantially exceeds the global mean temperature change (Fischer et al., 2014; Seneviratne et al., 2016). Following the approach used in the IPCC SR15 report, which is based on the sampling of responses at given global warming levels from transient simulations (see also Section 11.2 for details), we also provide here projections of changes in temperature extremes at different global warming levels, based on the CMIP5 simulations (Figs. 11.3 and 11.4). Updates based on CMIP6 simulations will be provided in the SOD. Figures 11.3 and 11.4 confirm that 1) there are already substantial increases in the temperature of hot and cold extremes at 1.5°C global warming, 2) that projected changes in 2°C are substantially larger than at 1.5°C in several regions, and 3) that a warming of temperature extremes of 5°C or more is already reached at 3°C global warming in several regions. As identified in previous analyses, hot spots of warming include mid-latitude and subtropical regions for hot extremes, and the Arctic for cold extremes.

[START FIGURE 11.3 HERE]

Figure 11.3: Projected changes in temperature of annual hottest daytime temperature (TXx) for projections at 1.5°C, 2°C, 3°C and 4°C of global warming compared to pre-industrial conditions (1851-1900), using empirical scaling relationship based on transient CMIP5 simulations. Cross-hatching highlights areas where at least two-thirds of the models agree on the sign of change as a measure of robustness.

[END FIGURE 11.3 HERE]

[START FIGURE 11.4 HERE]

Figure 11.4: Projected changes in temperature of annual coldest night-time temperature (TNn) for projections at 1.5°C, 2°C, 3°C and 4°C of global warming compared to pre-industrial conditions (1851-1900), using empirical scaling relationship based on transient CMIP5 simulations.Cross-hatching highlights areas where at least two-thirds of the models agree on the sign of change as a measure of robustness

[END FIGURE 11.4 HERE]

Figures 11.5 and 11.6 showschangesin the annual hottest daytime temperature (TXx) and the annual coldest night-time temperature (TNn) as function of global warming. Overall, the warming of temperature extremes tend to scale linearly with global warming (Seneviratne et al., 2016, Wartenburger et al., 2017; see also IPCC SR15, Ch3), but with a stronger warming on land. Regions and seasons of strongest warming include – as highlighted above and in the SR15 Ch3 – the mid-latitude summer, with warming in hot extremes that is up to double that of GMST (Fig. 11.5), and the Arctic winter, with the warming of the temperature of the coldest nights being up to 3 times the warming of GMST (Fig. 11.6).Figure 11.7 provides for comparison the scaling of the regional changes in mean temperature as function of global warming. From comparison of Figs. 11.5 and 11.6 with 11.7, it can be seen that projected changes in temperature extremes can deviate substantially from projected changes in mean warming in the same regions, showing that additional processes control the response of extremes in several regions as for instance highlighted in Orlowsky and Seneviratne (2012). As discussed in Section 11.1.6, these include in particular soil moisture-evapotranspiration-temperature feedbacks for hot extremes in mid-latitude and subtropical regions, and snow/ice-albedo-temperature feedbacks in high-latitude regions.

Despite the quasi-linear scaling of changes in the magnitude of temperature extremes as function of global warming, when assessing changes in the probability exceeding a certain hot extreme thresholdfor different global warming levels, projections tend to show on the other hand an exponential increase as a function of global warming (e.g. Fischer and Knutti, 2015, Kharin et al., 2018). Such nonlinearities in the characteristics of future regional extremes are shown, for instance, for Europe (Seneviratne et al., 2018; Dosio and Fischer, 2018), Asia (Harrington and Otto, 2018b; King et al., 2018) and Australia (Lewis et al., 2017a) under various global mean warming thresholds. The non-linear increase of fixed-threshold indices (e.g. percentile-based for a given reference period or based on an absolute threshold) as a function of global warming is consistent with a linear warming of the absolute temperature of the temperature extremes (e.g. Whan et al., 2015, WACE). Studies of projections of future temperature-related extremes under warming of 1.5˚C and 2˚C above pre-industrial values have also occurred at the regional and country-level, and for various heat metrics. For example, the number of marine heatwave days is projected to further increase on average by a factor of 16 for global warming of 1.5˚C above preindustrial levels and by a factor of 23 for 2.0˚C (Frölicher et al., 2018). At 3.5˚C of warming, marine heatwaves have an average spatial extent that is 21 times bigger than in preindustrial times. In some locations, models simulate substantially greater warming than is expected from linear scaling between global warming thresholds.

Several studies of future projections of observed hottest summer temperatures demonstrate decreases in the return times, i.e. a higher frequency, of such events (Lewis et al., 2017b; Mueller et al., 2016a). Tebaldi and Wehner (2018) analysed RCP4.5 and RCP8.5 projections from the CESM large ensemble (Kay et al., 2015a) of 20 year return values of both TXx and the running 3 day average of the daily maximum temperature (or TX3x). At the middle of the 21st century, 66% of the land surface area would experience present day 20-year return values every other year on average under the RCP8.5 scenario as opposed to only 34% under RCP4.5. By the end of the century these area fractions increase to 89% and 73% respectively. While long period return values of TX3x are slightly lower than for TXx, the relative changes are larger and more robust. These results further demonstrate that projections of temperature extremes are dependent on the metrics analysed and details of the definition of extreme temperatures.

Projections of temperature-related extremes in RCMs in CORDEX regions demonstrate robust increases in future scenarios and can provide information on finer spatial scales than GCMs. Five RCMs in the CORDEX-East Asia region show projected decreases in the 20 year return of temperature extremes (summer maxima), with models exhibiting warm biases projecting stronger warming (Park and Min, 2018). Similarly in the African domain, future increases in warm days (Tx90p) and nights (Tn90p) are projected (Dosio, 2017). This regional-scale analysis provides fine scale information, such as distinguishing increase in Tx90p over sub equatorial Africa (Democratic Republic of Congo, Angola and Zambia), with values over the gulf of Guinea, Central African Republic, South Sudan and Ethiopia.

As for the projected changes of extremes in 20-year return under stabilization targets, Wehner et al. (2018)analyzed five of the HAPPI atmosphere-only models and Sanderson et al., (2017a)analyzed an extension of the CESM large ensemble at these targets. Averaging the results of these two studies, the global land average of the 20-year return values of TX3x increases about the same as the global land average warm season (summer) temperatures. These amounts are about 0.3-0.4˚C larger than the targeted global average stabilized warming reflecting that land warms more than oceans as greenhouse gas concentrations are increased. There are significant differences in the occurrence and intensity of heat extremes under warming of 1.5˚C and 2˚C above pre-industrial values. Changes in nearly all heat extremes have a strong correlation to global mean temperature, so that scenarios and times with greater temperature change experience greater index changes for many regions (Aerenson et al., 2018)**.**

[START FIGURE 11.5 HERE]

Figure 11.5: Projected regional changes in temperature of annual hottest daytime temperature (TXx) compared to pre-industrial conditions (1850-1900) as function of mean global warming, using empirical scaling relationship based on transient CMIP5 simulations. Analyses for 37 AR6 regions, the global ocean and the global land.

[END FIGURE 11.5 HERE]

[START FIGURE 11.6 HERE]

Figure 11.6: Projected regional changes in temperature of annual coldest nighttime temperature (TNn) compared to pre-industrial conditions (1850-1900) as function of mean global warming, using empirical scaling relationship based on transient CMIP5 simulations. Analyses for 37 AR6 regions, the global ocean and the global land.

[END FIGURE 11.6 HERE]

[START FIGURE 11.7 HERE]

Figure 11.7: Projected changes in regional mean warming (Tmean) compared to pre-industrial conditions (1850-1900) as function of mean global warming, using empirical scaling relationship based on transient CMIP5 simulations. Analyses for 37 AR6 regions, the global ocean and the global land.

[END FIGURE 11.7 HERE]

[PLACEHOLDER FIGURE: AR5, Fig. 12.14]. 20-year return values for CMIP6 and for HighResMIP (there may be a difference in high altitudes.) Subtract out the appropriate seasonal mean change in a separate set of figures. Adapt for global warming levels (i.e. projections at 1.5°C, 2°C and 3°C global warming). Cite Kharin et al 2013 and Kharin et al. 2018.

Refer in text above

Summary: Climate models project substantial warming in maximum and minimum temperatures at the global scale due to changes in mean temperature, with some impacts from changes in the tails of distributions. It is *virtually certain* that increases in the magnitude of warm days and nights and decreases in the cold days and nights will occur through the 21st century at the global and continental scale. It is *virtually certain* that the length, frequency, and/or intensity of warm spells or heat waves (defined with respect to present regional climate) will increase over most land areas. Confidence in assessments depends on spatial and temporal scale of the extreme in question, with *high confidence* inprojections of temperature-related extremes at global and continental-scale for daily to seasonal-scales. There is *high confidence* that the magnitude of temperature extremes increases more strongly

on land than global mean temperature. This includes a projected warming of extreme hot daytime temperatures up to twice larger than global warming in mid-latitudes, i.e. about +3°C at +1.5°C global warming and about +8°C at +4°C global warming (*medium confidence*). The warming of extreme of cold night-time temperatures in the Arctic, in several northern high-latituderegions, and some mid-latitude regions.is additionally projected to be about three times larger than the warming of global mean temperature, i.e. about +4.5°C at +1.5°C global warming, and about +12°C at +4°C global warming (*medium confidence*). Changes in the intensity of temperature extremes at higher global warming levels are approximately linear (*high confidence*). There is *high confidence* that the frequency of hot and cold days, e.g. the number of hot days, does not respond linearly to levels of global mean warming, unlike their magnitude, which is a statistical property of exceedence frequencies above a given threshold in the presence of a mean warming and does not necessarily imply a stronger warming of temperature extremes.

11.4 Heavy precipitation

Definitions of extreme precipitation vary greatly throughout the literature, but most of available studies are based on precipitation accumulated over a short period of time, typically 5 days or one day. There is relatively limited literature on extreme precipitation for longer time periods, or for shorter duration at sub-daily scale. Most of the available studies have focused on long-term changes (trends) in the annual maximum 1-day or 5-day precipitation, while some studies have also examined changes in more extreme events such as those that occur once-in-20-year, in particular in model projections. Yet, some studies have also examined the proportion of annual total precipitation contributed by heavy precipitation events (defined as the top 5% or rarer daily precipitation events). The available literature limits the scope and type of extreme precipitation to be assessed in this section. Information on extreme precipitation for durations longer than a few days or shorter than a day is lacking in particular.

11.4.1 Mechanisms and drivers

SREX Ch3 assessed that the changes in heavy precipitation are associated with thermodynamic and dynamic changes (see also Box 11.1).The thermodynamic contribution mostly followsthe Clausius-Clapeyron relationship and is generally responsible for increase in heavy precipitation where the changes in circulation is low. However, this simplification does not apply in regions with significant changes in circulation patterns, such as mid to higher latitudes and tropics, where the dynamics of moisture supply from remote sources dominate. Further background on these processes is provided in Box 11.1.See also Chapter 8 for hydrological changes associated with monsoons.

Monsoon circulations are affected by both processes (Chapter 8). The tropical overturning circulation tends to be weaker with warming. The projected changes in the land-ocean heat contrast lead to changes in monsoon circulation patterns due to dynamical processes, with complicated effect on precipitation. The associated precipitation may be amplified under future global warming in some regions(Seth et al., 2019). There may be more precipitations over the rainy regions of the monsoon circulations both over land and ocean, and drier over in-land areas(Sherwood and Fu, 2014;Byrne and O'Gorman, 2015).

Changes in large-scale circulation patterns are associated with changes in SST distribution and land-ocean contrast (Chap 6 of SROCC). Changes in SST distribution modulate mean and variability of precipitation , such as affected by ENSO cycle (Watanabe et al. 2014) and by changes in monsoon circulations (Luong et al., 2017; Osakada and Nakakita, 2018). The changes in SST distribution modulate TC activities including distributions of genesis and intensification (see section 11.7.1) and then affects extreme precipitation due to TCs (Kitoh and Endo, 2019). Changes in the land-ocean contrast affects changes in monsoons in various regions (Chapter 8), hence leading to changes in heavy precipitation. Asian monsoon changes generally project increase in precipitation in the coastal regions of the East and South Asia (Freychet et al., 2015; Kitoh, 2017; Lee et al., 2018). For example, it is *likely* that SST is projected to increase more near the coast of the continents, and that this pattern of changes in SST might cause heavier rainfalls near the coastal areas in the East Asia via tropical cyclones (Mei and Xie, 2016) or the torrential areas over western Japan (Manda et al., 2014). Low-level monsoon westerlies with moisture surge towards Indian subcontinent is associated with the warming of Western Indian Ocean and this *likely* leads increase in the occurrences of precipitation extremes over the Central India (Roxy et al., 2017). Although there are a lot of studies showing enhances of extreme precipitations in various monsoon regions in observations and projections, it is *low-to-medium confidence* that the anthropogenic forcings contributed the enhancement of extreme precipitation in local scale. The changes in precipitation in dry inland areas are arguable (see section 11.1.6). Whether precipitation increases in dry regions is very sensitive to the definition of dry region, and a different classification based on aridity does not support the conclusions (Sippel et al., 2017).

There is *low to medium confidence* in the impacts of aerosols on heavy precipitation with a magnitude similar or higher than that caused by GHG forcings (Linet al. 2016, 2018). It is *likely* that this is primarily through the combined effects of the atmospheric energy balance, dynamical adjustment, and vertical structure of forcing, and not through cloud microphysics effect. Recent changes in circulation patterns by the aerosol forcing might have caused changes in distributions of extreme precipitation through changes in TC activities (Takahashi et al., 2017; Zhang et al., 2017). The effect of dust on TCs was found to induce complicated responses depending on whether it is predominantly absorbing or scattering (Strong et al., 2018). In this study, absorbing dust caused increases in Northern Hemisphere tropical precipitation and a decrease in the Southern Hemisphere. Predominantly scattering dust had the opposite effect.
Since SREX, the number of studies on the impacts of local land cover and land use change on heavy precipitation has increased. For example, there is growing number of literatures indicating increase in heavy precipitation in urban centers due to urbanization. There are three possible mechanisms: a) increase in atmospheric moisture associated with urban heat island effect (Shastri et al., 2015) ; b) increase in condensation due to urban aerosol emission (Han et al., 2011; Sarangi et al., 2017); and c) urban structures and resulting impediments to atmospheric motion and additional eddies (Ganeshan and Murtugudde, 2015; Paul et al., 2018; Shepherd, 2013). Other local factors such as reservoir operation may also have potential to impact heavy precipitation (Woldemichael et al., 2012). There is *low confidence* in the intensification of heavy precipitation due to urbanization and this attributes to lack of data availability at finer spatio-temporal resolution (Mishra et al., 2015; Paul et al., 2018).

11.4.2 Observed Trends

The SREX Ch3 concluded that more locations show statistically significant increases in the number of heavy precipitation (HP) events (e.g. 95th percentile) than statistically significant decreases. However, there are wide regional and seasonal variations, and trends in many regions are not statistically significant. Post-SREX studies report more evidence about HP detection. Alexander (2016) provides a recent review on the new progress since IPCC AR5, including a number of high-level coordination activities and papers around precipitation extremes [COMMENT: These are essentially based on the same dataset used in Donat et al. 2013 on which AR5 assessment is based. We will update this based on a new update that is currently underway]. According to Alexander (2016), heavy precipitation events appear to have increased in more regions than they have decreased, which is consistent to SREX. The study also finds similar conclusions for short-duration intense rainfall, though there is *low confidence* as data are more limited data and there are fewer studies (e.g. Westra et al., 2014).

Donat et al. (2016a) showed robust increase in extreme precipitation over both dry and wet land regions around the globe. They further found that in dry regions the total annual and extreme precipitation have similar trends, which is not observed in wet regions Their ‘wet’ grid cells are mainly found in Southeast Asia, India, eastern South America, the southeastern United States, Europe and small regions in northern tropical and eastern coastal Australia, eastern tropical Africa and southeastern Africa. Most of their ‘dry’ grid cells are located in central and northeast Asia, central Australia, northwestern North America, as well as north and southwestern Africa.

In North America, specifically in the United States, there is *medium tohigh confidence* in an overall increase of heavy precipitation, both in terms of intensity and frequency (Donat et al., 2013a; Huang et al., 2017a;

Villarini et al., 2012) except the southern part of the US (Hoerling et al., 2016). There has also been a widespread increase in heavy precipitation over Canada and this is associated with anthropogenic forcing (Zhang et al., 2013). In Central America trends in annual precipitation are generally non-significant, although small (but significant) upward trends are found in Guatemala, El Salvador and Panama (Hidalgo et al., 2017).

For South America the dominant signal is a wetting trend. The annual maximum 1-day (RX1day), consecutive 5-day (RX5day) precipitation and the heavy rainfall (R99p) exhibit upward trend when spatially averaged over large regions of South America including AMZ, NEB, SES and WSA (Skansi et al., 2013). Among all subregions, SES shows the highest rate of increases for rainfall extremes, followed by AMZ. According to (Skansi et al., 2013), moderate and non-statistically significant decreasing trends are also observed over Northeast Brazil, southern Peru and southern Chile.

Since SREX, there has been a growing number of studies on regional trends of extreme precipitation in Europe. There is *medium confidence* in an observed increasing trend in the intensity and frequency of extreme precipitation events (Cioffi et al., 2015; van den Besselaar et al., 2013). There are regions such as Portugal, where a mixed trend is observed (Pedron et al., 2017). In Romania, decreasing trend is observed for the total number of precipitation days (R0.1), increasing trends are found for the frequency of moderate and heavy precipitation (R5, R10) (Croitoru et al., 2016). Increase in extreme precipitation is observed in the Central Europe, which is associated with the warming of the Mediterranean Sea (Volosciuk et al., 2016). The trends in extreme precipitation over Asia is dominated by spatial variability. There is *high confidence* in the increase in extreme events over Western Himalayas (Cross chapter box) and over the central India (Roxy et al., 2017) with increase in spatial variability (Ghosh et al., 2012). Increasing trends in extreme precipitation dominated in northeastern Pakistan (Sheikh et al., 2015), whereas a reducing tendency towards extreme precipitation prevails in the southwestern part of the country (Hussain and Lee, 2013). There is *medium confidence* in the trends of extreme precipitation over China with high spatial variability and a mixture of regions with increasing and decreasing trends(Fu et al., 2013a; Jiang et al., 2013; Ma et al., 2015; Yin et al., 2015). High spatial variability is also observed in the observed trends of extreme precipitation over Australia (Bao et al., 2017) with limited evidences since SREX. There is also *low-to-medium confidence* in the observed trends of extreme precipitation over Africa. An increasing trend was observed in Central Sahel (Panthou et al., 2014), while drcreasing trend in observed extreme precipitation is observed by (Tramblay et al., 2012).

[START FIGURE 11.8 HERE]

Figure 11.8: Observed linear trend over 1951-2018 in the annual maximum pentadal (5-day) precipitation from the beta version of the most recent HadEX3 data set. Units: °C/decade.

[END FIGURE 11.8 HERE]

11.4.3 Model evaluation

The AR5, Chapter 9 concluded that statistics of extreme events are well represented in model simulations. Although the simulation of large-scale patterns of precipitation has improved, models continue to perform poorer for precipitation than for temperature. And the uncertainty in observed rainfall is larger than that for temperature and this makes the model evaluation for heavy precipitation more challenging. This has to do with the evolving patterns of weather responsible for extreme rainfall events (section 11.4.1) and how are they represented or captured in the models. A common issue when evaluating model output is the possible scale mismatch between simulated and observed data (Avila et al., 2015; Gervais et al., 2014). Gervais et al. 2014 estimated that the reduction in precipitation extremes can be as large as 30% when comparing point estimations with areal-mean values representative of GCM grid boxes. The scale mismatch implies that whenever the comparison between the observed and simulated data is not performed at common scales, the interpretation should be made cautiously. Regarding precipitation intensity, models have also been shown to reproduce the compensation between precipitation extremes and the rest of the distribution (Thackeray et al., 2018), a characteristic found in the observational record (Gu and Adler, 2018).

Studies evaluating the overall skill of the different generations of the Coupled Model Intercomparison Project (CMIP) models (Flato et al., 2013; Watterson et al., 2014) have found quite modest, although steady, improvements. Results showed improvements in representation of the magnitude of ETCCDI indices in CMIP5 over CMIP3 (Sillmann et al., 2013a;Chen and Sun, 2015a) and these improvements were attributed to higher resolution. And growing evidence suggest that high resolution models reproduce extreme rainfall comparable with observations (Sillmann et al., 2013b). These improvements appear more a property of the ensemble than of individual models. It should be noted that these overall assessments are usually based on relatively simple scores that use only a few observables and might not reflect much of the improvements in new generations of models related with a more comprehensive and better formulation of processes in model components (Di Luca et al., 2015). For annual Rx5day, the CMIP5 models were found to be consistently below the HadEX2 values as would be expected from resolution constraints (Wehner et al., 2014).

Studies over using regional climate models (RCMs), for example, the Coordinated Regional Downscaling Experiment (CORDEX; (Giorgi et al., 2009)) over Africa (Dosio et al., 2015; Gbobaniyi et al., 2014; Klutse et al., 2016; Pinto et al., 2016) , Australia , Europe (Prein et al., 2016a) and North America (Diaconescu et al., 2018) suggest that extreme rainfall events are better captured in RCMs due their ability to address regional characteristics, e.g., topography. However, CORDEX simulation do not show good skill over the South Asia for heavy precipitation and do not add value with respect to their parent CMIP5 GCMs (Mishra et al., 2014a; Singh et al., 2017)

Model evaluation of HighResMIP-class simulations is incomplete. Wehner et al., 2014b found that in a ~25km version of the Community Atmospheric Model (fvCAM5.1) long period return values of seasonal Rx5day were substantially increased over the same model at ~100km. While the high-resolution simulation mid-latitude winter extreme precipitation over land is in reasonable agreement with observations, simulation of the summer extreme precipitation has high bias. As simulated extreme precipitation in the tropics also appears to be too large, deficiencies in the parameterization of cumulus convection at this resolution are suspected.

There is a ***high confidence*** that the ability to simulate climate extremes has steadily increased since SREX and AR5 principally due to refinements in horizontal resolution of global and regional models. At about 25km, models begin to simulate tropical and other intense storms considerably with more realism, leading to higher values of extreme precipitation closer to observations especially in regions of highly variable topography [section 10.5.3]. However, cumulus convection must be parameterized in the HighResMIP models and current parameterizations are inadequate. Further progress in this regard awaits the computational advances necessary for explicit representation of convective processes in multi-decadal simulations. Despite of these few exceptions, in general the ability of the models to simulate the extreme events in the present improves the confidence on projected changes.

11.4.4 Detection and attribution, event attribution

Both SREX and AR5 concluded with *medium confidence* that anthropogenic forcing has contributed to a global scale intensification of heavy precipitation over the second half of the 20th century. These assessments were based on the evidence of anthropogenic influence on aspects of global hydrological cycle, in particular, human contribution to the observed increase in atmospheric moisture that should lead to an increase in heavy precipitation, and limited direct evidence of anthropogenic influence on extreme precipitation of durations from one to five days.

A few new studies have evaluated the large-scale observed changes in extreme precipitation. Updating Min et al., (2011) by using updated observational data and CMIP5 model data sets for an extended period of 1951-2005, Zhang et al. (2013) attributed the intensified annual maxima of daily (RX1day) and 5 day consecutive (RX5day) precipitation over the Northern Hemisphere land area tohuman influence (Figure

3.17:). They newly found that the anthropogenic signal is separable from the external natural forcing and that the intensification of extreme precipitation is consistent with the Clausius-Clapeyron relationship (~5.2%/K). Comparing spatially aggregated changes in RX5day over the global land area for 1960-2010, Fischer et al., (2014)found a large fraction of land that has experienced a strong intensification of heavy precipitation, which is generally captured by CMIP5 models including anthropogenic forcing but not by unforced simulations. CMIP5 models were, however, found to underestimate the observed trends in precipitation extremes. Applying a similar spatial aggregation to smaller areas, Donat et al., (2016a)found the robust increases in RX1day over the world's dry and wet regions during 1951-2010 from the observed and CMIP5 simulations. They also found that the future increases of RX1day in dry regions are closely related to the global mean temperature changes across models, supporting the C-C relationship, which is less robust over the wet regions. Shiogama et al., (2016)found human influence on the historical changes in the record-breaking 1-day precipitation to be statistically significant.

Adopting another spatial perspective, Dittus et al., (2015) utilized the areal extent of daily precipitation extremes to evaluate eight CMIP5 models in comparison with the observations over the period 1951-2005. They found that many CMIP5 models can reproduce the observed increasing trends in the area experiencing an extreme proportion of annual total precipitation from heavy precipitation (R95p/PRCTOT) for the Northern Hemisphere regions.

One study examined the volcanic impacts, showing detectable influence from natural forcing on extreme precipitation at the global scale. Paik and Min (2018) found substantial reduction in RX5day and SDII (simple daily intensity index) over the global summer monsoon regions after explosive volcanic eruptions from the HadEX2 observations and CMIP5 multi-models. From models, they found that the reduction in extreme precipitation is closely linked to the decrease in mean precipitation, for which both thermodynamic effect (moisture reduction due to surface cooling) and dynamic effect (monsoon circulation weakening) play important roles. The significant response in extreme precipitation to volcanic forcing has important implications for geoengineering based on solar radiation management (Curry et al., 2014; Tilmes et al., 2013).

Attribution of long-term changes in extreme precipitation at regional scale is more limited and the results tend to be less robust. For example, Li et al. (2017) detected anthropogenic influence on extreme precipitation in China using optimal fingerprint method while another one (Li et al., 2018d), based on a different method, did not, even though the underlying station data used in both studies are essentially same. This indicates that the details in the data process and analyses methods may contribute to this discrepancy. A weak signal to noise ratio is, however, the main cause for the lack of robustness as Li et al. (2018d) also showed that the signal would become robustly detectable 20 years in the future.

Studies that have led to the assessment of anthropogenic influence on extreme precipitation have mostly focused on extreme precipitation of durationsfrom one to five days. Systematic studies on long-term changes of heavy precipitation of time duration longer than 5-days are lacking. Instead, the focus has been on individual events i.e., the attribution of changes in the probability or the magnitude of a class of extreme precipitation events similar to those occurred recently between real world and counterfactual world. Many of those are summarised in the annual supplement report on "Explaining Extreme Events from a Climate Perspective" (Herring et al., 2014, 2015, 2016, 2018; Peterson et al., 2012, 2013b). Some studies found influence of climate change on the probability or magnitude of observed extreme precipitation events including European winters (Otto et al., 2018b; Schaller et al., 2016), parts of the US for individual events (Eden et al., 2016; Knutson et al., 2014; Szeto et al., 2015; van Oldenborgh et al., 2017) or China (Burke et al., 2016; Sun and Miao, 2018; Yuan et al., 2018b; Zhou et al., 2017). Other studies, however, suggested a lack of evidence about anthropogenic influences (Imada et al., 2013; Otto et al., 2015c; Schaller et al., 2014; Siswanto et al., 2015). Yet, there are also studies whose results are inconclusive because of limited reliable simulations (Angélil et al., 2016; Christidis et al., 2013b).

Anthropogenic influence may have affected the large scale meteorological patterns (LSMP) necessary for extreme precipitation and the localized thermodynamical and dynamical processes, both contributing to changes in extreme precipitation events. There are differences between attributing the causes of seasonal (or longer) extreme precipitation events and individual extreme storms (see section 11.6) as the relative roles of these two factors can vary greatly and appropriate attribution methods may also be different (see section 11.2.5). Several new methods have been propsoed to disentangle these effects by either conditioning on the circulation state or attributing analogues. In particular, evidence shows that the extremely wet winter of 2013/2014 in the UK can be attributed,approximately to the same degree, to both temperature induced increases in saturation vapor pressure and changes in the large scale circulation (Vautard et al., 2016; Yiou et al., 2017). There are multiple cases indicating an increase in very extreme precipitation in relation to temperature above thethe 6-7%/ºCClausius-Clayperonrate (Pall et al., 2017;Risser and Wehner, 2017; van der Wiel et al., 2017; van Oldenborgh et al., 2017;Wang et al., 2018). Many observational studies showed that this so-called "super C-C" relation occurs in particular at hourly rainfall extremes in many places, and the dynamic effect related to the enhanced convective activity has been suggested to be an important physical mechanism (e.g., Westra et al., 2014; Lenderink et al., 2017). However, the super C-C scaling is based on the day-to-day temperature variability and cannot provide a robust basis for the long-term attribution or projection of extreme precipitation changes (Zhang et al., 2017b). Over all, the events in question in these cases are exceedingly rare and the attribution statements are highly conditional on the observed LSMP (Wehner et al., 2018d). Yet, it is not known if and to what extend the LSMP properties have changed (see section 11.4.1).

Almost all existing event attribution studies on extreme precipitation are motivated by the need to understand the causes of a recent event that have caused flood leading to loss and damages. As precipitation is only one of the multiple factors, albeit an important one, that affects flood and as flood is only one of multiple factors causing damages, attribution of human influence to the probability of precipitation event does not by itself directly attribute human influence to the flood or to the related damages. For example, Teufel et al. (2017) showed that while human influence increased the odds of the flood-producing rainfall for the 2013 Alberta flood in Canada, it was not detected to have influenced the probability of flood itself. Similarly, Schaller et al.(2016) showed human influence in the increase of probabilities in heavy precipitation and its resulting flood of the river Thames flooding in winter 2014, but its contribution to the additional properties at risk was not found to be significant.

In summary, there is *highconfidence* that human influence has intensified heavy precipitation at the global scale. This is supported by multiple lines of new evidence since AR5 based on different methods. The observed global increase in annual maximum 1-day and 5-day precipitation can be attributed to human influence. A large fraction of land showed enhanced extreme precipitation and larger probability in record-breaking 1-day precipitation than expected by chance, both of which can only be explained when anthropogenic greenhouse gas forcing is considered.At regional scales, human influence on extreme precipitation is hardly detectable because of low signal-to-noise ratio, but there is some new evidence of human contribution to the increase in the probability or magnitude for some individual events in different parts of the world~~.~~

11.4.5 Projections

[To reviewers: TEXT WILL BE REORGANIZED TO DISCUSS CHANGES AT +1.5°C, +2°C and +3° AND PROJECTIONS BY CMIP6 SIMULATIONS]

As assessed earlier in AR5 and SREX, projected changes in the frequency of heavy rainfall and heavy rainfall amount is *likely* to increase in the 21st century over many land areas. There is a *medium to high confidence* that total rainfall amount is projected to decrease. And rare events such as 1 in 20 year annual maximum one day rainfall rate event are *likely* to become more frequent in many regions. Post AR5 studies using either GCMs and/or RCMs provide more lines of evidence supporting previous assessments. In many parts of Africa unser RCP8.5 scenario it is expected to see an increase in heavy rainfall amounts and rainfall intensity (Abiodun et al., 2017; Akinsanola and Zhou, 2018; Giorgi et al., 2014; Pinto et al., 2016). However, over western South Africa, heavy rainfall amounts are projected to decrease. This is mainly due to a decrease in frequency of the prevailing westerly winds south of the continent which translates into fewer cold fronts and closed mid-latitudes cyclones (Engelbrecht et al., 2009; Pinto et al., 2018). An increase in heavy rainfall are projected in most parts of Asia together with increases in rainfall intensity (Endo et al., 2017; Guo et al., 2018; Han et al., 2018; Kim et al., 2018b; Xu et al., 2016; Zhou et al., 2014). Over Australia there is *low confidence* in changes in extreme rainfall. This is due to a lack of consistency among climate models and no significant changes in extreme rainfall (Alexander and Arblaster, 2017; Evans et al., 2017). Over central Europe and southern Europe there is *low to medium confidence* in the changes in extreme raifall manly due to discrepancies among studies and strong seasonal seasonal differences (Casanueva et al., 2014; Croitoru et al., 2013; Fischer and Knutti, 2015; Roth et al., 2014). Over northern Europe there is *medium confidence* in increases in rainfall extremes in boreal winter and summer (Donnelly et al., 2017; Madsen et al., 2014; Thober et al., 2018). Over North America, the frequency and intensity of heavy rainfall are *likely* projected to increase (Easterling et al., 2017; Wu, 2015) with projected decreases over Mexico (Alexandru, 2018). Over South America, in general there is a decrease in heavy rainfall amount (Chou et al., 2014) with increases in South Eastern South America (Giorgi et al., 2014).

[START FIGURE 11.9 HERE]

Figure 11.9: Projected changes in annual maximum 5-day precipitation for projections at 1.5°C, 2°C, 3°C and 4°C of global warming compared to pre-industrial conditions (1850-1900), using empirical scaling relationship based on transient CMIP5 simulations. Cross-hatching highlights areas where at least two-thirds of the models agree on the sign of change as a measure of robustness.

[END FIGURE 11.9 HERE]

Model projections show that the extreme precipitation, in contrast to mean precipitation, depends on the total amount of warming and not really on the forcings (Pendergrass et al., 2015). Changes in RX1 extreme precipitation during the historic period for half a degree warming are consistent to the changes between the projections of the same for 1.5^{0}C and 2^{0}C warming scenarios as simulated by the global models (Fischer and Knutti, 2015). Dosio and Fischer, (2018) have shown a marked projected change in extreme precipitation in comparison to the mean precipitation in the Europe. In a 3^{0}C warmer world there will be a robust increase in extreme rainfall over the 80% of land areas in North Europe. Additional half degree warming in a 2˚C warmer world would result an increase in regional extreme precipitation over China irrespective of the return periods (Li et al., 2018e). Projections with HAPPI project show that the extreme precipitation will amplify in the Asian-Australian monsoon region due to additional half degree warming, though there is uncertainty in the projections for Australia (Chevuturi et al., 2018). Frequency of extreme precipitation will be more in East Asia and India. Increased daily extreme precipitation is projected for Africa due to an additional half degree warming by the CORDEX regional models and these projections are similar to the simulations by coarse resolution global climate models (Nikulin et al., 2018).

Figure 11.9 shows that 1) increases in heavy precipitation mostly over tropical Asia, Africa and polar regions at 1.5°C global warming, 2) increases in land areas with projected increase in heavy precipitation in 2°C warming scenario as compared to that of 1.5°C global warming, 3) projected widespread increase in heavy precipitation almost over the entire land region of the globe at the global warming of 3°C and 4°C. Figure 11.10 presents increase in extreme precipitation over majority of the regions with increase in the global warming levels; however, theses increases are associated with very high uncertainty as evident from high band widths.

[START FIGURE 11.10 HERE]

Figure 11.10: Projected changes in annual maximum 5-day precipitation (Rx5day) compared to pre-industrial conditions (1850-1900) as function of mean global warming, using empirical scaling relationship based on transient CMIP5 simulations. Analyses for 37 AR6 regions, the global ocean and the global land.

[END FIGURE 11.10 HERE]

In summary, there is *high confidence* that there are overall statistically significant upward trends in extremes rainfall events in a majority of land regions. Due to the highly spatial and temporal variability of precipitation the level of confidence of the trends depends on the region (*high confidence*). There is *high confidence* that anthropogenic influence has contributed to an increased severity of heavy rainfall events in majority of land regions. There is improved understanding of processes leading to extreme rainfall and representation in climate models. And climate models are improving in resolution and able to capture extreme rainfall, especially for shorter-lived events at regional scales. It is *likely* that past upwards trends in extreme rainfall will continue into the future. There are more land areas showing increases in extreme rainfall than decreases. A larger set of studies based on global and regional climate projections are becoming available and they will provide a more coherent picture of regional changes in extreme rainfall and snowfall with the associated uncertainties.

11.5 Floods, wet soils and water logging

Analysis of changes in intensity and occurrence frequency of flood is challenging due to the wide variety of related phenomena, such as flash floods, river floods, groundwater floods, surge floods, coastal floods, etc., which all depend on different drivers and processes (Nied et al., 2014) that may be changing due to greenhouse gas forcing, land use and/or infrastructural changes. Among these processes, rainfall intensity is of high importance, in particular with respect to flash floods, but antecedent soil moisture, snow depth and groundwater are also crucial (Sikorska et al., 2015). In the case of surge floods or coastal floods, flooding may also occur as a compound event resulting from the combination of heavy precipitation and sea level rise (see also Section 11.8). Confidence in detecting, attributing and projecting changes in flooding due to climate change, land use and/or infrastructural changes is often limited by poor spatial coverage of the flood data and the difficulty of models in reproducing this low-frequency phenomenon. On the other hand, relationships of some flood events to heavy precipitation and sea level rise provide a link to changes in the climate system that have overall a substantial footprint from greenhouse gas forcing in several regions (Section 11.4, Chapter 9).

11.5.1 Mechanisms and drivers

Climate models show that the frequency and intensity of extreme rainfall events that generate flash floods, overbank floods and urban floods (Hirabayashi et al., 2013; Kundzewicz et al., 2014) increase in several regions as the climate warms (Section 11.3). Since AR5, the number of studies on understanding and analysing extreme flooding has substantially increased. Several studies have highlighted some complex interactions at the basin scale between hydrology and climate (including snow processes, temperature – responsible for soil freezing, evapotranspiration and snowmelt – and precipitation intensity, duration, amount and timing), basin characteristics (e.g. topography, soil types), basin size and antecedent moisture conditions (Berghuijs et al., 2016; Paschalis et al., 2014). All these factors make it difficult to unravel the effects of greenhouse gas forcing and associated changes in precipitation from other drivers that affect flood generation, in particular for the attribution of single events, although the examination of changes in long-term flooding and corresponding changes in precipitation (Fig. 11.11) does reveal regional-scale similarity in some regions (Peterson et al., 2013a).

[START FIGURE 11.11 HERE]

Figure 11.11: Geographic distribution of century-scale changes in (a) flooding and (b) precipitation. In (a), the triangles are located at 200 stream gauges, which have record lengths of 85–127 years. The color and size of the triangles are determined by the trend slope of a regression of the logarithm of the annual flood magnitude vs time for the entire period of record at the site, ending with water year 2008. In (b), trends in total annual precipitation as percentages for a 100-yr period end the same year as the flood data (2008) shown in (a). There are regional similarities between the figures, such as increases in floods and precipitation in the northeastern Great Plains and drying in the Southwest, but not a one-to-one correspondence. From (Peterson et al., 2013a).

[END FIGURE 11.11 HERE]

While changes in the characteristics of mean or heavy precipitation, with some exceptions, have generally *medium to high confidence* (Section 11.4, Chapter 8), confidence in changing flood characteristics requires further understanding in three main areas: i) stream characteristics (river hydraulic structures, stream morphology -river training, flood plain removal, retention basins, reservoir dams, interactions sediment-flood-) (Borga et al., 2014; Nakayama and Shankman, 2013), ii) land-use and land-cover interactions and changes (Aich et al., 2016; Rogger et al., 2017) and iii) inter-system feedbacks not only between climate, soil, vegetation and landscape, but also between human actions and stream changes (Hall et al., 2014).

Increases in heavy rainfall events in a warming environment do not necessarily increase the streamflow and flooding (Sharma et al., 2018; Wasko and Sharma, 2017), although they tend to result in increases in flood intensity for small catchments and in case of high increases in extreme precipitation (Wasko and Sharma, 2017). Identifiying a link can be particularly challenging for the attribution of single events. Using the extreme 2011 flooding in Thailand as an example, Gale *et al.* (2013) calculated both the return time of the rainfall and of the river flow of the event, estimating the former to be between 1 and 8 years in the south of the country and 8 and 20 years in the north, and the associated river flow from satellite estimates to be between 10 and 20 years and between 5 and 6 years, respectively, when estimated from flood records. This illustrates that attribution results from rainfall alone can often not be directly transferred to hydrological measures of flooding like river flow. The absence of a strong association between extreme precipitation and extreme streamflow can be due to the importance of non-precipitation drivers, such as water demands/losses, antecedent moisture (Berghuijs et al., 2016; Paschalis et al., 2014, Fitsum and Ashish, 2016, Grillakis et al., 2016), rain on snow (Musselman et al., 2018); failure of dams (Kim and Sanders, 2016; Pisaniello et al., 2012), land use and land cover change (Lana-Renault et al., 2014; Arias et al., 2012; Pakorn et al., 2010) and mismanagement of reservoirs (Wei et al., 2015; Kundzewicz et al., 2014; Kundzewicz et al., 2018; Hall et al., 2014).

Flash floods, rapid local flooding, can be caused by extreme precipitation, glacier lake outburst (Schwanghart et al., 2016), by a dam break or a sudden release of water from upstream reservoirs (Calianno *et al.*, 2013). Urban flash flooding is often caused by brief but very extreme rainfall and a high fraction of impervious areas. Hence, changes in urban flooding have a more direct connection to changes in extreme precipitation. However, other factors also contribute to urban flooding including high overland flow, failure of urban storm water drainage system and water logging (Maksimović et al., 2009). Though the mechanisms of flood generation are similar across urban areas, variations in infrastructure and storage capacity result in a spectrum of responses in flood intensities to similar magnitude of changes in rainfall extremes (Smith et al., 2013).

Increases in temperature may lead to earlier and increased snowmelt rates, which together with the co-occurrence of extreme precipitation, often result in severe flooding (Vormoor et al., 2015, 2016). However, higher temperature can also lead to smaller snowpack. In mountainous regions, glacial lake outburst can also cause floods (Schwanghart et al., 2016). Coastal flooding is driven by multiple factors such as precipitation, winds, tides, tropical cyclones (Reed et al., 2015a), stormsurges(Little et al., 2015; Möller et al., 2014; Muis et al., 2016) and sea level rise (Chapter 9) (Woodruff et al., 2013). In fact, coastal flooding during tropical cyclones can be a mix of fresh water and salt water when large storm surges co-occur with heavy precipitation (Wahl et al., 2015) section 11.7.

Summary: In addition to contributions from extreme precipitation, floods are driven by catchment characteristics, antecedent soil moisture, coastal storm surge and tides, human intervention such as dam operation, and/or changes in land use and land cover. Some of these other conditions, such as antecedent soil moisture or coastal storm surge, may also be affected by greenhouse gas forcing. Overall, there is *high confidence* in the joint influence of climate, human intervention and catchment characteristics on flood generation, with the relative contribution of these factors depending on time and location, and the contribution of greenhouse gas forcing not being limited to possible changes in extreme precipitation. Hence, there is often not a one-to-one correspondence between trends in

extreme precipitation and flood events, in particular in terms of magnitude (*medium confidence*).

11.5.2 Observed trends

At the time of the SREX report (SREX Ch. 3) confidence in observed and projected flood trends was assessed as *low* given the limited available records, the influence of water regulation and land cover changes. This assessment was repeated by the AR5 report (AR5 Ch. 2), stressing a lack of evidence and strong spatial heterogeneity. The recent SR15 report (SR15 Ch. 3) assessed that there was *high confidence* that (mean) streamflow trends in most world's large rivers were not significant, but a *high confidence* in the increase in flood frequency and extreme streamflow in some regions. Some regions with decreases in flood frequency were also highlighted.

The number of studies analyzing flood trends has increased since the AR5 report, and there are also new analyses available since the SR15 (e.g. Gudmundsson et al., 2019). Nonetheless, as for other variables, it should be noted that runoff measurements are not homogeneously distributed, and that many regions have only sparse coverage, such as Africa, South America, and parts of Asia (e.g. Do et al. 2017). In an analysis of peak flow trends, Do et al. (2017) used annual maximum peak floods in more than 3500 streamflow stations in US, Central and North Europe, Africa, Brazil and Australia for 1961-2005, and found only 7.1% of the stations with significant positive and 11.9% with significant negative trends. This suggests that flood trends are not of consistent sign in different places at the global scale. Gudmundsson et al., (2019)have also highlighted the high regional dimension of runoff trends, with low-flow, median-flow and high-flow indices being often regionally consistent, showing that the entire flow distribution tends to move either upward or downward. Regions showing most consistent trends towards increases for the higher tail of the runoff distribution (90th percentile and/or maximum value) include Southern South America and Northern Asia, while those showing decreases over the last decades include the Mediterranean region and Northeastern Brazil (Gudmundsson et al., 2019). In Australia, Ishak et al. (2013) showed that negative trends in maximum annual floods dominated (22%) but that trends were mostly restricted to the southeast and southwest. In East Asia there are important regional differences. In Central China, Bai et al. (2016) showed a negative trend in maximum annual floods, connected to the decrease of precipitation intensity and increases in the number of dams. However, in the Pearl river basin, Zhang et al. (2015) showed that there were no changes in peak flows and no connection with precipitation changes and human activities. In the Amazon basin there is a significant increase of extreme floods associated with a more intense Walker circulation (Shkolnik et al., 2018), but in West Africa, Nka et al. (2015) did not find trends in annual maximum floods. In North America, Peterson et al., (2013a)documented strong spatial differences in the trends, with increases in the Northwest US and decreases in the Southeast US, possibly attributable to general drying and diminished snowpack. This is consistent with other studies at the continental and regional scale in North America (Armstrong et al., 2014; Archfield et al., 2016; Mallakpour and Villarini, 2015; Burn and Whitfield, 2016; Wehner *et al.*, 2018). In Europe, the long time series of high flows data do not show clear trends at the continental, national or regional levels (Hall et al., 2014; Mediero et al., 2015; Kundzewicz et al., 2018). Mangini et al. (2018) analysed flood peaks across central and North Europe using more than 600 gauging stations for the period 1961-2015 and found strong spatial heterogeneity with a similar percentage of positive (10%) and negative (8%) significant trends. Mudersbach et al. (2017) using 138 years of daily streamflow in the Elbe river found no long term trends.

Mallakpour and Villarini (2015) found an increase of the frequency of high floods in the northeast US using a peak over threshold approach. Nevertheless, in Europe, studies using the same approach suggest no general trends except in the UK (Mangini et al., 2018; Mediero et al., 2015). Changes in the flood frequency identified in regions of South Europe have been connected with dam management and irrigation practices (Vicente-Serrano et al., 2017b). Increased water use was also suggested by Mallakpour and Villarini (2015) to explain the decrease in flood frequency in Nebraska and Kansas, since although the frequency of heavy rainfall days increased, the water table decreased as a consequence of a higher groundwater withdrawal. Some changes have been recorded in the flood seasonality, mostly in snow dominated regions but not exclusively. In Canada, Burn and Whitfield (2016) showed that in some snow catchments flood events occur earlier, but also that some snow catchments experience a substantial decrease in regularity, interpreted to indicate a movement toward a mixed flood regime in which rainfall events are becoming an important flood generation mechanism. In Europe, Blöschl et al. (2017) analysed changes in the flood timing using a dataset of more than 4000 gauging stations from 1960 to 2010, and suggested that higher temperatures may have led to earlier spring floods connected with earlier snowmelt throughout north-eastern Europe. Nevertheless, they also suggested that other different greenhouse-gas forcing induced processes may be governing flood timing since delayed winter storms associated with polar warming might have caused later winter floods around the North Sea (despite *low confidence* in this proposed relationship; Section 11.1.5) and satuiration of soil earlier in the season could explain the earlier winter floods in Western Europe. Changes in flood seasonality not driven by snow processes have been shown by Ye et al. (2017) in their analysis of the flood evolution in 250 natural catchments of US between 1951 and 1999. They showed that in catchments with increases in storm rainfall, floods tended to occur with more seasonal irregularity.

Summary: There are important challenges in determining flood trends related to methodological issues, different flood metrics, and time windows, but also due to spatial gaps, with large parts of globe lacking runoff measurements. There is *high confidence* that significant flood trends have been recorded in some regions over the past decades, both positive (Northern Asia, Southern South America, Northeast US, UK and the Amazon) and negative (Mediterranean, northeastern Brazil, South Australia, central China, Southeast US). Because of the high regional variability of flood trends, there is generally *low confidence* in global trends in floods. There is *high confidence* that flood seasonality has changed in some regions dominated by snowmelt.

11.5.3 Model evaluation

Future flood scenarios strongly depend on changes in extreme precipitation, which have been projected to increase with a high degree of confidence in some world regions (Section 11.4.5), but there are still uncertainties given different theoretical and methodological constraints. Climate change impacts on flood severity depend also on basin characteristics in addition to changes in extreme precipitation. Spatial scales are also important since flooding processes and interactions are different in small catchments compared to the large basins. Future floodsalsodepend on flood preventionmeasures(Neumann et al., 2015; Şen, 2018) and flood control policies (Barraqué, 2017), on land cover changes and complex hydrological processes. The majority of regional to global climate change studies do not consider flood management changes in future scenarios, which is an important source of uncertainty in the projections. There are also uncertainties related to the modeling procedures. The studies at the scales from large basins to the entire globe show large uncertainties given the difficulties in properly representing the complex hydrological processes that drive floods, the use of different emission scenarios, the climate models (both RCMs and GCMs) (Hundecha et al., 2016; Krysanova et al., 2017), the use of multiple runs of a single models and the influence of downscaling and bias correction techniques (Muerth et al., 2013), and the hydrological models used for simulations (Roudier et al., 2016), even if they are forced by the same GCMs (Thober et al., 2018). Over-fitting of complex hydrological models is also an important source of uncertainty (Orth et al., 2015).

In general, studies that use different hydrological models show wide spread in flood simulations (Dankers et al., 2014; Krysanova et al., 2017; Roudier et al., 2016). Huang et al. (2017) used nine hydrological models in different large basins of the world. They showed that although models reproduced river flow well, the flood quantiles exhibited a wide spread among the hydrological models, independent of the climatic and physiographic characteristics of the basins. Moreover, the issue is not restricted to the hydrological models. Studies that use different GCMs to force a single hydrological model suggest large differences among simulations. For example, Arnell and Gosling (2016) downscaled simulations by twenty-one GCMs under the CMIP3 A1B scenario to force a hydrological model at the global scale. They showed low consistency among projections in large parts of the world. Additionally, the use of different hydrological models forced by a single GCM also show spatial differences caused by differences among hydrological models (Dankers et al., 2014).

Summary: Complex hydrologic processes, driving factors acting at multiple scales, and human influences on the river courses render flood modeling challenging. Moreover, there are several sources

of uncertainty in modeling approaches and strong differences in simulations as a consequence of differences in climate models, the downscaling techniques and the hydrological models (*high evidence, medium agreement*).

11.5.4 Attribution

Case studies using the optimal fingerprinting method for Detection and Attribution have been applied to observed streamflow, finding a decline in streamflow attributable to anthropogenic forcing in British Columbia (Najafi et al., 2017) and in Southern Europe (Gudmundsson et al., 2017), whereas for Northern Europe and Japan an attributable increase in freshwater resources (Gudmundsson et al 2017; Meng et al., 2016) is found. All studies highlight however a very large uncertainty in their findings (Ahn et al., 2016); confidence in the results is therefore *low* in particular as studies are isolated and generally using a single model only.

In the case of event attribution, while two of the three relevant event attribution studies discussed in the AR5 analysed floods experienced as a result of heavy precipitation, most event attribution studies since then have focused on the attribution of the flood-inducing rainfall event rather than the flooding itself. There are a few studies attributing hydrological extreme events like river runoff and other hydrological properties to anthropogenic climate change (in contrast to attribution to observed changes in rainfall), but they are localized and do not allow to draw any global conclusions.

Event attribution studies focused on runoff using hydrological models include river basins in the UK (Kay et al., 2018; Schaller et al., 2016) (see section 11.4.4) the Okavango river in Africa (Wolski et al., 2014) and the Brahmaputra in Bangladesh (at least 2 in review). Structural differences in hydrological models are very large compared to climate models, making it difficult to compare results employing the same multi-method approach to individual event attribution studies but does allow for an estimate of modeling uncertainty. In a review on the UK, Hannaford (2015) highlights that the methodologies used in different studies do not allow for general conclusions to be drawn. Philip *et al.* (2018) have employed the multi-method approach recommended for the attribution of extreme weather events (National Academies of Sciences, Engineering, 2016) for hydrological modeling approaches on the floods in Bangladesh in the Brahmaputra basin. They found that despite large modeling differences, there is an attributable signal in the river flow that is significantly different from no change and that has the same order of magnitude of the signal in the precipitation that produced the flood event. Other attribution frameworks have been suggested(Feng et al., 2018) but have so far not been applied.

Summary: There are few flood attribution studies and there are important differences between models and methods used for individual event attribution. This causes important uncertainties and limited confidence in the attribution of specific floods to anthropogenic forcing. In addition, there is limited confidence on a global anthropogenic flood attribution.

11.5.5 Future projections

The SREX report (SREX Ch. 3) stressed the low availability of studies on flood projections under different emission scenarios and concluded there was *low confidence* in projections of flood events given the complexity of the mechanisms driving floods at the regional scale. The AR5 report (WG II, Ch. 7) justified a *medium confidence* statement on global flood trends despite stated uncertainties in coupled GCMs and hydrological models. SR15 (SR15 Ch. 3; IPCC 2018) assessed based on more recent literature that there was *medium confidence* that a global warming of 2°C would lead to an expansion of the fraction of global area affected by flood hazard, compared to conditions at 1.5°C of global warming, as a consequence of changes in heavy precipitation.

There is an increasing number of studies that have coupled GCMs and hydrological models to determine projected changes in floods under climate change scenarios. At the global scale, Alfieri et al., (2016) used downscaled projections from seven GCM to force a hydrodynamic model, which suggested an increase in the frequency of high floods with increasing levels of global warming (1.5°C, 2°C, 4°C) in all continents, with the exception of Europe. Nevertheless, previous studies suggested that flood hazard would possibly increase less uniformly on global scale, although many generally show a larger fraction of regions with increases than decreases. Dankers et al. (2014) used nine hydrological models forced by GCMs, and recorded an increase in floods in more than half of the global land grid points, with a consistent signal in central and eastern Siberia, Southeast Asia and India. Hirabayashi et al. (2013) used a high concentration scenario finding a consistent increase in the flood frequency in Southeast Asia, Peninsular India, eastern Africa and the northern half of the Andes, and a decrease in Europe (except for the British Isles), Southern South America and South US, although these conclusions have some limitations since this study used a limited grid-box run-off model that does not consider the transport along the stream. In a global study based on twenty-one GCMs for the CMIP3 A1B scenario, Arnell and Gosling (2016) found a significant decrease in the 100 year flood in the Mediterranean and in large areas of central and Eastern Europe, south West Africa and Central America, but no general changes in East Asia; on the other hand, that study found an increase in flood magnitude across humid tropical Africa, south and East Asia, the majority of South America and the high latitudes of Asia and North America. Based on 7-day flood magnitude and using four GCMs, Döll *et al.* (2018) showed no change in global flood frequency but a pattern with an increase in some regions and decrease in other regions. These changes include a decrease in flood frequency in East Europe and South Canada and an increase in Southeast Asia, although the agreement between models was low, except in Eastern Europe.

Continent-wide assessments show little consistency in the flood projections. In Europe, an increase in the flood frequency is found in a pair of analyses (Alfieri et al., 2015; Roudier et al., 2016), consistent with the projected changes in extreme precipitation (Rajczak and Schär, 2017). Nevertheless, flood projections show low spatial agreement between different studies. Kundzewicz et al. (2017) reviewed flood projections in this region and stressed the low agreement between studies developed at large spatial scales. In South Europe, Roudier et al.(2016) and Alfieri et al. (2015) found an increase in future flood intensity, while Giuntoli et al. (2015)found no changes and Dankers et al., (2014) a possible decrease in the magnitude of floods. Inconsistencies are also found in the Alps, with both increases and decreases being projected when applying different hydrological models (Köplin et al., 2014; Thober et al., 2018). Similarlyinconsistentassessments are found in Scandinavia(Alfieri et al., 2015; Arheimer and Lindström, 2015; Hall et al., 2014), central and East Europe (Hall et al., 2014; Roudier et al., 2016; Shkolnik et al., 2018) and the British Isles (Dankers et al., 2014; Hall et al., 2014; Thober et al., 2018).

In East Asia there are also inconsistencies between projections since some studies project increases (Dankers et al., 2014; Hirabayashi et al., 2013; Gu et al., 2014), decreases (Liu et al., 2017) or no changes (Arnell and Gosling, 2016) in future flood magnitude. On ther other hand, there is a consistent signal towards an increase in flood intensity in the basins of northern Eurasia (Shkolnik et al., 2018), an area where extreme precipitation is also projected to increase independently of methodological approaches.

In North and South America there are also strong differences among studies (Salathé et al., 2014). Naz et al. (2016) forced a hydrological model with dynamically downscaled and bias corrected outputs of GCMs and showed an increase of the flood frequency in the central US but low agreement between models in West and East US. An increase in maximum flow wasprojected by Wobus et al (2017) where they modeled more than 50000 streams in US under the RCP 8.5 scenario. In any case, these regional studies do not match with other global studies that suggest a decrease in the magnitude and frequency of floods across North America (e.g., Hirabayashi et al., 2013; Arnell and Gosling, 2016). On the contrary, most of global modelling aproaches but also regional studies show agreement in the increase of floods in regions like the Amazon (Sorribas et al., 2016; Langerwisch et al., 2013; Guimberteau et al., 2013; Zulkafli et al., 2016) and the Andes (Bozkurt et al., 2018). Although regional studies use more detailed orography and land cover, the models also have problems to reproduce hydrological processes that drive floods at these spatial scales (Bout and Jetten, 2018) and even uncertainties may increase more in high spatial resolution studies (Mateo et al., 2017) (so regional projections would be also effected by methodological uncertainties).

Summary: Impact models show limitations to reproduce flood events, affecting the confidence of the

future projections. There is *medium confidence* that increasing global warming would lead to a larger fraction of the globe affected by flood increases, although there are high geographical variations in the projections and some discrepancies in regional to continental studies. Consistent regional projections are found in the Amazon, the Andes and northern Eurasia in which there is *high confidence* in a projected increase of floods.

11.6 Droughts

Drought is an impact-dependent phenomenon: it may refer to agricultural impacts (e.g., crop yield reductions or failure), ecological impacts (e.g., tree mortality), or hydrological impacts (e.g., reductions in streamflow, and storages such as reservoirs, soil moisture and groundwater). Drought cannot be defined (Lloyd-Hughes, 2014) or directly measured based on a single variable (SREX Ch3, Vicente-Serrano, 2016). In simple terms, drought is a temporal anomaly from average moisture conditions during which limitations in water availability results in negative impacts of various components of natural systems and economic sectors. Droughts are often analysed using climate drought indices, which are synthetic measures of drought severity, duration and frequency calculated from time series of different climate variables (Mukherjee et al., 2018), and remotesensingbasedmethods(AghaKouchak et al., 2015). There are several drought indices published in the scientific literature, such as the Palmer Drought Severity Index (PDSI) or the Standardized Precipitation Evapotranspiration Index (SPEI), which were discussed in the SREX report (SREX Ch3), although these indices have some limitations. Furthermore, observations of the terrestrial water cycle (e.g. evapotranspiration, runoff, and soil moisture) are used to characterize drought severity (Berg et al., 2017) but they are also affected by uncertainties related to the availability of observations, land surface models used to make the estimations, land cover changes and other human influences. Table 11.SM.1 shows a list of drought metrics used for drought quantification and the analysis of drought trends and projections.

11.6.1 Mechanisms and drivers

Similar to many other extreme events (see Box 11.1), droughts occur as the combination of thermodynamical and dynamical processes. While dynamical processes affecting droughts are particularly important on interannual time scales, there is limited evidence of circulation changes attributable to greenhouse gas forcing. On the other hand, thermodynamical processes, including heat and moisture exchanges which are at least in part modulated by plant physiology at the land surface, are substantially affected by greenhouse gas forcing both at global and regional scale.

Atmospheric circulation patterns, which vary on interannual, decadal and longer time scales, is a strong contributor to the occurrence of single drought events (Schubert et al., 2016). Nonetheless, there is *low confidence* that changes in global circulation may explain long-term global drought trends. Sea Surface Temperature (SST) anomalies connected with El Niño-Southern Oscillation (ENSO) are important drivers of drought in large regions of the world (e.g., North and South America, South Africa, Australia) (Seager and Hoerling, 2014; Burgman and Jang, 2015; Dai, 2013; Schubert et al., 2016). In other regions droughts are affected by the combination of ENSO and other mechanisms (e.g. the Indian Ocean Dipole in East Africa and Indonesia) (Funk et al., 2018b; Lestari et al., 2018). Other regions like Northern Eurasia, Europe and North Africa, central and eastern Canada and the middle East are not SST-driven and other circulation patterns dominate (Schubert et al., 2016; Kingston et al., 2015; Raymond et al., 2018) but there is no evidence of changes in large scale circulation mechanisms driving drought trends in these regions (see Chapter 2). Future global mechanisms of drought could be affected by possible changes in the characteristics of ENSO events (Power et al., 2013). In tropical and subtropical regions recent drought occurrences have been linked to expansions and contractions of the Hadley cell (Davis and Birner, 2016; Feldl and Bordoni, 2016; Nguyen et al., 2015). However, multi-decadal changes in the position of the Hadley cell are part of the natural climate variability (Bronnimann et al., 2015), and there is still *low confidence* in a climate change signal independent of the natural climate variability (Staten et al., 2018).

The radiative forcing due to increase in atmopsheric CO_2 concentrations has warmed the atmosphere that, in absence of other influences, is a thermodynamical mechanism that could increase the potential evaporation (Epot) and subsequently, if leading to changes in actual evapotranspiration (ETa), the drought severity during low precipitation periods (Dai and Zhao, 2017). Potential evaporation is the amount of evaporation that would occur if sufficient water sources were available. It is sometimes refered as the drying –or evaporating- power of the atmosphere. It can be estimated using different methods. Some methods may overestimate it, such as those solely based on temperature. It is thus important to use equations that include both the radiative and aerodynamic controls of evaporation (Mcvicar et al., 2012; Sheffield et al., 2012). Epot is also the main variable used in the definition of the "aridity index". Vegetation can play a role since a higher CO_2 concentration may lead to a decrease of plant transpiration through physiological effects on plant photosynthesis (so called "anti-transpirant effect", e.g. (Roderick et al., 2015; Swann et al., 2016, Box 11.1). Nonetheless, the actual evapotranspiration (ETa) is a different variable from Epot that corresponds to the water fluxes from soil and vegetation to the atmosphere. ETa is a key hydrological variable and it is often much smaller than Epot (in particular in arid environments) since if soil moisture is limited, soil evaporation and/or plant transpiration cannot be sustained; Box 11.1). For soil moisture availability, ETa is the variable directly affecting how much moisture is evaporated and thus the more relevant variable than Epot.

Overall, soil moisture levels play an important role for drought development and intensification via its effects on evapotranspiration and associated land-atmospheric feedbacks (Miralles et al., 2018). If soil moisture becomes limited, plant transpiration is reduced, which on one hand may decrease the rate of soil drying, but on the other hand can lead to further drying through the following feedback loop (Seneviratne et al., 2010; Vogel et al., 2018): Because of decreased evapotranspiration, latent heat flux is reduced and there is an enhancement of the sensible heat flux that warms the atmosphere, which will tend to increase vapor pressure deficit (VPD) and advection and again increases Epot, potentially contributing to enhanced drought severity (Teuling, 2018). Seneviratne et al. (2013) showed that soil moisture-climate feedbacks are responsible for a substantial fraction of the simulated mid-latitude warming in climate projections for the 21st century (see also Box 11.1), with strong response of the relative partitioning of available energy into the latent and sensible heat fluxes. The process can be complex since vegetation coverage plays a role modulating albedo and providing access to deeper stores of water (both in the soil and groundwater), and land cover changes may alter evapotranspiration (Sterling et al., 2013; Döll et al., 2016; Woodward et al., 2014). Although there are methodological limitations to observe these thermodynamical processes, remote sensing estimations of the land evapotranspiration and combination with eddy-covariance towers allow to identify clear land-atmospheric feedbacks that affect land evapotranspiration (Miralles et al., 2018) and the main driver "flash droughts" (Otkin et al., 2016, 2018).

The assessment of drought mechanisms under future climate change scenarios is hampered by the limited availability of reliable model simulations, which is both the result of a large climate model dependency of drought projections in some regions (Section 11.6.5) as well as of methodogical choices. Some studies support wetting tendencies as a response to a warmer climate when considering globally-averaged changes in precipitation and runoff over land (Berg and Sheffield, 2018; Greve et al., 2017; Roderick et al., 2015; Scheff, 2018; Scheff et al., 2017; Yang et al., 2018c; Zhang et al., 2016c). On the other hand, drying tendencies are identified when focusing on increased Epot and related drought indices (Dai et al., 2018; Zhao and Dai, 2017), as well as to a smaller extent when considering projected changes in soil moisture (Dirmeyer et al., 2013; Greve et al., 2017). These differences can be partly explained by the fertilization effect of the CO_2 under enhanced concentrations for the end of this century, since CO_2 would affect plant stomata conductance and the water use efficiency (WUE) by vegetation (Greve et al., 2017; Lemordant et al., 2018; Milly and Dunne, 2016; Scheff et al., 2017; Swann et al., 2016). Thus, streamflow projections clearly respond to enhanced CO_2 concentrations in CMIP5 models (Yang et al., 2019). Nevertheless, there are still uncertainties regarding associated drought impacts, since although increased WUE could reduce hydrological droughts, the role of the CO_2 fertilization on vegetation growth and activity under water-limited conditions is still under debate (Allen et al., 2015) and recent studies indicate that models overestimate the plant benefits of the CO_2 fertilization (Kolby Smith et al., 2015), and also do not consider changes in the vegetation type (Roderick et al., 2015), and in the rooting depth (Trancoso et al., 2017). Finally, there are also uncertainties in the CO_2 forcing since fertilization effect of CO_2 will be probably smaller than the radiative role of CO_2(Dai et al., 2018).

Summary: There are several definitions of droughts and these definitions may affect assessments regarding their changes under increased greenhouse gas forcing (*high confidence*). It is important to distinguish meteorological drought (precipitation deficits) from soil drought (lack of soil moisture, also termed "agricultural drought", relevant for agriculture and ecosystems), hydrological drought (lack of streamflow), atmospheric dryness (lack of moisture in the air), and overall atmospheric evaporative demand (associated with Epot). In addition, there is *medium confidence* that the relative importance of these drought measures may change under enhanced CO_2 concentrations due to physiological effects of the latter on plant transpiration Drought events are both the result of dynamical and thermodynamical processes. There is *low confidence* that observed long-term changes in drought frequency and severity are primarily driven by changes in atmospheric circulation processes There is *medium confidence* that thermodynamical processes have enhanced the severity of drought and atmospheric dryness in some water limited regions and/or seasons.

11.6.2 Observed trends

The SREX report (SREX Ch3) and the AR5 (AR Ch2) assessed that there was *low to medium confidence* in trends in global droughts. However, the mean global drought trend is not a very meaningful metric since drought trends are strongly regional in scope (e.g. Sheffield et al., 2012). In addition, the publicly available climate data for the last century also have limitations for estimating global drought trends due to large uncertainties in precipitation data products (Trenberth et al., 2014; Dai and Zhao, 2017). The varyingnumber of meteorological stations in time introduce a bias in the spatial variance of the griddeddatasetswith implications in trend estimation in drought(Beguería et al., 2016). Some key climate variables (e.g. relative humidity, wind speed) show high uncertainties (Trenberth et al., 2014), low spatial coverage (Willett et al., 2014), and temporal inhomogeneities (Azorin-Molina et al., 2014). Moreover, the naturalclimatevariability(Dai et al., 2018) driven by large-scale mechanisms (e.g., ENSO, PDO) may mask drought trends (Trenberth et al., 2014).

Severe drought events have been recorded in recent decades in the Amazon (2005, 2010), south China (2009-2010), southwest North America (2011-2014), Australia (2001-2009), California (2014), the middle East (2012-2016) among others (Van Dijk et al., 2013;Marengo and Espinoza, 2016; Marengo et al., 2017; Dai and Zhao, 2017; Cook et al., 2018; Mann and Gleick, 2015;Rowell et al., 2015). It is difficult to identify any trends in precipitation-based drought indices such as the Standardized Precipitation Index (SPI) (Orlowsky and Seneviratne, 2013; Spinoni et al., 2014), with the exception of small increases in the drought frequency, duration and severity in Central and West Africa, Northeast China and small areas of the Amazon, the Mediterranean and Southeast Australia. Based on the two most widely used observational precipitation datasets (CRU and GPCC), trends are not significant in the annual and seasonal values of the SPI in the majority of the world, but are significant in some regions of West Africa and South America. Similar results are also observed for drought frequency and severity based on data by Spinoni *et al.*(2019) (Figure 11.SM.1).

[START FIGURE 11.12 HERE]

Figure 11.12: Observed Standardized Precipitation Index (SPI) for 12-month (Ann) and 3-month (JJA and DJF) time scales using the Climate Research Unit (CRU) and Global Precipitation Climatology Centre (GPCC) precipitation datasets from 1950 to 2016.

[END FIGURE 11.12 HERE]

SPI tends to underestimate drought in regions where evapotranspiration and/or Epot strongly contribute to drying. Ideally, a better measure of drought limitation for ecosystems or agriculture would be soil moisture, which is the amount of water available to plants (Seneviratne et al., 2010). However, there are only limited measurements of soil moisture from ground observations (Dorigo et al., 2011), which impedes their use in the analysis of trends. Alternatively, satellite measurements may be used, but the available records are only a few decades long and they are affected by uncertainties (Dorigo et al., 2012; Rodell et al., 2018). Finally, new centennial land surface model soil moisture simulations will be computed as part of CMIP6 and will be assessed as part of the SOD.

Global studies have often been based on drought indices that combine precipitation and Epot estimates, such as the PDSI (Dai, 2013; Dai and Zhao, 2017) or the SPEI (Vicente-Serrano et al., 2017a). The PDSI is a simplified water-balance model, which as highlighted in the SREX Ch3, is known to have several limitations. The SPEI compares available moisture from precipitation with atmospheric demand for evaporation (Epot). It should be noted that the PDSI and SPEI metrics are not estimates of soil moisture or runoff availability, and will generally provide higher drying estimates than soil moisture or runoff from a global climate model due to their reliance on potential evaporation (e.g. Milly and Dunne, 2016). SPEI- or PDSI-based metrics suggest a higher increase in the percentage of the world area affected by drying conditions over the last decades in comparison to the SPI (See Figure 11.SM.1 based on (Spinoni et al., 2019)), but there is *low confidence* in these trends given the stressed complexity of using Epot in drought indices, as its effect can be different in humid and dry environments but also between agricultural/ecological vs. hydrological drought conditions. Overall, regions showing dryness increases based on the SPI display higher dryness increases based on SPEI- or PDSI metrics. Additionally, enhanced drought severity expands to regions including central Europe, West Africa and North Canada with these metrics. Other regional studies suggest a drought increase associated to higher Epot in the Amazon (Marengo and Espinoza, 2016b; Fu et al., 2013), Iran (Tabari and Aghajanloo, 2013), the Fertile Crescent (Kelley et al., 2015; Mathbout et al., 2018) and Southern Europe (González-Hidalgo et al., 2018; Stagge et al., 2017). These findings are based on limited data and also potentially overestimate Epot effects on drought severity in humid environments (Berg and Sheffield, 2018;Milly and Dunne, 2016). It has been suggested that increased Epot could explain the occurrence of recent “flash droughts” in different world regions (Ford and Labosier, 2017; Hunt et al., 2014; Zhang et al., 2017c), although there is *low confidence* in this assessment due to limited evidence.

The assessment of hydrological drought trends is more complex as hydrological droughts are affected by land cover, groundwater and soil characteristics (Van Lanen et al., 2013; Van Loon and Laaha, 2015; Barker et al., 2016) as well as human activities (water management and demand, damming and land use changes.He et al., 2017; Veldkamp et al., 2017). Wada et al. (2013) estimate that human water consumption have intensified the magnitude of hydrological droughts by 20%-40% over the last 50 years. Thus, these authors stressed that in the Mediterranean (Vicente-Serrano et al., 2017b), and the central US, as well as in parts of Brazil (Martins et al., 2017; Otto *et al.*, 2015), the human water use contribution to hydrological droughts was more important than climatic factors. Groundwater abstractions mayalso affect streamflowdrought duration (Tijdeman et al., 2018).

There are few studies analysing hydrological drought trends but there is evidence of increased hydrological droughts in the Mediterranean (Giuntoli et al., 2013; Lorenzo-Lacruz et al., 2013), China (Zhang et al., 2018a) and southern Africa (Gudmundsson et al., 2019). In the US, depending on the methods, datasets and study periods, there are differences between studies that suggest an increase (Shukla et al., 2015; Udall and Overpeck, 2017) vs a decrease in hydrologicaldroughtfrequency(Mo and Lettenmaier, 2018). Shukla et al. (2015)suggesteded that the high temperatures observed in 2014 in California increased hydrological drought severity, and Udall and Overpeck (2017) estimated that between 1/6 and 1/2 of the flow reduction in the Colorado river between 2000-2014 was related to the unprecedented high temperatures. In the Mediterranean region there is also hydrological drought intensification that, in addition to human and land drivers, seems to be partially related to precipitation trends (Giuntoli et al., 2013; Gudmundsson et al., 2017) and increasedEpot(Vicente-Serrano et al., 2014), including associated effects related to actual evapotranspiration.

Summary: The limited data quality and availability, different drought definitions, and the regional variations in drought trends hinder definitive conclusions regarding *global* trends in drought severity and frequency. There is *medium confidence* that in some regions drought severity has increased due to precipitation decrease. There is *high confidence* that regions with increased drought severity are more expanded if increases in potential evaporation are considered; however there is *low confidence* in the extent to which such estimates can be used to approximate changes in drought severity. There is

***medium confidence* in increase in drought in the Mediterranean, West and Central Africa, and Southeast Australia. There is *high confidence* that human activities related to water management, damming and land use changes affect hydrological drought trends, making it difficult to isolate climate change signals.**

11.6.3 Model evaluation

Comparisons between observed and simulated droughts often show different results for different drought metrics, the regions analysed, the models used and the spatial resolution selected. Stegehuis et al., (2013) used an ensemble of regional model simulations for Europe and showed that models dry the soil too much in early summer, resulting in an excessive decrease of the latent heat fluxes, with potential implications for more severe drought in dry environments (Teuling, 2018). Vogel et al., (2018) have identified a trimodal distribution of hydrological and temperature projections of CMIP5 global climate models in Central Europe, whereby the driest models which project the most warming are found to have substantial bias in soil moisture-temperature coupling in present climate.

There can be a large spread in mean and temporal variability among drought simulations (Zhao and Dai, 2017), and the level of spread is affected by the drought metrics used. Ukkola *et al.* (2018) compared results from different CMIP5 models, and showed that although the spread among models is small for precipitation-based drought metrics, soil moisture- and runoff-based drought metrics have larger differences among models and stronger spatial contrasts in the agreement. In addition, the spread is higher in the regions where an enhanced drought condition is projected and under high-emission scenarios (Orlowsky and Seneviratne, 2013). Model selection based on their ability to reproduce observed indices may artificially reduce the range of drought projections due to model structural uncertainty (Herrera-Estrada and Sheffield, 2017).

There is some evidence that models reproduce a consistent drought signal at the global or the hemispheric scales (Nasrollahi et al., 2015; Zhao and Dai, 2017), but model disagreement at the regional scale is high. RegionalClimateModels do not reduce the prevailingbiases(Senatore et al., 2018) and have difficulties in reproducing the severity, duration and frequency of observed droughts in Canada (PaiMazumder and Done, 2014) and the US (Ganguli and Ganguly, 2016), and to reproduce spatial variability of drought in East Africa (Diasso and Abiodun, 2017), and to identify drought events and their trends in East Asia (Um et al., 2017). .

Orlowsky and Seneviratne (2013) compared drought trends using three different observation precipitation datasets and simulations by 32 CMIP5 models from 1950 to 2009 and showed agreement only in high latitudes (i.e., > 55° degrees from the equator). Nasrollahi et al. (2015) compared the area in drought conditions using 41 CMIP5 models for 1901–2005 and showed that the majority of models overestimated extreme drought conditions, particularly in the Southern Hemisphere. Zhao and Dai (2017) showed low spatial agreement between observed and modeled PDSI by CMIP3 and CMIP5 models from 1950 to 2014. Nevertheless, in some regions models reproduced the observed trends well (Mediterranean or South Asia (Zhao and Dai, 2017), Northwest US (Abatzoglou and Rupp, 2017) or the Amazon (Duffy et al., 2015)).

Finally, simulations of hydrological drought metrics show uncertainties related to the contribution of both GCMs and hydrological models (Bosshard et al., 2013; Giuntoli et al., 2015; Samaniego et al., 2017), but hydrological models forced by the same climate input data also show large spread (Van Huijgevoort et al., 2013).

Summary: There is *medium confidence* that climate models simulate the observed drought trends overall. There is, however, *medium confidence* that models reproduce recent drought trends in some regions (the Mediterranean, High North latitudes, Amazonia, South Asia and Northwest US).

11.6.4 Attribution

Anthropogenic influence on drought and water scarcity is complex, it includes climate influences, land use influences, and socio-economical influences (high confidence). Drought attribution studies are limited and do not adequately sample droughts over all regions. Attribution techniques and observed data sources also vary between these analyses. Many drought-focused attribution studies are inconclusive due to lack of observational data (e.g. Philip et al., 2017) and a lack of sufficiently reliable model simulations to determine the reliability of the attributable signal (Otto et al., 2018a; Philip et al., 2018a; Uhe et al., 2017). Furthermore, the attributable signal varies depending on the region, event timescale considered and the attributable signal of large-scale modes of variability, such as ENSO.

There have been a number of attribution studies of drought events or drying trends occurring in various regions in recent years, which have predominantly focused on meteorological drought. Some studies have determined an attributable signal being the severity or likelihood of observed drought events, particularly in the Mediterranean-type climates of South Africa and Europe. In addition, the observed increases in the land surface area affected by drought (defined by soil moisture deficits) can be reproduced by CMIP5 models only if anthropogenic forcings are involved (Mueller and Zhang, 2016).

In Europe, precipitation deficits of the magnitude of the 2011-2012 winter drought over the Iberian Peninsula were found to have decreased between the 1960s and 2000s (Trigo et al., 2013; Angélil et al., 2017). A multi-method and multi-model attribution study on the 2015 Central European drought found that it was inconclusive whether human-induced climate change was a driver of the rainfall deficit, because the results were very model and method dependent (Hauser et al., 2017). However, there is evidence that human emissions have contributed to drying trends in Southern Europe, and to an observed contrast in pan-European river flow, with tendencies towards wetter conditions in the north and drier conditions in the south (Gudmundsson et al., 2017).

In Africa, two studies determined that drought in southern Africa in 2016 was worsened by greenhouse gas forcing. The first study found that the likelihood of flash drought over southern Africa was tripled during the last 60 years mainly due to anthropogenic climate change (Yuan et al., 2018a). The second was a multi-step attribution study. It showed that climate change likely increased the intensity of the 2015/16 El Niño, contributing to further decreases in southern African precipitation, crop production and food availability (Funk et al., 2018a). However, there is only low confidence in the results, as the study was based on a single model. A study on the three-year 2015-2017 drought in the Western Cape region of South Africa also found a threefold increase in the likelihood of the lack of rainfall (Otto et al., 2018c). There are also some contradictory results among studies of a single event. In a study of the 2014 southern Levant drought (Bergaoui et al., 2015) found an anthropogenic influence on both magnitude of the event and its likelihood. However, a study focused on the 2014 low rainfall over the Horn of Africa found no anthropogenic influence (Marthews et al. 2015). In terms of dependence on event timescales, Lott et al. (2013) examined East African drought and found no evidence for human influence on the 2010 short rain failure, but an attributable increase in 2011 long rain failure, although the magnitude of increase depended on the estimated pattern by which human influence changed observed SSTs. Further studies have provided attribution statements of African drought events to large-scale modes of variability, such as the strong 2015 El Niño episode which increased the severity of Ethiopian drought (Philip et al., 2018a).

In addition to investigating drought in different locations and of varying duration, drought attribution studies in North America (Wehner et al., 2017) also explore different drought measures (meteorological, agricultural and hydrological). This re-examination demonstrates that, in addition to the region and event definition, attribution statements are potentially dependent on the model dataset examined, model treatment of human influence on observed SSTs and overall attribution framework used. Overall, the anthropogenic influence on US droughts is complex, with *limited evidence* for an attributable anthropogenic signal on observed precipitation deficits.

An attributable anthropogenic signal in observed droughts has not been found in regions of Asia and South America. No climate change signal was found in the record dry spell over Singapore-Malaysia in 2014 (Mcbride et al., 2015) or the drought in central southwest Asia in 2013/2014 (Barlow and Hoell, 2015). Similarly, in recent droughts occurring in South America, specifically in the southern Amazon region in

2010 (Hideo et al., 2013) and in northeast Brazil in 2014 (Otto, et al. 2015) and 2016 (Martins, E.S.P.R., Coelho, C.A.S., Haarsma, R., Otto, F.E.L., King, A.D., van Oldenborgh, G.J., Kew, S., Philip, S., Vasconcelos Junior, F.C. and Cullen, 2017; Quan et al., 2018) anthropogenicclimate change was not a dominant influence.

Results of drought event attribution studies in Australasia show either an increase in drought likelihood or no change depending on methods, regions and season. While the meteorological conditions associated with the 2013 New Zealand drought were attributed by Harrington et al. (2014) using the fully coupled CMIP5 models to be more probable as a result of anthropogenic climate change, Angélil et al. (2017) did not find a corresponding change in the dry end of simulated precipitation from a stand-alone atmospheric model. Several studies of Australian droughts of varying length demonstrate no significant change in meteorological droughts in the region related to anthropogenic climate change based on analysis of precipitation deficits (Cai et al., 2014b; King et al., 2014). However, co-occurring hot and dry conditions, such as in 2006 across southeast Australia are *likely* to have increased due to climate change (King et al., 2017).

Studies also highlight a complex interplay of anthropogenic and non-anthropogenic climatological factors. For example, anthropogenic warming contributed to the 2014 east African drought by increasing east African and west Pacific temperatures, and increasing the gradient between standardized western and central Pacific SST causing reduced rainfall, evapotranspiration, and soil moisture (Funk et al., 2015b). Several events have been independently re-examined using a single analytical approach and climate model datasets (Angélil et al., 2017), identifying several instances of diverging claims of the anthropogenic attributable change.

Summary:Anthropogenic influence on drought and water scarcity is complex, it includes climate influences, land use influences, and socio-economical influences (*high confidence*).There is *low confidence* in a global attribution of trends in large drought events over the last decades. There is *medium confidence* that recent severe drought events affecting the Mediterranean-type climates, in particular in Europe have an attributable anthropogenic component. There is *medium confidence* that an increasing trend in the severity or likelihood of observed drought events in Southern Africa and Southern Europe is due to anthropogenic effects.

11.6.5 Projections

The SREX report (SREX Ch3) highlighted projections of increased drought severity in some regions, including southern Europe and the Mediterranean, central Europe, Central America and Mexico, northeast Brazil, and southern Africa. Nevertheless, the report stressed *low confidence* in global drought projections given large spread between models and scenarios. The AR5 (AR5 Ch11 and 12) also stressed large uncertainties in drought projections at the regional and global scales.

Uncertainties in drought projections are affected by different processes, including the possible role of the CO_2 fertilization on the water use by vegetation (Roderick et al., 2015; Milly and Dunne, 2016; Swann, 2018), but also different thermodynamical processes that operate differently in dry and humid environments (see also Box 11.1). Huang et al. (2017) showed that humid areas warmed between 60-80% in comparison to dry regions, and stressed that this differential warming is not well represented in GCMs. This issue could underestimate warming in dry areas for future scenarios, reinforcing thermodynamic processes in water limited environments, which would contributing to more severe drought events (Dai et al., 2018). The different role of the Epot in humid and dry environments, but also the different influence on hydrological and agricultural/environmental droughts is an issue under future projections. Under water limited conditions a higher Epot could have negative impacts since it would cause increased water stress as a consequence of a higher evapotranspiration deficit, but also reductions in surface water by direct evaporation (Ukkola et al., 2016). Nonetheless, increases in evapotranspiration could also be limited compared to the increased Epot due to soil moisture limitation and effects of enhanced CO_2 on plant physiology (Berg et al., 2016). Therefore, under future warmer conditions, while dry regions could experience reinforced drought conditions as a consequence of land-atmospheric feedbacks and drought self-intensification (Miralles et al., 2018; Sherwood and Fu, 2014; Teuling, 2018), there remains substantial uncertainty with respect to the underlying mechanisms. For instance, in a recent study regarding changes in droughts and heatwaves in Central Europe, Vogel et al. (2018)) found that the CMIP5 ensemble displayed a trimodal distribution of projections, with distinct behaviours between “very dry”, “dry” and “wet” models. The application of an observational constraint for present-day land-atmosphere conditions revealed that the “very dry” models were less realistic (Vogel et al., 2018). Another study found using observational constraints for precipitation that the spread in projections of precipitation minus evaporation as a measure of water availability is reduced, suggesting that both extreme dry or wet projections are less realistic (Padrón et al., 2019). However, the constrained ensemble in this study also projected a stronger drying in the Amazon region.

Studies based on CMIP5 projections show a consistent signal in the sign and spatial pattern of drought projections in some regions. In terms of precipitation droughts, Orlowsky and Seneviratne (2013) and Martin (2018) showed that the model ensemble displayed robust signal-to-noise ratio in the Mediterranean, South Africa, Southern North America, Central America and Northeast Brazil, regions in which more frequent and severe droughts are projected. Projections of the 12-month SPI for different levels of warming relative to 1850-1900 mean show such spatial patterns, with an increase of drought severity according to the level of warming (Figure 11.13). Similar conclusions can be drawn for the number of consecutive dry days (Figure 11.14). In some regions such as the Mediterranean and South Africa, projected increase in the frequency of CDD becomes larger with higher level of warming (Figure 11.SM.2)

[START FIGURE 11.13 HERE]

Figure 11.13: Projected changes in 12-month Standardized Precipitation Index for projections at 1.5°C, 2°C, 3°C and 4°C of global warming compared to pre-industrial conditions (1850-1900), using empirical scaling relationship based on transient CMIP5 simulations. Cross-hatching highlights areas where at least two-thirds of the models agree on the sign of change as a measure of robustness.

[END FIGURE 11.13 HERE]

[START FIGURE 11.14 HERE]

Figure 11.14: Projected changes in consecutive dry days for projections at 1.5°C, 2°C, 3°C and 4°C of global warming compared to pre-industrial conditions (1850-1900), using empirical scaling relationship based on transient CMIP5 simulations. Cross-hatching highlights areas where at least two-thirds of the models agree on the sign of change as a measure of robustness.

[END FIGURE 11.14 HERE]

These geographic patterns are consistent with studies based on drought indices that consider Epot in the formulation. In general, the inclusion of Epot expands the spatial extent with drought conditions in the future (expanded to regions in the Amazon, most of North America, central Europe and East China) as well increase in drought severity in areas with projected precipitation decrease (Cook *et al.*, 2014; Dai *et al.*, 2018; Naumann *et al.*, 2018; Zhao and Dai, 2015). There is, however, *low confidence* in these findings, as the reliability of the models and the relevant physical processes, and relevance of Epot for drought stress are not well established. In particular, Milly and Dunne (2016)have highlighted that using Epot as a proxy for drought change will tend to overestimate projected drying, because of lack of consideration of decoupling of actual evapotranspiration and potentiation evaporation, when actual evapotranspiration is reduced due to soil moisture limitation or CO_2 effects on plant water use efficiency (Section 11.6.1), which can contribute to maintain the available surface water resources (Yang et al., 2019) .

Areas with projected soil moisture decreases do not fully coincide with areas with projected precipitation decreases, although there are substantial consistent patterns (Berg and Sheffield, 2018; Dirmeyer et al., 2013). Soil moisture is projected to decrease in some regions with projected precipitation increases including central North America, central Europe (Samaniego et al., 2018), the Amazonia and Northeast Brazil

(Orlowsky and Seneviratne, 2013) and East Africa(Rowell et al., 2015). Moisture in the top soil layer (10 cm.) is projected to have stronger drought severity than projected precipitation-based drought at all warming levels, extending the regions affected by severe soil moisture drought over most of South and Central Europe, North and South America, South Africa and East Asia (Figure 11.3, Figure 11.SM.1), possibly as a consequence of enhanced drying power of the atmosphere and thus associated increased evapotranspiration as highlighted by some studies (Dai et al., 2018; Orlowsky and Seneviratne, 2013).

There are substantial increases in risks of drying from 1.5°C to 2°C global warming as well as for further additional increments of global warming (Figs. 11.3 and 11.4). These findings, which are based on CMIP5 analyses are consistent with the conclusions of the SR15 Ch3 and Greve et al. (2018). Corresponding analyses based on CMIP6 projections will be provided in the SOD.

[START FIGURE 11.15 HERE]

Figure 11.15: Projected changes in surface soil moisture for projections at 1.5°C, 2°C, 3°C and 4°C of global warming compared to pre-industrial conditions (1850-1900), using empirical scaling relationship based on transient CMIP5 simulations. Cross-hatching highlights areas where at least two-thirds of the models agree on the sign of change as a measure of robustness.

[END FIGURE 11.15 HERE]

[START FIGURE 11.16 HERE]

Figure 11.16: Projected changes in surface soil moisture compared to pre-industrial conditions (1850-1900) as function of mean global warming, using empirical scaling relationship based on transient CMIP5 simulations. Analyses for 37 AR6 regions, the global ocean and the global land.

[END FIGURE 11.16 HERE]

Global averages of hydrological drought are projected to display a decrease in drought frequency but an increase in drought severity and duration (Wanders and Van Lanen, 2015). The regions that are more affected are those already stressed by drought including the Mediterranean, the middle East, South Africa, South Australia and Southern South America (Prudhomme et al., 2014; Wanders and Van Lanen, 2015). Models have smaller spread in future projections for northern latitudes, the Horn of Africa and Indonesia where a reduction of drought severity is projected. Streamflow droughts are projected to become more severe in Europe, except for north and northeast Europe. Streamflow in southern Europe can bereduce by 10-30% (Forzieri et al., 2014; Roudier et al., 2016). There is, however, only *medium confidence* in these projections due to large model uncertainties (Prudhomme et al., 2014; Gosling et al., 2017) and uncertainty in the projection of future human activities including water demands, land cover changes, etc., which may represent more than 50% of the projected changes in hydrological droughts (Wanders and Wada, 2015).

In addition, regions dependent on mountainous snowpack as a temporary reservoir are at risk of severe hydrological droughts in a warmer world. For instance, in the western United States, a 22% reduction in winter snow water equivalent is projected under a high emissions scenario by 2050 relative to historical levels with a further decrease to a 70% reduction by 2100 (Rhoades et al. 2018). The exact magnitude of the influence of higher temperatures on snow droughts is, however, difficult to estimate (Mote et al., 2016).

Summary: There is *medium confidence* in projected increases in drought frequency and severity in the Mediterranean, Southern Africa, Southern North America, Central America and Northeast Brazil. The *confidence* is assessed to be *medium* because while there is high agreement among climate models, there are uncertainties in drought representation in the climate models, the use of drought metrics in the projections, and lack of observations in several regions to evaluate models. Additionally, there are different types of drought (*climate, soil moisture and hydrology*) and there is also a lack of clear

understanding on the role of climate variables (precipitation and potential evaporation) on drought severity and the relevant physical processes. Streamflow drought projections have*lower confidence* than meteorological or soil moisture drought projections in general, though there is *medium confidence* for an increase in hydrological droughts in the Mediterranean, South Africa, South Australia and Southern South America.

11.7 Extreme storms

Extreme storms, such as tropical and extratropical cyclones, severe convective storms, and atmospheric rivers often have substantial societal impacts. Quantifying the relationship between climate change and extreme storms is challenging, partly because extreme storms are rare, short-lived, and local, and individual events are largely influenced by stochastic variability. The high degree of random variability makes detection and attribution of extreme storm trends more uncertain than detection and attribution of trends of other aspects of the environment in which the storms evolve (e.g., larger-scale temperature trends). Projecting changes in extreme storms is also challenging because of constraints in the models' ability to accurately represent small-scale physical processes. Despite the challenges though, good progress has been and continues to be made. The SREX assessed:

There is *low confidence* in observed long-term (40 years or more) trends in tropical cyclone (TC) intensity, frequency, and duration, and any observed trends in phenomena such as tornadoes and hail.
It is *likely* that extratropical storm tracks have shifted poleward in both the Northern and Southern Hemispheres and that heavy rainfalls and mean maximum wind speeds associated with TCs will increase with continued greenhouse gas (GHG) warming.

- It is *likely* that the global frequency of TCs will either decrease or remain essentially unchanged while it is *more likely than not* that the frequency of the most intense storms will increase substantially in some ocean basins.
- There is *low confidence* in projections of small-scale phenomena such as tornadoes and hail.
- There is *medium confidence* that there will be reduced frequency and a poleward shift of mid-latitude cyclones due to future anthropogenic climate change.

The AR5 maintained an assessment of *low confidence* in observed long-term trends in TC metrics but modified this statement from the SREX to state that it is *virtually certain* that there are increasing trends in the North Atlantic since the 1970s with *medium confidence* that anthropogenic aerosol forcing has contributed to these trends. Unchanged from the SREX, the AR5 concluded that it is *likely* that TC precipitation and mean intensity will increase and *more likely than not* that the frequency of the strongest storms increase with continued GHG warming. *Confidence* in projected trends in overall TC frequency remained *low*. *Confidence* in observed and projected trends in hail and tornado events also remained *low*.

The SROCC assessment of past and projected tropical and extratropical cyclones essentially follows the conclusions of the AR5 with some additional detail. Literature subsequent to the AR5 adds support to the likelihood of increasing trends in TC intensity and precipitation and frequency of the most intense storms while some newer studies have added uncertainty to projected trends in overall frequency. A growing body of post-AR5 research on the poleward migration of TCs led to a new assessment in the SROCC of *low-to-medium confidence* that the migration in the western North Pacific represents a detectable climate change contribution from anthropogenic forcing.

The conclusions of the SR1.5 essentially mirror the AR5 assessment of tropical and extratropical cyclones adding that heavy precipitation associated with TCs is projected to be higher at 2°C compared to 1.5°C global warming (medium confidence).

The SREX, AR5, SROCC, and SR1.5 do not provide assessments of the atmospheric river literature and the SROCC and SR1.5 do not assess severe convective storms. In this section, we assess the state of knowledge on the four phenomena of tropical and extratropical cyclones, severe convective storms, and atmospheric rivers. In this respect, our report will closely mirror the SROCC assessment of tropical and extratropical cyclones while updating the SREX and AR5 assessment of severe convective storms and introducing an assessment of atmospheric river literature.

11.7.1 Tropical cyclones

The SREX and AR5 stated that there is *low confidence* that any observed long-term increases in tropical cyclone (TC) –based metrics are robust, after accounting for past changes in observing capabilities and resultant data heterogeneity. The AR5 further stated that it is *virtually certain* that the frequency and intensity of the strongest tropical cyclones in the North Atlantic has increased since the 1970s and there is *medium confidence* that a reduction in aerosol forcing over the North Atlantic has contributed at least in part to these increases.

For 21st century projections of TC activity, the SREX and AR5 stated that it is *likely* that the global frequency of TCs will either decrease or remain essentially unchanged, concurrent with a *likely* increase in both global mean TC maximum wind speed and precipitation rates.

In Section 3.3.6 of SR1.5 (Hoegh-Guldberg et al., 2018), the following assessments are provided: “Tropical cyclones are projected to increase in intensity (with associated increases in heavy precipitation) although not in frequency (low confidence, limited evidence)”.
“there is only low confidence regarding changes in global tropical cyclone numbers under global warming over the last four decades.”

“Under 3 to 4 °C of warming it is *more likely than not (medium confidence)* that the global number of tropical cyclones would decrease whilst the number of very intense cyclones would increase.”
“There is thus limited evidence that the global number of tropical cyclones will be less under 2°C of global warming compared to 1.5 °C of warming, but with an increase in the number of very intense cyclones (low confidence).”

In Section 3.3.5 of SR1.5, “In coastal regions, increases in heavy precipitation associated with tropical cyclones combined with increased sea levels may lead to increased flooding.”

11.7.1.1 Mechanisms and drivers

Tropical cyclones (TCs) respond to their ambient environment in a number of ways. For example, latent and sensible surface heat fluxes provide energy that can be converted to wind, upper-level atmospheric temperatures modulate the thermodynamic limit on the peak winds that can be achieved, mid-to-upper-level winds steer the TCs and largely determine their translation speed (which strongly affects local rainfall totals), and vertical wind shear generally affects TC genesis and intensification. Changes in these and other environmental factors, whether as natural variability or by external forcing, are expected to manifest in changes in TC characteristics. This is true for both past and future changes.

The genesis of TCs and their development and tracks depend on conditions of the large-scale circulations of the atmosphere and ocean. The large-scale atmospheric circulations, such as the Hadley and Walker circulations and the monsoon circulations, affect climatalogical aspects of TC activities. Various types of internal atmospheric variabilities including intra-seasonal oscillations (e.g., the Madden-Julian oscillations, the Boreal Summer Intraseasonal Variabilities) and equatorial waves modulate TC activities. TCs also affect these large-scale circulations in various ways. The sea surface temperature distributions together with thermodynamic condition of the ocean mixed layer directly affects TC activities together with acting as driving forces of the large-scale circulations of the atmosphere. TC activities are also affected by interannual variabilities caused by the atmosphere-ocean coupled modes represented as ENSO, PDO, and AMO. It has been shown that other types of the ocean variabilities such as the Pacific meridional mode (PMM) have impacts on TC activity (Murakami et al., 2017; Zhang et al., 2016b). Because the time-scale of these modes is long such as multi-decadal, detection of anthropogenic effects from natural variabilities of these modes is generally difficult, it is *highly uncertain* that TC changes will be driven by projected changes of these modes. Aerosol forcing also affects SST patterns, and it is *likely* that the observed changes in TC activities are partly caused by changes in aerosol forcing (Takahashi et al., 2017). Among possible changes from these drivers, there is *medium-to-high confidence* that the Hadley cell is widening and will be wider in the future (Chapter 3, 4, and 5). This *likely* causes the latitudinal shifts of TC tracks (Sharmila and Walsh, 2018). Regional TC activity changes are strongly affected by projected change in sea surface temperature warming patterns (Yoshida et al., 2017), whichishighlyuncertain (Chapter 4, 9 [TBC]).

11.7.1.2 Observed trends

Identifying past trends in tropical cyclone (TC) metrics remains a challenge due to the heterogeneous character of the historical data. There are ongoing efforts to homogenize the data (e.g., Landsea et al. 2015; Kossin et al., 2013;Emanuel et al., 2018), but confidence remains low that any reported long-term (multidecadal to centennial) trends in TC frequency- or intensity-based metrics are not affected by changes in technology used to collect the data. This should not be interpreted as implying that no physical trends exist, but rather as indicating that either the quality or the availability of data are not high enough to provide statements with high confidence. There is evidence that the period of highest quality post-satellite era data is shorter than the timescale required for TC intensity trends to emerge from the noise, given the observed changes in the environment (Bender et al., 2010; Kossin et al., 2013). That is, given the observed trends in the background environment, and our theoretical understanding of how these trends affect TC intensity, it is not expected that a trend in TC intensity should be detectable over the past 40 years or so. Consistent with this, an increasing intensity trend remains after homogenization of the data over this period, but statistical confidence in the trend is presently less than 95%, although it is near 90% (Kossin et al., 2013) and there is evidence that the proportion of strong TCs has increased although the signal is much weaker in the homogenized data (Holland and Bruyère, 2014). This is also consistent with numerical modeling simulations, which generally indicate an increase in mean TC peak intensity and the frequency of very intense TCs in a warming world (Knutson et al., 2015; Walsh et al., 2015, 2016a).

Subsequent to the AR5, two new metrics that are comparatively less sensitive to data issues than frequency- and intensity-based metrics have been analyzed, and trends in these metrics have been identified over the past ~70 years. There has been a global poleward migration of the location where TCs reach their peak intensity (Kossin et al., 2014) and a global slowing of TC translation speed (Kossin, 2018). The poleward migration is consistent with the independently-observed expansion of the tropics (Lucas et al., 2014), and has been linked to changes in the Hadley circulation (Altman et al., 2018; Sharmila and Walsh, 2018; Studholme and Gulev, 2018). The migration is also apparent in the locations where TCs exhibit eyes (Knapp et al. 2018), which is when they are most intense. Part of the northern hemisphere poleward migration is due to interbasin changes in TC frequency (Kossin et al., 2014; Moon et al. 2015; Kossin et al. 2016b; Moon et al. 2016), and the trends, as expected, can be sensitive to the time period chosen (Song and Klotzbach 2018; Tennile and Ellis 2017; Kossin 2018b) and to subsetting of the data by intensity (Zhan and Wang 2017). The poleward migration is particularly pronounced in the western North Pacific basin, which has changed regional TC hazard exposure patterns (Park et al. 2014; Choi et al. 2016; He et al. 2017; Liang et al 2017; Oey and Chou 2016; He et al. 2015; Kossin et al. 2016a; Daloz and Camargo 2018; Wang et al. 2011; Liang et al. 2017), and a significant poleward trend remains after accounting for the known modes of dominant interannual to decadal variability in the region (Kossin et al. 2016a; Kossin 2018b; Knutson et al. 2018). A poleward trend in the western North Pacific is also found in CMIP5 model-simulated TCs (1980–2005) although it is weaker than observed and is not statistically significant (Kossin et al. 2016a). However, the trend is significant in 21st century CMIP5 projections under the Representative Concentration Pathway8.5 scenario, with a similar spatial pattern and magnitude to the past observed changes in that basin over the period 1945–2016 (Figure 11.7), supporting a possible anthropogenic contribution to the observed trends (Kossin et al. 2016a; Kossin 2018b).

[START FIGURE 11.17 HERE]

Figure 11.17: A multipanel figure showing polar migration pf tropical cyclones in Atlantic and Pacific basins in the

observations and CMIP5 simulations. [This is a placeholder (from a presentation). Jim will put something more aesthetically together for FOD.]

[END FIGURE 11.17 HERE]

Another recently-analyzed metric that is comparatively less sensitive to data issues than frequency- and intensity-based metrics is TC translation speed (Kossin, 2018), which has slowed globally by about 10% over the period 1949-2016. TC translation speed is a measure of the speed at which TCs move across the Earth's surface and is very closely related to local rainfall amounts (i.e., slower translation speed causes greater local rainfall). TC translation speed also affects structural wind damage and coastal storm surge by changing hazard event duration. The slowdown is observed in all basins except the Northern Indian Ocean and is also found in a number of regions where TCs interact directly with land. The slowing TC translation speed is expected to increase local rainfall totals, which would increase coastal and inland flooding. It is not yet clear what the cause of the slowdown is, but it is consistent, at least in sign, with expectations for weakening atmospheric circulation in a warming world (e.g., Held and Soden, 2006; He and Soden, 2015).

11.7.1.3 Model evaluation

Projecting future TC activity has two principal sources of uncertainties: changes in the relevant environmental factors (e.g. SST) that can affect TC activity, and the actual changes in TC activity under a given environmental condition. For evaluation of projections of TC-relevant environmental variables, the confidence statements of AR5 were based on global temperature and moisture, but not on the detailed regional structure of SST and atmospheric circulation changes such as steering flows and vertical shear, which affect characteristics of TCs (genesis, intensity, tracks, etc). For evaluation of TC simulation, the capabilities of models at simulating present-day TC climatologies and variability for certain TC metrics have been evaluated in various aspects, as reviewed in (Walsh et al., 2015; Camargo and Wing, 2016; Knutson et al., 2018a, 2018b)). Examples of TC climatology/variability metrics are spatial distributions of TC occurrence and genesis (Walsh et al., 2015) and seasonal cycles and interannual variability of basin-wide activity (Kodama et al., 2014; Shaevitz et al., 2014; Zhao et al., 2009) or landfalling activity (Lok and Chan, 2017).

CMIP5/6 class climate models (~100-200 km grid spacing) generally do not simulate TCs of Category 4-5 intensity. HighResMIP-class global models (~10-60 km grid spacing) begin to capture some structures of TCs more realistically as well as produce intense TCs of Category 4-5 despite the need to still parameterize deep cumulus convection processes (Roberts et al. 2018; Wehner et al., 2015). Convection permitting models, (~1-10 km grid-spacing) such as used in some dynamical downscaling studies provide further realism. Model characteristics besides resolution, especially details of convective parameterization, can influence a model's ability to simulate intense TCs (He and Posselt, 2015; Kim et al., 2018; Reed and Jablonowski, 2011). However, models' dynamical cores also affect simulated TC properties (Reed et al., 2015b). Both wide-area regional and global convective-permitting models (1-10 km grid spacing) without the need for parameterized convection are becoming more useful for TC projection studies (regional model projection studies: Kanada et al. (2017), Gutmann et al. (2018); global model projection studies: Satoh et al., 2015; Yamada et al., 2017; Satoh et al., 2017)), as they capture more realistic eye-wall structures of TCs (Kinter et al., 2013) and are becoming more useful for investigation of changes in TC structures (Kanada et al., 2013; Yamada et al., 2017). Large ensemble simulations of the global climate mode with 60 km grid spacing provides TC statistics with more detectable projection which are not well captured in a single experiment (Yoshida et al., 2017). The operational models have great capability of simulating TCs and their use for climate projection studies is promising. However, there is only limited application of direct use of the operational models for future projection as they are highly tuned for operational purposes and development is ongoing. In particular, enhancement of horizontal resolution offers promise for more credible projections of TCs (Nakano et al., 2017).

Even with higher resolution models, TC projection studies generally include assumptions in experimental design that introduce uncertainty. For example, many studies use specified SST experimental designs, in which the atmosphere does affect the surface ocean to avoid the high computational cost of spinning up high resolution models. The lack of a trailing cold wake in SST could be an important limitation in analysis of intense TCs. Even for specified SST experiments, computational constraints often limit the number of simulations permitted resulting in relatively small ensemble sizes and an incomplete analysis of possible future SST magnitude and pattern changes (Knutson et al., 2013; Zhao and Held, 2011). Uncertainties in aerosol forcings also are reflected in TC projection uncertainty (Wang et al., 2014).

In a case study of Hurricane Harvey, Trenberth et al. (2018) suggest that the lack of realistic hurricane activity within coupled climate models hampers the models' ability to simulate SST and ocean heat content and their changes.

11.7.1.4 Detection and attribution, event attribution

There is general agreement in the literature that anthropogenic greenhouse gases and aerosols have measurably affected observed oceanic and atmospheric variability in the North Atlantic and in the Pacific. This led to the AR5 assessment of medium confidence that humans have contributed to the observed increase in Atlantic hurricane activity since the 1970s. Literature subsequent to the AR5 lends further support to this statement (Knutson et al., 2019a). However, there is still no consensus on the relative magnitude of human and natural influences on past changes in hurricane activity, and particularly which factor has dominated the observed increase. This remains a very active area of research.

The recent active TC seasons particularly in 2015 have been tested for an anthropogenic influence by (Murakami et al., 2017)(Murakami et al., 2017)Murakami et al. (2017) for the unusually high TC frequency near Hawaii and in the eastern Pacific basin, by Zhang et al. (2016) for high Accumulated Cyclone Energy (ACE) in the western North Pacific, and by Yang et al. (2017) for TC intensification in the western North Pacific. These studies suggest that the anomalous TC activity in 2015 was not only explained by the effect of a super El Nino (see section 11.11.x Case study: 2015 global extreme and Super El Nino), implying anthropogenic contribution to TC frequency. Takahashi et al. (2017)suggeted that the decrease in sulfate aerosol emissions caused about half of the observed decreasing trends in TC genesis frequency in the southeastern western North Pacific during 1992–2011. Murakami et al. (2018) concluded that the active 2017 Atlantic hurricane season was mainly caused by pronounced SSTs in the tropical North Atlantic and infered that this seasonal event will intensify by projected anthropogenic forcing.

In a case study of Hurricane Sandy's (2012), Lackmann (2014) finds no statistically significant impact of anthropogenic climate change on the intensity while projection in a warmer world showed significantly increased intensity. As for typhoon Haiyan, which struck the Philippines on 8 November 2013, Takayabu et al. (2015) took an event attribution approach with cloud system-resolving (~1km) downscaling ensemble experiments to evaluate anthropogenic effect on typhoons and showed that the intensity of the simulated worst case storm in the actual conditions was stronger than that in a hypothetical condition without historical anthropogenic forcing. However, in a similar approach with two coarser parameterized convection models, Wehner et al. (2018) found conflicting human influences on Haiyan's intensity. Kanada et al. (2017) obtained robust anthropogenic intensification on a strong typhoon using 5-km mesh multi-models whose resuoltion is required to simulate realistic rapid intensification of a TC (Kanada and Wada, 2016). In contrast to these convection permitting simulations, Patricola and Wehner (2018) found little evidence of an attributable change in intensity in 15 different TCs using a regional climate model configured between 3 and 4.5 km. They did however find that attributable increases in heavy precipitation totals for some of the 15 TCs that could be traced to a storm structural change.

The dominant factor in the extreme rainfall amounts during Hurricane Harvey's passage onto the U.S. in 2017 was its slow translation speed. But studies published after the event have argued that anthropogenic climate change contributed to an increase in rain rate, which compounded the extreme local rainfall amounts due to this slow translation. Emanuel (2017) used a large set of synthetically-generated storms and showed that the occurrence of extreme rainfall as observed in Harvey was substantially enhanced by anthropogenic changes to the large-scale environment. Trenberth et al. (2018) linked Harvey's rainfall totals to the anomalously large ocean heat content from the Gulf of Mexico. van Oldenborgh et al. (2017) and Risser and Wehner (2017) applied extreme value analysis to extreme rainfall records in the Houston, TX region both attributing large increases to climate change. Large precipitation increases during Harvey due to warming were also found using climate models (van Oldenborgh et al., 2017; Wang et al., 2018b). Similar precipitation increases in excess to that expected from Clausius-Clapeyron scalingwere predicted in advance from a forecast model for Hurricane Florence in 2008 by Reed et al., (2019). Urbanization was also found to be a contributing factor to the large precipitation totals of Harvey (Zhang et al., 2018c).

11.7.1.5 Projections

A summary of the studies on the TC projections for the late 21st century, particularly studies covering after AR5, is given by Knutson et al. (2018b). AR6 confidence levels stated above from the SREX and AR5 for either essentially unchanged or the decrease in global frequency of TCs and the increases in global mean TC maximum wind speed and precipitation rates remain the same. At the individual basin scale, confidence levels are broadly similar though slightly less than for the global scale.

Projections of future changes in the frequency of TCs are highly uncertain. Genesis Potential Indices (GPI) from climate models project general increases as the climate warms (Zhang et al., 2010). However, while a traditional GPI well describes the observed interannual variability of current TC frequency (Camargo et al., 2007), it fails to predict the decreased TC frequency found in warmer simulations of a high resolution model (Wehner et al., 2015). In fact, most but not all TC permitting global simulations project significant reductions in the total number of tropical cyclones with the bulk of the reduction at the weaker end of the intensity spectrum as the climate warms (Knutson et al., 2019b) except for a recent high-resolution coupled model result (Bhatia et al., 2018). Additionally, most of these simulations also project increases in the numbers of intense TC (Category 4-5 in the Saffir-Simpson scale) as well as an increase in the intensity of the very strongest TC. Summary of projection of TC characteristics in each basins is shown in Fig. 11.X. [Waiting for HighResMIP results].

The bottom-left panel of Figure 11.X shows the global number of TCs produced by a single TC permitting global model (CAM5) under stabilized warming levels of 1.5, 2 and 3C above preindustrial temperatures (Wehner et al., 2018c). The reduction in the total number of tropical storms is concentrated in categories 0 and 1 even though the number of intense storms is increased. However, uncertainty in such projections stemming from both the climate models as well as the details of the future SST and aerosol forcings magnitudes and patterns is high.

In a different approach, a seeded downscaled multi-model projection (Emanuel, 2013) exhibited increases in TC frequency consistent with GPI-based projections. This disparity in the sign of the projected change in global TC frequency is a reflection of the lack of a generally accepted theory of the climatology of tropical cyclogenesis (Walsh et al., 2015). Changes in SST are not the only controlling large scale environmental factor as the thermal and moisture vertical structures also were demonstrated to play a role in a series of idealized experiments (Walsh et al., 2015). Reductions in vertical convective mass flux due to increased tropical stability have been associated with a reduction in cyclogenesis (Held and Zhao, 2011; Sugi et al., 2012). Satoh et al. (2015a) further posits that the robust simulated increase in intense TCs, and hence increased vertical mass flux per TC, must lead to a decrease in TC frequency because of this association. GPI can be modified to mimic the TC frequency decreases of a model by altering the treatment of humidity (Camargo et al., 2014) supporting the idea that increase mid-tropospheric saturation deficit (Emanuel et al., 2008) controls TC frequency but the approach remains empirical. Other possible controlling factors, such as a decline in the number of seeds (which were held constant in Emanuel's downscaling), again due to increased atmospheric stability have also been proposed but questioned as an important factor (Patricola et al., 2018).

The projected increase in the number and intensity of the strongest TC is, however, on firm theoretical footing. Emanuel's (1987) model of intense TCs as a Carnot engine transporting heat from the surface to the top of the storm has worked well to describe the maximum intensity of observed TCs. The most intense TCs occur in a near perfect environment of low wind shear and high sensible and latent available energy. As such available energy must increase in a warmer world, this theoretical model provides a plausible explanation for the increased numbers of intense TC in nearly every TC permitting simulation of the future. Hence, confidence in this part of the projection is *high*.

Projected increase of intensity of TCs means the increase in the number of intense TCs or the ratio of the intence TCs to the total TCs, because the number of weak TC decreases in most projections while the number of intense TC increases. Intense TCs are generally defined as stronger categories such as Category 4-5 of the Saffir-Simpson scale, which is based on maximum sustained wind speeds of a TC. The mean projected increase in the proportion of Category 4–5 TCs is +23%, while the mean decrease in the global TC frequency is -10%, then it is inferred that global Category 4–5 TC frequency has a modest increase +11% (Knutson et al., 2019b Part II). The average increase in the global average TC maximum surface windspeeds is about 5% for a 2ºC global warming across a number of high resolution multi-decadal studies (Knutson et al., 2019b). TC intensities are also measued by quantities related to wind speeds by a TC such as Accumulated Cyclone Energy (ACE) or TC power dissipation index (PDI) (Murakami et al., 2014). Several TC modeling studies(Kim et al., 2014; Knutson et al., 2015; Yamada et al., 2010) project little change or decreases in global accumulated value of PDI or ACE, which is due to effects of decrease in the total number of TCs. Thus, it is projected that surface winds associated with a TC become stonger, while future probability of stronger winds associated with TCs decreases. However, at basin scale, significant differences exist between models and SST warming patterns. The number of the intense TCs in each basin might decrease depending on SST patterns, while the proportion of Category 4-5 TCs*likely* increases in most of basins as revealed by large-ensemble TC-resolving simulations (Sugi et al., 2017; Yoshida et al., 2017).

AR5 indicates projected increases in precipitation associated with TCs. While there are various metrics for TC precipitation, Knutson et al. (2019b Part II) suggested the use of TC-relative rainfall rate changes rather than accumulated rainfall at a given geographical location. In general, existing modeling studies agree on a projected increase in global average TC rainfall rates; a representative quantitative estimate for the increase is about 12% for a 2ºC global warming consistent with Clausius-Clapeyron scaling. Projection of TC precipitation using large-ensemble experiments (Kitoh and Endo, 2018, in revew) show that the annual maximum 1-day precipitation total is projected to increase, except for the western North Pacific where there is only a small change or even a reduction is projected, mainly due to a projected decrease of TC frequency in the western North Pacific. They also show that the 10 year return value of extreme Rx1day associated with TCs will greatly increase in a region extending from Hawaii to the south of Japan.. The confidence in an increase in globally averaged TC precipitation rates for individual storms is *medium-to-high*. Maximum accumulated rainfall rates in intense TCs may locally exceed Clausius-Clapeyron scaling by a large factor due to changes in storm structure even if the total storm rainfall rate follows this scaling (Patricola and Wehner, 2018).

Projected changes in TC tracks or TC areas of occurrence have considerable diversity of results from available studies, except for over the North Pacific. Several studies project either poleward or eastward expansion of TC occurrence over the North Pacific region, and more TC occurrence in the central North Pacific. A poleward expansion of the latitude of maximum TC intensity in the western North Pacific is consistent with the detected observed signals (Kossin et al., 2014, 2016) with a Hadley circulation expansion (Sharmila and Walsh, 2018). The bottom-right panel of Figure 11.X shows the zonal average TC storm track density from single model results by (Wehner et al., 2018a) at three warming levels and exhibits a poleward increase in the Northern Hemisphere as warmer SST will support TC-class wind speeds farther north until wind shear causes transition to extra-tropical storm properties. The southern hemisphere changes are due to a cyclogenesis shift in the Indian Ocean that may be model and forcing specific.

A slow down of the global TC propagation speeds is observationally detected (Kossin, 2018) and is consistent with the weakening of the atmospheric circulation projected with global warming. Weakening of steering flows are projected with global warming. However, the current model projection studies of TC propagation speeds show diverse results. Therefere, future projections of TC propagation speed are uncertain.

TC size is an important determinant of the area of the TC damages. No detectable anthropogenic influences on TC size have been identified to date. However, projection by high resolution models indicates future widening of TC scales if compared in the same categories of TCs (Yamada et al., 2017) although details may be basin dependent (Knutson et al., 2015). A plausible mechanism is that as the tropopause height becomes higher with global warming, the eye wall areas become wider because the eye walls are inclined to the tropopause. This effect is only reproduced in high resolution convection-permitting models capturing eye walls, and such modeling studies are not common. Moreover, the projected TC size changes are generally of the order of 10% or less, and these size changes are still highly variable between basins and studies. Thus, the projected change in TC size is uncertain.

The projection of coastal effects due to TCs depend on all the factors of TC characteristics, intensity, size, tracks, and transition speeds. Projected increases in sea level, average TC intensity, and TC rainfall rates each generally act to further elevate future storm surge risk. Changes in TC frequency could contribute toward increasing or decreasing future storm surge risk, depending on the net effects of changes in weaker vs stronger storms. Several studies (Garner et al., 2017; Little et al., 2015; McInnes et al., 2014, 2016) have explored future storm surge risk in the context of anthropogenic climate change with the influence of both sea level rise and the changes in future TC changes. Garner et al. (2017) investigated the near future changes in risks of New York City's coastal flood, and suggested a small change in storm-surge height because effects of TC intensification is compensated by the offshore shifts in TC tracks, but concluded that the overall effect due to the rising sea levels would likely increase of the flood risk. For the Pacific islands, McInnes et al. (2014) find that the future projected increase in storm surge risk in Fiji is dominated by sea level rise, and projected TC changes cause only a minor contribution. Among various storm surge risks, there is *highconfidence* that sea level rise will lead to higher risk due to extreme coastal water levels combined with storm surge due to TCs.

Confidence in projection of future TC activity relies not only on a consensus of models but also on whether the projection can be explained by a plausible theory. Hence, confidence is *very low* that the global frequency of TCs over all categories will decrease. Confidence is *very high* that the global frequency of intense TC will increase and the most intense TCs will become yet more so. Confidence is also *high* that average total TC precipitation will increase at Clausius-Clapeyron scaling rates globally. Local TC precipitation rates will increase in some intense TC at greater rates with *medium confidence*. A poleward shift in tropical cyclogenesis is projected with *medium confidence* and a slowdown in TC translational speed is projected with *low confidence*. Increases in TC size are projected with *low confidence*.

[START FIGURE 11.18 HERE]

Figure 11.18: Global view of basin level TC changes. [After (Knutson et al., 2019b), as an update of Fig. TS. 26 of AR5. (Waiting for HighResMIP results) with additional metrics such as ACE.] Bottom two panels show (left) projected global TC annual frequency by Saffir-Simpson scales from the high resolution version of CAM5 under present day, 1.5, 2.0 and 3.0C above stabilized preindustrial temperatures warming scenarios and (right) zonal mean TC track density for the same model and warming levels. Updated from (Wehner et al., 2018a).

[END FIGURE 11.18 HERE]

11.7.2 Extratropical cyclones (ETCs)

Mechanisms and drivers, detection and attribution and projections of weak and moderate ETCs are covered in Section 8.3.2.10 of Chapter 8. In this section we focus on trends and future changes related with the most extreme ETCs.

11.7.2.1 Observed trends

As discussed in Section 8.3.2.10 of Ch. 8, inconsistencies in reanalysis data, mostly related with changes in the type and/or amount of observed data assimilated by the reanalysis systems (Chang and Yau, 2016; Tilinina et al., 2013; Wang et al., 2016), prevent the estimation of reliable historical trends in ETC characteristics.

Observation shows an increase trend inPacific Ocean for theextreme winds of the 95 percentile of the surface winds estimated by microwave satellite data (Kruk et al., 2015)consistent with the trend of the average surface winds (Tokinaga and Xie, 2010), though these studies did not focused on ETCs. This is contrasted to the decreasing trend in the tropical region (Gastineau and Soden, 2011).

11.7.2.2 Model evaluation

The representation of extratropical cyclones in climate models has been assessed in terms of their frequency and intensity at global, hemispheric and regional scales (Di Luca et al., 2016b; Zappa et al., 2013a, 2013b) and their "signature" in different fields such as surface wind speeds, cloudiness, latent heat (Hawcroft et al., 2017) and precipitation(Catto et al., 2015; Hawcroft et al., 2016).

The evaluation of the frequency and intensity of ETCs commonly employs reanalysis data due to the need of homogeneous data in time and space. As both frequency and intensity of ETCs depend strongly on the horizontal resolution of the data, data is either preprocessed or the tracking algorithms tunned so that common spatial scales are assessed in both reanalysis and simulated datasets. For example, Zappa et al. (2013a) identify and track ETCs in 850-hPa vorticity fields from CMIP5 and the ERA-Interim reanalysis after removing spectral components of total wavenumbers larger than T42. More details on the evaluation of ETCs are provided in Chapter 8, in Section 8.3.2.10.2.

11.7.2.3 Detection and attribution, event attribution

The assessment on this topic is provided in Chapter 8, in Section 8.3.2.10.

11.7.2.4 Projections

Projected changes in ETCs show a variety of responses depending on the hemisphere, the season and the horizon of the projection (e.g., Grise and Polvani, 2014; Zappa et al., 2013). These differences are related with the interplay of several drivers whose role vary spatially and seasonally, often contributing in opposite ways to ETCs changes (e.g., Geng and Sugi, 2003; Grise et al., 2014; Grise and Polvani, 2014; Lehmann et al., 2014; Shaw et al., 2016). For example, in the NH the zonal-mean equator-to-pole temperature gradient decreases in the lower troposphere (due to polar amplification) but increases in the upper-troposphere and lower-stratosphere (due to tropical amplification) thus driving opposite changes in baroclinicity in the lower and upper troposphere. The absence of polar amplification at lower levels over the SH leads to a robust increase in the projected zonal-mean meridional temperature gradient that is largest at higher levels.
A second driver with conflicting responses is related with the general increase in water vapour. On one hand, the increase availability of water vapour leads to larger rates of diabatic heating within ETCs thus contributing to make them stronger (Li et al., 2014b; Shaw et al., 2016; Willison et al., 2013). On the other hand, more water vapour in the atmosphere means that weaker ETCs are needed to transport the same amount of latent heat thus imposing a constraints via the energetics of the large-scale circulation (Li et al., 2014b; Shaw et al., 2016). More water vapor also affects modification of trajectories of storm tracks; it leads to increased poleward propagation of ETCs together with to increased upper-level winds (Tamarin-Brodsky and Kaspi, 2017; Tamarin and Kaspi, 2017).

Another major driver of changes with opposing effects in ETC activity is associated with the changes in the sea surface temperature patterns. While the direct effect of the increase in greenhouse gases is to shift poleward the storm tracks in both hemispheres, the response of SSTs shows a nonsymmetric response with a poleward shift in the SH and a zonally dependent response in the NH (Grise and Polvani, 2014). Finally, particularly during austral summer in the SH, ozone recovery is projected to oppose the response to greenhouse gases at least for low-emission scenarios or for the near future (Grise and Polvani, 2014). There are also other more uncertain drivers that might change in the future such as the cloud-radiative effects and the vertical stratification as quantified for example using the static stability (Shaw et al., 2016).

Over the SH, projections suggest an overall poleward shift of the storm tracks and the ETC activity by the end of the century for all seasons with positive changes in ETC activity to the south of 45°S and negative changes to the north (Chang, 2017; Yettella and Kay, 2017). In austral winter, CMIP5 and other large ensembles (e.g., CESM Large Ensemble) projections suggest a widespread increase over most mid and high-latitudes (e.g., Yettella and Kay, 2017a). Over the SH, future changes (1980-1999 to 2081-2100) in extreme ETCs were studied by Chang (2017) in 26 CMIP5 models using a variety of cyclone intensity metrics. They showed an overall decrease in the total number of cyclones in the band 30-60° S by about 6% while the number of strong cyclones is projected to increase by at least 20% but as much as 50% depending on the specific criteria used to defined extreme cyclones. While the overall increases in the number of strong cyclones are observed in all seasons, regional variations are important with generally weaker and less robust increases over the South Pacific Ocean.

Over the NH, future changes in storm tracks and ETC activity show a less clear picture, with larger zonal and seasonal asymmetries (Grise and Polvani, 2014; Yettella and Kay, 2017; Zappa et al., 2013b). In boreal winter, CMIP5 projections show reduction in track density and the intensity of individual cyclones in the Norwegian and Mediterranean Seas and subtropical central Atlantic, while the track density increases close to the British Isles (Zappa et al., 2013a). In summer, the North Atlantic storm track shows a shift to the north with decreases in the frequency of ETC between 35 and 45° N and increases at around 60° N.

Changes in the intensity of cyclones are projected to be small (Li et al., 2014b; Yettella and Kay, 2017). New studies confirm that the precipitation associated with ETCs will increase in the future as reported in AR5 (e.g., Zappa et al., 2013). Based on an ensemble of simulations by a single model, Yettella and Kay (2017) found that the mean precipitation associated with ETCs will increase in the future following the increase in water vapour (i.e., due to thermodynamic effects; See Box 11.2) with the exception of the Mediterranean and some areas in North America in winter.

Projection of extreme winds show reduction in the tropics and increase in high-latitudes (Gastineau and Soden, 2009; McInnes et al., 2011). In regional scales, projections show increase in the northern Europe and decrease in the southern Europe including Mediterranean and the northern Africa (Donat et al., 2011) consistent with global tendency, while no robust change in China (Chen et al., 2012). A specific modeling study by (Booth et al., 2013) indicates that future more humidity may lead more rapid development of extratropical cyclone and more frequency of extreme winds.

11.7.2.5 Summary

Confidence in past changes in the frequency and intensity of extratropical cyclones is *low* due to inhomogeneities in the data and inconsistencies between studies. Medium confidence might be associated to an observed poleward shift in the SH storm tracks in summer largely explained by ozone depletion.
By the end of the century, there is *medium confidence* on a poleward shift in the SH storm track which will be more visible in winter and shoulder seasons. In summer season, the ozone recovery partially compensates the GHGs poleward shift thus increasing the uncertainty. It is *likely* that changes in the NH storm track will be more complicated than a simple poleward shift with polar amplification and SST pattern changes modifying the response. It is *very likely* that the precipitation associated with ETCs will increase in the future largely due to the thermodynamic effects. There is *low confidence* on changes in the intensity of ETCs.

Both observation and modeling shows trends and projections of reduction of extreme winds in the tropics and increase in high-latitudes, although no robust change is detected in regional scale such as in China. It is *likely* that these changes are drived by weakening of tropical overturning circulation and poleward shift and intensification of strom-track, as consistent with the wind change in general.

11.7.3 Severe convective storms

The assessment of changes in severe convective storms in the SREX and AR5 is quite limited and focused mainly on tornadoes and hail. In Chapter 3 of SREX (Seneviratne et al., 2012), it is assessed as "There is low confidence in observed trends in small-scale phenomena such as tornadoes and hail because of data inhomogeneities and inadequacies in monitoring systems". Subsequent works assessed in the CSSR (Kossin et al., 2017) led to the statement: "Tornado activity in the United States has become more variable, particularly over the 2000s, with a decrease in the number of days per year with tornadoes and an increase in the number of tornadoes on these days (*medium confidence*). Confidence in past trends for hail and severe thunderstorm winds, however, is low. Climate models consistently project environmental changes that would putatively support an increase in the frequency and intensity of severe thunderstorms (a category that combines tornadoes, hail, and winds), especially over regions that are currently prone to these hazards, but confidence in the details of this projected increase is low", while in SREX "Regarding other phenomena associated with extreme winds, such as thunderstorms, tornadoes, and mesoscale convective complexes, studies are too few in number to assess the effect of their changes on extreme winds. As well, historical data inhomogeneities mean that there is low confidence in any observed trends in these small-scale phenomena."

11.7.3.1 Mechanisms and drivers

Severe convective storms are convective systems that are associated with extreme phenomena such as tornadoes, hail, heavy precipitation (rain or snow), strong winds, and lightning. They sometimes are embedded in synoptic-scale weather systems such as tropical and extratropical cyclones and fronts (Kunkel et al., 2013). They are also generated as individual events not clearly embedded within larger-scale weather systems including meso-scale convective systems (MCSs) and mesoscale convective complex (MCC) (a special type of a large-organized and long-lived MCS) MCS and MCC are commonly associated with heavy rainfall, strong winds, hail, lightning and tornadoes. Characteristics of MCSs are viewed in new perspectives in recent years, probably because of both development of dense meso-scale observing networks (where?) and advances in high-resolution meso-scale modeling (see sections 11.7.3.2 and 11.7.3.3). The horizontal scale of MCSs is discussed with their organization of the convective structure and it is examined with a concept of "convective aggregation" in recent years (Holloway et al., 2017). MCSs sometimes take a linear shape and stay almost stationary with successive production of cumulonimbus on the upstream side (back-building type convection), and cause heavy rainfall (Schumacher and Johnson, 2005). Many of recent severe rainfall events in Japan are associated with line-shaped precipitation systems (Kunii et al., 2016; Oizumi et al., 2018; Tsuguti et al., 2018), suggesting common characteristics of severe precipitation at least in the Eastern Asia. Cloud microphysics characteristics of MCSs are examined and roles of warm rain processes on extreme precipitations are also stressed recently (Hamada et al., 2015; Sohn et al., 2013). It is unknown whether these types of MCSs are becoming more frequent in recent periods nor observed ubiquitously all over the world.

Severe convective storms occur under conditions preferable for deep convection, that is, conditionally unstable stratification, sufficient moisture both in lower and middle levels of the atmosphere, and a strong vertical shear. These large-scale environmental conditions are viewed as (necessary conditionsfor the?) occurrence of severe convective systems, or theresulting tornadoes and lightning. Frequently used metrics are atmospheric static stability, moisture content, conditional available potential energy (CAPE) and convective inhibition(CIN), wind shears or helicity including storm-relative environmental helicity (SREX) (Elsner et al., 2019; Tochimoto and Niino, 2018). These metrics, largely controlled by large-scale atmospheric circulations or synoptic weather systems such as TCs and ETCs, are then generally used to examine severe convective systems. In early June of the Eastern Asia, associated with the Baiu/Changma/Mei-yu, severe precipitations are frequently caused with MCSs. Severe precipitations are also caused by remote effects of TCs known as predecessor rain events (PREs) (Galarneau et al., 2010). Atmospheric rivers and other coherent types of enhanced water vapor flux also have the potential to induce severe convective systems (Kamae et al., 2017a; Ralph et al., 2018; Waliser and Guan, 2017). Combined with the above drivers, topographical effects also enhances intensity and duration of severe convective systems and associated precipitation (Piaget et al., 2015).

11.7.3.2 Observed trends

Observed trends of severe convective storms or MCSs are not so much documented, but climatology of MCSs are analyzed in specific regions (North America, Southe America, Europe, Asia). Because definition of MCSs depends on literatures, it is not straightfoward to make a synthetic view of MCSs in different regions. However, analysis using satellite observations provides global view of MCSs (Kossin et al., 2017).

The observed trends of severe storms in the United States are extensively reviewed by (Kossin et al., 2017; Kunkel et al., 2013) including severe convective storms which are associated with tornades, hail, and severe thunderstorms, and severe snow- and ice-storms. There is no significant increase of convective storms, and hails and severe thunderstorms. It is likely that tornado activity has increased in the United States particularly over the 2000s, with a decrease in the number of days per year where tornadoes are observed but an increase in the number of tornadoes on days when they occur (Elsner et al., 2015, 2019; Kossin et al., 2017). Trends of MCSs are realtively more visible for particular aspects of MCSs such as activities in seasons and dependency on duration; Feng et al. (2016)analyzed that the observed increases in springtime total and extreme rainfall in the central United States are dominated by MCSs, with increased frequency and intensity of long-lasting MCSs. Westra et al. (2014) found that there is an increase in the intensity of short-duration convective events (minutes to hours) over the whole world. In Sahelian region, Taylor et al. (2017)analyzed MCSs using satellite observations since 1982 and showed increase in frequency of extreme storms. Prein and Holland (2018) estimated hail hazard from largescale environmental conditions using a statistical approach and showed increase trends in the United States, Europe, and Australia.

Studies on trends of severe convective storms and their ingredients out of the United States are limited. Tochimoto and Niino (2018) analyzed structure and environment of tornado associated with extratropical cyclones in Japan and compared with those in the United States. Global distribution of thunderstorms was analyzed by using the satellite TRMM data (Zipser et al., 2006). In Europe, climatology of tornadoes are compiled by (Antonescu et al., 2016b, 2016a), reporting increase of detected tornadoes between 1800 to 2014 in Europe, but this trend might be affected by density of observations. Thunderstorm climatology in the Mediterranean is analized by Galanaki et al. (2018). In South America, Durkee and Mote (2010) shows climatology of MCC. Climatology of MCS over Amazon is analyzed by Rehbein et al. (2018) using 14-year long infrared geostationary satellite image. TRMM classification of topographyc convection over South America is given by Rasmussen and Houze (2011). Climatology of MCC in marine time continent is analyzed by Trismidianto and Satyawardhana (2018).

11.7.3.3 Model evaluation

The explicit representation of MCSs require non-hydrostatic models with horizontal grid spacings below 5 km denoted as convection-permitting models or storm resolving models (see section X in Chapter 10). Such high resolution simulations are computationally too expensive to perform at the global scale and for long periods and alternative methods are generally used. For climate projection purposes, convection-permitting models are becoming available to run over a wide domain such as a continental scale or even over the global area and show realistic climatological characteristics of MCSs (Prein et al., 2015; Satoh et al., 2019). Future projections of MCSs are usually studied using a time slice approach by comparing simulations performed using historical conditions with those using future hypothesized conditions (Satoh et al., 2018). Convective-permitting models are used as the flagship project of CORDEX to particularly study projections of thunderstorms (Chapter 10). Upto now, individual studies use convective-permitting models for projection of MCSs. North American MCSs simulations by a convection-permitting model are conducted by Prein et al. (2017 ClimDyn) and used for future projections of MCSs in North America (Prein et al., 2017 NatCC). Future projections of precipitation is conducted using convective-permitting simulations around Japan

(Murata et al., 2015, 2017 Clim Dyn).

11.7.3.4 Detection and attribution, event attribution

It is extremely difficult to detect differences in time and space of severe convective storms (Kunkel et al., 2013). Although some ingredients that are favorable for severe thunderstorms have increased over the years, others have not; thus, overall, changes in the frequency of environments favorable for severe thunderstorms have not been statistically significant. Event attribution studies on severe convection events are now undertaken for some of cases, such as the case of the July 2018 heavy rainfall event in Japan (BOX 11.3 global extremes).

11.7.3.5 Projections

Only a limited number of papers is published on the projection of MCSs. Prein et al. (2017b) investigated future projection of North American MCSs simulations by a convection-permitting model and show increase in MCS frequency and increase in total MCS precipitation volume by the combined effect of increases in maximum precipitationrates associated with MCSs and increases in their size. Rasmussen et al. (2017) investigated future changes in the diurnal cycle of precipitation using a convection-permitting model which captures organized and propagating convection and showed that weak to moderate convection will decrease and strong convection will increase in frequency in the future.

Severe thunderstorms are generally formed in environments with large CAPE and strong vertical wind shear. Climate model simulations project an increase in CAPE in the future and no changes or decreases in the vertical wind shear, suggesting thatfavorable conditions for tornadoes and hails might increase in the future. Thus, it is suggested that activities of tornades will increase in future: Brooks (2013) for the United States, Muramatsu et al. (2016) for Japan, and Púčik et al. (2017) for Europe.

11.7.3.6 Summary

Severe convective storms are convective systems that associate with severe events such as tornadoes, hail, heavy precipitation (rain or snow), strong winds, and lightning. Their characteristics are viewed in new perspectives in recent years, such as convective aggregation, line-shaped convective systems, or warm rain processes. Because definition of severe convective storms depends on literature, it is not straightforward to make a synthetic view over the world. However, observation shows *medium confidence* of intensification of severe convective storms in different regions. For projection, there is *low-to-medium confidence*of future intensification of severe convective storms. There is limited evidence that severe convective storms show increase in frequency and increase in total precipitation, and it is that any projected changes.

11.7.4 Atmospheric rivers

Section 8.4.2.6.4 discusses the qualitative and quantitative definitions of atmospheric rivers, their association with extratropical cyclones (ETC), their role in transporting moisture poleward from the equator and future changes in frequency and magnitude. If an AR makes landfall, its interaction with local orography determines the pattern of precipitation. Orographic lifting by upslope flow can release much of the available moisture leading to very extreme precipitation and flooding (Konrad and Dettinger, 2017). In regions with frequent ARs, most extreme precipitation events are associated with this class of storm (Dettinger et al., 2018; Ralph and Dettinger, 2012; Ramos et al., 2015). Significant inland penetration can occur through low elevation gaps in otherwise high topography (Lavers and Villarini, 2015; Rutz et al., 2014).

As with other classes of storms (section 11.4.5), AR extreme precipitation is robustly projected to increase as saturation atmospheric water vapour increases. Hence, the number of AR extreme precipitation days is projected to increase in North American west coast regions (Hagos et al., 2016; Jeon et al., 2015) and can be expected to in other regions as well. Increases in extreme daily precipitation may scale with temperature below the C-C relationship if on-shore winds weaken. However, confidence is limited by the coarse resolution of CMIP5 and an inability to realistically represent orographic enhancement (Gao et al., 2016). Radić et al. (2015) found that IVT patterns associated with extreme precipitation in British Columbia increase in frequency in a warmer world in 4 of the 5 CMIP5 models analysed, suggesting that changes in large scale dynamics will also contribute to increases in extreme precipitation event frequency. Weak changes in spatial dependence in extreme precipitation may also occur but confidence is low (Jeon et al., 2015)

[PLACEHOLDER for figure: A projection result from the ARTMIP study of CMIP5 models. This will be RCP8.5 but not ready for the FOD. However, it would encompass both model and AR definition structural uncertainty.]

In some regions, mostly near or downwind a west coast, atmospheric rivers produce the most extreme precipitation events. Extreme precipitation due to atmospheric rivers is *very likely* to increase in a warmer climate. Resolution constraints in CMIP5 limit the important orographic lifting component of extreme precipitation and hence confidence in the magnitude of this increase is *low*. Confidence in changes in future AR landfall location is also *low* due to biases in simulated large-scale circulation features, especially mid-latitude jets.

11.7.5 Synthesis across storms

[PLACEHOLDER FOR SOD: Put some synthesis paragraph including summary of this section]

Very few of the various aspects of observational trends and future changes of extreme storms are robust and attributable to anthropogenic changes. It is likely that poleward shifts of storm tracks is associated with the expansion of Hadley cell, and about as likely as not that a slow down of TC translation speed is associated with the slowing down of mean TC steering flow. It is *likely* that increased specific humidty due to anthropogenic global warming leads to more frequent intense TCs (categories 4 and 5) and increased TC precipitation as well as intensification of ETCs and severe storms. There is *low to medium considence* that hail, tornades, and thunderstorms embedded in severe storms are more frequent and have intensified due to the short length of high quality data records. Both observation and modeling show a reduction of extreme winds in the tropics and an increase in high-latitudes. It is *likely* that these changes are driven by a weakening of tropical overturning circulation and poleward shift and intensification of storm-track.

11.8 Compound events

The occurrence of multiple extremes concurrently or in succession, or the so-called “compound events” (SREX Ch3), can lead to impacts that are much larger than the sum of the impacts due to the occurrence of individual extremes alone. This is because multiple stressors can exceed the coping capacity of a system more quickly. For instance, co-occurring extreme precipitation and extreme winds can result in massive infrastructural damage (Martius et al., 2016); the compounding of storm surge and precipitation extremes can cause devastating coastal floods (Wahl et al., 2015); and combination of drought and heat can lead to tree mortality (Allen et al., 2015). The driving variables for compound extremes are often statistically dependent (Zscheischler and Seneviratne, 2017), which may amplify the associated impacts compared to what would be expected if the same variables were independent (Zscheischler et al., 2014; Wahl et al., 2015; Martius et al., 2016).

The IPCC SREX first introduced compound events in an IPCC assessment (SREX Ch3). In the SREX Ch3, compound events were defined as “(1) two or more extreme events occurring simultaneously or successively,

(2) combinations of extreme events with underlying conditions that amplify the impact of the events, or (3) combinations of events that are not themselves extremes but lead to an extreme event or impact when combined. The contributing events can be of similar (clustered multiple events) or of different type(s). Leonard et al. (2014) sought to unify these concepts with a particular emphasis on how processes relate to each other, defining compound events as "an extreme impact that depends on multiple statistically dependent variables or events". In an attempt to harmonize previous definitions with a clear focus on the risk framework established by the IPCC, and also highlighting that compound events may not necessarily result from dependent drivers, Zscheischler et al., (2018b) define compound weather/climate events as "the combination of multiple drivers and/or hazards that contributes to societal or environmental risk". We use this definition in the present assessment. Drivers include processes, variables and phenomena in the climate and weather domain that may span over multiple spatial and temporal scales. Hazards are usually the immediate physical precursors to negative impacts (such as floods, heatwaves, wildfire), but can occasionally have positive outcomes (Flach et al., 2018). This definition of compound events includes concurrent climate extremes, but also includes events with extreme impacts associated with climate drivers that might not be extremes themselves. Linking compound events to risk highlights the needed interaction of WG I of the IPCC, dealing with the physical domain, with WG II, which focuses on impacts of climate change (also relevant for Chapter 12 of the present report).

Many major climate-related catastrophes are inherently of a compound nature (Zscheischler et al., 2018). This has been highlighted for a broad range of Australian hazards such as droughts, heatwaves, wildfires, coastal extremes, and floods(Westra et al., 2016). It also holds for other regions of the world. As a natural extension of analyses of univariate climate extremes, many studies investigate the likelihood of concurrent extremes that are known to cause potential impacts at the same location. This likelihood can change due to a change in the likelihood of individual drivers or extremes/hazards but also due to a change in the dependence between extremes. For instance, the dependence between dry and hot summers is projected to intensify in the future in many regions (Zscheischler and Seneviratne, 2017). Similarly, the dependence between precipitation extremes and storm surge increased at US coasts during the observational period (Wahl et al., 2015). Spatial dependencies of extremes may change as well, affecting the likelihood of compound events. A decreasing spatial dependence in extreme snowfall in the French Alps has been observed over recent decades (Nicolet et al., 2016). Changes in the co-occurrence of extreme rainfall in West Africa since 1950 affect drought and flood patterns (Blanchet et al., 2018). Finally, clear associations have been shown between the spatial extent of individual storms and the atmospheric temperature (Wasko et al., 2016). Current assessments of such changes in dependence are often uncertain, and future changes are typically very difficult to quantify.

Extremes may occur at different locations but affect the same system, for instance heat waves affecting crop yields and possibly global food prices. Finally, large impacts may occur not because of multiple climate extremes but because of large multivariate anomalies in the climate drivers, if systems are adapted to the historical multivariate climate variability (Flach et al., 2017). For instance, ecosystems are typically adapted to the local covariability of temperature and precipitation such that a bivariate anomaly may have a large impact even though neither temperature nor precipitation may be extreme based on a univariate assessment (Mahony and Cannon, 2018). Given that almost all systems are affected by weather and climate phenomena at multiple space-time scales, it is natural to consider extremes in a compound event framework. Despite this recognition, the literature on past and future changes in compound event is limited. Section 11.8 assesses a few types of compound events warranted by available literature.

11.8.1 Concurrent extremes at coastal regions

Coastal zones are often prone to a number of meteorological extreme events. Sea level extremes and their physical impacts in the coastal zone arise from a complex set of atmospheric, oceanic and terrestrial processes that interact on a range of spatial and temporal scales and will be modified by a changing climate, including sea level rise (McInnes et al., 2016). A major hazard in coastal regions around the world is floods. Due to the lack of representative data, the assessment of flood likelihoods is often not based on actual flood measurements. More often, flood risk is estimated from its main drivers including astronomical tide, storm surge, heavy precipitation and high streamflow. A single driver analysis might underestimate flood risk if multiple correlated drivers contribute to the risk (e.g., van den Hurk et al., 2015). Floods with multiple drivers are often referred as “compound floods” (Moftakhari et al., 2017; Wahl et al., 2015).

At US coasts, the likelihood of co-occurring storm surge and heavy precipitation is higher for the Atlantic/Gulf coast relative to the Pacific coast (Wahl et al., 2015). Furthermore, all 6 studied locations at the US coast with long overlapping time series show an increase in the dependence between heavy precipitation and storm surge over the last century, leading to more frequent co-occurring storm surge and heavy precipitation events at the present day (Wahl et al., 2015). Storm surge and extreme rainfall are also dependent in most locations at the Australian coast (Zheng et al., 2013). The dependence is strongest in the north and northwest of Australia, followed by the west and northeast of Australia. In contrast, the dependence is weak and/or statistically insignificant along southeast coast of Western Australia, along small parts of the South Australian coastline, and along the eastern part of the Victorian coast near Bass Strait (Wu et al., 2018). There are significant seasonal differences in the dependence between extreme storm surge and rainfall along the north and northwest coast of Australia, where dependence is very strong in summer and autumn, and becomes insignificant in spring and winter (Wu et al., 2018). Storm surge and heavy precipitation are also related at coasts in the Netherlands. In the Noorderzijlvest area, this dependence leads to a more than two-fold increase in frequency of exceeding the highest warning level compared to the case if storm surge and heavy precipitation were independent (van den Hurk et al., 2015). At European coasts, storm surge and heavy precipitation show strong dependence in particularly along the Mediterranean Sea (Bevacqua et al., 2018). Under strong warming, the risk of compound flooding increases most strongly along the Atlantic coast and the North Sea. The increasing risk of compound flooding is mostly driven by an intensification of precipitation extremes and aggravates flooding risk due to sea level rise (Bevacqua et al., 2018).

Flood risk may also be influenced by the dependence between storm surge and river flow, and is increased by sea level rise due to climate change (Moftakhari et al., 2017). For instance, the occurrence of a North Sea storm surge directly after an extreme Rhine river discharge is much more likely due to their dependence compared to if both events would be independent (Kew et al., 2013).

Many coastal areas are prone to the occurrence of compound precipitation and wind extremes, which can cause great damages. For example, if strong winds destroy the roofs of buildings, the concomitant heavy rain causes substantially more damage. Another impact example is the hindered access to affected areas for rescue personnel as a consequence of blocked roads, e.g., by fallen trees or intense snowfall in winter. Martius et al. (2016) show a high percentage of co-occurring wind and precipitation extremes are found in coastal regions and in areas with frequent tropical cyclones.

11.8.2 Concurrent drought and heatwaves

Concurrent droughts and heatwaves have a number of negative impacts on human society and natural ecosystems. Concurrent droughts and heat can lead to crop failure (Barnabas et al., 2007), a reduction of carbon uptake potential of ecosystems (Ciais et al., 2005); Zscheischler et al., 2014; von Buttlar et al., 2018; Sippel et al., 2018b), tree mortality (Allen et al., 2010, 2015), increase wildfire risk (Brando et al., 2014; Ruffault et al., 2018), and higher risk of failure of electric power plants (Bartos and Chester, 2015; Cook et al., 2015). Drought and heatwaves are highly correlated in summer over land (Zscheischler and Seneviratne, 2017), mostly due to land-atmosphere feedbacks (Seneviratne et al., 2010). In addition to warmer mean temperatures, the correlation between drought and high temperatures in summer is expected to increase in the future (Zscheischler and Seneviratne, 2017), leading to immense challenges for adaptation.
Studies since SREX and AR5 show several occurrences of observed combinations of drought and heatwaves in various regions. Drought events characterized by low precipitation and extreme high temperatures occurred, for example, in 2014 in California (AghaKouchak et al., 2014), in 2013 in inland eastern Australia (King et al., 2014) and in 2015 in large parts of Central Europe (Orth et al., 2016b). In these regions, temperature and precipitation are strongly negatively correlated, with drought conditions (including low antecedent rainfall and soil moisture) enhancing summer temperatures extremes (Mueller and Seneviratne,

2012). There has been an increase in observed concurrence of meteorological drought and heatwaves across the United States (Mazdiyasni and AghaKouchak, 2015), however heatwave flash droughts (associated with high temperatures, increase evapotranspiration rates and decrease in soil moisture) decreased in the US over 1913-2011 and then increased (Mo and Lettenmaier, 2015). In India, the impact of meteorological drought is also amplified by the co-occurrence of heatwaves, which additional increase evapotranspiration rates and increase soil moisture deficits (Sharma et al., 2017).

Uncertainties in future projections of combined drought and heatwave events relate to model biases in precipitation, near-surface air temperature, evapotranspiration and land–atmospheric coupling strength. Accurate simulation of physical processes and their interactions are required. Overall, projections of increase in co-occurring drought and heatwaves are reported in northern Eurasia (Schubert et al., 2014), Europe (Orth et al., 2016b; Sedlmeier et al., 2018) and multiple regions of the United States (Diffenbaugh et al., 2015; (Herrera-Estrada and Sheffield, 2017).The dominant signal is related to the dominant increase of heatwave occurrence, which means that even if drought occurrence is unaffected, compound hot and dry events will be more frequent. The likelihood of co-occurring meteorological droughts and heatwaves has increased in the observational period in the United States (Mazdiyasni and AghaKouchak, 2015) and India (Sharma & Mujumdar, 2017) and will continue to do so under unabated warming (Hao et al., 2013; Herrera-Estrada and Sheffield, 2017; Zscheischler and Seneviratne, 2017).

Drought and heatwaves are also associated with wildfires, related through high temperatures, low soil moisture and low humidity. Concurrent hot and dry conditions amplifies wildfire risks in southern Europe (Russo et al., 2017), northern Eurasia (Schubert et al., 2014), USA (Littell et al., 2016) and Australia (Hope et al., in review BAMS). In the US, studies find fire seasons become longer in the future, mainly due to temperature increases. Fire potential increases in the Southwest, Rocky Mountains, northern Great Plains, Southeast, and Pacific coast, region (Liu et al., 2013). Uncertainties in projections of future compound wildfire risks relate to uncertainties in droughts and heatwaves, as well as their interactions with fire and the multiple characteristics of wildfire (frequency of events, severity of fire weather, spatial extent, duration of fire season). These characteristics have been examined in both process-based physical climate models and empirical statistical models. A study of the western USA examined the correlation between historical water-balance deficits and annual area burned, across a range of vegetation types f temperate rainforest to desert (McKenzie and Littell, 2017). The relationship between temperature and dryness, and wildfire, varied with ecosystem, and the fire-climate relationship was both nonstationary and vegetation-dependent. In the Mediterranean, projections for increased severity of future drought and heatwaves may lead to increased frequency of wildfires (Ruffault et al., 2018). In China’s Daxing’anling region, fire weather indices, together with temperature and moisture deficits (Drought and Duff Moisture Codes) were projected to increase for the period 2021-2050, relative to 1971-2000 (Tian et al., 2017).

PLACEHOLDER :*Synthesis statement in calibrated confidence language*

High temperature and droughts are also often strongly correlated with high ozone concentrations (Tai and Val Martin, 2017; Tai et al., 2014; Wang et al., 2017c; Zhang et al., 2018b). Ozone can negatively affect ecosystem carbon uptake (Oliver et al., 2018c; Franz et al., 2018, in review). Hence, there is a risk that dry and hot conditions could reduce carbon uptake through ozone effects.

11.8.3 Hot extremes and high humidity

Humans are very susceptible to extremely hot and humid conditions, which can induce hyperthermia in humans and other mammals, as dissipation of metabolic heat becomes impossible. The effect of extremely hot and dry conditions on humans is often measure with combined indicators such as the Wet Bulb Globe Temperature (WBGT) or variants thereof, which integrate temperature and relative humidity. Global warming of 7°C will create uninhabitable zones in the world because of extended periods of very hot and humid conditions (Sherwood and Huber, 2010). The Arabian Gulf is very likely to approach uninhabitability by the end of the century under a business as usual scenario (Pal and Eltahir, 2016). Humid heat stress may also strongly reduce labour capacity, up to 20% in peak months by 2050 under a business as usual scenario

(Dunne et al., 2013). Projections of combined indices such as Wet Bulb Globe Temperature are associated with large uncertainties associated with climate sensitivity, model uncertainty and the choice of bias correction (Zscheischler et al., 2019). However, because models that are biased cold typically show higher relative humidity and vice versa, model projections of WBGT are more certain due to a compensation of uncertainties in the contributing variables temperature and relative humidity (Fischer and Knutti, 2012).

11.8.4 Other types of compound events

[PLACEHOLDER, TO BE COMPLETED FOR SOD ; COULD FOR INSTANCE DISCUSS GEOMORPHOLOGICAL EXTREMES (SEE SREX) DEPENDING ON AVAILABLE LITERATURE]

11.9 Regional information on extremes

Chapter 11, like Chapters 10 and 12 from the AR6, is a regional chapter from the WG 1 assessment. For this reason, we provide hereafter detailed regional assessments of observed, attributed and projected changes in extremes across the AR6 regions (see Chapter 1 for definition). The assessments are organized by continents: Africa (11.9.1), Asia (11.9.2), Australasia (11.9.3), Europe (11.9.4), Central and South America (11.9.5) and North America (11.9.6). We also provide a synthesis across regions in Subsection 11.9.7.

[PLACEHOLDER for SOD: Possibly include Small Islands Developing States]

11.9.1 Africa

The SREX Ch3 had the following assessment for this region. There is *low to medium confidence*, depending on the sub-regions an increase in temperature extremes over Africa. For southern Africa, there is *medium confidence* in the increase of warm days and warm nights and decrease of cold days and cold nights. An increasing trend in warm nights was reported with *medium confidence* over northen Africa. This warming is *likely* to continue in the future in all sub-regions. For extreme precipitation, there is *low tomedium confidence* in regional trends due to lack of data and lack of consistency in reported patterns in some regions. In West Africa, there is *medium confidence* in an increase in observed precipitation intensity and increases in drought duration and intensity. There is *high confidence* in a *likely* increase in heavy precipitation in east Africa, and *medium confidence* in projected increase in the duration and intensity of drought in southern Africa.

An overview of assessments regarding changes in weather and climate extremes in Africa is provided in Table 11.3. The following paragraphs provide a summary of the main assessments.

Recent observational studies show considerable warming trend over most part of Africa accompanied by an increase in high temperature extremes. These include an increase in frequency of warm days and nights and decrease in frequency of cold days and nights over almost all the continent, where data are available. Additionally, heat waves, regardless definition, have been becoming more frequent, longer lasting and hotter over more than three decades in Africa. Future projections under two representative concentrations pathways (RCP4.5 and RCP8.5) show an increase in mean and extreme temperatures over Africa. Increases are also projected in the frequency of hot extremes such as warm days, warm nights and heat waves over most of the continent with the exception of Central Africa.

Precipitation extremes show spatially non-homogenous trends over the continent where data are available. Over Sahara and Sub-Saharan Africa, increases in the frequency and intensity of extreme precipitation have been observed. Significant upward trends for extreme precipitation-related indices are identified: in R10mm over Western Sahara and Sudan, in R20mm, SDII and R95p over western Sahel and in SDII, RX5day and consecutive wet day (CWD) counts over western and southern Africa. With regard to dryness, there is insufficient evidence to make an overall statement for the whole continent. Over Western Africa, there has been a significant decrease of consecutive dry day (CDD) counts, consistent with a weting tendency. An increase in CDD and in the frequency of meteorological droughts have been reported in Southern and Eastern Africa.

A strong increase in heavy precipitation (R95p) and in the length of dry spells (CDD) is projected under high emission scenarios (RCP8.5) by the end of 21st century over most of the continent with exception of central and eastern Africa. Further, models project a change in precipitation regime towards more scarce and intense precipitation over the continent. Particularly, in West and South Africa, projections show an increase in precipitation intensity and drought duration and intensity.

[START TABLE 11.3 HERE]

Table 11.3: Regional assessments for Africa (D&A stands for detection and attribution; EA stands for event attribution).

[END TABLE 11.3 HERE]

11.9.2 Asia

The SREX Ch3 had the following assessment for Asia. There is in an increase in warm days/nights and a decrease in cold days/nights. The confidence is *high* for the North, Central, East and West Asia and over the Tibetan Plateau, and *medium* over the Southeast and South Asia. There is *low* to *medium confidence* in increase in heavy precipitation and in dryness for most regions due to insufficient evidence or inconsistency in the direction of trends in several regions. There is *high confidence* to project an increase warm days/nights and decrease in cold days/nights. It is *likely* heavy precipitation will increase over the North Asia. The projected increase in heavy precipitation has *medium confidence* over the Southeast Asia, East Asia and Tibetan Plateau and *low confidence* over the South and West Asia. There is *low* confidence for projected changes in drought because projections by different models are inconsistent.

An overview of assessments regarding changes in weather and climate extremes in Asia is provided in Table 11.4. The following paragraphs provide a summary of the main assessments.

Recent studies provide *high confidence* in the observed increase in daily temperature extremes in the past few decades over most of the Asian continent including the Himalaya and Tibetan Plateau. During the period 1961-2013, the Excess Heat Factor (EHF) and 90th percentile of maximum temperatures have increased over the central and the northwestern parts of South Asia. Such increases are associated with an anti-cyclonic flow, along with clear skies and reduced soil moisture. Decreases in cold extremes and increases in warm extremes are observed across the western parts of East Asia since the 1960s. There is *high confidence* that anthropogenic forcing has contributed to changes in extreme temperatures in the western parts of East Asia, including changes in magnitude, frequency, and duration. Moreover, there is *high confidence* that anthropogenic warming has contributed to an increase in the probability of occurrence of the August 2015 heat wave in Japan. Warming is projected to continue in the region, along with changes in temperature extremes. The frequency of heatwaves in India is *likely* to increase by 30 times, under the 2°C global warming level, and this would be reduced by half under the 1.5°C global warming level. Projections based on statistically downscaled temperatures over the central parts of South Asia show a 140% increase of urban heat island by 2090 under the RCP 8.5 scenario.

There is *high confidence* in observed increase in precipitation extreme over the Central Asia, most of the South Asia, the southern and northern Tibetan Plateau, the northwest Himalaya, the Indochina and east-central Philippines, Jakarta, the eastern and northwestern China, Japan and Korea. There is *medium confidence* in observed decrease in precipitation extreme in the central Tibetan Plateau, the south-western part of Pakistan, and a southwest–northeast belt from Southwest China to Northeast China. There is *low confidence* that human influence has contributed to the increase in daily precipitation extremes over China in recent decades,contributing to the observed shift from light to heavy precipitation over eastern China.

There is *high confidence* that extreme precipitation is projected to increase in most parts of Asia under both RCP4.5 and RCP8.5 scenarios. Consecutive Dry Days is projected to increase in the south China and decrease in the north China. There is *high confidence* that warming will result in more droughts and flooding in West Asia.

[START TABLE 11.4 HERE]

Table 11.4: Regional assessments for Asia

[END TABLE 11.4 HERE]

11.9.3 Australasia

The SREX Ch3 had the following assessment for the region. It is *likely* or *very likely* (depending on the region) that since 1950 there has been a decrease in the number of cold days and nights, and an increase in the number of warm days and nights over Australia and New Zealand. It is *very likely* that warm days/nights will increase and cold days/nights will decrease in the future over Australasia. It is *likely* that heavy precipitation has decreaseed in many areas in South Australia, especially in regions where mean precipitation has decreased. In New Zealand, there is *high confidence* that trends in heavy precipitation are positive in the western North and South Islands and negative in the eastern part of the country. There is *low confidence* in projecting changes in extreme precipitation over North Australia and South Australia/New Zealand regions by the end of the 21st century due to lack of agreement regarding sign of change for different models and different indices.

An overview of assessments regarding changes in weather and climate extremes in Australasia is provided in Table 11.5. The following paragraphs provide a summary of the main assessments.

There are more than 30 new studies published since 2013 regarding changes in extremes over Australia and New Zealand. These studies support and enhance the previous assessments. It is *very likely* that temperature extremes have increased over North and South Australia and New Zealand for monthly to daily temporal scales. Due to limited evidence, there is *low-to-medium confidence* that temperature extremes have increased in Pacific Islands. Increases in extreme minimum temperatures, typically exceeding increases in extreme maximum temperatures, occur in all seasons over most of Australia.Statistically significant increases in extreme maximum temperatures have been observed in spring and winter over the southern and eastern part of Australia over the period 1960-2010. Extremes of cold temperatures on monthly to annual timescales have changed in way consistent with warming over the historical period over Australia. In some locations in southwest and southeast Australia, increases in the number of frost days have been observed, but this usually linked to changes in precipitation. Over New Zealand, warming trends have been observed for cold and warm extremes although with important spatial heterogeneity according to records from 22 stations available since 1951. In the tropical western Pacific region, spatially coherent warming trends in maximum and minimum temperature extremes have been reported for the period 1951–2011.

CMIP5 models project a reduction in the number of cold temperature extremes and an increase in the number of warm temperature extremes for the future over Australasia. Over most Australia, increases in extremes are dominated by increases in mean temperatures except for the southern part of Australia that shows larger warming rates for warm extremes. Future projections indicate a decrease in the number of frost days regardless the region and season considered. There is little updated information since SREX and AR5 on temperature projections for New Zealand, where New Zealand temperature change was projected to increase by a range of 0.1–4.6°C by 2090.

There have been *likely* increases in heavy precipitation in northwest Australia and decreases in many areas of southern Australia. Over Australia, there are nearly as many stations showing significant increases as significant decreases in the maximum daily rainfall over the period 1900-2009, although stations are not evenly spatially distributed. There is a significant reported increase in RX5day, PRCPTOT, R10mm, R20mm, R95p, CWD in northwest Australia over the period 1951-2015, and significant decrease in SDII in coastal eastern Australia. A significant decrease in CWD, PRCTOT, R10mm, R20mm, SDII is reported in southeast Australia. Over southeast Australia, gridded observations show an overall increase in rainfall extremes (e.g., Rx1day) for the period 1911-2014 although trends vary spatially and seasonally. There is *low confidence* that the number of heavy snowfall events have remain unchaged in the last 25 years over the Snowy Mountains (Fiddes et al., 2015). Over New Zealand, negative trends are observed for moderate-heavy precipitation events but no significant trends for very heavy events (more than 64 mm in a day) for the period 1951-2012.

There is *low confidence* in projected changes in extreme precipitation over Australia and New Zealand for thr future by the end of the 21st century. Over Australia, different climate models agree little in the direction and magnitude of future changes in precipitation extremes and most regions do not show significant and robust changes over the 21st century. Over southeast Australia, a regional climate model ensemble shows an overall increase in extreme rainfall indices (e.g., R20mm, Rx1day and R95p) although with important differences between models. According to the same ensemble, drought indices (SPEI) suggest significant drying in Australia's southwest and southeast during spring. Less intense drying occurs in Australia's southwest during winter and summer, and some significant drying although with high model disagreement occurs over north Australia during winter.

There is *low confidence* in a decrease in the frequency of tropical cyclones affecting the northern Australian region since 1982 (Dowdy, 2014). No significant trends in extreme extratropical cyclones have been observed over the east coast of Australia. There is *low confidence* about future changes in the most extreme tropical and extratropical cyclones occurring over the east coast Australia (Pepler et al., 2016).

[START TABLE 11.5 HERE]

Table 11.5: Regional assessments for Australasia

[END TABLE 11.5 HERE]

11.9.4 Europe

The SREX Ch3 had the following assessment for this region. It is *likely* that warm days and nights have increased and cold days and night have decreased in the observation in Europe. There is *medium confidence* for an increase in observed heatwaves in all of Europe as well as in observed winter precipitation in parts of the region. There is *medium confidence* in an observed increase in extreme winter precipitation in Northern Europe. With respect to droughts there are overall small changes, and they depend on the drought metric, the season and region. For the Mediterreanean there is *medium confidence* in an observed drying trend. Over the Alps there is a little additional evidence since AR5

An overview of assessments regarding changes in weather and climate extremes in Europe is provided in Table 11.6. The following paragraphs provide a summary of the main assessments.

Recent studies show *high confidence* in the increase of maximum temperatures and in the frequency of heat waves, with little differences among studies and regions. Over NEU there is a *high confidence* in a strong increase in extreme winter warming events but conflicting evidence on whether and to what extent this influences large scale teleconnections. There is *high confidence* that human-induced climate change has contributed to the increase in the frequency and intensity of short-term heat waves. There are few attribution studies on Scandinavia but over Britain there is *high confidence* that extreme heat in summer and decrease in cold extremes can be attributed to climate change. There is *high confidence* of projected increase in summer heat waves, similar to 2003 and 2010, and in an increase in high temperature extremes over the whole continent.

Regarding precipitation, there is a*medium confidence* in increase in extreme wet events over CEU with large discrepancies among studies and regions and strong seasonal differences. Over SEU, recent studies show a *medium confidence* in evolution of rainfall extremes with strong regional differences even at local scales. Dominant decrease in the Western Mediterranean and some increase in Eastern Mediterranean although there is high spread between studies and regions. Over NEU, there is *high confidence* in increase in rainfall extremes in winter and *medium confidence* in summer which is projected to continue into the future with *medium confidence*. There is *low confidence* in an observed increase in extratropical cyclones over NEU. Further, in the Arctic, there is a *medium confidence* in extreme snow melt events. Over the Alps, models show a high uncertainty in precipitation extremes with high orography and changes in seasonality particularly important. For snowfall, recent studies show decrease with *high confidence* in observations and in projections; and increase in flood risk despite declining snow. Attribution studies show no evidence of human influence on observed extreme wet events over CEU but with *medium confidence* in the attribution of wet winters to climate change. Wet summers over the British Isles are with *low confidence* attributed to climate change. Over SEU, extremes wet events are associated with natural variability also with *low confidence.*

[START TABLE 11.6 HERE]

Table 11.6: Regional assessments for Europe

[END TABLE 11.6 HERE]

11.9.5 Central and South America

The SREX Ch3 had the following assessment for the region. There is *low* to *medium confidence* in the observed changes in daily temperature extremes due to inconsistencies of changes across the region and lack of evidence in some cases. The observed changes in temperature extremes were consistent with warming though in the southern half of South America a decrease in warm days was detected. There is *high confidence* in the projected warming of temperature extremes by the end of the 21st century over Central and South America. There is *low* to *medium confidence*in trends of extreme precipitation over Central and South America depending on the region. For the western coast of South America, a decrease of extreme rainfall in many areas and an increase in a few areas were observed. In Central America and northern South America, heavy precipitation is projected to remain the same or to decrease. In some regions with projected decreases in total precipitation, such as the west coast of South America, heavy precipitation is nevertheless projected to increase. Over South Eastern South America (SES) the frequency of rainfall extremes is projected to increase by the end of the 21st century, possibly due to an intensification of the moisture transport from Amazonia by a more frequent/intense low-level jet east of the Andes. There is *medium confidence* in projected increase in duration and intensity of droughts in Northeast Brazil.

An overview of assessments regarding changes in weather and climate extremes in Asia is provided in Table 11.7. The following paragraphs provide a summary of the main assessments.

There are many more studies since the SREX report examining regions that were nearly unexplored at the time of SREX, including Amazon (AMZ) and Northeast Brazil (NEB). In South (Central) America there is a *high (medium) confidence* that observed temperature extremes have increased over recent years. There is *medium* to *high confidence* that extremes derived based on daily minimum temperatures (TN) have warmed faster than those derived based on daily maximum temperatures (TX), with the largest warming rates observed over Northeast Brazil (NEB) and Amazon (AMZ) for cold nights. There is *high confidence* that hot extremes (TXx and TX90p) have decreased in the last decades over most of South East South America (SES) during austral summer. There is *medium confidence* that the decrease in hot extremes over SES is related to an increase in precipitation over the region due to more intense extratropical cyclones and anomalous easterly flow related with a southward shift of the tropospheric jet as a result of ozone depletion in summer months.

It is *extremely likely* that temperature extremes will warm more over Central and South America by the end of the 21st century, with the largest changes projected over the South American Monsoon (SAM) region (Chou et al., 2014). Over SES, during the austral summer, the projected increase in the frequency of warm nights (TN90p) is larger than that projected for warm days (TX90p), consistent with observed past changes. The larger increases in TN compared to TX have been related with changes in cloud cover that affect differently day- and night-time temperatures.

There is *medium confidence* that extreme precipitation has increased in South America, though trends (both upward and downward) in precipitation indices are not statistically significant at most stations. The annual total precipitation (PRCPTOT), the annual maximum 1-day (RX1day) and consecutive 5-day (RX5day) precipitation and the heavy rainfall (R99p) exhibit increase trend when averaged over large areas of South America including AMZ, NEB, SES and WSA. Among all subregions, SES shows the highest rate of increases for rainfall extremes, particularly during the warm season, followed by AMZ. Despite the overall increase in rainfall extremes over South America, moderate decreasing trend which are usually not statistically significant are also found in regions including Northeast Brazil, southern Peru and southern Chile. The consecutive dry days (CDD), a proxy for dryness, show mostly upward trends (*medium confidence*), suggesting that a wetter continent might be associated more with rainfall intensification rather than with an increase in the frequency of wet days. In Central America trends in annual precipitation are generally not statistically significant, although small but significant positive trends are found in Guatemala, El Salvador and Panama.

There is *medium confidence* in the projected increase in R95p in the western AMZ and SES. Over eastern AMZ, there is *medium confidence* for intensification of drought in the 21st century, with rainfall reduction and longer dry seasons. There is *medium confidence* for increasd dryness in the second half of tyeh 21st century over NEB, including rainfall reductions, temperature increases, more water deficits and longer dry spells. Projected trends in Central America suggests future drier conditions in the northern part of the continent and wetter conditions in the southern Panama, consistent with the future south displacement of ITCZ (*low confidence*).

[START TABLE 11.7 HERE]

Table 11.7: Regional assessments for Central and South America

[END TABLE 11.7 HERE]

11.9.6 North America

The SREX Ch3 had the following assessment for this region. It is *likely* that there has been an overall decrease in the number of cold days and nights, and an overall increase in the number of warm days and nights at the continental scale in North America. Changes in temperature extremes over central North America and the eastern United States was consistent with the cooling of average temperatures. It is *very likely* that warm (cold) days and warm (cold) nights will increase (decrease) in all subregions. There is *medium confidence* in increases in warm days and warm nights in summer particularly over the United States and in large decreases in cold days in Canada in fall and winter. It is *likely* the number of heavy precipitation days will increase over Alaska, Canada, Greenland and Iceland and there is *medium confidence* in the intensification of meteorological droughts in the future in central North America and Mexico.

An overview of assessments regarding changes in weather and climate extremes in North America is provided in Table 11.8. The following paragraphs provide a summary of the main assessments.

Our assessment is similar to that from the SREX, with a few modifications. There is an overall decrease in the number of cold days and nights, and an overall increase in the number of warm days and nights at the continental scale in North America, including over central North America and the eastern United States where warming has been small, albeit smaller than elsewhere in North America. Furthermore, the number of high temperature records set in the past two decades far exceeds the number of low temperature records with high confidence. Projections in temperature extremes for the end of 21st century, show that warm (cold) days and warm (cold) nights are *very likely* or *likely* to increase (decrease) in all regions. There is *medium confidence* in large increases in warm days and warm nights in summer particularly over the United States and in large decreases in cold days in Canada in fall and winter.

There is *high confidence* that precipitation extremes have increased throughout North America since 1950 especially in the eastern half of the United States. A recent body of literature provides evidence that there has been a detectable long-term increase in the occurrence of Hurricane Harvey-like extreme precipitation events in the eastern Texas region of the U.S., and that anthropogenic forcing has contributed to this increase. There is *medium confidence* that droughts have become less frequent, less intense, or shorter in North America since 1950 although some and associated heat waves have reached record intensity in some regions of the United States.It is *likely* that both moderate and rare precipitation extremes in all regions of the United States and Canada will increase. There is also *high confidence* for future increases in agricultural drought through North America and severe hydrological drought in the western United States.

[START TABLE 11.8 HERE]

Table 11.8: Regional assessments for North America

[END TABLE 11.8 HERE]

11.9.7 Regional changes : Synthesis

We provide hereafter a short summary of the main assessed regional changes, ordered by continents.

In Africa, there is *medium to high confidence* in the increase in the number of warm days and nights and decrease in the number of cold days and night over North, West and South Africa since 1951.Heat waves have increased with *medium confidence* over Africa except Central and East Africa. These changes are expected to continue in the future with *medium to high confidence*. There is *low confidence* in observed change in heavy precipitation over the most part of the continent owing to lack of information. Positive trends in the intensity of extreme precipitation over West and South Africa have been observed with *medium confidence* which is projected to continue in the future (*medium to high confidence*). With respect to dryness, there is *medium confidence* in increase (decrease) of CDD over South Africa (West Africa). In the future, there is *medium to high confidence* in projected increase in dryness over the continent exceptSahara,central and eastern Africa .

In Asia, there is *high confidence* in the increase of daily temperature extreme during the last decades over most part of Asian continent including the Himalaya and Tibetan Plateau. Observed precipitation extreme shows an increasing trend with *high confidence* over most part of Asia. However, there is *medium confidence* in observed decrease in precipitation extreme in the central Tibetan Plateau, the south-western part of Pakistan, and a southwest–northeast belt from Southwest China to Northeast China. Projections of extreme precipitation show with *high confidence* a general wetting with increases of heavy precipitation in most parts of Asia.

In Australasia, there is *high confidence* that it is *very likely* that temperature extremes have increased over South and North Australia, New Zealand and western Pacific islands. There is *high confidence* that it is *extremely likely* that by the end of the century there will be a reduction in the number of cold temperature extremes and an increase in the number of warm temperature extremes in Australasia. There is *medium* *confidence* that heavy precipitation has increased in North Australia and low confidence that it has decreased in South Australia with important regional and seasonal variations. There is *low confidence* on trends over New Zealand where also important seasonal and spatial variations are observed. There is *low to medium confidence* that extreme precipitation will increase over Australia and New Zealand by the end of the 21st century. There is *low confidence* in a decrease in the frequency of tropical cyclones affecting the northern Australian region since 1982 and *medium confidence* that no changes have been observed in extreme extratropical cyclones over the east coast of Australia.

In Europe, there is *high confidence* in the increase of maximum temperatures and in the frequency of heat waves. There is also *high confidence* that human-induced climate change has contributed to the increase in the frequency and intensity of short-term heat waves. There is *high confidence* of projected increase in high temperature extremes over the whole continent. Regarding precipitation, there is *medium confidence* in the increase in extreme wet events which are also projected to continue into the future with *medium confidence*.

In South (Central) America, there is a *high* (*medium*) *confidence* in the *very likely* increase in the number of warm days and nights and decrease in the number of warm days and nights in the last decades, except over South East South America (SES) where hot extremes have decreased during austral summer. With *high confidence*, projected changes in temperature extreme indices show a widespread *extremely likely* warming over Central and South America by the end of the 21st century. Observations since 1950 suggest an overall increase in precipitation extremes (*medium confidence*) and a *likely* increase over South East South America with *high confidence*. There is *medium confidence* on projected increase in precipitation extremes over SES and *low confidence* on decrease over Central America and northern South America.

In North America, dominant changes in observed extremes include *very likely* increase (*high confidence*) in the number of warm days and nights and decrease in the number of cold days and nights, also over central North America and the eastern United States, albeit with changes smaller than elsewhere in North America. Projections in temperature extremes for the end of 21st century (*high confidence*), show that warm (cold) days and warm (cold) nights are *very likely* or *likely* to increase (decrease) in all regions. There is *medium confidence* in large increases in warm days and warm nights in summer particularly over the United States and in large decreases in cold days in Canada in fall and winter. There is *high confidence* that precipitation extremes have been increasing throughout North America, especially in the eastern half of the United States. There is *medium confidence* that droughts have become less frequent, less intense, or shorter in North America since 1950. Increases in both moderate and rare precipitation extremes in all regions of the United States have been projected. Increases in agricultural drought through North America and severe hydrological drought in the western United States are also projected.

11.10 Storylines, potential surprises and low-probability high-impact extremes

The SREX assessed that there was *low confidence* for potential surprises resulting from tipping points of the climate system such as the shutdown of the Atlantic thermohaline circulation or from poor understanding of climate processes including climate feedbacks that may enhance or damp extremes in several climate variables. The low confidence does not by itself exclude the possibility of such surprises or neither implies that abrupt and thus surprising changes in climate extremes will occurr, it is instead an indication of the poor state of knowledge.

The difficulties in determining the likelihood of occurrence and timeframe of potential tipping points and surprises persist, hence there is still *low confidence* in this area but new literature has emerged on two categories of surprises and low-probability events. One category includes events that are sufficiently rare that they have not been observed in the historical climate, but whose occurrence is nonetheless plausible within the current state of the climate system. These events can be surprises to many in that the events have not been experienced, although their occurrence could be inferred by statistical means or physical modelling approaches which take the non-stationarity of the distribution of many extremes in a changing climate into account (Chen et al., 2017; Harrington and Otto, 2018a; van Oldenborgh et al., 2017). Another approach in particular to estimate consequences of low-probability events and of events whose likelihood of occurrence is unknown is to nudge physical climate models into an extreme atmospheric state and thus create a non-probabilistic physically self-consistent storyline of plausible extreme events and assess their impacts and driving factors (Cheng et al., 2018; Shepherd, 2016; Shepherd et al., 2018; Zappa and Shepherd, 2017).

It is important to note again that the magnitude of impact of a particular extreme event is always affected by exposure and vulnerability and changes in these aspects of risk (see discussion of risk framework in chapter 1) are often as large or larger than changes in the meteorological hazard. For example, the location of where people live has an equally large or larger influence on how many people are exposed to extreme heat in the future than that is due to additional warming from 1.5°C to 2°C of global warming (Harrington and Otto, 2018b) and the share of land used for agriculture and land-use in general are most central for the occurrence of extremes in temperature (Seneviratne et al., 2018b; Vogel et al., 2017). However, here we focus only on the changes in climate extremes, i.e. in the hazard component of climate risks (see also Chapter 12).

11.10.1 Unprecedented events that can be anticipated

In many parts of the world, observational data are limited to 50-60 years. This means that the chance to observe an extreme event that occurs once in several hundred years or more is small. Thus when a very extreme event occurs, it becomes a surprise (Bao et al., 2017) to many and very rare events are often associated with high impact (Philip et al., 2018a; van Oldenborgh et al., 2016). Such events do occur somewhere on the Earth from time to time, however. For example, hurricane Harvey was estimated to be at least a 1 in 9000 year event by van Oldenborgh et al., 2017) while (Risser and Wehner, 2017) give a cautious estimate of several thousand years without being able to quantify it based on observations alone. Even when such a rare event has not been observed, they can still be conceived under a particular state of the climate. For example, Lin and Emanuel (2016) showed that storm surge can reach 6 meters in Tampa, Florida, U.S.A. in the 1985-2005 climate though such an event is associated with a low probability of over 10,000 years. The estimation of the probability for such events is usually highly uncertain.

As warming continues, the climate moves further away from the historical state that we are familiar with, resulting in more unprecedented events and surprises. This is particularly the case under high warming level such as the climate at the late 21st century under the RCP8.5 scenario (i.e. associated with 4°C of global warming or higher, Chapter 4). By combining the observed current maximum values to future climate simulated by the CMIP6 under the RCP8.5 scenario, (Bador et al., 2017) 'mega-heatwaves' defined as reaching anomalies of 6°C -13°C above the historical maxima in Europe are projected to have some probability to occur. More severe storm surges of above 8m up to 11m in Tampa has a negligible probabilities in the 1980-2005 climate and are projected to occur as 5000-150000 year event in the late 20th century (Lin and Emanuel, 2016). The lower estimate of the uncertainty range is comparable to the events that did occur in Chennai or Houston.

The rare nature of such events and the limited availability of data make it difficult to estimate their associated occurrence probability and thus gives little evidence on whether to include such hypothetical events in planning decisions and risk assessments. The estimation of such potential surprises is often limited to events that have historical analogues albeit the magnitude of the event may differ. Additionally, there is also a limitation of available resources such as computing capability to exhaust all plausible trajectories of the climate system. As a result, there will still be events that cannot be anticipated.

11.10.2 Unprecedented events conditional on tipping points

As in the SREX report, while this chapter does not assess the existence of possible tipping points in the climate system, we do assess future extremes conditional on the occurrence of such tipping points. Such tipping points include the occurrence of super El Niños (Latif et al., 2015), collapse of regional convection in the North Atlantic (Drijfhout et al., 2015), or abrupt changes in the West African Monsoon (Dong and Sutton, 2015). Assessments on the plausibility and timescale of such tipping elements can be used to anticipate potential surprises in future extremes in addition to High-End Climate Change (HECC) simulations.

In recent studies evidence has been found that the extreme negative phase of the North Atlantic Oscillation (NAO) observed during the boreal winter of 2009/10 (Jung et al., 2011) triggered extreme ice loss over Greenland (Bevis et al., 2019) which can lead to extreme ice loss and thus fresh water intrusion into the North Atlantic Ocean which in turn is suggested to trigger instabilitiy in the ocean circulation (Thornalley et al., 2018) and thus potentially triggering tipping elements. Even without providing a tipping point, the extreme negative NAO index is further linked to an extreme sea level rise event on the US American East coast (Goddard et al., 2015). While all studies use very different modelling approaches and thus do not allow for quantitative conclusions to be drawn the fact that these independent studies all point to the negative NAO index as a potential trigger provide evidence that studies on the likelihood of very negative NAO index under a warming climate can provide a lower bound of the likelihood of the associated extreme events to occur.

11.11 Knowledge gaps

[PLACEHOLDER, WILL BE FURTHER DEVELOPED FOR SOD]

There are some remaining areas associated with knowledge gaps in extremes research at present. Some topics are still unsufficiently investigated such has hail. Also, possible changes associated with global and regional tipping points (high-risks low probability events) are associated with *low confidence*, but cannot be excluded, especially at high global warming levels (>3°C). Finally, there are still remaining important observational gaps in several world’s regions, in particular in Africa.

[START BOX 11.2 HERE]

BOX 11.2: Extremes in palaeoclimate archives

Anthropogenic and natural forcings play a substantial role in driving climate variability on hemispheric scales prior to the twentieth century, with volcanic aerosol forcing being the most significant contributor to pre-industrial temperature variability on multi-decadal timescales (Bindoff et al., 2013). Examining extremes in pre-instrumental information can help to put extremes occurring in the instrumental records in a longer-term context, even though human influence on the occurrence or magnitude of those extremes may still be difficult to quantify. Here we focus on the Common Era (the last 2000 years) and discuss extreme events in palaeoreconstructions, documentary evidence (such as grape harvest data, gazettes, newspapers, diaries and logbooks) and model-based analyses. This focus is because we have generally higher confidence in pre-instrumental information gathered from the more recent archives from the Common Era, than from earlier evidence. Many factors affect confidence in information on pre-instrumental extremes, including the availability of data (Smerdon and Pollack, 2016), the event type and region examined, and the reconstruction methods (Christiansen and Ljungqvist, 2017) and the quality of those reconstructions.

Based on studies of palaeoclimate reconstructions, documentary evidence and early instrumental data, AR5 concluded with high confidence that droughts of greater magnitude and of longer duration than those observed occurred in many regions during the last millennium, and with high confidence that floods during the past five centuries in northern and central Europe, western Mediterranean region and eastern Asia were of greater magnitude than those observed (Masson-Delmotte et al., 2013). AR5 noted with high confidence the occurrence of regions in which 20th century summer temperatures (1971-2000) were higher than other 30-year periods over the period reconstructed within the Common Era (e.g. last 580 years in Australasia) (Masson-Delmotte et al., 2013).

Overall, we have the most complete pre-instrumental evidence of extremes for long-duration, large spatial-scale extremes, such as for multi-year meteorological droughts or seasonal- and regional- scale temperature extremes. Palaeoreconstructions provide, for example, evidence of the occurrence droughts prior to the commencement of instrumental records in many locations. Studies indicate that in some locations the recent observed drought extremes do not have precedents within the multi-century periods reconstructed, including for the Levant (Cook et al., 2016a), Sahel (Ljungqvist et al., 2016), California in the United States (Cook et al., 2014b; Griffin and Anchukaitis, 2014) and the Andes (Domínguez-Castro et al., 2018). In some regions,the recent drought extremes may have had historical precedents, including in Southwest North America (Asmerom et al., 2013; Cook et al., 2015a) and the Great Plains region (Cook et al., 2004), the Middle East (Kaniewski et al., 2012) and China (Gou et al., 2015). Liu et al. (2017) compared the variability in PDSI over a record from Mongolia extending from 1680-2012 AD and suggested that the post-1960 increase in drought years related to global warming effects in the region. This record is, however, notably shorter than many multi-century reconstructions attempting to provide insights into recent extremes. In Australia, there is conflicting evidence for the severity of pre-instrumental droughts compared to observed extremes, depending on the length of reconstruction and seasonal perspective provided (Cook et al., 2016b; Freund et al., 2017). There can also be differing conclusions for the severity or even the occurrence of specific pre-instrumental droughts when different evidence is compared. For example, 1540 AD was not an exceptional event in the tree ring record, but documentary sources suggest that it was an extreme year (Büntgen et al., 2015; Wetter et al., 2014). We have clearer insights into recent extremes where multiple studies have been undertaken, compared to the confidence we have in drought extremes reported at single sites or in single studies which may not necessarily be representative of large-scale changes, or for reconstructions that synthesise multiple proxies over large areas, such as drought atlases (Cook et al., 2015b). In summary, there is high confidence for the occurrence of large duration and severe drought events during the Common Era for many locations, although their severity compared to recent drought events differs for locations and length of reconstruction provided.

There is also evidence of the occurrence of regional and seasonal-scale temperature-related extremes from data products synthesizing many proxy records. These products combine palaeoclimate temperatures reconstructions and cover sub-continental- to hemispheric-scale regions to provide continuous records of seasonal- to annual- scale temperature over the Common Era (Ahmed et al., 2013; Neukom et al., 2014). Multiple studies have further examined the unusualness of present-day European summer temperature records in a long-term context, particularly in comparison to exceptionally warm 1540 AD in Central Europe. Several studies focused on evidence from documentary and palaeoclimate sources show that the recent extreme summers of 2003 and 2010 in Europe have been unusually warm in the context of individual summer temperatures over the last 500 years (Barriopedro et al., 2011). Luterbacher(2016) determined that the mean average European summer temperature of the last 3 decades (1986–2015CE) exceed temperatures in all 30 yr reconstructed periods of the last two millennia. The anomalous recent warmth was identified particularly in Southern Europe where variability is generally smaller. Orth (2016), however, determined that summer mean temperatures (TJJA) and maximum temperatures (TXx) in Central Europe in 1540 were warmer than the present-day mean summer temperatures (assessed between 1966–2015), though noted that it is difficult to assess if the summer in 1540 AD was warmer than current records. Further studies using grape harvest and tree ring data suggest that the extreme summer temperatures of 1540 in Central Europe exceed the observed instrumental extremes (Wetter and Pfister, 2013). In summary, there is high confidence that the magnitude of large-scale, seasonal-scale extreme temperatures in observed records exceed those reconstructed from over the Common Era.

The clearest information of palaeofloods occurs in high temporally resolved records, such as annually laminated lake deposits. These reconstructions provide evidence, for example, of floods exceeding probable maximum flood levels in the Upper Colorado River, USA (Porat et al., 2014) and peak discharges that are double gauge levels along the middle Yellow River, China (Liu et al., 2014). Annually resolved lake records of flooding provide evidence of pre-instrumental periods of high and low extreme rainfall and flooding in various riverine systems, particularly in Europe (e.g. Corella et al., 2014; Wirth et al., 2013). We have higher confidence in extreme historical flood episodes determined from documentary evidence, compared to low-resolution natural archives. Historical data includes, for example, peak flow recorded on infrastructure, paintings, photographs, diaries, newspapers and harvest records, which provide information on flood frequency and magnitude over many centuries (Kjeldsen et al., 2014). In regions such as Europe and China that have rich historical flood documents, there is strong evidence of high flood events over historical periods (Benito et al., 2015; Kjeldsen et al., 2014; Liu et al., 2014; Macdonald and Sangster, 2017). While pre-instrumental records provide additional insights prior flood characteristics, we note that pre-instrumental floods often occurred in considerably different contexts in terms of land use, irrigation and infrastructure and may not be directly insightful into modern river systems, which further prevents long term assessments of flood changes being made based on these sources. In summary, we have high confidence that the magnitude of floods over the Common Era have exceeded observed records in some locations, including central Europe and eastern Asia.

High temporal resolution palaeotempest archives provide insights into previous tropical cyclone characteristics in some locations. Haig et al. (2014a) used stalagmite records over the past 550-1500 years to show current levels of tropical cyclone activity (defined by a tropical cyclone activity index) in northeast Queensland are lower than at any time in the past 1500 years. This result supports earlier multi-millennium reconstructions from northeastern Australian beach ridges that extreme storms occur considerably more frequently in the pre-instrumental period than observed (Nott et al., 2009). Tropical storm changes recorded in archives of longer-duration (several millennia) but lower temporal resolution (see Muller et al., 2017), show periods of anomalously high and low storm frequency compared to observed, and the average number of storms per century (e.g., Brandon et al., 2013). Overall, palaeotempest studies cover a limited number of locations, and provide information on specific locations that cannot be extrapolated basin-wide. In summary, we have medium confidence that periods of both more and less tropical cyclone activity than observed occurred over the Common Era in many regions.

It remains difficult for various reasons to assess long-term changes and trends in extremes even for large-scale long-duration events. First, the geographical coverage of palaeoclimate reconstructions of extremes is not spatially uniform and depends on both the availability of archives and records, which are environmentally dependent, and also the differing attention and focus from the scientific community. In Australia, for example, the palaeoclimate network is sparser than for other regions, such as Europe and North America, and synthesised products rely on remote proxies and assumptions about the relationship of remote climates spatial coherence of precipitation. Second, pre-instrumental evidence of extremes is often focused on a small number of archetypal events, such as the climatic impact of the 1816 eruption of Mount Tambora, Indonesia (Brohan et al., 2016; Veale and Endfield, 2016). These studies provide narrow evidence of extremes in response to specific forcings(Li, 2017) in particular locations, for specific epochs. Third, many natural archives tend to provide information about extremes in one season only. Given these limitations and spatial and temporal inhomogeneities, it is not possible to assess potential long-term observed changes in the characteristics of most extremes from a systematic long-term perspective in many locations.

Evidence of shorter duration extreme event types, such as floods and tropical storms, is further restricted by the comparatively low chronological controls and temporal resolution (e.g. monthly, seasonal, yearly, multiple years) of most archives compared to events (e.g. minutes to hours or days). Natural archives may be sensitive only to large magnitude environmental disturbances, and so only sporadically record short duration or small spatial scale extremes. Interpreting sedimentary records as evidence of past short-duration extremes is also complex and requires clear understandings of natural processes. For example, palaeoflood reconstructions of flood recurrence and intensity produced from geological (eg. river and lake sediments, speleothems (Denniston and Luetscher, 2017), botanical (e.g. flood damage to trees, or tree ring reconstructions) and faunal (e.g. diatom fossil assemblages) require understandings of sediment sources and flood mechanisms. Pre-instrumental records of tropical storm intensity and frequency (also called palaeotempest records) derived overwash deposits of coastal lake and marsh sediments are difficult to interpret, with many factors affecting whether disturbances are deposited in archives (Muller et al., 2017) and deposits providing sporadic and incomplete preservation histories (e.g. Tamura et al., 2018).

While there is pre-instrumental evidence that some recently observed extremes have not been exceeded in the Common Era (last 2000 years), due to data limitations and available we cannot obtain a systematic long-term perspective of changes in many locations, or assessments of the potential unusualness of observed extremes. The probability of finding an unprecedented extreme event also increases with an increase of length of past record-keeping, in the absence of trends. Thus, there is also a comparatively higher chance for a very rare extreme events to have occurred at some prior time in the combined palaeoclimate and historical records which provided extended records length. Given the rarity of such extreme event and limited data samples available, it remains difficult to quantify systematically the likelihood of such an event occurring in the past and whether the likelihood has changed in the instrumental period. As such, it is also difficult to determine whether human or natural external forcing is having an influence on their likelihood from these data. Nevertheless, such events may provide a basis for possibly constructing storylines.

[END BOX 11.2 HERE]

[START BOX 11.3 HERE]

BOX 11.3: Case study: Global-scale concurrent climate anomalies at the example of the 2015 Super El Niño and the 2018 boreal spring/summer extremes

[PLACEHOLDER: PRELIMINARY VERSION OF THIS BOX; TO BE FURTHER DEVELOPED FOR SOD]

Occurrence of concurrent or near-concurrent extremes in different parts of a region, or in different places of the world challenges adaptation and risk management capacity. Yet, this does occur from time to time because climates in different parts are inter-connected through teleconnections. In addition, in a warming climate, the probability of having several locations being affected simultaneously by e.g. temperature hot extremes and heatwaves increases strongly for each 0.5°C of additional global warming, since these are increasing worldwide at high rate (Section 11.3; Box 11.1, Figure 1). Recent articles have highlighted the risks associated with concurrent extremes over large spatial scales (e.g. (Lehner and Stocker, 2015)). There is evidence that such global-scale extremes associated with hot temperature extremes are increasing in occurrence (Sippel et al. 2015; Vogel et al., submitted). Hereafter, we focus on two recent global-scale events that featured concurrent extremes happening at several locations at the same time.

[START BOX 11.3, FIGURE 1 HERE]

Box 11.3, Figure 1: Analysis of the percentage of land area affected by temperature extremes larger than a) two or b) three standard deviations in June-July-August (JJA) between 30°N and 80°N using an approach using a standard normalization (orange) and a corrected normalization (grey). The more appropriate estimate is the corrected normalization. These panels show for both estimates a substantial increase in the overal land area affected by very high hot extremes since 1990 onward. From Sippel et al. 2015. [THIS FIGURE WILL BE UPDATED UP TO 2018 FOR THE SOD]

[END BOX 11.3, FIGURE 1 HERE]

2015/2016 El Niño or "Super El Niño"

El Niño is one of the phenomena that have the ability to bring multitudes of extremes in different parts of the world, especially in the extreme cases of El Niño. Additionally, the background climate warming associated with greenhouse gas forcing can significantly exacerbate extremes in parts of the world even under normal El Niño conditions. According to some measures, the 2015/16 El Niño was the strongest El Niño over the past 145 years (Barnard et al., 2017). A brief summary of what happened that year is provided hereafter. We provide some highlights illustrating extremes that occurred in different parts of the world during the 2015/16 El Niño event, hereafter referred to as "Super El Niño".

The state of the climate in 2015 reviewed by Blunden and Arndt (2016) summarized extreme aspects due to the super El Niño, as overlaying a general increase in the hydrologic cycle, the strong El Niño enhanced precipitation variability around the world and drought conditions prevailed across many areas for most of the year. Emissions from tropical Asian biomass burning in 2015 were also severely enhanced (Cross-Chapter Box 11.1, Figure 1).

Several regions were strongly affected by droughts in 2015, including Indonesia, the Amazon region and Ethiopia. In 2015, Indonesia experienced a severe drought and forest fire causing pronounced impact on economy, ecology and human health due to haze crisis (Hartmann et al., 2018). The extent of drought season in Indonesia during 2015 has intensified the flammability of forest and peatlands leading to a severe fire season (Field et al., 2016). During 2015, forest and peatland fires have released 227 ± 67 Tg C (Huijnen et al., 2016; Patra et al., 2017), which was in between 2013 CO_2 emission from fossil fuel in Japan and India (Field et al., 2016). The Amazon region experienced the most intense droughts of this century in 2015/2016. This drought was more severe than the previous major droughts that occurred in the Amazon in 2005 and 2010 (Erfanian et al., 2017; Panisset et al., 2018), which had been both assessed as 1-in-100 year types of events (Lewis et al. 2011). The 2015/2016 Amazon drought impacted the entirety of South America north of 20°S during the austral spring and summer (Erfanian et al., 2017). According to Panisset et al. (2018), 80,1% of the Amazon Basin area was stricken by precipitation deficit during this drought, which spanned from September 2015 to May 2016 (Ribeiro et al., 2018). Jiménez-Muñoz et al. (2016), using the self-calibrating Palmer Drought Severity Index (van der Schrier et al. 2013 ; note, however, some limitations with this index, Section 11.6), showed that the 2015 El Niño event, combined with the regional warming trend, was associated with unprecedented warming and a larger extent of extreme drought in Amazonia compared to the earlier strong El Niño events in 1982/83 and 1997/98. The 2015/2016 anomalous dryness increased the forest fire incidence by 36% compared to the preceding 12 years (Aragão et al., 2018). The active fires occurred over an area of 799,293 km^2, impacting areas in central Amazonia barely affected by fires in the past (Aragão et al., 2018). As a consequence, forest fires increased the biomass burning outbreaks and the carbon monoxide (CO) concentration in the area, affecting air quality (Ribeiro et al., 2018). This out-of-season drought affected the water availability for human consumption and agricultural irrigation and it also left rivers with very low water levels, without conditions of ship transportation, due to large sandbanks, preventing the arrival of food, medicines, and fuels. Eastern African countries, including Ethiopia, Somalia, and parts of Kenya, were impacted by drought in 2015. The drought in Ethiopia was the worst in several decades. It was found that the Ethiopian drought was associated with the super El Niño in 2015 that developed early in the year (Blunden and Arndt, 2016; Philip et al., 2018a). Because the Ethiopian drought is well correlated with ENSO in the observations, it is *likely* that the strong 2015 El Niño did increase the severity of the drought in Ethiopia (Philip et al., 2018a). It should be noted that 2015 was a year that displayed a particularly high CO_2 growth rate, possibly related to some of the mentioned droughts, in particular in Indonesia and the Amazon region, leading to CO_2 release or less CO_2 uptake from land areas (Humphrey et al. 2018).

In 2015, the activity of tropical cyclones was notably high in the North Pacific (Blunden and Arndt, 2016). Over the western North Pacific, the number of category 4 and 5 Tropical Cyclones (TCs) was 13, which is more than twice its typical annual value of 6.3 (Zhang et al., 2016a). Similarly, a record-breaking number of TCs was observed in the eastern North Pacific, particularly in the western part of that domain (Collins et al., 2016; Murakami et al., 2017). These extraordinary TC activities were related to the average SST anomaly during that year, which were associated with the super El Niño event in 2015 and the positive phase of the Pacific Meridional Mode (PMM) (Murakami et al., 2017). However, it has been suggested that the intense TC activities in both the western and the eastern North Pacific in 2015 were not only due to the El Niño, but also to a contribution of anthropogenic forcing (Murakami et al., 2017; Yang et al., 2018b). In the 2015/2016 Super El Niño years, the TC activities were similarly strong in the western Pacific as in the 1997 super El Niño. However, differences in possible TC characteristics between the two super El Niño years in 1997 and 2015 were suggested to be due to the additional effect of PMM(Hong et al., 2018; Yamada et al., 2019). It was also suggested that the impact of the Indian Ocean SST also contributes to the extreme TC activity in 2015 (Zhan et al., 2018).

[START BOX 11.3, FIGURE 2 HERE]

Box 11.3, Figure 2: Geographical distribution of notable climate anomalies and events occurring around the world in 2015 (Adopted from Fig. 1.1 of Blunden and Arndt, (2016) and to be updated).

[END BOX 11.3, FIGURE 2 HERE]

Global-scale temperature extremes in boreal 2018 spring and summer

In the 2018 boreal spring-summer season (May-August), wide areas of the mid-latitudes in the Northern Hemisphere experienced extremes heat extremes and in part enhanced drought (Box 11.3, Figure 3). Between May and August 2018, the reported impacts included the following (Vogel et al., submitted): 90 deaths from heat strokes in Quebec (Canada), 119 deaths from heat strokes in Japan, heat warning affecting 90’000 students in the USA, fires in numerous countries (Canada (British Columbia), USA (California), Lapland, Latvia)), crop losses in the UK, Germany and Switzerland, fish deaths in Switzerland, and melting of roads in the Netherlands and the UK), among others.

In addition to the numerous hot and dry extremes, an extremely heavy rainfall occurred over wide areas of Japan from 28 June to 8 July 2018 (Tsuguti et al., 2018), which was succeeded by a heatwave (Japan Meteorological Agency, 2018). The heavy precipitation event was named as “the Heavy Rain Event of July 2018” and was characterized by line-shaped precipitation systems which recently are frequently associated with heavy precipitation events in the East Asia (Kunii et al., 2016; Oizumi et al., 2018; Tsuguti et al., 2018; section 11.7.3). This precipitation event and the subsequent heatwave are related to abnormal condition of the jet and North Pacific Subtropical High in this month (Japan Meteorological Agency, 2018), which caused extreme conditions from Europe, Eurasia, and North America (Cross-Chapter Box 11.2, Figure 1). The cause of the meandering jets and their relation to SST and external forcing are under investigated.

[START BOX 11.3, FIGURE 3 HERE]

Box 11.3, Figure 3: Global extreme climate events in July 2018 (Japan Meteorological Agency, 2018). This figure shows overlaid climate extremes (warm, cold, wet and dry) from weekly reports for July 2018. [SOD PLACEHOLDER: WILL INCLUDE AN UPDATED FIGURE PROVIDING ANOMALIES OVER THE WHOLE DURATION OF THE EVENT, I.E. AT LEAST MAY-AUGUST 2018]

[END BOX 11.3, FIGURE 3 HERE]

Regarding the hot extremes that occurred across the Northern Hemisphere in the 2018 boreal May-July time period, Vogel et al. (submitted) find that the event was unprecedented in terms of the total area affected by hot extremes (on average about 22% every day during this whole 3-month period) for that period, but was consistent with a +1°C climate which is the estimated present-day global mean temperature anomaly (SR15). Indeed, the probability of such an event is about 12% under a 1°C global warming (Box 11.3, Figure 4). This study also finds that events similar to the 2018 May-July temperature extremes would approximately occur every other year under 1.5°C global warming, and every year under +2°C of global warming (Box 11.3, Figure 4). Hence, while the 2018 had a strong circulation component (Box 11.3, Figure 3), the widespread temperatures anomalies that occurred in that year should not be unexpected given climate simulations for present-day warming, and are projected to happen more frequently under higher levels of global warming.

[START BOX 11.3, FIGURE 4 HERE]

Box 11.3, Figure 4: CMIP5-based multi-model range of probabilities for exceeding concurrent hot days areas for global warming of +1°C (orange), +1.5°C (red) and +2°C (dark red) with respect to 1870-1900, with area experienced in 2018 May-July indicated with dashed blue line. Corresponding box plots for the probabilities of occurrence of the 2018 area at +1°C, +1.5° and +2°C global warming are shown on the right.From Vogel et al. (submitted).

[END BOX 11.3, FIGURE 4 HERE]

[END BOX 11.3 HERE]

[START BOX 11.4 HERE]

BOX 11.4: Reasons for concern related to weather and climate extremes: Informing on changes in extremes supportingrelated adaptability assessments

(Sonia Seneviratne, Claudia Tebaldi, Xuebin Zhang; Preliminary draft, additional WG1 and WG2 authors will contribute for SOD; to be coordinated with chapter 12 for SOD)

[PLACEHOLDER WITH BRIEF OVERVIEW; TO BE DEVELOPED FOR THE SOD]

Discussion points:

- The AR5 WG2 chapter 19 (Oppenheimer et al., 2014, IPCC AR5 WG2) included an assessment of risk as function of global warming for five identified "Reasons For Concern" (RFCs). The risk assessment was subdivided in four categories (Box 11.4, Fig. 1): undetectable (white), moderate (yellow), high (red), very high (purple). Very high risk indicates a level of risk at which limits to adaptability may be reached.
- The Reason For Concern #2 on climate extremes assessed "high risk" for global warming at 1.5°C and above, but was not able to provide an assessment of a possible transition to "very high risk" at higher warming levels because there was not enough literature at the time to determine the global warming level at which a "very high risk" could occur (purple shading)
- It has been recognized in the SR15 that +0.5C of warming in addition to +1.5C global warming would substantially increase the frequency and severity of extremes.
- This box builds on the SR15 report and the assessment conducted in this chapter, providing new physical evidence on projected changes in extremes at different global warming levels and show large incremental increases in extremes that should inform the assessment of limits to adaptability to changes in extremes at different global warming levels and at high level in particular.
- Important new evidence to consider:
    - Increase in extremes in general
        - Consider spatial dimension of extremes (Box 11.3): e.g. at ca 4°C (RCP8.5), near 75% of the world population could be affected by extreme hot days of up to 5 standard deviations (Lehner and Stocker, 2015; Box 11.4, Figure 3)
    - Compounding of events, i.e. several extremes happening at the same time/location which can potentially lead to more impacts than if they had happened in isolation (Section 11.8)
        - New analyses showing that several locations could be affected simultaneously, or very repeatedly by different types of extremes (Mora et al., 2018; Box 11.4, Figure 2; also several new articles currently in review)
    - [PLACEHOLDER FOR SOD: FURTHER ASPECTS TO BE CONSIDERED, E.G. PROJECTIONS FOR CHANGES IN COMPOUND EVENTS AND RATE OF CHANGE IN CLIMATE EXTREMES FOR DIFFERENT SCENARIOS]

The box will be developed in collaboration with chapter 12 and WG2 authors, focusing on physical aspects of (past and projected) changes in extremes which could be of particular challenge for society and/or ecosystems.

[START BOX 11.4, FIGURE 1 HERE]

Box 11.4, Figure 1: "Reasons for concerns" (RFCs), highlighting RFC2 on "Risks associated with extreme weather events. From Oppenheimer, M. et al (2014), IPCC AR5 WG2).

[END BOX 11.4, FIGURE 1 HERE]

[START BOX 11.4, FIGURE 2 HERE]

Box 11.4, Figure 2: Cumulative climate hazards within RCP 8.5 scenario, which reaches ca. 4°C of global warming in 2100. The main map shows the cumulative index of climate hazards, which is the summation of the rescaled change in all hazards between 1955 and 2095. Most of the considered hazards are associated with weather and climate extremes. From (Mora et al., 2018).

[END BOX 11.4, FIGURE 2 HERE]

[START BOX 11.4, FIGURE 3 HERE]

Box 11.4, Figure 3:(Lehner and Stocker, 2015)

[END BOX 11.4, FIGURE 3 HERE]

[END BOX 11.4 HERE]

[START CROSS-CHAPTER BOX 11.1 HERE]

Cross-Chapter Box 11.1: Cross-Chapter (Ch11-Ch08-Ch10-Ch12) case study: The Himalayan heavy precipitation and flooding events

THIS BOX IS NOT YET WELL DEVELOPED. HERE WE OUTLINE MAIN POINTS THAT WILL BE DISCUSSED IN THE BOX. THE BOX WILL BE REWORKED FOR THE SOD.

Lesson learnt:
Extreme precipitation and resulting flooding events are common in Bangladesh, Bhutan, India, Nepal and Pakistan during the summer monsoon season (June to September); they are however, rare in the northwestern part of the sub-continent (Hunt et al., 2018). Research shows an increase in frequency and intensity of extreme precipitation events (and warming trend in temperature extremes) over the western and central Himalayas (Adnan et al., 2016; Dimri et al., 2017; Sheikh et al., 2015), whereas no trend is observed over the Eastern Himalayas or contrasting evidence exists (Sheikh et al., 2015; Talchabhadel et al., 2018). Most intense and frequent floods have been reported in the last decade. The Himalayan floods are complex geophysical phenomena associated with extreme precipitation events, complex topography, Glacier Lake Outburst Floods (Cook et al., 2018b) and contributions from glaciers and snow-melt due to rise in temperature (Immerzeel, Petersen, Ragettli, & Pellicciotti, 2014, Ali et al., 2015). Variability of the extreme precipitation events and resulting floods can be linked with climate change (Adnan et al., 2017). However, there is low agreement on the effect of projected increase in extreme precipitation on flooding events (Philip et al., 2018b; Rimi et al., 2019).

Rationale:
The Himalayas are the freshwater reserves, and major source of the river systems in South Asia (such as; the Indus, the Ganges and the Brahmaputra). The Himalayas are also known as the “Third Pole”. The Himalayan region encounter frequent devastating landslides, heavy cloudbursts, flash floods, monsoonal floods, glacial avalanches, Glacier Lake Outburst Floods (GLOFs), and hailstorms. These incidents caused sudden and severe damage to life and property in many parts of the region (Gupta and Uniyal, 2015). This complex geomorphology, together with high socio-economic vulnerability (Elalem and Pal, 2015;Dewan, 2015; Gupta & Uniyal, 2015) and an observed increase in extreme precipitation over the Western Himalayas, that reportedly increased intense floods in the Himalayan region during the recent decade (Elalem and Pal, 2015), makes the case-study area an important hot-spot for climate induced extreme events study (Adnan et al., 2017; Hunt et al., 2018). However data availability is limited rendering confidence low (You et al., 2017).

Concepts, Drivers, and Projections:
Extreme precipitation in the eastern and middle Himalayas are associated with south-western monsoon circulations, while the Western Himalayas are affected by both Western Disturbances (WDs) and monsoon Circulations. Extreme Precipitation events occur during both summer and winter in the Western Himalayas; summer extremes are generally associated with the tropical lows (Hurley and Boos, 2015) and their interactions with WDs, whereas the winter extremes are associated with only WDs (Dimri et al., 2015). Increasing trends (during 1950s to date) have been observed in precipitation extremes of WDs (Dimri et al., 2015; Madhura et al., 2015; Ridley et al., 2013) over the Western Himalayas, which has also experienced surface warming since 1950s. The monsoon extremes over the Western Himalayas show an increasing trends associated with declining south-west monsoon circulation and increased activities of westerly troughs of upper-air (Priya et al., 2017).

Recent high occurrences of floods over the Western Himalayas are essentially pluvial floods associated with cloud burst extreme precipitation events (Dimri et al., 2017;Devrani et al., 2015). Two recent major flood events over the Himalayan region occurred in Pakistan (during 2010) and in Uttarakhand (India) during 2013. The Pakistan Meteorological Department (PMD) reported that over 200 millimetres (7.9 in) of rain fell over a 24-hour period during the Pakistan flood of 2010. The extreme rainfall resulted from the convergence of extratropical and monsoonal circulations. The Uttarakhnad flood during June 2013 was caused by merging of eastward-propagating and southward extended upper-level trough in the westerlies with monsoon low (Houze et al., 2017). There is a high agreement that such events have high predictability and both the events could have been predicted well in advance with an extended range prediction system (Houze et al., 2017Webster, Toma, & Kim, 2011, J. et al. 2011, Joseph et al., 2015).

In addition, glacier retreat and or mass gain, can cause hazards such as Glacier Lake Outburst Floods (GLOFs), which could increase with future warming (Bolch, 2012). A significant lake normally develops if the glacier tongue gradient slopes < 2 degree (Quincey, 2007; Bolch, 2012). GLOFs can be in the shape of cross-valley ice dams in the case of mass gain, or side/frontal moraines in the case of glacier retreat (UNEP, 2010). Both types of glacial lake can cause devastating floods, which can adversely affect the downstream population and infrastructure (especially hydro-power). One example of this occurred during the period 1941-1970, when more than 27,000 people were killed by GLOFs in the Cordillera Blanca region of Peru; a hazard where climate change could have increased the likelihood due to high glacier retreat since 1980 (Carey, 2005). Another example is the LuggyeTsho, Bhutan GLOF, which produced a flood wave of 2m over 200km in 1994 (Richardson, 2000). GLOFs are also major cause of extreme floods over the Himalayas where e.g. the severity of the 2013 Uttarakhand flood has partially been attributed to the GLOF based on observed Satellite images (Das et al., 2015). GLOFS are also the major reason driver of floods in Nepal, where intensity and frequency of such floods is very high (Kropáček et al., 2015). Over the last 50 years, the Himalayan glaciers generated 20 GLOFs and more than 33 glacial lakes have been identified as a possible cause of future flooding (Qiu, 2008). In addition to this, since the 1860s, the western Himalayan glaciers have encountered more than 34 surges, and these have become more frequent since 1985 (Hewitt, 2007), while Campbell (2005) identified 52 potential outburst floods in Pakistan.

Furthermore, extreme precipitation on the Himalayas may generate catastrophic fluvial floods in India and Bangladesh due to excessive direct runoff in the Ganges and Brahmaputra rivers (Masood et al., 2014; Wesselink et al., 2015). However, the causes of the fluvial floods are not only due to heavy precipitation or glacier- and snow-melt but also affected by other factors such as deforestation, sedimentation of the river bed, flood control infrastructures, backwater effect and synchronization of flood peaks (Mirza, 2011). There is some evidence that climate change will increase the likelihood of hydrological floods in Bangladesh (Masood et al., 2014) and other countries. There is a high confidence that monsoon floods in the Ganges and Brahmaputra river basins will be more intense in a 2 ℃ warmer environment than 1.5 ℃(Mirza, 2011; Mohammed et al., 2017, 2018). In the upper Ganges river basin, climate change will bring more extreme precipitation in the monsoon (Kumar Mishra and Herath, 2015). With respect to the duration of floods, the severity of extreme events is projected to be increased (Masood and Takeuchi, 2015)(Paltan et al., 2018).Although an increasing likelihood of extreme precipitation and discharge is projected in the future recent attribution studies on discharge in 2017 in the Brahmaputra basin (Philip et al., 2018b), the 2013 extreme precipitation in Uttarakhand (Prasad et al.in review) and extreme rainfall in Bangladesh in 2017 (Rimi et al., 2019) found no significant increase in the likelihood of these events attributable to anthropogenic climate change. There is however evidence that current aerosol pollution masks an existing climate change signal (Patil et al., 2018; Rimi et al., 2019). At the downstream of the Ganges and Brahmaputra rivers where about 170 million people are living in a low lying delta, risks of flooding and sea level rise are very likely (Auerbach et al., 2015)(Brown et al., 2018; Kay et al., 2015b). Sediment loads are also likely to be increased in the Brahmaputra and Ganges by the end of the century under the influence of the anthropogenic climate change which would worsen the fluvial flood conditions (Darby et al., 2015) (Dunn et al., 2018).

[END CROSS-CHAPTER BOX 11.1 HERE]

Synthesis tables

[START TABLE 11.1 HERE]

Table 11.1: Synthesis table on observed changes in extremes and contribution by human influences. Note that observed changes in marine extremes are assessed in the cross-chapter box 9.1 in Chapter 9.

Phenomenon and direction of trend	Observed/detected trends since 1950 (for +0.5°C global warming[3] or higher)	Human contribution to the observed trends since 1950 (for +0.5°C global warming[a] or higher)
Warmer and/or more frequent hot days and nights over most land areas	***Virtually certain*** **on global scale** ---------------------------------- Regional signals : North America, Europe, Australia, Asia, South America: *Very likely* Central America, Southern Africa: *Medium confidence* Africa, except southern Africa: *Low confidence* because of lack of observations	***Very likely*** **on global scale** ---------------------------------- Regional signals : North America, Europe, Australia, Asia: *Likely*. In North America, Europe, and India: *Medium confidence* in partial counteracting of warming of hottest extremes due to land use changes (crop expansion, irrigation) Central and South America, Southern Africa: *Medium confidence* Africa, except southern Africa: *Low confidence* because of lack of observations
Warmer and/or fewer cold days and nights over most land areas	***Virtually certain*** **on global scale** *Australasia: Very likely* *Asia: Very likely* *South America: Low evidence, High agreement*	***Very likely*****on global scale**

Notes:
(a) See IPCC SR15 (IPCC, 2018)

Warm spells/heatwaves; Increases in frequency or intensity over most land areas *[changes in duration are not assessed, may be assessed for SOD]*	***Virtually certain* on global scale** *Australasia: Very likely* *Asia: Very likely* *South America: Low evidence, high agreement*	***Very likely* on global scale**
Cold spells/cold waves: Decreases in frequency or intensity over most land areas *[changes in duration are not assessed, may be assessed for SOD]*	***Virtually certain* on global scale** *South America: Low evidence, medium agreement*	***Very likely* on global scale**
Heavy precipitation events: increase in the frequency, intensity, and/or amount of heavy precipitation	***Likely* more regions with positive than negative trends** ---------------------------------- Regional signals: Northern high-latitude: *Very likely* increase in frequency, intensity and total amount Southern high-latitudes: Low confidence because of lack of observations and studies Mid-latitudes: *Likely* increase in intensity of wet days during cold season*; Low confidence* in other characteristics Tropics: *Low confidence*	***High confidence in* human contribution to the observed intensification of heavy precipitation** ---------------------------------- Regional signals: Northern hemisphere: *High confidence*
Drought events: Increases in frequency, intensity and/or duration	High-latitudes: *Low confidence* Mid-latitudes/subtropics, transitional regions between dry and wet climates, semi-arid regions*: Medium confidence* in increased drying in some regions with these climate characteristics; *medium confidence* in increased drying in Mediterranean region Tropics: *Low confidence*	High-latitudes: *Low confidence* Mid-latitudes/subtropics, transitional regions between dry and wet climates, semi-arid regions*: Medium confidence* in attribution of increased drying in Mediterranean region to human-induced emissions; *low confidence* elsewhere Tropics: *Low confidence*

Floods and water logging: Increases in intensity and/or frequency	Streamflow trends mostly not statistically significant (*high confidence*) *Low confidence* in the majority of the world regions with the exception of increases in the Amazon (*high confidence*), Northwest US and UK (*medium confidence*). *High confidence* in changes of flood seasonality, mostly in snow dominated regions.	*Low confidence* due to little evidence and high seasonality. In some areas mean streamflow is declining. The attributable signal in flooding does not scale linearly with that in rainfall.
Increase in precipitation associated with tropical cyclones	*Low confidence* for detectable global trend in tropical cyclone (TC) rain rates, due to data limitations. *Low confidence* for detectable global change in TC translation speed.	*Low confidence* for global TC rain rates and changes in translation speed. *Low to medium confidence* for contribution of TCs to detectable anthropogenic contribution to extreme rainfall events. *Medium confidence* for detectable anthropogenic contribution to global near-surface water vapor increases, which is expected to increase TC rainfall, all other things equal. *Medium confidence* for anthropogenic contribution to extreme rainfall events, which TCs contribute to, over the United States and other regions with sufficient data coverage.
Increase in tropical cyclone intensity (maximum surface wind speed)	Generally *low confidence* in detection of trends in historical tropical cyclone intensity in any basin or globally due to lack of confidence resulting from data inhomogeneities.	Generally *low confidence* in attribution of any anthropogenic influence on historical changes in tropical cyclone intensity in any basin or globally due to lack of confidence resulting from data inhomogeneities, with exception of North Atlantic. North Atlantic: *Medium confidence* that a <u>reduction in aerosol forcing</u> has contributed at least in part to the observed increase in tropical cyclone intensity since the 1970s.*Low confidence* for direct role of greenhousegas

		forcing.
Changes in frequency of tropical cyclones	*Low confidence* in detection of trends in historical tropical cyclone frequency in any basin or globally due to lack of confidence resulting from data inhomogeneities. Furthermore, physical process understanding is still unclear and there is no clear expectation for an increase in overall frequency with increasing greenhouse gas concentration.	*Low confidence* in attribution of any anthropogenic influence on historical changes in tropical cyclone frequency in any basin or globally due to lack of confidence resulting from data inhomogeneities, with exception of North Atlantic. North Atlantic: *Medium confidence* that a reduction in aerosol forcing has contributed at least in part to the observed increase in tropical cyclone frequency since the 1970s. *Low confidence* for direct role of greenhousegas forcing.
Poleward migration of tropical cyclones	*Low confidence* for a detectable global signal. *Low-to-medium confidence* for a detectable migration rate in the western North Pacific.	*Low confidence* for global migration. *Low-to-medium confidence* for migration in the western North Pacific.
Slowdown of tropical cyclone translation speed	*Low confidence* due to a present limited literature and lack of consensus on model results.	*Low confidence.*
Severe convective storms (tornadoes, hail, rainfall, wind, lightning)	*Low confidence* in past trends in hail and winds and tornado activity due to short length of high quality data records.	*Low confidence*.
Increase in compound events	*High confidence* that some compound events, for instance co-occurrent heatwaves and droughts, are becoming more frequent under enhanced greenhouse gas forcing. *[MORE DETAILED ASSESSMENT, E.G. TRENDS IN OTHER TYPES OF COMPOUND EVENTS, IN SOD]*	*TO BE ASSESSED FOR SOD*

[END TABLE 11.1 HERE]

[START TABLE 11.2 HERE]

Table 11.2: Synthesis table on projected changes in extremes. Note that projected changes in marine extremes are assessed in the cross-chapter box 9.1 in Chapter 9.

Phenomenon and direction of trend	Projected changes at +1.5°C global warming	Projected changes at +2°C global warming	Projected changes at +3°C global warming or higher
Warmer and/or more frequent hot days and nights over most land areas	All continents: *Likely;* warming of hottest days of up to +3°C in mid-latitudes	All continents: *Very likely;* warming of hottest days of up to +4°C in mid-latitudes	All continents: *Extremely likely; ;*warming of hottest days of up to +6°C or larger in mid-latitudes
Warmer and/or fewer cold days and nights over most land areas	All continents: *Likely;* warming of coldest nights of up to +4.5°C in Arctic, several northern high-latitude regions, and some northern mid-latitude regions	All continents: *Very likely*; warming of coldest nights of up to +6°C in Arctic, several northern high-latitude regions, and some northern mid-latitude regions	All continents: *Extremely likely* warming of coldest nights of up to +9°C or larger in Arctic, several northern high-latitude regions, and some northern mid-latitude regions
Warm spells/heatwaves; frequency and/or duration increases over most land areas	All continents:*Likely*	All continents:*Likely*	All continents:*Very likely*
Cold spells/cold waves: Decreases in frequency, intensity and/or duration over most land areas	All continents:*Likely*	All continents:*Likely*	All continents:*Very likely*
Heavy precipitation events: increase in the frequency, intensity, and/or amount of heavy precipitation (to be updated with CMIP6 simulations in SOD)	*High confidence* in most continents but *low confidence* in Australasia, Central and South America	*Likely* in most continents but *low confidence* in Australasia, Central and South America	*Very likely* in most continents but *low confidence* in Australasia, Central and South America
Increases in intensity and/or duration of drought events	*Medium confidence* in increase in drought probability in subtropical regions: Mediterranean, Southern Africa, Northeast Brazil, Southern North America and Central America *High confidence* in higher probability of atmospheric ariditiy, i.e. drier atmosphere, in subtropical and mid-latitude regions	*Medium confidence* in increase in drought probability in subtropical regions (Mediterranean, Southern Africa, Northeast Brazil, Southern North America and Central America), with higher probability of intense/frequent droughts than at 1.5°C global warming *Medium confidence*in expansion of drought probability outside these regions given increased radiative forcing (e.g. central Europe and Central North America, the Amazon) *High confidence* in higher probability of atmospheric ariditiy, i.e. drier atmosphere,	*Medium confidence* in increase in drought probability in subtropical regions (Mediterranean, South Africa, Northeast Brazil, Southern North America and Central America), with probability of intense droughts being higher than for 2°C of global warming *Medium confidence*in expansion of drought probability outside these regions given increased radiative forcing (e.g. central Europe and Central North America, the Amazon), with probability of intense droughts being higher than for 2°C of global warming

		in subtropical and mid-latitude regions	*High confidence* in higher probability of atmospheric ariditiy, i.e. drier atmosphere, in subtropical and mid-latitude regions
Increases in floods and water logging	*Medium confidence* that an increase in global warming to 1.5°C would lead to a larger fraction of land area affected by flood hazard at global scale compared to present	*Medium confidence* that an increase in global warming to 2°C compared to 1.5°C or present-day conditions would lead to a larger fraction of land area affected by flood hazard at global scale.	*High confidence* that flood hazard would be even more widespread at +3°C compared to +2°C given projected changes in heavy precipitation; in part lack of literature to quantitatively assess projected changes.
Increase in precipitation associated with tropical cyclones (TC)	*Medium-to-high confidence* in a 11% projected increase of TC rain-rates at the global scale and *medium confidence* that rain-rates will increase in every basin.	*Medium-to-high confidence* in a 14% projected increase of TC rain-rates at the global scale and *medium confidence* that rain-rates will increase in every basin.	*Medium-to-high confidence* in a 21% projected increase of TC rain-rates at the global scale and *medium confidence* that rain-rates will increase in every basin.
Increase in mean tropical cyclone lifetime-maximum wind speed (intensity)	*Medium-to-high confidence* for a 3.75% increase.	*Medium-to-high confidence* for 5% increase.	*Medium-to-high confidence* for a 7.5% increase.
Changes in frequency of tropical cyclones	*Low confidence* for overall frequency. *Medium-to-high confidence* for a 10% increase in the frequency of the strongest (Category 4-5) storms	*Low confidence*for overall frequency. *Medium-to-high confidence* for a 13% increase in the frequency of the strongest (Category 4-5) storms	*Low confidence*for overall frequency. *Medium-to-high confidence* for a 20% increase in the frequency of the strongest (Category 4-5) storms
Severe convective storms	*High confidence* in projected environmental changes that would putatively support an increase in the frequency and intensity of severe convective storms (a category that combines tornadoes, hail, and winds), especially over regions that are currently prone to these hazards, but *low confidence* in how this will impact	Same	same

	the storms themselves.		
Increase in compound events (frequency, intensity)	*High confidence* that some compound events, for instance co-occurrent heatwaves and droughts, will continue to increase under higher levels of global warming, with higher frequency/intensity with every additional 0.5°C of global warming.		

[END TABLE 11.2 HERE]

[START TABLE 11.11 HERE]

Table 11.3: Regional assessments for Africa (D&A stands for detection and attribution; EA stands for event attribution). [to be further completed for SOD]

	Temperature extremes *[coordinated with section 11.3]*			Precipitation extremes and flooding (including effects of TC, ETC and atmospheric rivers) *[coordinated with sections 11.4, 11.5 and 11.7]*			Droughts, dryness and aridity *[coordinated with section 11.6]*		
	Observed trends	D&A; EA	Projections	Observed trends	D&A; EA	Projections	Observed trends	D&A; EA	Projections
North Africa (S.MED)	*High confidence*: Increase in WD,WN , HWand decrease in CN,CD and CW since 1981 (Donat et al., 2013a, 2014a, 2016b; Filahi et al., 2016)		*Medium confidence*: Increase of heat waves by end 21 century) (Giorgi et al., 2014) Increase of WD, WN and HW (Lelieveld et al., 2016)	*Low confidence*: Increase in R10mm in West (Donat et al., 2014a) Decrease in the East R10mm (Donat et al., 2014a; Mathbout et al., 2018b)		*Low confidence*: Lack of agreement in sign of change of R95p (Giorgi et al., 2014; Sillmann et al., 2013a).	*Low confidence*: Increase in CDD East (Donat et al., 2014a; Mathbout et al., 2018b) and decrease in West (Donat et al., 2014a)	*Low confidence*: Drying attributable to climate change (Bergaoui et al., 2015)	*Medium confidence*: Increase of CDD (Giorgi et al., 2014; Han et al., 2019; Sillmann et al., 2013a)
Sahara (SAH)	*Medium confidence*: Increase in WD, WN and HW and decrease CD,CN, and CW since 1981. (Donat et al., 2014a; Moron et al., 2016).		*Medium confidence*: Increase of HW by end 21 century) (Giorgi et al., 2014) Increase of WD, WN and HW. (Dosio, 2017).	*Low confidence*: Increase of R10 mm in west Sahara and Soudan (Donat et al., 2014a).		*Medium confidence*: Increase of R95 by end of 21 century (Giorgi et al., 2014; Sillmann et al., 2013a)).	*Low confidence*: insufficient evidence to assess trends		*Low confidence*: Lack of agreement in sign of change of CDD (Giorgi et al., 2014; Han et al., 2019; Sillmann et al., 2013a)

West Africa (WAF)	*Medium confidence*: Increase in WD and WN and decrease in CD and CN (Barry et al., 2018)(Chaney et al., 2014).		*Medium confidence*: Increase in HW by end 21 century) (Giorgi et al., 2014). Increase of WD ,WN and HW in summer and winter(Dosio, 2017).	*Medium confidence*: Increase in heavy precipitation R10mm,R20mm,R95, R99p, SDII and RX5day (Barry et al., 2018; Chaney et al., 2014).		*High confidence*: Increase in R95p,SDII (Dosio el al 2019 in review) by the by end of 21 century(Akinsanola and Zhou, 2018; Giorgi et al., 2014; Sillmann et al., 2013a)	*Medium confidence*: Decrease of CDD (Barry et al., 2018; Chaney et al., 2014).	*Low confidence* that late onset of rainy season is not attributable to climate change (Lawal et al., 2016)	*Low confidence*: Lack of agreement in sign of change of CDD (Akinsanola and Zhou, 2018, Dosio el al 2019 in review)(Han et al., 2019; Sillmann et al., 2013a)
Central Africa (CAF)	*Low confidence*: Insufficient evidence to assess trends		*Low confidence*: Insufficient evidence to assess trends	*Low confidence*: Insufficient evidence to assess trends		*Low confidence*: due to low model agreement	*Low confidence*: Insufficient evidence to assess trends		*Low confidence*: Insufficient evidence to assess trends
North East Africa (NEAF) and Central East Africa (CEAF)	*Medium confidence*: Increases in WD	*Medium confidence*: Increased temperature attributable to climate change (Otto et al., 2015a) Philp et al., in review	*High confidence*: Likely increases in WD and decreases in CD	*Low confidence*: Insufficient evidence to assess trends		*Low confidence*: insufficient evidence to assess trends	*Medium confidence*: Increase in frequency of meteorological droughts (Funk et al., 2015a; Nicholson, 2017)	(Funk et al., 2018b; Otto et al., 2018a; Philip et al., 2018a; Uhe et al., 2017) *Low confidence* high evidence that observed drying is not attributable to anthropogenic climate change	*Low confidence*: lack of agreement in the sign of change (SREX suggest decreases in CDD but (Osima et al., 2018, Dosio el al 2019 in review) suggest in increases) (need to explore more)

South WestAfrica (SWAF)	*High confidence* : *likely* increases in WD and decreases in CD (Donat et al., 2013a) *Medium confidence*: Increases in heatwaves frequency (Russo et al., 2016)		*High confidence*: *likely* increases in WD and decreases in CD *High confidence*: *very likely* increases in heat waves frequency (Dosio, 2017; Engelbrecht et al., 2015; Russo et al., 2016)	*Medium confidence*: increases in heavy precipitation but with spatially varying trends. Increases in precipitation intensity (SDII) (Donat et al., 2013a)		*Medium confidence*: increases in heavy precipitation but varying spatially (Pinto et al., 2016) *High confidence*: *likely* increases in precipitation intensity (Pinto et al., 2016, Dosio el al 2019 in review,)	*Medium confidence*: increase in dryness (CDD)	*Medium confidence*: Recent meteorological drought attributable to anthropogenic climate change (Otto et al., 2018c)	*High confidence*: *Likely* increases in dryness (Giorgi et al., 2014; Pinto et al., 2016)(Maúre et al., 2018, Dosio el al 2019 in review) (CDD and SPEI,SPI*)
South East Africa (SEAF)	*High confidence* : *likely* increases in WD and decreases in CD (Donat et al., 2013a) *Medium confidence*: Increases in heatwaves frequency (Russo et al., 2016)		*High confidence*: *likely* increases in WD and decreases in CD *High confidence*: *very likely* increases in heat waves frequency(Dosio, 2017; Engelbrecht et al., 2015; Russo et al., 2016)	*Medium confidence*: increases in heavy precipitation but with spatially varying trends. Increases in precipitation intensity (SDII) (Donat et al., 2013a)		*Medium confidence*: increases in heavy precipitation but varying spatially (Pinto et al., 2016) *High confidence*: *likely* increases in precipitation intensity (Pinto et al., 2016, Dosio el al 2019 in review)	*Medium confidence*: increase in dryness (CDD)	*Medium confidence*: Recent meteorological drought attributable to anthropogenic climate change (Bellprat et al., 2015)	*High confidence*: *Likely* increases in dryness(Giorgi et al., 2014; Pinto et al., 2016)(Maúre et al., 2018, Dosio el al 2019 in review) (CDD and SPEI,SPI*)

[END TABLE 11.11 HERE]

[START TABLE 11.12 HERE]

Table 11.4: Regional assessments for Asia [to be further completed for SOD]

	Temperature extremes			Precipitation extremes and flooding			Droughts, dryness and aridity		
	Observed trends	Detection and attribution;event attribution	Projections	Observed trends	Detection and attribution;event attribution	Projections	Observed trends	Detection and attribution;event attribution	Projections
Central Asia	*High confidence*: Increase in warm nights/days, decrease in cool nights/days (Hu et al., 2016) The warming in most warm extreme occured in spring, that in most cold extreme occured in autum(Feng et al., 2017).		*Medium confidence*: Increase in warm events and decrease in cold events are projected by the end of the 21st century under RCP4.5 and RCP8.5 scenarios (Han et al., 2018).	*High confidence*: Very wet days, maximum 1-day precipitation and the heavy precipitation days had slight increasing trend (Hu et al., 2016)		SDII and precipitation extreme indices, including RX5day, R95p, days of heavy precipitation (i.e.,R10mm), are all projected to increase under RCP4.5 and RCP8.5 scenarios (Han et al., 2018).			Small changes in CDD are projected under RCP4.5 and RCP8.5 (Han et al., 2018)
Northern Asia			*Medium confidence*: Increase in warm extremes and decrease in cold exremes(Han et al., 2018; Xu et al., 2017)			SDII, RX5day, R95p, are projected to increase (Han et al., 2018; Xu et al., 2017)			Decreases in CDD are projected in most regions under RCP4.5 and RCP8.5 (Han et al., 2018)
Himalaya, Tibetan Plateau (TIB)	*High confidence*: Extreme cold days/nights has decreased and extreme warm days/nights has increased (Sun et al., 2017)		*Medium confidence*: Increase in warm extremes and decrease in cold exremes(Gao et al., 2018; Singh and Goyal, 2016; Zhang et al., 2015b; Zhou et al., 2014a)	*High confidence*: Increasing trends over northwest Himalaya (Nishant et al., 2016), and southern and northern TP (You et al., 2008), while decreasing trends in the central TP (You et al., 2008)		A general wetting across the whole TP with increases of heavy precipitation (Gao et al., 2018; Zhang et al., 2015b; Zhou et al., 2014a)	Decreasing trends in CDD (You et al., 2008)		A general decrease is projected under RCP4.5 and RCP8.5 but with large uncertainty (Zhou et al., 2014a)

South Asia (SAS)	*High confidence*: Warm extremes have become more common and cold extremes less common (Rohini et al., 2016; Sheikh et al., 2015; Zahid and Rasul, 2012)	*Medium confidence*: Anti-cyclonic flow, along with clear skies and depleted soil moisture are responsible for the warming over India (Rohini et al., 2016). Observed changes in minimum temperature over Mahandi river basin during the pre-monsoon and monsoon season can be attributed to an anthropogenic effect (Kumar, 2017).	*Medium confidence*: In creases in warm extremes and decreases in cold extremes are projected (Han et al., 2018; Xu et al., 2017). More intense heatwaves of longer duration at a higher frequency in India (Murari et al., 2015) and in Pakistan (Nasim et al., 2018) .	*High confidence*: Increasing trends over most of South Asia (Sheikh et al., 2015)Asia (Nishant et al., 2016; Rohini et al., 2016; Roxy et al., 2017; Sheikh et al., 2015; Zahid and Rasul, 2012). Extreme precipitation shows decreasing trends in the south-western part of Pakistan (Hussain and Lee, 2013)		RX5day and R95p are projected to increase e (Han et al., 2018; Xu et al., 2017)	Frequency of droughts shows increasing trend (Niranjan Kumar et al., 2013).		Small changes in CDD are projected under RCP4.5 and RCP8.5 (Han et al., 2018). Frequency and area extents of severe, extreme, and exceptional agricultural droughts are projected to increase in India during near term and mid 21st Century (Mishra et al., 2014b; Salvi and Ghosh, 2016).
East Asia (EAS)	Decreases in cold extremes and increases in warm extremes (Lu et al., 2016, 2018; Yin et al., 2017; Zhou et al., 2016)	*High confidence*: Anthropogenic influences on extreme temperature in China, including their magnitude, frequency, and duration (Lu et al., 2016, 2018; Yin et al., 2017)	*Medium confidence*: Increase in warm extremes and decrease in cold extremes (Guo et al., 2018; Li et al., 2018c; Seo et al., 2014; Sui et al., 2018; Wang et al., 2017a, 2017c; Xu et al., 2016; Zhou et al., 2014a)	*High confidence*: Annual total precipitation amount, average daily precipitation rate, and the proportion of heavy precipitation show negative trends in a southwest–northeast belt from Southwest China to Northeast China while positive trends in eastern China and northwestern China (Zhou et al., 2016). Observed increase in extreme	*Low confidence*: Human influence has increased daily precipitation extremes over China in recent decades (Chen and Sun, 2017c; Li et al., 2017), and contribution to the shift from light to heavy precipitation over eastern China(Ma et al., 2017).	*Medium confidence*: Intensification of precipitation extremes (Guo et al., 2018; Li et al., 2018c; Seo et al., 2014; Sui et al., 2018; Wang et al., 2017a, 2017c; Xu et al., 2016; Zhou et al., 2014a). Increase in extreme precipitation intensity over Japan in future climate scenarios (Nayak et al., 2017)	Since the 1950s some regions of China have experienced a trend to more intense and longer droughts, in particular in North China and Northeast China, but in some regions	There is evidence that the droughts have changed as a result of anthropogenic influences, including the drought occurrences, severity, and the drought regimes across China (Chen and Sun, 2017a, 2017b)	CDD is projected to increase in south China and decrease in north China (Zhou et al., 2014a) The occurrence probability of hot drought events (SPEI < -1.0) will increase to nearly 100% by the year 2050 (Chen and Sun, 2017a, 2017b)

				precipitation intensity over Japan (Nayak et al., 2017) and Korea(Baek et al., 2017)			droughts have become less frequent, less intense, or shorter, especially in northwestern China (Chen and Sun, 2015b; Yu et al., 2014)		
Southeast Asia (SEA)	Frequency of warm days/nights shows increasing trend (Supari et al., 2017).		In creases in warm extremes and decreases in cold extremes are projected (Han et al., 2018; Xu et al., 2017).	*High confidence*: RX1day over the Indochina and east-central Philippines increases, while that over most parts of the Maritime Continent shows decreasing trend (Villafuerte and Matsumoto, 2015). Increasing trends have also been observed over Jakarta (Siswanto et al., 2015)	These trends are linked to the rising global mean temperature and ENSO variability (Villafuerte and Matsumoto, 2015)	Precipitation extreme indices, including RX5day, R95p, are projected to increase under RCP4.5 and RCP8.5 (Basconcillo et al., 2016; Han et al., 2018).		No link to climate change could be made for the 2015 drought in Singapore/Malaysia (Mcbride et al., 2015). Drought in Indonesia was found to be made more likely by El nino and climate change (King et al., 2016b)	Increasing frequency of drought events as a consequence of increasing frequency of extreme El Nino (Cai et al., 2014a, 2015, 2018)

[END TABLE 11.12 HERE]

[START TABLE 11.13 HERE]

Table 11.5: Regional assessments for Australasia [to be further completed for SOD]

	Temperature extremes			Precipitation extremes and flooding (including effects of TC, ETC and atmospheric rivers)			Droughts, dryness and aridity		
	Observed trends	Detection and attribution; event attribution	Projections	Observed trends	Detection and attribution; event attribution	Projections	Observed trends	Detection and attribution; event attribution	Projections
N. Australia (NAU)	*High confidence*: Likely increases in the number of warm days and warms nights and very likely decreases in the number of cold days and cold nights since 1950 (Alexander and Arblaster, 2017; Wang et al., 2013b; Jakob and Walland, 2016; Lewis and King, 2015). Increases in minimum temperature extremes are likely to be larger than those in extremes of maximum temperature (Alexander and Arblaster, 2017; Wang et al., 2013b; Jakob and Walland, 2016).	*High confidence*: Increases in trends in increasing temperature extremes, and in the likelihood of extremes events on daily to annual timescales due to anthropogenic warming (Lewis and Karoly, 2013; Lewis and King, 2015; Perkins et al., 2014a)	*High confidence*:*Very likely* increases in warm temperature extremesand very likely decreases in cold temperature extremes (Alexander and Arblaster, 2017; Lewis et al., 2017; Herold et al., 2018).	*Low to medium confidence*: Likely positive trends are observed over the northwest for various rainfall extreme indices (Dey et al., 2019). Evidence is limited due to the lack of observation in the region. *Low confidence*: there is a likely negative trends in the number of TCs over North Australia (Dowdy, 2014) Thunderstorms and hail: insufficient evidence (Walsh et al., 2016b)	*Low confidence*: Trends in northwest Australia rainfall attributable to anthropogenic aerosols, but large spread in models (Dey et al., 2019)	*Low confidence*: Extreme precipitation is projected to increase in most regions mainly to the north of NAU. Future changes are however more uncertain and do not show agreement among models. (Alexander and Arblaster, 2017; Dey et al., 2018; Evans et al., 2017; Perkins et al., 2014b).	*Low confidence*: Historical trends since 1911 show decreases in the number, duration and intensity of droughts over northwest Australia (Gallant et al., 2013).	*Low confidence*: No evidence has been found.	*Low confidence*: Projections do not show significant trends in this region (Herold et al., 2018)
South	*High confidence*:	*High confidence*:	*High confidence*:	*Low confidence*:	*Low confidence*:	*Low confidence*:	*Low confidence*:	*Low confidence*:	*Medium*

Australia (SAU)	Likely increases in the number of warm days and warms nights and very likely decreases in the number of cold days and cold nights since 1950 (Alexander and Arblaster, 2017; Wang et al., 2013b; Jakob and Walland, 2016; Lewis and King, 2015). *Medium confidence*: *likely* increase in the number of frost days in early spring over southeast Australia and in winter over southwest Australia since 1980 (Crimp et al., 2016; Dittus et al., 2014)). For southeast Australia the increase in frost days have been linked with a decline in precipitation and a drying trend (Dittus et al., 2014).	As above	Very likely increases in warm temperature extremesand very likely decreases in cold temperature extremes (Alexander and Arblaster, 2017; Lewis et al., 2017; Herold et al., 2018).In contrast with historical observations, future projections indicate a likely decrease in the number of frost days in southeast and southwest Australia regardless the region and season considered (Gobbett et al., 2018; Herold et al., 2018)	Over the whole Australia trends (1911-2010) in extreme precipitation indices are usually positive but their magnitude depend strongly on the dataset (HadEX2 or WAP) and on the specific index being conisdered(Alexander and Arblaster, 2017) Overall increases over southeast Australia (1911-2014) although trends are generally not significant for several extreme rainfall indices including Rx1day (Evans et al., 2017) As many positive as negative significant trends over SAU (Westra et al., 2013) The number of heavy snowfall events have remain unchanged in the last 25 years over the Snowy Mountains (Fiddes et al., 2015). Lack of any statistically significant trend in ETCs in Southeast Australia (Walsh et al., 2016b) Thunderstorms and hail: reliable trends are not available (Walsh et al.,	Anthropogenic greenhouse gas influence on extreme rainfall events in southern and eastern Australia is highly uncertain (Christidis et al., 2013a; King et al., 2013; Lewis and Karoly, 2014a)	Extreme precipitation is projected to increase but the agreement among models is quite low (Alexander and Arblaster, 2017; Evans et al., 2017) Quite robust decrease in ETCs in winter in the Australian east coast based on GCMs and RCMs (Dowdy et al., 2013b, 2013a; Ji et al., 2015; Pepler et al., 2016)	Across much of south Australia, droughts became less frequent, shorter and less intense from 1911 to 2009. Exceptions include far southwest Western Australia, which has had statistically significant increases in drought intensity and southeast Australia which has shown a significant increase in the average length of droughts. (Gallant et al., 2013)	Single study shows probability of drought conditions in 2013 in Queensland were not signficantly altered by anthropogenic forcings (King et al., 2014)	*confidence*: Robust decrease in precipitation, soil moisture and SPEI in spring over all southern Australia and in winter/summer mainly over the southwest (Herold et al., 2018; Olson et al., 2016; Zhao and Dai, 2017). Southwest Australia identified as a hot spot for drough risks in the future (Prudhomme et al., 2014)

				2016b)					
New Zealand	*High confidence*: Most stations show positive and generally significant trends for monthly minimum and maximum temperatures over the period 1951-2012. All daily temperature extremes show warming trends with cold extremes (TN10 and TX10) increasing faster than warm extremes (TN90 and TX90) (Caloiero, 2017).	*Low confidence*:	*High confidence*: Moderately extreme rainfall is likely to increase in most areas, with the largest increases being seen in areas where mean rainfall is also increasing, such as the West Coast. Very extreme rainfall is likely to increase in all areas with increases more pronounced for shorter duration events.	*Low confidence*: Some suggestion of changes in the frequency of heavy rain days with mostly decreases (Caloiero, 2015; Harrington and Renwick, 2014)	*Low confidence*: Single study of exteme 2011 rainfall in northern South Island indicates amount was 1%–5% higher as a result of the emission of anthropogenic greenhouse gases (Dean et al., 2013)	*Medium confidence*: Extreme rainfall as measured using the 99th percentile is likely to increase in most areas, with the largest increases being seen in areas where mean rainfall is also increasing, such as the West Coast.	*Low confidence*: Some indication of a trend towards more drought in most areas of NZ (Salinger, 2013)	*Low confidence*: Single study of 2013 North Island drought found dry conditions more favorable as a result of anthropogenic climate change (Harrington et al., 2014)	*Low confidence*: Drought severity (measured using potential evapotranspiration deficit, PED) is projected to increase in most areas of the country, except for Taranaki-Manawatu, West Coast and Southland
Western Pacific Islands	*High confidence*: Western Pacific islands show warming trends, mostly significant, for all temperature extreme indices including TN10, TX10, TN90 and TX90 for the period 1951-2011 based on 46 stations (Whan et al., 2014). Largest warming trends are found in the hottest day (night) of the year with weaker warming trends in the coolest								

	day (night) of the year(Whan et al., 2014)								

[END TABLE 11.13 HERE]

[START TABLE 11.14 HERE]

Table 11.6: Regional assessments for Europe [to be further completed for SOD]

	Temperature extremes			Precipitation extremes and flooding			Droughts		
	Observed trends	Detection and attribution; event attribution	Projections	Observed trends	Detection and attribution; event attribution	Projections	Observed trends	Detection and attribution; event attribution	Projections
Central Europe (CEU) (without Alps)	*High confidence*: Increase in the maximum temperatures and the frequency of heat waves. Consistent signal among studies and regions (Christidis et al., 2015; Scherrer et al., 2016; Shevchenko et al., 2014; Twardosz and Kossowska-Cezak, 2013).	*High confidence*: Human-induced climate change has contributed to the increase in the frequency and intensity of short-term heat waves and heat stress (Sippel et al., 2017, 2018a).	*High confidence*: Increase of extreme temperatures and increased frequency of heat waves similar to 2003 and 2010 (Lau and Nath, 2014; Lhotka et al., 2018; Rasmijn et al., 2018; Russo et al., 2015; Vogel	*Medium confidence*: Increase of extreme precipitation events. Large discrepancies among studies and regions and strong seasonal differences (Casanueva et al., 2014; Croitoru et al., 2013; Fischer et al., 2015; Roth et al., 2014; Willems, 2013).	*Low confidence*: Attribution of extreme wet events to human climate signal (Wilcox et al., 2018).	*Medium confidence*: Increase in extreme precipitation events, although important seasonal differences (Rajczak et al., 2013; Rajczak and Schär, 2017)	*High confidence*: No relevant changes in the frequency of dry spells (Zolina et al., 2013) and in droughtseverity(Cook et al., 2014a; Orlowsky and Seneviratne, 2013; Spinoni et al., 2017).	*Medium confidence*: Attribution of the 2017 drought event to climate change (García-Herrera et al., 2018).	*Low confidence*: Drought projections in central Europe based on precipitation (Orlowsky and Seneviratne, 2013). *High confidence:* drought projections based on soil moisture and drought indices (Dai

			et al., 2017).						et al., 2018; Lehner et al., 2017; Samaniego et al., 2018; Zhao and Dai, 2017).
South Europe (SEU)	*High confidence*: Increase of heat waves, tropical nights with few differences among studies and regions, No important differences between West and East Mediterranean (Christidis et al., 2015; Croitoru and Piticar, 2013; El Kenawy et al., 2013; Fioravanti et al., 2016; Kawase et al., 2016; Nastos and Kapsomenakis, 2015; Ruml et al., 2017; Türkeş and Erlat, 2018)	*High confidence*: Human attribution of extreme temperature events (Sippel and Otto, 2014; Wilcox et al., 2018).	*High confidence*: Projected increase in summer heat waves and maximum temperature extremes (Cardoso et al., 2019; Ozturk et al., 2015; Schoetter et al., 2015).	*Medium confidence*: Evolution of precipitation events, with strong regional differences even at the local scale. Dominant decrease in the Western Mediterranean and some increase in Eastern Mediterranean (Casanueva et al., 2014; de Lima et al., 2015; Gajić-Čapka et al., 2015; Rajczak et al., 2013; Ribes et al., 2018; Sunyer et al., 2015).	*Medium confidence*: Extreme events associated to natural variability (Añel et al., 2014; U.S. Department of Agriculture Economic Research Service, 2016).	*Low confidence*: Increase of extreme precipitation events. High spread between studies and regions (Argüeso et al., 2012; Monjo et al., 2016; Patarčić et al., 2014; Paxian et al., 2014; Rajczak et al., 2013)	*High confidence*: Increased dryness caused by an increase in atmospheric evaporative demand and increase of hydrological droughts (Cook et al., 2014a; González-Hidalgo et al., 2018; Gudmundsson et al., 2017; Ozturk et al., 2015; Roudier et al., 2016; Stagge et al., 2017).	*Medium confidence*: Attribution of the 2014 eastern Mediterranean drought events to climate change (Bergaoui et al., 2015).	*High confidence*: Increase of climatic and hydrological droughts based on precipitation, soil moisture, runoff and drought indices (Cook et al., 2014a; Dai et al., 2018; Orlowsky and Seneviratne, 2013; Ozturk et al., 2015; Prudhomme et al., 2014; Samaniego et al., 2018; Schewe et al., 2014).
North Europe (NEU)	*High confidence*: Strong increase in extreme winter warming events (Matthes et al., 2015; Vikhamar-Schuler et al., 2016). *Low*	*High confidence*: Attribution studies of temperature extremes in Central England (King et al., 2015; Roth et al.,	*High confidence*: strong decrease in heating degree days (Spinoni et al., 2018a). Medium	*High confidence*: Change in flood seasonality in Scandinavia (Matti et al., 2017). Extreme rainfall trends are different depending on season(Irannezhad et al., 2017). Evidence for more extreme	*High confidence*: Wet summer of 2012 not attributable to climate change (Otto et al., 2015c; Schaller et	*High confidence*: Reduction of flows from snow melt but increase river flow through increased precip(Donnelly et al., 2017; Madsen et al., 2014; Thober et al., 2018). High confidence: Shift of strong ETCs and ARs closer to Scandinavia (Ramos et al., 2016; Romero and Emanuel, 2017).	*High confidence*: No important changes in drought severity based on different metrics (Dai et al., 2018; Orlowsky and Seneviratne, 2013; Spinoni et al., 2014, 2017). High	*Medium confidence*: Decrease of dry years in Scandinavia (Gudmundsson and Seneviratne,	*Low confidence*: Increase in droughts in Northern Scandinavia (Spinoni et al., 2018b): Medium

	confidence:Warming in the arctic induces cooling on the Eurasian continent (Christiansen et al., 2018)	2018). *High confidence*: Cold winter of 2009/2010 has become less likely (Otto et al., 2012)(Massey et al., BAMS 2012, (Christiansen et al., 2018)). *Low confidence*: evidence of detectable circulation change attributable to climate change (Nilsen et al., 2017).	confidence: Frequent ice-free arctic summers projected even under moderate warming scenarios (Laliberté et al., 2015; Sigmond et al., 2018).	precipitation in summer and winter but not other seasons (Yiou and Cattiaux 2013, BAMS, Dong et al. 2013 BAMS, (Grams et al., 2014; Helama et al., 2018; Held and Soden, 2006; Madsen et al., 2014). Medium confidence: Snow cover is declining but by how much and how it effects large scale teleconnections not straightforward (Bokhorst et al., 2016; Cohen et al., 2014). High confidence: Increased extreme snow-melt events (Hansen et al., 2014; Pedersen et al., 2015)	al., 2014; Wilcox et al., 2018). High confidence: Recent extreme wet winters are attributable to climate change (Otto et al., 2018b; Schaller et al., 2016; Vautard et al., 2016).		confidence: Small changes in drought frequency (Kay et al., 2018)	2016).	confidence decrease in droughts in NEU (Spinoni et al., 2015).
Alps	*High confidence*: Increase in temperature extremes (Gobiet et al., 2014; Stoffel and Corona, 2018). High confidence: Strong increase in heatwave duration and intensity and decrease in cold spells (Brugnara et al., 2016)		*High confidence*: Projected increase in temperature extremes in all seasons (Gobiet et al., 2014).	*High confidence*: Negative trends in snow cover below 2000m (Beniston et al., 2018) and glaciers (Beniston et al., 2018; Fischer et al., 2015; Gardent et al., 2014; Roudier et al., 2016). Medium confidence: increase in Rain on snow events that lead to flood (Beniston and Stoffel, 2016). Low confidence: floodsincrease(Roudier et al., 2016).		*High confidence*: Intensity of precipitation extremes increase in all seasons (Gobiet et al., 2014)particularlywinter(Fischer et al., 2015). Medium confidence: flood increase(Roudier et al., 2016)despitedecliningsnowamounts(Frei et al., 2018; Hanzer et al., 2018). High confidence: Elevationincrease of the snowlines(Beniston et al., 2018)(Marty et al., 2017). Medium confidence: decrease in snowfall extremes (Vries et al., 2014). Medium confidence: Changes in rainfallseasonality(Brönnimann et al., 2018)	*Medium confidence*: Wet days decrease in summer, (Gobiet et al., 2014). Runoff decreases in particular in summer (Hanzer et al., 2018).		*Medium confidence*: Decrease in wet days in summer projected to continue (Fischer et al., 2015). ;edium confidence: Drought probabilities increase in summer (Haslinger et al., 2016)

[END TABLE 11.14 HERE]

[START TABLE 11.15 HERE]

Table 11.7: Regional assessments for Central and South America [to be further completed for SOD]

	Temperature extremes			Precipitation extremes and flooding (including effects of TC, ETC and atmospheric rivers)			Droughts, dryness and aridity		
	Observed trends	Detection and attribution; event attribution	Projections	Observed trends	Detection and attribution; event attribution	Projections	Observed trends	Detection and attribution; event attribution	Projections
Central America (CAM):	*High confidence*: Warming in most of CAM (Donat et al., 2016b; Hidalgo et al., 2017) and cooling in parts of Honduras and northern Panama (Hidalgo et al., 2017)		*High confidence*: Warming (Hidalgo et al., 2017; Imbach et al., 2018; Sillmann et al., 2013a)	*Low confidence*: Increase in precipitation extremes most of CAM (Donat et al., 2016b) and in Guatemala, El Salvador and Panama (Hidalgo et al., 2017)		*Low confidence*: Decrease during the rainy season (Imbach et al., 2018) Decrease (increase) in the northern part of CAM (Southern Panama) consistent with the future south displacement of ITCZ (Hidalgo et al., 2017) Mostly decrease (Chou et al., 2014; Giorgi et al., 2014)	*Low confidence*: Drying trends in the Central Pacific slope of Costa Rica and a small part in the middle of Panama (Hidalgo et al., 2017)		*Low confidence*: Increase the Mid-Summer Drought (Imbach et al., 2018) Mostlyincrease in CDD (Chou et al., 2014; Giorgi et al., 2014)
Amazon (AMZ)	*High confidence*: Warming: increases in TN and TX(Almeida et al., 2017; Donat et al., 2016b; Skansi et al., 2013)		*High confidence*: Warming(Chou et al., 2014; López-Franca et al., 2016; Sillmann et al., 2013b)	*Medium confidence*: Increasing (decreasing) trends in the annual and wet (dry) season rainfall (Almeida et al., 2017). Mostly increasing trends in precipitation extremes (Skansi et al., 2013)		*Low confidence*: Decreasing of PRCPTOT, R95p and CWD (Chou et al., 2014; Seiler et al., 2013)while(Giorgi et al., 2014) shows an increase in R95p.	*Low confidence*: Increase in CDD (Skansi et al., 2013)		*Low confidence*: Increase in dryness (Marengo and Espinoza, 2016) Increase in the frequency and geographic extent of meteorological drought in the eastern Amazon, and the opposite in the West (Duffy et al., 2015)
Northeastern Brazil (NEB)	*High confidence*: Warming in Pernambuco (Lacerda et al., 2015) and MATOPIBA region (Salvador and de Brito, 2018)		*High confidence*: Warming(Chou et al., 2014; Lacerda et al., 2015; López-Franca et al., 2016; Marengo and Bernasconi, 2015;	*Low confidence*: Decrease in PRCPTOT, RX1day, RX5day, R50mm, R95p, R99p in Custódia and Sta Maria da Boa Vista (PE)		*Low confidence*: Decrease in R95p (Chou et al., 2014; Giorgi et al., 2014)	*Low confidence*: Mostly upward trends in CDD (Skansi et al., 2013)		*Medium confidence*: Increase in dryness, (Marengo and Bernasconi, 2015) Increase in CDD (Chou et al., 2014; Giorgi et al., 2014; Sillmann et al., 2013a)

			Sillmann et al., 2013b)	(Bezerra et al., 2018) Mostly decrease in precipitation extremes (Luiz Silva et al., 2018; Skansi et al., 2013)					
North Western South America (NWS)	*High confidence*: Warming in Peru (Skansi et al., 2013; Vicente-Serrano et al., 2018) and in Equator(Skansi et al., 2013)		*High confidence*: Warming(Chou et al., 2014; López-Franca et al., 2016; Sillmann et al., 2013b)	*Low confidence*: Increase in precipitationextremes(Donat et al., 2016b; Skansi et al., 2013)		*Low confidence*: Decreasing of PRCPTOT, R95p and CWD (Chou et al., 2014)whileGiorgi et al. (2014 and Seiler et al. (2013) show an increase in R95p and PRCPTOT	*Low confidence*: Mostly upward trends in CDD (Donat et al., 2016b; Skansi et al., 2013)		*Low confidence*: Increase in CDD) (Chou et al., 2014; Giorgi et al., 2014) Decrease in the frequency and geographic extent of meteorological drought in the western Amazon, and (Duffy et al., 2015)
South Western South America (SWS)	*High confidence*: Warming in SWS (Skansi et al., 2013) and in northern Chile (Meseguer-Ruiz et al., 2018)		*High confidence*: Warming(Chou et al., 2014; López-Franca et al., 2016; Sillmann et al., 2013b)	*Low confidence*: Positive trends over southern Pacific and Titicaca (Heidinger et al., 2018) Mostly positive trends ober SWS (Skansi et al., 2013)		*Low confidence*: Drier conditions (Reduction of PRCPTOT, and R95p) (Chou et al., 2014) Increase in R95p (Giorgi et al., 2014)	*Medium confidence*: Robust drying trend in Chile (30-48°S) (Boisier et al., 2018; Saurral et al., 2017)	*Low confidence*: Global warming: reduce precipitation in subtropical arid-semi arid zone and increase rainfall in the ITCZ (Minetti et al., 2014) Main character of the observed long term drying signal in Chile attributable to anthropogenic forcing (Boisier et al., 2018)	*Low confidence*: Increase in CDD) (Chou et al., 2014; Giorgi et al., 2014) Drying in Chile will likely prevail (Boisier et al., 2018)
South America Monsoon (SAM)	*Medium confidence*: Increasing in TN10p (Donat et al., 2016b)		*High confidence*: Warming at Pantanal (Marengo et al., 2016), over Bolivia (Seiler et al., 2013) and over SAM (Chou et al., 2014; Sillmann et al., 2013b)	*Low confidence*: Mostly increasing trends in precipitation extremes (Skansi et al., 2013)		*Low confidence*: Reduction oin rainfall at Pantanal (Marengo et al., 2016) Reduction in R95p (Chou et al., 2014) Increase in R95p (Giorgi et al., 2014)	*Low confidence*: Mostly upward trends in CDD (Skansi et al., 2013)		*Low confidence*: Mostlyincrease in CDD (Chou et al., 2014; Giorgi et al., 2014)
South Eastern South America (SES)	*High confidence*: Decrease in TX extremes over south western SES (Donat et al., 2016b; Skansi et al., 2013; Wu	*Low confidence*: Decrease in warm day extremes	*High confidence*: Warming at RJ, SP and Santos, mainly during the summer (Lyra et	*High confidence*: Increase in maximum precipitation extremes over SES	*Medium confidence*: Stratospheric ozone depletion	*Medium confidence*: Increase in the total monsoon precipitation over southern Brazil,	*Low confidence*: Mostly upward trends in CDD (Skansi et al., 2013)		*Low confidence*: Mostly downward trends in CDD (Chou et al., 2014; Giorgi et al., 2014)

	and Polvani, 2017) Warming in SP (Zilli et al., 2017), RJ, SC (Ávila et al., 2016) Increasing in intensity and in frequency of heat waves. No significant changes detected for cold waves (Ceccherini et al., 2016)	linked with stratospheric ozone depletion (Wu and Polvani, 2017) Anthropogenic forcings increased the risk of heatwaves by a factor of five (Hannart et al., 2015)	al., 2018) Warming in TN stronger than in TX (López-Franca et al., 2016) Warming(Chou et al., 2014; Sillmann et al., 2013b)	(Wu and Polvani, 2017), over most of subtropical Argentina (Barros et al., 2015) Increase in annual rainfall (Saurral et al., 2017) Increase in summer rainfall (Vera and Díaz, 2015) Intense precipitation events in most of the northeastern Argentina increased since 1970 (Lovino et al., 2018) Wet grid cells in PRCPTOT and RX1day over SES (Donat et al., 2016a)	causing increase in precipitation and decrease in maximum temperature extremes (Wu and Polvani, 2017) Hadley cell has shrunk and shifted towards the equator in winter over the SES which has caused an enhancement of the sinking motion over much of Argentina, Chile and Brazil, while increasing the baroclinicity (and associated precipitation) over Patagonia (Saurral et al., 2017) Antropogenic forcing explaining the precipitation changes observed in SES (Vera and Díaz, 2015)	Uruguay, and northern Argentina under RCP8.5(Jones and Carvalho, 2013) Wetting condition (increase in PRCPTOT and R95p) under RCP4.5 and RCP8.5 (Chou et al., 2014) Drierclimate in RJ, SP and Santos (Lyra et al., 2018)			
Southern South America (SSA)	*Medium confidence*: Warming (Skansi et al., 2013)		*High confidence*: Warming(Chou et al., 2014; López-Franca et al., 2016; Sillmann et al., 2013b)	*Low confidence*: Increase in maximum precipitationextremes over SSA (Skansi et al., 2013)	*Low confidence*: Antropogenic forcing explaining the precipitation	*Low confidence*: Increase in R95p (Giorgi et al., 2014)	*Low confidence*: Downward trends in CDD (Skansi et al., 2013)		*Low confidence*: Projecteddecreasing in CDD (Giorgi et al., 2014)

				Negative trends in austral summer rainfall in southern Andes (Vera and Díaz, 2015)	changes observed in southern Andes (Vera and Díaz, 2015)				

[END TABLE 11.15 HERE]

[START TABLE 11.16 HERE]

Table 11.8: Regional assessments for North America [to be further completed for SOD]

	Temperature extremes			Precipitation extremes and flooding (including effects of TC, ETC and atmospheric rivers)			Droughts, dryness and aridity		
	Observed trends	Detection and attribution; event attribution	Projections [including assessment of model evaluation for confidence]	Observed trends	Detection and attribution; event attribution	Projections [including assessment of model evaluation for confidence]	Observed trends	Detection and attribution; event attribution	Projections [including assessment of model evaluation for confidence]
Canada	Increase in hot days and decraese in cold days, incraese in TXx, TNn(Wang et al. 2014, Wan et al. 2017, Vincent et al. 2018)	Incraese in TXx, TNn (Wan et al. 2017, Wang et al. 2017)	Increasing in TNn and TXx during winter and summer (Grotjahn et al., 2016), Li et al. 2018 Increase in the number of warm spell days (Alexandru, 2018), Li et al. 2018	No detectable trend in obsered annual maximum daily (or shorter duration) precipitation (Shephard et al. 2014, Mekis et al. 2015, Vincent et al. 2018)		Increase in precipitation during the year, except in JJA over Central Canada and increase in the number of days with daily precipitation larger than the 90th present-climate percentile (Alexandru, 2018)	Defer to Canada's Climate Change Assessmen Report		Based on SPI Swain and Hayhoe (2015) project for MAM (JJA) wetter (drier) conditions over most of Canada. Also add Canada's climate change assessment report when it is released
USA	Increasing hot days and cold nights (Vose et al., 2017)		Increasing hot days and cold nights (Vose et al., 2017) Increasing in TNn and TXx during winter and summer (Grotjahn et al., 2016)	Increase in precipitationextremesacross CONUS (Easterling et al., 2017; Wu, 2015) Increase in extreme hurricane rainfall events (Emanuel, 2017; Risser and Wehner, 2017; Trenberth et al., 2018; van Oldenborgh et al., 2017; Wang et al., 2018b).	Hurricane Harvey increased rate of occurrence associated with anthropogenic warming (Emanuel, 2017; Risser and Wehner, 2017; Trenberth et al., 2018; van Oldenborgh et al., 2017; Wang et al., 2018b)	Increase in precipitation extremes across CONUS (Easterling et al., 2017) Projected increase in hurricane rain rates (medium to high confidence) (Knutson et al., 2015; Kossin et al., 2017) Increased rainfall volume associated with severe convective storms (Prein et al., 2017c). Increased	None		Based on SPI Swain and Hayhoe (2015) project for MAM and JJA drier conditions in most of the U.S.

						occurrenec of large hail (Brimelow et al., 2017)			
Rockies	Increasing hot days and cold nights (Grotjahn et al., 2016; Vose et al., 2017)		Increase (decrease) in TN90p and TX90p (TN10p and TX10p) (Yang et al., 2018a) Increasing in TNn and TXx during winter and summer (Grotjahn et al., 2016) Increase in the number of warm spell days (Alexandru, 2018)	Increase in precipitation extremes (Easterling et al., 2017; Wu, 2015)					Based on SPI Swain and Hayhoe (2015) project for MAM, wetter (drier) conditions in the northern (southern) Rockies and for JJA drier conditions.
Mexico	Increase (decrease) in TX90p, TXx and TNn (TN10p) (Donat et al., 2016b) Decrease in TNn(Donat et al., 2014b)		Increase (decrease) in TN90p and TX90p (TN10p and TX10p) (Yang et al., 2018a) Increase in the number of warm spell days (Alexandru, 2018)	Increase in R10mm and R95p (Donat et al., 2016b) Increase in PRCPTOT and RX1day (Donat et al., 2016a)		Decrease in precipitation(Alexandru, 2018; Cook et al., 2014a) and in the number of days with daily precipitation larger than the 90th present-climate percentile (Alexandru, 2018) Mixed trends (Meyer and Jin, 2017)	Decrease in CDD (Donat et al., 2016b)		Increase in duration and intensity of droughts over northern and northwestern Mexico (Escalante-Sandoval and Nuñez-Garcia, 2017; Feng and Fu, 2013) Increase in CDD (Pascale et al., 2016)

[END TABLE 11.16 HERE]

Frequently Asked Questions

FAQ 11.1: How do extreme changes compare with mean climate changes?

Changes in temperature and precipitation extremes are at times larger and spatially more robust than their average counterpart. Yet changes in means and extremes can be governed by different processes, thereby challenging their intercomparison.

When comparing extreme changes to mean changes in climate, the answer depends on the aspect of extremes, as well as on the questions being asked. One can, for instance, consider variations in (i) the magnitude of the change, (ii) the spatial scale, or (iii) the underlying processes driving the changes.

Magnitude. While changes in global mean temperature have been used as an important indicator of global climate change, changes in regional mean land temperature are often larger than changes in global mean temperature. This is due to the lower heat capacity of land compared to oceans, and because land absorbs energy at the surface, whereas solar radiation penetrates into the water column and oceans subsequently transport it further down through mixing and circulation. This leads to land warming – on average – faster than oceans, and hence faster than the global average. In addition, for several variables and regions, absolute changes in extremes are larger than changes in global – and sometimes even local – means. This is exemplified in Figure 1, showing that past and future warming during the hottest day in the Mediterranean is consistently larger than the rise in global mean temperature. In contrast, in a few regions observational records do not show a rise in extreme temperatures despite a mean warming. For instance, observations show no increase in warm temperature extremes in recent decades over most of India and the US Midwest. For precipitation, percentage changes in wet extremes are usually larger than that changes in annual mean amounts (see below).

[START FAQ 11.1, FIGURE 1 HERE]

FAQ 11.1, Figure 1: In the Mediterranean, warming of hot extremes is consistently larger than the rise in global mean temperature.

[END FAQ 11.1, FIGURE 1 HERE]

This is illustrated by the modelled relation between daily maximum temperature during warmest day of the year and global mean temperature change (red band) lying consistently above the 1:1 line (dashed line). Full lines represent the CMIP5 multi-model mean changes under past (black), moderate future (RCP4.5, blue) and business-as-usual future (RCP8.5, red) emissions, whereas the red band represents the multi-model envelope including uncertainties from emission scenarios, model deficiencies and natural variability. From Seneviratne et al. (2016), see ref for technical details.

Spatial scale. While local-scale changes in extreme may be subject to considerable uncertainty, spatial aggregation of temperature and precipitation extremes highlights a robust response to climate change with increased likelihood of both hot extremes and heavy precipitation. Moreover, a small change in the mean conditions shifts the entire distribution, resulting in a relatively large change in the probability of extremes.

Processes driving mean and extreme change. Some processes amplify extreme events rather than mean conditions, resulting in the tail of variable distributions showing a higher increase than the median values. This is for instance the case with hot extremes in regions that are projected to become drier during the warm season. Also changes in surface albedo have been shown to affect hot extremes more than median temperatures: because there tends to be more incident shortwave radiation on hot days, an increased surface reflectivity associated with higher albedo will induce a stronger net cooling. Likewise, also the absence of warming during hot days may be explained by processes affecting extremes rather than mean. Notably, the absence of warming in India and the US Midwest has been ascribed to cooling from aerosols and local land management including irrigation and cropland intensification.

In case of precipitation, changes in wet extremes are largely constrained by moisture availability, leading to extreme precipitation changing consistent with the Clausius-Clapeyron relation in absence of a moisture limitation (that is, an increase by about 7% per degree of warming). In contrast to this thermodynamic control on extremes, changes in mean precipitation rather tend to be determined by changes in atmospheric circulation, moisture transport and the surface energy balance, generally leading to more complex patterns and rates of change. Additionally, there is evidence for dynamics to modulate such that larger change is associated with more extreme precipitation.

FAQ 11.2: Could new types of extreme events develop from climate change?

As the climate changes, the associated unusual or extreme events will also change. Most future extreme events will be similar to past events, but some will occur with magnitudes much larger than experienced in the past and some events will occur much more frequently. The compound occurrence of multiple extreme events may change the type and severity of future impacts.

The climate we have experienced is one to which both human and natural systems have adapted. This climate state includes the occurrence of unusual and extreme events. As the climate changes, it moves away from that which the human and natural systems are accustomed. When extreme events occur in the new climate state, they have the potential to be different from those events experienced in the past. For example, we have seen an increased occurrence of record-breaking hot temperatures globally and throughout many regions. In addition, warming may have resulted in more precipitation brought by tropical cyclones and continued warming is projected to increase tropical cyclone rainfall even more. In this sense, new extremes that have never been experienced before may emerge.

In general, many extreme events in a warmer climate will be similar to what we have experienced in the past. This is because the projected changes in large-scale circulation and thus, the associated weather systems that generate extreme events, are relatively small. However, these extreme events will often be more severe or occur more frequently. For example, we have experienced heatwaves in the past and we will experience heatwaves in the future. However, under a warmer climate, the heatwaves will have hotter temperatures and last longer than past heatwaves. A severe heatwave event that occurs once in five years in China today is projected to become an annual event under a high level of global warming.

Compound events are also an important consideration for future extremes. They occur when multiple hazards combine to produce increased risks and impacts. For example, the occurrence of drought combined with extreme heat will increase the risk of wildfires and agriculture losses. A changing climate may alter the interaction between hazards or see the combination of multiple unprecedented events. It is possible that compound events will exceed the adaptive capacity or resilience of the human and natural systems more quickly than individual events. The result could include types or levels of impacts not seen previously.

FAQ 11.3: Did climate change cause that recent extreme event in my country?

The climate and weather we experience varies from day to day and from year to year. As a result, there will always be unusual or extreme weather and climate events. However, there is strong evidence that characteristics of many types of extreme events have already changed because of changes in the climate. These events are occurring more often and becoming more severe.

Many factors contributed to the occurrence of any specific extreme event. While some factors may include the built environment or human behavior (e.g., increased pavement in an urban area that contributed to increased flooding), many factors involve the local or global climate. These climate factors are driven by natural variability on the backdrop of a changing climate. While it is difficult to answer if climate change has caused particular extreme events, it is possible, through a process called event attribution, to quantify how climate change has altered the characteristics of some types of extreme events.

There is strong evidence that characteristics of extreme events, including their frequency or magnitude, may have changed as a result of climate change. Precipitation extremes have intensified over large scales and in some regions. Heatwaves around the globe have consistently increased in frequency, and many in magnitude as well. That is, heatwaves are occurring more often and with hotter temperatures. With warming, cold extremes are less frequent and less cold.

[START FAQ 11.3, FIGURE 1 HERE]

FAQ 11.3, Figure 1:Demonstration of changing temperature extremes with a warming climate. Return periods for hot (a) and cold (b) extremes are shown with a log scale for a natural only climate (dark blue) and a climate that includes human-driven climate change (light blue). A return period describes the average time between events of a certain magnitude; shorter return periods indicate more frequent occurrence. An extreme hot temperature in the natural climate increases in both frequency (red arrow) and magnitude (orange arrow) under climate change. Similarly, an extreme cold temperature in the natural climate decreases in frequency (dark green arrow) and increases in magnitude (light green arrow) with climate change.

[END FAQ 11.3, FIGURE 1 HERE]

The change in temperature extremes is illustrated in FAQ 11.3, figure 1. A climate that is influenced by only natural factors will still experience extreme hot and extreme cold events. However, including the effects of anthropogenic climate change results in a warmer climate. In this case, the cold events of the natural climate occur less often, while the hot events occur much more frequently. Similarly, the cold event that occurs once in 50 years, for example, will be much warmer under the influence of climate change. The same is true for hot events; an event that occurs with the same frequency in both climates will be warmer with climate change.

While a specific event may not be entirely attributable to human-driven changes in the climate, there is already evidence that climate change is resulting in certain extreme events occurring more frequently or becoming more intense. With continued warming, it is expected that many extreme events will continue to occur more often or become more severe in the future.

References

Abatzoglou, J. T., and Rupp, D. E. (2017). Evaluating climate model simulations of drought for the northwestern United States. *Int. J. Climatol.* 37, 910–920. doi:10.1002/joc.5046.

Adnan, M., Rehman, N., Ali, S., Mehmood, S., Mir, K. A., Khan, A. A., et al. (2017). Prediction of summer rainfall in Pakistan from global sea-surface temperature and sea-level pressure. *Weather* 72, 76–84. doi:10.1002/wea.2784.

Adnan, M., Rehman, N., and Shahbir, J. (2016). Predicting the Frequency and Intensity of Climate Extremes by Regression Models. *J. Climatol. Weather Forecast.* 04. doi:10.4172/2332-2594.1000185.

Aerenson, T., Tebaldi, C., Sanderson, B., and Lamarque, J.-F. (2018). Changes in a suite of indicators of extreme temperature and precipitation under 1.5 and 2 degrees warming. *Environ. Res. Lett.* 13, 035009. doi:10.1088/1748-9326/aaafd6.

AghaKouchak, A., Cheng, L., Mazdiyasni, O., and Farahmand, A. (2014). Global warming and changes in risk of concurrent climate extremes: Insights from the 2014 California drought. *Geophys. Res. Lett.* 41, 8847–8852. doi:10.1002/2014GL062308.

AghaKouchak, A., Farahmand, A., Melton, F. S., Teixeira, J., Anderson, M. C., Wardlow, B. D., et al. (2015). Remote sensing of drought: Progress, challenges and opportunities. *Rev. Geophys.* 53, 452–480. doi:10.1002/2014RG000456.

Ahmed, M., Anchukaitis, K. J., Asrat, A., Borgaonkar, H. P., Braida, M., Buckley, B. M., et al. (2013). Continental-scale temperature variability during the past two millennia. *Nat. Geosci.* 6, 339–346. doi:10.1038/ngeo1797.

Ahn, K.-H., Merwade, V., Ojha, C. S. P., and Palmer, R. N. (2016). Quantifying relative uncertainties in the detection and attribution of human-induced climate change on winter streamflow. *J. Hydrol.* 542, 304–316. doi:https://doi.org/10.1016/j.jhydrol.2016.09.015.

Aich, V., Liersch, S., Vetter, T., Fournet, S., Andersson, J. C. M., Calmanti, S., et al. (2016). Flood projections within the Niger River Basin under future land use and climate change. *Sci. Total Environ.* 562, 666–677. doi:10.1016/j.scitotenv.2016.04.021.

Akinsanola, A. A., and Zhou, W. (2018). Projections of West African summer monsoon rainfall extremes from two CORDEX models. *Clim. Dyn.* doi:10.1007/s00382-018-4238-8.

Alexander, L. V. (2016). Global observed long-term changes in temperature and precipitation extremes: A review of progress and limitations in IPCC assessments and beyond. *Weather Clim. Extrem.* 11, 4–16. doi:10.1016/J.WACE.2015.10.007.

Alexander, L. V., Zhang, X., Peterson, T. C., Caesar, J., Gleason, B., Klein Tank, A. M. G., et al. (2006). Global observed changes in daily climate extremes of temperature and precipitation. *J. Geophys. Res.* 111, D05109. doi:10.1029/2005JD006290.

Alexander, L. V, and Arblaster, J. M. (2017). Historical and projected trends in temperature and precipitation extremes in Australia in observations and CMIP5. *Weather Clim. Extrem.* 15, 34–56.

Alexandru, A. (2018). Consideration of land-use and land-cover changes in the projection of climate extremes over North America by the end of the twenty-first century. *Clim. Dyn.* 50, 1949–1973. doi:10.1007/s00382-017-3730-x.

Alfieri, L., Bisselink, B., Dottori, F., Naumann, G., de Roo, A., Salamon, P., et al. (2016). Global projections of river flood risk in a warmer world. *Earth's Futur.* 5, 171–182. doi:10.1002/2016EF000485.

Alfieri, L., Burek, P., Feyen, L., and Forzieri, G. (2015). Global warming increases the frequency of river floods in Europe. *Hydrol. Earth Syst. Sci.* 19, 2247–2260. doi:10.5194/hess-19-2247-2015.

Alkama, R., and Cescatti, A. (2016). Biophysical climate impacts of recent changes in global forest cover. *Science (80-.).* 351, 600–604. doi:10.1126/science.aac8083.

Allen, C. D., Breshears, D. D., and McDowell, N. G. (2015). On underestimation of global vulnerability to tree mortality and forest die-off from hotter drought in the Anthropocene. *Ecosphere* 6, art129. doi:10.1890/ES15-00203.1.

Allen, C. D., Macalady, A. K., Chenchouni, H., Bachelet, D., McDowell, N., Vennetier, M., et al. (2010). A global overview of drought and heat-induced tree mortality reveals emerging climate change risks for forests. *For. Ecol. Manage.* 259, 660–684. doi:10.1016/j.foreco.2009.09.001.

Almeida, C. T., Oliveira-Júnior, J. F., Delgado, R. C., Cubo, P., and Ramos, M. C. (2017). Spatiotemporal rainfall and temperature trends throughout the Brazilian Legal Amazon, 1973-2013. *Int. J. Climatol.* 37, 2013–2026. doi:10.1002/joc.4831.

Altman, J., Ukhvatkina, O. N., Omelko, A. M., Macek, M., Plener, T., Pejcha, V., et al. (2018). Poleward migration of the destructive effects of tropical cyclones during the 20th century. *Proc. Natl. Acad. Sci.* 115, 11543 LP-11548. doi:10.1073/pnas.1808979115.

Añel, J. A., López-Moreno, J. I., Otto, F. E. L., Vicente-Serrano, S. M., Schaller, N., Massey, N., et al. (2014). The extreme snow accumulation in the Western Spanish Pyrenees during winter and spring 2013. *Bull. Am. Meteorol. Soc.* 95, S73–S74.

Angélil, O., Perkins-Kirkpatrick, S., Alexander, L. V, Stone, D., Donat, M. G., Wehner, M., et al. (2016). Comparing

regional precipitation and temperature extremes in climate model and reanalysis products. *Weather Clim. Extrem.* 13, 35–43. doi:https://doi.org/10.1016/j.wace.2016.07.001.
Angélil, O., Stone, D. A., Tadross, M., Tummon, F., Wehner, M., and Knutti, R. (2014). Attribution of extreme weather to anthropogenic greenhouse gas emissions: Sensitivity to spatial and temporal scales. *Geophys. Res. Lett.* 41, 2150–2155. doi:10.1002/2014GL059234.
Angélil, O., Stone, D., Perkins-Kirkpatrick, S., Alexander, L. V., Wehner, M., Shiogama, H., et al. (2018). On the nonlinearity of spatial scales in extreme weather attribution statements. *Clim. Dyn.* 50, 2739–2752. doi:10.1007/s00382-017-3768-9.
Angélil, O., Stone, D., Wehner, M., Paciorek, C. J., Krishnan, H., and Collins, W. (2017). An Independent Assessment of Anthropogenic Attribution Statements for Recent Extreme Temperature and Rainfall Events. *J. Clim.* 30, 5–16. doi:10.1175/JCLI-D-16-0077.1.
Antonescu, B., Schultz, D. M., Holzer, A., and Groenemeijer, P. (2016a). Tornadoes in Europe: An Underestimated Threat. *Bull. Am. Meteorol. Soc.* 98, 713–728. doi:10.1175/BAMS-D-16-0171.1.
Antonescu, B., Schultz, D. M., Lomas, F., and Kühne, T. (2016b). Tornadoes in Europe: Synthesis of the Observational Datasets. *Mon. Weather Rev.* 144, 2445–2480. doi:10.1175/MWR-D-15-0298.1.
Archfield, S. A., Hirsch, R. M., Viglione, A., and Blöschl, G. (2016). Fragmented patterns of flood change across the United States. *Geophys. Res. Lett.* 43, 10,232-10,239. doi:10.1002/2016GL070590.
Argüeso, D., Hidalgo-Muñoz, J. M., Ga´ Miz-Fortis, S. R., Esteban-Parra, M. J., and Castro-Díez, Y. (2012). Evaluation of WRF Mean and Extreme Precipitation over Spain: Present Climate (1970-99). *J. Clim.* 25, 4883–4895. doi:10.1175/JCLI-D-11-00276.1.
Arheimer, B., and Lindström, G. (2015). Climate impact on floods: Changes in high flows in Sweden in the past and the future (1911-2100). *Hydrol. Earth Syst. Sci.* 19, 771–784. doi:10.5194/hess-19-771-2015.
Armstrong, W. H., Collins, M. J., and Snyder, N. P. (2014). Hydroclimatic flood trends in the northeastern United States and linkages with large-scale atmospheric circulation patterns. *Hydrol. Sci. J.* 59, 1636–1655. doi:10.1080/02626667.2013.862339.
Arnell, N. W., and Gosling, S. N. (2016). The impacts of climate change on river flood risk at the global scale. *Clim. Change* 134, 387–401. doi:10.1007/s10584-014-1084-5.
Asmerom, Y., Polyak, V. J., Rasmussen, J. B. T., Burns, S. J., and Lachniet, M. (2013). Multidecadal to multicentury scale collapses of Northern Hemisphere monsoons over the past millennium. *Proc. Natl. Acad. Sci. U. S. A.* 110, 9651–9656. doi:10.1073/pnas.1214870110.
Auerbach, L. W., Goodbred Jr, S. L., Mondal, D. R., Wilson, C. A., Ahmed, K. R., Roy, K., et al. (2015). Flood risk of natural and embanked landscapes on the Ganges–Brahmaputra tidal delta plain. *Nat. Clim. Chang.* 5, 153. Available at: http://dx.doi.org/10.1038/nclimate2472.
Ávila, A., Justino, F., Wilson, A., Bromwich, D., and Amorim, M. (2016). Recent precipitation trends, flash floods and landslides in southern Brazil. *Environ. Res. Lett.* 11, 114029. doi:10.1088/1748-9326/11/11/114029.
Avila, F. B., Dong, S., Menang, K. P., Rajczak, J., Renom, M., Donat, M. G., et al. (2015). Systematic investigation of gridding-related scaling effects on annual statistics of daily temperature and precipitation maxima: A case study for south-east Australia. *Weather Clim. Extrem.* 9, 6–16. doi:10.1016/j.wace.2015.06.003.
Azorin-Molina, C., Vicente-Serrano, S. M., Mcvicar, T. R., Jerez, S., Sanchez-Lorenzo, A., López-Moreno, J.-I., et al. (2014). Homogenization and assessment of observed near-surface wind speed trends over Spain and Portugal, 1961-2011. *J. Clim.* 27. doi:10.1175/JCLI-D-13-00652.1.
Bador, M., Terray, L., and Boé, J. (2016). Detection of anthropogenic influence on the evolution of record-breaking temperatures over Europe. *Clim. Dyn.* 46, 2717–2735. doi:10.1007/s00382-015-2725-8.
Bador, M., Terray, L., Boé, J., Somot, S., Alias, A., Gibelin, A. L., et al. (2017). Future summer mega-heatwave and record-breaking temperatures in a warmer France climate. *Environ. Res. Lett.* 12. doi:10.1088/1748-9326/aa751c.
Baek, H.-J., Kim, M.-K., and Kwon, W.-T. (2017). Observed short- and long-term changes in summer precipitation over South Korea and their links to large-scale circulation anomalies. *Int. J. Climatol.* 37, 972–986. doi:10.1002/joc.4753.
Bai, P., Liu, X., Liang, K., and Liu, C. (2016). Investigation of changes in the annual maximum flood in the Yellow River basin, China. *Quat. Int.* 392, 168–177. doi:10.1016/j.quaint.2015.04.053.
Ban, N., Schmidli, J., and Schär, C. (2014). Evaluation of the new convective-resolving regional climate modeling approach in decade-long simulations. *J. Geophys. Res. Atmos.* 119, 7889–7907. doi:10.1002/2014JD021478.
Ban, N., Schmidli, J., and Schär, C. (2015). Heavy precipitation in a changing climate: Does short-term summer precipitation increase faster? *Geophys. Res. Lett.* 42, 1165–1172. doi:10.1002/2014GL062588.
Bao, J., Sherwood, S. C., Alexander, L. V, and Evans, J. P. (2017). Future increases in extreme precipitation exceed observed scaling rates. *Nat. Clim. Chang.* 7, 128–132. doi:10.1038/nclimate3201.
Barker, L. J., Hannaford, J., Chiverton, A., and Svensson, C. (2016). From meteorological to hydrological drought using standardised indicators. *Hydrol. Earth Syst. Sci.* 20, 2483–2505. doi:10.5194/hess-20-2483-2016.
Barlow, M., and Hoell, A. (2015). Drought in the Middle East and Central–Southwest Asia During Winter 2013/14. *Bull. Am. Meteorol. Soc.* 96, S71–S76. doi:10.1175/BAMS-D-15-00127.1.
Barnabas, B., Jager, K., and Feher, A. (2007). The effect of drought and heat stress on reproductive processes in cereals.

Plant. Cell Environ., 11–38. doi:10.1111/j.1365-3040.2007.01727.x.
Barnard, P. L., Hoover, D., Hubbard, D. M., Snyder, A., Ludka, B. C., Allan, J., et al. (2017). Extreme oceanographic forcing and coastal response due to the 2015–2016 El Niño. *Nat. Commun.* 8, 14365. doi:10.1038/ncomms14365.
Barraqué, B. (2017). The common property issue in flood control through land use in France. *J. Flood Risk Manag.* 10, 182–194. doi:10.1111/jfr3.12092.
Barriopedro, D., Fischer, E. M., Luterbacher, J., Trigo, R. M., and Garcia-Herrera, R. (2011). The Hot Summer of 2010: Redrawing the Temperature Record Map of Europe. *Science (80-.).* 332, 220–224. doi:10.1126/science.1201224.
Barros, V. R., Boninsegna, J. A., Camilloni, I. A., Chidiak, M., Magrín, G. O., and Rusticucci, M. (2015). Climate change in Argentina: trends, projections, impacts and adaptation. *Wiley Interdiscip. Rev. Clim. Chang.* 6, 151–169. doi:10.1002/wcc.316.
Barry, A. A., Caesar, J., Klein Tank, A. M. G., Aguilar, E., McSweeney, C., Cyrille, A. M., et al. (2018). West Africa climate extremes and climate change indices. *Int. J. Climatol.* 38, e921–e938. doi:10.1002/joc.5420.
Bartos, M. D., and Chester, M. V. (2015). Impacts of climate change on electric power supply in the Western United States. *Nat. Clim. Chang.* 5, 748–752. doi:10.1038/nclimate2648.
Basconcillo, J., Lucero, A., Solis, A., Sandoval Jr, R., Bautista, E., Koizumi, T., et al. (2016). Statistically downscaled projected changes in seasonal mean temperature and rainfall in Cagayan Valley, Philippines. *J. Meteorol. Soc. Japan. Ser. II* 94, 151–164.
Beguería, S., Vicente-Serrano, S. M., Tomás-Burguera, M., and Maneta, M. (2016). Bias in the variance of gridded data sets leads to misleading conclusions about changes in climate variability. *Int. J. Climatol.* 36. doi:10.1002/joc.4561.
Bellprat, O., García-Serrano, J., Fučkar, N. S., Massonnet, F., Guemas, V., and Doblas-Reyes, F. J. (2016). The Role of Arctic Sea Ice and Sea Surface Temperatures on the Cold 2015 February Over North America. *Bull. Am. Meteorol. Soc.* 97, S36–S41. doi:10.1175/BAMS-D-16-0159.1.
Bellprat, O., Lott, F. C., Gulizia, C., Parker, H. R., Pampuch, L. A., Pinto, I., et al. (2015). Unusual past dry and wet rainy seasons over Southern Africa and South America from a climate perspective. *Weather Clim. Extrem.* 9, 36–46. doi:10.1016/J.WACE.2015.07.001.
Bender, M. A., Knutson, T. R., Tuleya, R. E., Sirutis, J. J., Vecchi, G. A., Garner, S. T., et al. (2010). Modeled Impact of Anthropogenic Atlantic Hurricanes. *Science (80-.).* 327, 454–458.
Beniston, M., Farinotti, D., Stoffel, M., Andreassen, L. M., Coppola, E., Eckert, N., et al. (2018). The European mountain cryosphere: a review of its current state, trends, and future challenges. *Cryosph.* 12, 759–794. doi:10.5194/tc-12-759-2018.
Beniston, M., and Stoffel, M. (2016). Rain-on-snow events, floods and climate change in the Alps: Events may increase with warming up to 4°C and decrease thereafter. *Sci. Total Environ.* 571, 228–236. doi:https://doi.org/10.1016/j.scitotenv.2016.07.146.
Benito, G., Brázdil, R., Herget, J., and Machado, M. J. (2015). Quantitative historical hydrology in Europe. *Hydrol. Earth Syst. Sci.* 19, 3517–3539. doi:10.5194/hess-19-3517-2015.
Berg, A., Findell, K., Lintner, B., Giannini, A., Seneviratne, S. I., Van Den Hurk, B., et al. (2016). Land-atmosphere feedbacks amplify aridity increase over land under global warming. *Nat. Clim. Chang.* 6, 869–874. doi:10.1038/nclimate3029.
Berg, A., and Sheffield, J. (2018). Climate Change and Drought: the Soil Moisture Perspective. *Curr. Clim. Chang. Reports* 4, 180–191. doi:10.1007/s40641-018-0095-0.
Berg, A., Sheffield, J., and Milly, P. C. D. (2017). Divergent surface and total soil moisture projections under global warming. *Geophys. Res. Lett.* 44, 236–244. doi:10.1002/2016GL071921.
Bergaoui, K., Mitchell, D., Otto, F., Allen, M., Zaaboul, R., McDonnell, R., et al. (2015). The Contribution of Human-Induced Climate Change to the Drought of 2014 in the Southern Levant Region. *Bull. Am. Meteorol. Soc.* 96, S66–S70. doi:10.1175/BAMS-D-15-00129.1.
Berghuijs, W. R., Woods, R. A., Hutton, C. J., and Sivapalan, M. (2016). Dominant flood generating mechanisms across the United States. *Geophys. Res. Lett.* 43, 4382–4390. doi:10.1002/2016GL068070.
Bevacqua, E., Maraun, D., Vousdoukas, M. I., Voukouvalas, E., Vrac, M., Mentaschi, L., et al. (2018). Higher potential compound flood risk in Northern Europe under anthropogenic climate change. *EarthArXiv*. doi:10.31223/osf.io/ta764.
Bevis, M., Harig, C., Khan, S. A., Brown, A., Simons, F. J., Willis, M., et al. (2019). Accelerating changes in ice mass within Greenland, and the ice sheet's sensitivity to atmospheric forcing. *Proc. Natl. Acad. Sci.*, 201806562. doi:10.1073/pnas.1806562116.
Bezerra, B. G., Silva, L. L., Santos e Silva, C. M., and de Carvalho, G. G. (2018). Changes of precipitation extremes indices in São Francisco River Basin, Brazil from 1947 to 2012. *Theor. Appl. Climatol.* doi:10.1007/s00704-018-2396-6.
Bhatia, K., Vecchi, G., Murakami, H., Underwood, S., and Kossin, J. (2018). Projected response of tropical cyclone intensity and intensification in a global climate model. *J. Clim.* 31, 8281–8303. doi:10.1175/JCLI-D-17-0898.1.
Biasutti, M., Voigt, A., Boos, W. R., Braconnot, P., Hargreaves, J. C., Harrison, S. P., et al. (2018). Global energetics and local physics as drivers of past, present and future monsoons. *Nat. Geosci.* 11, 392–400. doi:10.1038/s41561-

018-0137-1.
Bindoff, N. L., Stott, P. A., AchutaRao, K., Allen, M. R., Gillett, N., Gutzler, D., et al. (2013). "Detection and Attribution of Climate Change: from Global to Regional," in *Climate Change 2013 - The Physical Science Basis*, ed. Intergovernmental Panel on Climate Change (Cambridge: Cambridge University Press), 867–952. doi:10.1017/CBO9781107415324.022.
Blanchet, J., Aly, C., Vischel, T., Panthou, G., Sané, Y., and Diop Kane, M. (2018). Trend in the Co-Occurrence of Extreme Daily Rainfall in West Africa Since 1950. *J. Geophys. Res. Atmos.* doi:10.1002/2017JD027219.
Blöschl, G., Hall, J., Parajka, J., Perdigão, R. A. P., Merz, B., Arheimer, B., et al. (2017). Changing climate shifts timing of European floods. *Science (80-.).* 357, 588–590. doi:10.1126/science.aan2506.
Blunden, J., and Arndt, D. S. (2016). State of the Climate in 2015. *Bull. Am. Meteorol. Soc.* 97, Si-S275. doi:10.1175/2016BAMSStateoftheClimate.1.
Boisier, J. P., Alvarez-Garretón, C., Cordero, R. R., Damiani, A., Gallardo, L., Garreaud, R. D., et al. (2018). Anthropogenic drying in central-southern Chile evidenced by long-term observations and climate model simulations. *Elem Sci Anth* 6, 74. doi:10.1525/elementa.328.
Bokhorst, S., Pedersen, S. H., Brucker, L., Anisimov, O., Bjerke, J. W., Brown, R. D., et al. (2016). Changing Arctic snow cover: A review of recent developments and assessment of future needs for observations, modelling, and impacts. *Ambio* 45, 516–537. doi:10.1007/s13280-016-0770-0.
Booth, J. F., Wang, S., and Polvani, L. (2013). Midlatitude storms in a moister world: lessons from idealized baroclinic life cycle experiments. *Clim. Dyn.* 41, 787–802. doi:10.1007/s00382-012-1472-3.
Borga, M., Stoffel, M., Marchi, L., Marra, F., and Jakob, M. (2014). Hydrogeomorphic response to extreme rainfall in headwater systems: Flash floods and debris flows. *J. Hydrol.* 518, 194–205. doi:10.1016/j.jhydrol.2014.05.022.
Bosshard, T., Carambia, M., Goergen, K., Kotlarski, S., Krahe, P., Zappa, M., et al. (2013). Quantifying uncertainty sources in an ensemble of hydrological climate-impact projections. *Water Resour. Res.* 49, 1523–1536. doi:10.1029/2011WR011533.
Bout, B., and Jetten, V. G. (2018). The validity of flow approximations when simulating catchment-integrated flash floods. *J. Hydrol.* 556, 674–688. doi:10.1016/j.jhydrol.2017.11.033.
Bozkurt, D., Rojas, M., Boisier, J. P., and Valdivieso, J. (2018). Projected hydroclimate changes over Andean basins in central Chile from downscaled CMIP5 models under the low and high emission scenarios. *Clim. Change* 150, 131–147. doi:10.1007/s10584-018-2246-7.
Brando, P. M., Balch, J. K., Nepstad, D. C., Morton, D. C., Putz, F. E., Coe, M. T., et al. (2014). Abrupt increases in Amazonian tree mortality due to drought-fire interactions. *Proc. Natl. Acad. Sci.* 111, 6347–6352. doi:10.1073/pnas.1305499111.
Brandon, C. M., Woodruff, J. D., Lane, D. P., and Donnelly, J. P. (2013). Tropical cyclone wind speed constraints from resultant storm surge deposition: A 2500 year reconstruction of hurricane activity from St. Marks, FL. *Geochemistry, Geophys. Geosystems* 14, 2993–3008. doi:10.1002/ggge.20217.
Brimelow, J. C., Burrows, W. R., and Hanesiak, J. M. (2017). The changing hail threat over North America in response to anthropogenic climate change. *Nat. Clim. Chang.* 7, 516–522. doi:10.1038/nclimate3321.
Brohan, P., Compo, G. P., Brönnimann, S., Allan, R. J., Auchmann, R., Brugnara, Y., et al. (2016). The 1816 'year without a summer' in an atmospheric reanalysis. *Clim. Past Discuss.*, 1–11. doi:10.5194/cp-2016-78.
Bronnimann, S., Fischer, A. M., Rozanov, E., Poli, P., Compo, G. P., and Sardeshmukh, P. D. (2015). Southward shift of the northern tropical belt from 1945 to 1980. *Nat. Geosci.* 8, 969–974. doi:10.1038/ngeo2568.
Brönnimann, S., Rajczak, J., Fischer, E. M., Raible, C. C., Rohrer, M., and Schär, C. (2018). Changing seasonality of moderate and extreme precipitation events in the Alps. *Nat. Hazards Earth Syst. Sci.* 18, 2047–2056. doi:10.5194/nhess-18-2047-2018.
Brooks, H. E. (2013). Severe thunderstorms and climate change. *Atmos. Res.* 123, 129–138. doi:10.1016/j.atmosres.2012.04.002.
Brown, S., Nicholls, R. J., Lázár, A. N., Hornby, D. D., Hill, C., Hazra, S., et al. (2018). What are the implications of sea-level rise for a 1.5, 2 and 3° C rise in global mean temperatures in the Ganges-Brahmaputra-Meghna and other vulnerable deltas? *Reg. Environ. Chang.*, 1–14.
Brugnara, Y., Auchmann, R., Brönnimann, S., Bozzo, A., Berro, D. C., and Mercalli, L. (2016). Trends of mean and extreme temperature indices since 1874 at low-elevation sites in the southern Alps. *J. Geophys. Res. Atmos.* 121, 3304–3325. doi:10.1002/2015JD024582.
Bucchignani, E., Zollo, A. L., Cattaneo, L., Montesarchio, M., and Mercogliano, P. (2017). Extreme weather events over China: assessment of COSMO-CLM simulations and future scenarios. *Int. J. Climatol.* 37, 1578–1594. doi:10.1002/joc.4798.
Büntgen, U., Tegel, W., Carrer, M., Krusic, P. J., Hayes, M., and Esper, J. (2015). Commentary to Wetter et al. (2014): Limited tree-ring evidence for a 1540 European 'Megadrought.' *Clim. Change* 131, 183–190. doi:10.1007/s10584-015-1423-1.
Burgman, R. J., and Jang, Y. (2015). Simulated U.S. drought response to interannual and decadal pacific SST variability. *J. Clim.* 28, 4688–4705. doi:10.1175/JCLI-D-14-00247.1.
Burke, C., Stott, P., Ciavarella, A., and Sun, Y. (2016). Attribution of Extreme Rainfall in Southeast China During May

2015. *Bull. Am. Meteorol. Soc.* 97, S92–S96. doi:10.1175/BAMS-D-16-0144.1.

Burn, D. H., and Whitfield, P. H. (2016). Changes in floods and flood regimes in Canada. *Can. Water Resour. J.* 41, 139–150. doi:10.1080/07011784.2015.1026844.

Byrne, M. P., and O'Gorman, P. A. (2015). The response of precipitation minus evapotranspiration to climate warming: Why the "Wet-get-wetter, dry-get-drier" scaling does not hold over land. *J. Clim.* 28, 8078–8092. doi:10.1175/JCLI-D-15-0369.1.

Cai, W., Borlace, S., Lengaigne, M., Van Rensch, P., Collins, M., Vecchi, G., et al. (2014a). Increasing frequency of extreme El Niño events due to greenhouse warming. *Nat. Clim. Chang.* 4, 111–116. doi:10.1038/nclimate2100.

Cai, W., Purich, A., Cowan, T., Van Rensch, P., and Weller, E. (2014b). Did climate change-induced rainfall trends contribute to the australian millennium drought? *J. Clim.* 27, 3145–3168. doi:10.1175/JCLI-D-13-00322.1.

Cai, W., Santoso, A., Wang, G., Yeh, S. W., An, S. Il, Cobb, K. M., et al. (2015). ENSO and greenhouse warming. *Nat. Clim. Chang.* 5, 849–859. doi:10.1038/nclimate2743.

Cai, W., Wang, G., Gan, B., Wu, L., Santoso, A., Lin, X., et al. (2018). Stabilised frequency of extreme positive Indian Ocean Dipole under 1.5°C warming. *Nat. Commun.* 9, 4–11. doi:10.1038/s41467-018-03789-6.

Calianno, M., Ruin, I., and Gourley, J. J. (2013). Supplementing flash flood reports with impact classifications. *J. Hydrol.* 477, 1–16. doi:10.1016/J.JHYDROL.2012.09.036.

Caloiero, T. (2015). Analysis of rainfall trend in New Zealand. *Environ. Earth Sci.* 73, 6297–6310. doi:10.1007/s12665-014-3852-y.

Caloiero, T. (2017). Trend of monthly temperature and daily extreme temperature during 1951–2012 in New Zealand. *Theor. Appl. Climatol.* 129, 111–127. doi:10.1007/s00704-016-1764-3.

Camargo, S. J., Emanuel, K. A., and Sobel, A. H. (2007). Use of a Genesis Potential Index to Diagnose ENSO Effects on Tropical Cyclone Genesis. *J. Clim.* 20, 4819–4834. doi:10.1175/JCLI4282.1.

Camargo, S. J., Tippett, M. K., Sobel, A. H., Vecchi, G. A., and Zhao, M. (2014). Testing the performance of tropical cyclone genesis indices in future climates using the HiRAM model. *J. Clim.* 27, 9171–9196. doi:10.1175/JCLI-D-13-00505.1.

Camargo, S. J., and Wing, A. A. (2016). Tropical cyclones in climate models. *Wiley Interdiscip. Rev. Clim. Chang.* 7, 211–237. doi:10.1002/wcc.373.

Cardoso, R. M., Soares, P. M. M., Lima, D. C. A., and Miranda, P. M. A. (2019). Mean and extreme temperatures in a warming climate: EURO CORDEX and WRF regional climate high-resolution projections for Portugal. *Clim. Dyn.* 52, 129–157. doi:10.1007/s00382-018-4124-4.

Casanueva, A., Rodríguez-Puebla, C., Frías, M. D., and González-Reviriego, N. (2014). Variability of extreme precipitation over Europe and its relationships with teleconnection patterns. *Hydrol. Earth Syst. Sci.* 18, 709–725. doi:10.5194/hess-18-709-2014.

Catto, J. L., Madonna, E., Joos, H., Rudeva, I., and Simmonds, I. (2015). Global relationship between fronts and warm conveyor belts and the impact on extreme precipitation. *J. Clim.* 28, 8411–8429. doi:10.1175/JCLI-D-15-0171.1.

Ceccherini, G., Russo, S., Ameztoy, I., Romero, C. P., and Carmona-Moreno, C. (2016). Magnitude and frequency of heat and cold waves in recent decades: the case of South America. *Nat. Hazards Earth Syst. Sci.* 16, 821–831. doi:10.5194/nhess-16-821-2016.

Chaney, N. W., Sheffield, J., Villarini, G., and Wood, E. F. (2014). Development of a high-resolution gridded daily meteorological dataset over sub-Saharan Africa: Spatial analysis of trends in climate extremes. *J. Clim.* doi:10.1175/JCLI-D-13-00423.1.

Chang, E. K. M. (2017). Projected Significant Increase in the Number of Extreme Extratropical Cyclones in the Southern Hemisphere. *J. Clim.* 30, 4915–4935. doi:10.1175/JCLI-D-16-0553.1.

Chang, E. K. M., and Yau, A. M. W. (2016). Northern Hemisphere winter storm track trends since 1959 derived from multiple reanalysis datasets. *Clim. Dyn.* 47, 1435–1454. doi:10.1007/s00382-015-2911-8.

Chen, H., and Sun, J. (2015a). Assessing model performance of climate extremes in China: an intercomparison between CMIP5 and CMIP3. *Clim. Change* 129, 197–211. doi:10.1007/s10584-014-1319-5.

Chen, H., and Sun, J. (2015b). Changes in Drought Characteristics over China Using the Standardized Precipitation Evapotranspiration Index. *J. Clim.* 28, 5430–5447. doi:10.1175/JCLI-D-14-00707.1.

Chen, H., and Sun, J. (2017a). Anthropogenic warming has caused hot droughts more frequently in China. *J. Hydrol.* 544, 306–318.

Chen, H., and Sun, J. (2017b). Characterizing present and future drought changes over eastern China. *Int. J. Climatol.* 37, 138–156. doi:10.1002/joc.4987.

Chen, H., and Sun, J. (2017c). Contribution of human influence to increased daily precipitation extremes over China. *Geophys. Res. Lett.* doi:10.1002/2016GL072439.

Chen, L., Pryor, S. C., and Li, D. (2012). Assessing the performance of Intergovernmental Panel on Climate Change AR5 climate models in simulating and projecting wind speeds over China. *J. Geophys. Res. Atmos.* 117. doi:10.1029/2012JD017533.

Chen, S., Li, Y., Kim, J., and Kim, S. W. (2017). Bayesian change point analysis for extreme daily precipitation. *Int. J. Climatol.* 37, 3123–3137. doi:10.1002/joc.4904.

Cheng, L., Hoerling, M., Smith, L., and Eischeid, J. (2018). Diagnosing Human-Induced Dynamic and Thermodynamic

Drivers of Extreme Rainfall. *J. Clim.* 31, 1029–1051. doi:10.1175/JCLI-D-16-0919.1.

Chevuturi, A., Klingaman, N. P., Turner, A. G., and Hannah, S. (2018). Projected Changes in the Asian-Australian Monsoon Region in 1.5°C and 2.0°C Global-Warming Scenarios. *Earth's Futur.* 6, 339–358. doi:10.1002/2017EF000734.

Chou, S. C., Lyra, A., Mourão, C., Dereczynski, C., Pilotto, I., Gomes, J., et al. (2014). Assessment of Climate Change over South America under RCP 4.5 and 8.5 Downscaling Scenarios. *Am. J. Clim. Chang.* 03, 512–527. doi:10.4236/ajcc.2014.35043.

Christiansen, B., Alvarez-Castro, C., Christidis, N., Ciavarella, A., Colfescu, I., Cowan, T., et al. (2018). Was the Cold European Winter of 2009/10 Modified by Anthropogenic Climate Change? An Attribution Study. *J. Clim.* 31, 3387–3410. doi:10.1175/JCLI-D-17-0589.1.

Christiansen, B., and Ljungqvist, F. C. (2017). Challenges and perspectives for large-scale temperature reconstructions of the past two millennia. *Rev. Geophys.* 55, 40–96. doi:10.1002/2016RG000521.

Christidis, N., Jones, G. S., and Stott, P. A. (2015). Dramatically increasing chance of extremely hot summers since the 2003 European heatwave. *Nat. Clim. Chang.* 5, 46–50. doi:10.1038/nclimate2468.

Christidis, N., and Stott, P. A. (2014). Change in the Odds of Warm Years and Seasons Due to Anthropogenic Influence on the Climate. *J. Clim.* 27, 2607–2621.

Christidis, N., and Stott, P. A. (2016). Attribution analyses of temperature extremes using a set of 16 indices. *Weather Clim. Extrem.* 14, 24–35. doi:10.1016/j.wace.2016.10.003.

Christidis, N., Stott, P. A., and Ciavarella, A. (2014). The effect of anthropogenic climate change on the cold spring of 2013 in the United Kingdom. *Bull. Am. Meteorol. Soc.* 95, S15–S18. doi:10.1175/1520-0477-95.9.S1.1.

Christidis, N., Stott, P. A., Karoly, D. J., and Ciavarella, A. (2013a). An Attribution Study of the Heavy Rainfall Over Eastern Australia in March 2012. *Bull. Am. Meteorol. Soc.* 94, S58-61.

Christidis, N., Stott, P. A., Scaife, A. A., Arribas, A., Jones, G. S., Copsey, D., et al. (2013b). A New HadGEM3-A-Based System for Attribution of Weather- and Climate-Related Extreme Events. *J. Clim.* 26, 2756–2783. doi:10.1175/JCLI-D-12-00169.1.

Ciais, P., Reichstein, M., Viovy, N., Granier, A., Ogée, J., Allard, V., et al. (2005). Europe-wide reduction in primary productivity caused by the heat and drought in 2003. *Nature* 437, 529–533. doi:10.1038/nature03972.

Cioffi, F., Lall, U., Rus, E., and Krishnamurthy, C. K. B. (2015). Space-time structure of extreme precipitation in Europe over the last century. *Int. J. Climatol.* 35, 1749–1760. doi:10.1002/joc.4116.

Cohen, J., Furtado, J. C., Jones, J., Barlow, M., Whittleston, D., and Entekhabi, D. (2014). Linking Siberian Snow Cover to Precursors of Stratospheric Variability. *J. Clim.* 27, 5422–5432. doi:10.1175/JCLI-D-13-00779.1.

Collins, J. M., Klotzbach, P. J., Maue, R. N., Roache, D. R., Blake, E. S., Paxton, C. H., et al. (2016). The record-breaking 2015 hurricane season in the eastern North Pacific: An analysis of environmental conditions. *Geophys. Res. Lett.* 43, 9217–9224. doi:10.1002/2016GL070597.

Collins, M., Knutti, R., Arblaster, J., Dufresne, J.-L., Fichefet, T., Friedlingstein, P., et al. (2013). "Long-term Climate Change: Projections, Commitments and Irreversibility Pages 1029 to 1076," in *Climate Change 2013 - The Physical Science Basis*, ed. Intergovernmental Panel on Climate Change (Cambridge, United Kingdom and New York, NY, USA: Cambridge University Press), 1029–1136. doi:10.1017/CBO9781107415324.024.

Cook, B. I., Anchukaitis, K. J., Touchan, R., Meko, D. M., and Cook, E. R. (2016a). Spatiotemporal drought variability in the Mediterranean over the last 900 years. *J. Geophys. Res. Atmos.* 121, 2060–2074. doi:10.1002/2015JD023929.

Cook, B. I., Ault, T. R., and Smerdon, J. E. (2015a). Unprecedented 21st century drought risk in the American Southwest and Central Plains. *Sci. Adv.* 1. doi:10.1126/sciadv.1400082.

Cook, B. I., Mankin, J. S., and Anchukaitis, K. J. (2018a). Climate Change and Drought: From Past to Future. *Curr. Clim. Chang. Reports* 4, 164–179. doi:10.1007/s40641-018-0093-2.

Cook, B. I., Palmer, J. G., Cook, E. R., Turney, C. S. M., Allen, K., Fenwick, P., et al. (2016b). The paleoclimate context and future trajectory of extreme summer hydroclimate in eastern Australia. *J. Geophys. Res.* 121, 12,812-820,838.

Cook, B. I., Smerdon, J. E., Seager, R., and Coats, S. (2014a). Global warming and 21st century drying. *Clim. Dyn.* 43, 2607–2627. doi:10.1007/s00382-014-2075-y.

Cook, B. I., Smerdon, J. E., Seager, R., and Cook, E. R. (2014b). Pan-Continental Droughts in North America over the Last Millennium. *J. Clim.* 27, 383–397. doi:10.1175/JCLI-D-13-00100.1.

Cook, E. R., Seager, R., Kushnir, Y., Briffa, K. R., Büntgen, U., Frank, D., et al. (2015b). Old World megadroughts and pluvials during the Common Era. *Sci. Adv.* 1. doi:10.1126/sciadv.1500561.

Cook, E. R., Woodhouse, C. A., Mark Eakin, C., Meko, D. M., and Stahle, D. W. (2004). Long-Term Aridity Changes in the Western United States. *Science (80-.).* 306, 1015–1018. doi:10.1126/science.1102586.

Cook, K. L., Andermann, C., Gimbert, F., Adhikari, B. R., and Hovius, N. (2018b). Glacial lake outburst floods as drivers of fluvial erosion in the Himalaya. *Science (80-.).* 362, 53 LP-57. doi:10.1126/science.aat4981.

Cook, M. A., King, C. W., Davidson, F. T., and Webber, M. E. (2015c). Assessing the impacts of droughts and heat waves at thermoelectric power plants in the United States using integrated regression, thermodynamic, and climate models. *Energy Reports* 1, 193–203. doi:10.1016/j.egyr.2015.10.002.

Corella, J. P., Benito, G., Rodriguez-lloveras, X., Brauer, A., and Valero-garcés, B. L. (2014). Annually-resolved lake record of extreme hydro-meteorological events since AD 1347 in NE Iberian Peninsula. *Quat. Sci. Rev.* 93, 77–90. doi:10.1016/j.quascirev.2014.03.020.
Crimp, S. J., Zheng, B., Khimashia, N., Gobbett, D. L., Chapman, S., Howden, M., et al. (2016). Recent changes in southern Australian frost occurrence: Implications for wheat production risk. *Crop Pasture Sci.* 67, 801–811. doi:10.1071/CP16056.
Croitoru, A.-E., Chiotoroiu, B.-C., Ivanova Todorova, V., and Torică, V. (2013). Changes in precipitation extremes on the Black Sea Western Coast. *Glob. Planet. Change* 102, 10–19. doi:10.1016/j.gloplacha.2013.01.004.
Croitoru, A.-E., and Piticar, A. (2013). Changes in daily extreme temperatures in the extra-Carpathians regions of Romania. *Int. J. Climatol.* 33, 1987–2001. doi:10.1002/joc.3567.
Croitoru, A.-E., Piticar, A., and Burada, D. C. (2016). Changes in precipitation extremes in Romania. *Quat. Int.* 415, 325–335. doi:10.1016/J.QUAINT.2015.07.028.
Dai, A. (2013). Increasing drought under global warming in observations and models. *Nat. Clim. Chang.* 3, 52. Available at: http://dx.doi.org/10.1038/nclimate1633.
Dai, A., and Zhao, T. (2017). Uncertainties in historical changes and future projections of drought. Part I: estimates of historical drought changes. *Clim. Change* 144, 519–533. doi:10.1007/s10584-016-1705-2.
Dai, A., Zhao, T., and Chen, J. (2018). Climate Change and Drought: a Precipitation and Evaporation Perspective. *Curr. Clim. Chang. Reports* 4, 301–312. doi:10.1007/s40641-018-0101-6.
Dankers, R., Arnell, N. W., Clark, D. B., Falloon, P. D., Fekete, B. M., Gosling, S. N., et al. (2014). First look at changes in flood hazard in the Inter-Sectoral Impact Model Intercomparison Project ensemble. *Proc. Natl. Acad. Sci. U. S. A.* 111, 3257–3261. doi:10.1073/pnas.1302078110.
Darby, S. E., Dunn, F. E., Nicholls, R. J., Rahman, M., and Riddy, L. (2015). A first look at the influence of anthropogenic climate change on the future delivery of fluvial sediment to the Ganges–Brahmaputra–Meghna delta. *Environ. Sci. Process. Impacts* 17, 1587–1600.
Das, S., Kar, N. S., and Bandyopadhyay, S. (2015). Glacial lake outburst flood at Kedarnath, Indian Himalaya: a study using digital elevation models and satellite images. *Nat. Hazards* 77, 769–786. doi:10.1007/s11069-015-1629-6.
Davin, E. L., Seneviratne, S. I., Ciais, P., Olioso, A., and Wang, T. (2014). Preferential cooling of hot extremes from cropland albedo management. *Proc. Natl. Acad. Sci.* 111, 9757–9761. doi:10.1073/pnas.1317323111.
Davis, N., and Birner, T. (2016). Climate model biases in the width of the tropical belt. *J. Clim.* 29, 1935–1954. doi:10.1175/JCLI-D-15-0336.1.
de Lima, M. I. P., Santo, F. E., Ramos, A. M., and Trigo, R. M. (2015). Trends and correlations in annual extreme precipitation indices for mainland Portugal, 1941–2007. *Theor. Appl. Climatol.* 119, 55–75. doi:10.1007/s00704-013-1079-6.
Dean, S. M., Rosier, S., Carey-Smith, T., and Stott, P. A. (2013). The role of climate change in the two-day extreme rainfall in Golden Bay, New Zealand, December 2011. *Bull. Am. Meteorol. Soc.* 94, S61–S63.
Denniston, R. F., and Luetscher, M. (2017). Speleothems as high-resolution paleo fl ood archives. 170, 1–13. doi:10.1016/j.quascirev.2017.05.006.
Dettinger, M. D., Ralph, F. M., and Rutz, J. J. (2018). Empirical Return Periods of the Most Intense Vapor Transports during Historical Atmospheric River Landfalls on the U.S. West Coast. *J. Hydrometeorol.* 19, 1363–1377. doi:10.1175/JHM-D-17-0247.1.
Devrani, R., Singh, V., Mudd, S. M., and Sinclair, H. D. (2015). Prediction of flash flood hazard impact from Himalayan river profiles. *Geophys. Res. Lett.* 42, 5888–5894. doi:10.1002/2015GL063784.
Dewan, T. H. (2015). Societal impacts and vulnerability to floods in Bangladesh and Nepal. *Weather Clim. Extrem.* 7, 36–42. doi:10.1016/J.WACE.2014.11.001.
Dey, R., Lewis, S., Arblaster, J., and Abram, N. (2018). A Review of Past and Projected Changes in Australia's Rainfall. *Wiley Interdiscip. Rev. Clim. Chang.*
Dey, R., Lewis, S. C., and Abram, N. J. (2019). Investigating observed northwest Australian rainfall trends in Coupled Model Intercomparison Project phase 5 detection and attribution experiments. *Int. J. Climatol.* 39, 112–127. doi:10.1002/joc.5788.
Di Luca, A., Argüeso, D., Evans, J. P. J. P., De Elía, R., Laprise, R., Elía, R., et al. (2016a). Quantifying the overall added value of dynamical downscaling and the contribution from different spatial scales. *J. Geophys. Res. Atmos.* 121, 1575–1590. doi:10.1002/2015JD024009.Received.
Di Luca, A., de Elía, R., and Laprise, R. (2015). Challenges in the Quest for Added Value of Regional Climate Dynamical Downscaling. *Curr. Clim. Chang. Reports* 1, 10–21. doi:10.1007/s40641-015-0003-9.
Di Luca, A., Evans, J. J. P., Pepler, A. S. A., Alexander, L. V. L., and Argüeso, D. (2016b). Evaluating the representation of Australian East Coast Lows in a regional climate model ensemble. *J. South. Hemisph. Earth Syst. Sci.* 66, 108–124. doi:10.22499/3.6602.003.
Diaconescu, E. P., Mailhot, A., Brown, R., and Chaumont, D. (2018). Evaluation of CORDEX-Arctic daily precipitation and temperature-based climate indices over Canadian Arctic land areas. *Clim. Dyn.* 50, 2061–2085. doi:10.1007/s00382-017-3736-4.
Diallo, I., Giorgi, F., Sukumaran, S., Stordal, F., and Giuliani, G. (2015). Evaluation of RegCM4 driven by CAM4 over

Southern Africa: mean climatology, interannual variability and daily extremes of wet season temperature and precipitation. *Theor. Appl. Climatol.* 121, 749–766. doi:10.1007/s00704-014-1260-6.
Diasso, U., and Abiodun, B. J. (2017). Drought modes in West Africa and how well CORDEX RCMs simulate them. *Theor. Appl. Climatol.* 128, 223–240. doi:10.1007/s00704-015-1705-6.
Diffenbaugh, N. S., Singh, D., Mankin, J. S., Horton, D. E., Swain, D. L., Touma, D., et al. (2017). Quantifying the influence of global warming on unprecedented extreme climate events. *Proc. Natl. Acad. Sci.* 114, 4881–4886.
Diffenbaugh, N. S., Swain, D. L., and Touma, D. (2015). Anthropogenic warming has increased drought risk in California. *Proc. Natl. Acad. Sci.* 112, 3931 LP-3936. doi:10.1073/pnas.1422385112.
Dimri, A. P., Chevuturi, A., Niyogi, D., Thayyen, R. J., Ray, K., Tripathi, S. N., et al. (2017). Cloudbursts in Indian Himalayas: A review. *Earth-Science Rev.* 168, 1–23. doi:10.1016/J.EARSCIREV.2017.03.006.
Dimri, A. P., Niyogi, D., Barros, A. P., Ridley, J., Mohanty, U. C., Yasunari, T., et al. (2015). Western Disturbances: A review. *Rev. Geophys.* 53, 225–246. doi:10.1002/2014RG000460.
Dirmeyer, P. A., Jin, Y., Singh, B., and Yan, X. (2013). Trends in land-atmosphere interactions from CMIP5 simulations. *J. Hydrometeorol.* 14, 829–849. doi:10.1175/JHM-D-12-0107.1.
Dittus, A. J., Karoly, D. J., Donat, M. G., Lewis, S. C., and Alexander, L. V (2018). Understanding the role of sea surface temperature-forcing for variability in global temperature and precipitation extremes. *Weather Clim. Extrem.*, 0–1.
Dittus, A. J., Karoly, D. J., Lewis, S. C., and Alexander, L. V. (2014). An investigation of some unexpected frost day increases in southern Australia. *Aust. Meteorol. Oceanogr. J.* 64, 261–271. doi:10.22499/2.6404.002.
Dittus, A. J., Karoly, D. J., Lewis, S. C., and Alexander, L. V. (2015). A multiregion assessment of observed changes in the areal extent of temperature and precipitation extremes. *J. Clim.* 28, 9206–9220. doi:10.1175/JCLI-D-14-00753.1.
Do, H. X., Gudmundsson, L., Leonard, M., and Westra, S. (2018). The Global Streamflow Indices and Metadata Archive (GSIM) – Part 1: The production of a daily streamflow archive and metadata. *Earth Syst. Sci. Data* 10, 765–785. doi:10.5194/essd-10-765-2018.
Do, H. X., Westra, S., and Leonard, M. (2017). A global-scale investigation of trends in annual maximum streamflow. *J. Hydrol.* 552, 28–43. doi:10.1016/j.jhydrol.2017.06.015.
Döll, P., Douville, H., Güntner, A., Müller Schmied, H., and Wada, Y. (2016). Modelling Freshwater Resources at the Global Scale: Challenges and Prospects. *Surv. Geophys.* 37, 195–221. doi:10.1007/s10712-015-9343-1.
Döll, P., Trautmann, T., Gerten, D., Schmied, H. M., Ostberg, S., Saaed, F., et al. (2018). Risks for the global freshwater system at 1.5 °c and 2 °c global warming. *Environ. Res. Lett.* 13. doi:10.1088/1748-9326/aab792.
Domínguez-Castro, F., García-Herrera, R., and Vicente-Serrano, S. M. (2018). Wet and dry extremes in Quito (Ecuador) since the 17th century. *Int. J. Climatol.* 38. doi:10.1002/joc.5312.
Donat, M. G., and Alexander, L. V. (2012). The shifting probability distribution of global daytime and night-time temperatures. *Geophys. Res. Lett.* 39, n/a-n/a. doi:10.1029/2012GL052459.
Donat, M. G., Alexander, L. V., Yang, H., Durre, I., Vose, R., Dunn, R. J. H. H., et al. (2013a). Updated analyses of temperature and precipitation extreme indices since the beginning of the twentieth century: The HadEX2 dataset. *J. Geophys. Res. Atmos.* 118, 2098–2118. doi:10.1002/jgrd.50150.
Donat, M. G., Alexander, L. V, Yang, H., Durre, I., Vose, R., and Caesar, J. (2013b). Global Land-Based Datasets for Monitoring Climatic Extremes. *Bull. Am. Meteorol. Soc.* 94, 997–1006.
Donat, M. G. G., Peterson, T. C. C., Brunet, M., King, A. D. D., Almazroui, M., Kolli, R. K. K., et al. (2014a). Changes in extreme temperature and precipitation in the Arab region: long-term trends and variability related to ENSO and NAO. *Int. J. Climatol.* 34, 581–592. doi:10.1002/joc.3707.
Donat, M. G., Leckebusch, G. C., Wild, S., and Ulbrich, U. (2011). Future changes in European winter storm losses and extreme wind speeds inferred from GCM and RCM multi-model simulations. *Nat. Hazards Earth Syst. Sci.* 11, 1351–1370. doi:10.5194/nhess-11-1351-2011.
Donat, M. G., Lowry, A. L., Alexander, L. V., O'Gorman, P. A., and Maher, N. (2016a). More extreme precipitation in the world's dry and wet regions. *Nat. Clim. Chang.* 6, 508–513. doi:10.1038/nclimate2941.
Donat, M. G. M. G. G., Alexander, L. V., Herold, N., and Dittus, A. J. (2016b). Temperature and precipitation extremes in century-long gridded observations, reanalyses, and atmospheric model simulations. *J. Geophys. Res. Atmos.* 121, 11174–11189. doi:10.1002/2016JD025480.
Donat, M. G., Pitman, A. J., and Seneviratne, S. I. (2017). Regional warming of hot extremes accelerated by surface energy fluxes. *Geophys. Res. Lett.* 44, 7011–7019.
Donat, M. G., Sillmann, J., Wild, S., Alexander, L. V., Lippmann, T., and Zwiers, F. W. (2014b). Consistency of Temperature and Precipitation Extremes across Various Global Gridded In Situ and Reanalysis Datasets*. *J. Clim.* 27, 5019–5035. doi:10.1175/JCLI-D-13-00405.1.
Dong, B., and Sutton, R. (2015). Dominant role of greenhouse-gas forcing in the recovery of Sahel rainfall. *Nat. Clim. Chang.* 5, 757. Available at: http://dx.doi.org/10.1038/nclimate2664.
Dong, B., Sutton, R. T., Chen, W., Liu, X., Lu, R., and Sun, Y. (2016). Abrupt summer warming and changes in temperature extremes over Northeast Asia since the mid-1990s: Drivers and physical processes. *Adv. Atmos. Sci.* 33, 1005–1023. doi:10.1007/s00376-016-5247-3.

Dong, B., Sutton, R. T., and Shaffrey, L. (2017). Understanding the rapid summer warming and changes in temperature extremes since the mid-1990s over Western Europe. *Clim. Dyn.* 48, 1537–1554. doi:10.1007/s00382-016-3158-8.
Dong, S., Sun, Y., Aguilar, E., Zhang, X., Peterson, T. C., Song, L., et al. (2018). Observed changes in temperature extremes over Asia and their attribution. *Clim. Dyn.* 51, 339–353. doi:10.1007/s00382-017-3927-z.
Dong, S., Xu, Y., Zhou, B., and Shi, Y. (2015). Assessment of indices of temperature extremes simulated by multiple CMIP5 models over China. *Adv. Atmos. Sci.* 32, 1077–1091. doi:10.1007/s00376-015-4152-5.
Donnelly, C., Greuell, W., Andersson, J., Gerten, D., Pisacane, G., Roudier, P., et al. (2017). Impacts of climate change on European hydrology at 1.5, 2 and 3 degrees mean global warming above preindustrial level. *Clim. Change* 143, 13–26. doi:10.1007/s10584-017-1971-7.
Dorigo, W. A., Wagner, W., Hohensinn, R., Hahn, S., Paulik, C., Xaver, A., et al. (2011). The International Soil Moisture Network: a data hosting facility for global in situ soil moisture measurements. *Hydrol. Earth Syst. Sci.* 15, 1675–1698. doi:10.5194/hess-15-1675-2011.
Dorigo, W., de Jeu, R., Chung, D., Parinussa, R., Liu, Y., Wagner, W., et al. (2012). Evaluating global trends (1988-2010) in harmonized multi-satellite surface soil moisture. *Geophys. Res. Lett.* 39. doi:10.1029/2012GL052988.
Dosio, A. (2017). Projection of temperature and heat waves for Africa with an ensemble of CORDEX Regional Climate Models. *Clim. Dyn.* 49, 493–519. doi:10.1007/s00382-016-3355-5.
Dosio, A., and Fischer, E. M. (2018). Will Half a Degree Make a Difference? Robust Projections of Indices of Mean and Extreme Climate in Europe Under 1.5°C, 2°C, and 3°C Global Warming. *Geophys. Res. Lett.* 45, 935–944. doi:10.1002/2017GL076222.
Dosio, A., Panitz, H.-J., Schubert-Frisius, M., and Lüthi, D. (2015). Dynamical downscaling of CMIP5 global circulation models over CORDEX-Africa with COSMO-CLM: evaluation over the present climate and analysis of the added value. *Clim. Dyn.* 44, 2637–2661.
Douville, H., Colin, J., Krug, E., Cattiaux, J., and Thao, S. (2016). Midlatitude daily summer temperatures reshaped by soil moisture under climate change. *Geophys. Res. Lett.* 43, 812–818. doi:10.1002/2015GL066222.
Douville, H., and Plazzotta, M. (2017). Midlatitude Summer Drying: An Underestimated Threat in CMIP5 Models? *Geophys. Res. Lett.* 44, 9967–9975. doi:10.1002/2017GL075353.
Dowdy, A. J. (2014). Long-term changes in Australian tropical cyclone numbers. *Atmos. Sci. Lett.* 15, 292–298. doi:10.1002/asl2.502.
Dowdy, A. J., Mills, G. A., and Timbal, B. (2013a). Large-scale diagnostics of extratropical cyclogenesis in eastern Australia. *Int. J. Climatol.*, n/a--n/a. doi:10.1002/joc.3599.
Dowdy, A. J., Mills, G. A., Timbal, B., and Wang, Y. (2013b). Changes in the risk of extratropical cyclones in eastern Australia. *J. Clim.* 26, 1403–1417. doi:10.1175/JCLI-D-12-00192.1.
Drijfhout, S., Bathiany, S., Beaulieu, C., Brovkin, V., Claussen, M., Huntingford, C., et al. (2015). Catalogue of abrupt shifts in Intergovernmental Panel on Climate Change climate models. *Proc. Natl. Acad. Sci.* 112, E5777 LP-E5786. Available at: http://www.pnas.org/content/112/43/E5777.abstract.
Duffy, P. B., Brando, P., Asner, G. P., and Field, C. B. (2015). Projections of future meteorological drought and wet periods in the Amazon. *Proc. Natl. Acad. Sci.* 112, 13172–13177. doi:10.1073/pnas.1421010112.
Dunn, R. J. H., Donat, M. G., and Alexander, L. V (2014). Investigating uncertainties in global gridded datasets of climate extremes. *Clim. Past Discuss.* 10, 2105–2161.
Dunne, J. P., Stouffer, R. J., and John, J. G. (2013). Reductions in labour capacity from heat stress under climate warming. *Nat. Clim. Chang.* 3, 563–566. doi:10.1038/nclimate1827.
Durkee, J. D., and Mote, T. L. (2010). A climatology of warm-season mesoscale convective complexes in subtropical South America. *Int. J. Climatol.* 30, 418–431. doi:10.1002/joc.1893.
Easterling, D. R., Kunkel, K. E., Arnold, J. R., Knutson, T., LeGrande, A. N., Leung, L. R., et al. (2017). "Precipitation change in the United States," in *Climate Science Special Report: Fourth National Climate Assessment, Volume I*, eds. D. J. Wuebbles, D. W. Fahey, K. A. Hibbard, D. J. Dokken, B. C. Stewart, and T. K. Maycock (Washington, DC, USA: U.S. Global Change Research Program), 207–230. doi:10.7930/J0H993CC.
Easterling, D. R., Kunkel, K. E., Wehner, M. F., and Sun, L. (2016). Detection and attribution of climate extremes in the observed record. *Weather Clim. Extrem.* 11, 17–27. doi:https://doi.org/10.1016/j.wace.2016.01.001.
Eden, J., Wolter, K., Otto, F. E. L. O., and van Oldenborgh, G. J. (2016). Multi-method attribution analysis of extreme precipitation in Boulder, Colorado. *Environ. Res. Lett.* 11, 124009. Available at: http://stacks.iop.org/1748-9326/11/i=12/a=124009.
El Kenawy, A., López-Moreno, J. I., and Vicente-Serrano, S. M. (2013). Summer temperature extremes in northeastern Spain: Spatial regionalization and links to atmospheric circulation (1960-2006). *Theor. Appl. Climatol.* 113, 387–405. doi:10.1007/s00704-012-0797-5.
Elalem, S., and Pal, I. (2015). Mapping the vulnerability hotspots over Hindu-Kush Himalaya region to flooding disasters. *Weather Clim. Extrem.* 8, 46–58. doi:10.1016/J.WACE.2014.12.001.
Elsner, J. B., Elsner, S. C., and Jagger, T. H. (2015). The increasing efficiency of tornado days in the United States. *Clim. Dyn.* 45, 651–659. doi:10.1007/s00382-014-2277-3.
Elsner, J. B., Fricker, T., and Schroder, Z. (2019). Increasingly powerful tornadoes in the United States. *Geophys. Res. Lett.*, 1–10. doi:10.1029/2018GL080819.

Emanuel, K. (2017). Assessing the present and future probability of Hurricane Harveys rainfall. *Proc. Natl. Acad. Sci.* 114, 12681–12684. doi:10.1073/pnas.1716222114.
Emanuel, K. A. (1987). The dependence of hurricane intensity on climate. *Nature* 326, 483.
Emanuel, K. A. (2013). Downscaling CMIP5 climate models shows increased tropical cyclone activity over the 21st century. doi:10.1073/pnas.1301293110.
Emanuel, K., Caroff, P., Delgado, S., Guard, C. "Chip," Guishard, M., Hennon, C., et al. (2018). On the Desirability and Feasibility of a Global Reanalysis of Tropical Cyclones. *Bull. Am. Meteorol. Soc.* 99, 427–429. doi:10.1175/BAMS-D-17-0226.1.
Emanuel, K., Sundararajan, R., and Williams, J. (2008). Hurricanes and Global Warming: Results from Downscaling IPCC AR4 Simulations. *Bull. Am. Meteorol. Soc.* 89, 347–368. doi:10.1175/BAMS-89-3-347.
Engelbrecht, F., Adegoke, J., Bopape, M.-J., Naidoo, M., Garland, R., Thatcher, M., et al. (2015). Projections of rapidly rising surface temperatures over Africa under low mitigation. *Environ. Res. Lett.* 10, 085004. doi:10.1088/1748-9326/10/8/085004.
England, M. H., Mcgregor, S., Spence, P., Meehl, G. A., Timmermann, A., Cai, W., et al. (2014). Recent intensification of wind-driven circulation in the Pacific and the ongoing warming hiatus. *Nat. Clim. Chang.* 4, 222–227. doi:10.1038/nclimate2106.
Erfanian, A., Wang, G., and Fomenko, L. (2017). Unprecedented drought over tropical South America in 2016: significantly under-predicted by tropical SST. *Sci. Rep.* 7, 5811. doi:10.1038/s41598-017-05373-2.
Escalante-Sandoval, C., and Nuñez-Garcia, P. (2017). Meteorological drought features in northern and northwestern parts of Mexico under different climate change scenarios. *J. Arid Land* 9, 65–75. doi:10.1007/s40333-016-0022-y.
Evans, J. P. J. P., Argueso, D., Olson, R., and Di Luca, A. (2017). Bias-corrected regional climate projections of extreme rainfall in south-east Australia. *Theor. Appl. Climatol.* 130, 1085–1098. doi:10.1007/s00704-016-1949-9.
Feldl, N., and Bordoni, S. (2016). Characterizing the Hadley circulation response through regional climate feedbacks. *J. Clim.* 29, 613–622. doi:10.1175/JCLI-D-15-0424.1.
Feng, D., Zheng, Y., Mao, Y., Zhang, A., Wu, B., Li, J., et al. (2018). An integrated hydrological modeling approach for detection and attribution of climatic and human impacts on coastal water resources. *J. Hydrol.* 557, 305–320. doi:https://doi.org/10.1016/j.jhydrol.2017.12.041.
Feng, S., and Fu, Q. (2013). Expansion of global drylands under a warming climate. *Atmos. Chem. Phys.* 13, 10081–10094. doi:10.5194/acp-13-10081-2013.
Feng, S., Trnka, M., Hayes, M., and Zhang, Y. (2017). Why do different drought indices show distinct future drought risk outcomes in the U.S. Great Plains? *J. Clim.* 30, 265–278. doi:10.1175/JCLI-D-15-0590.1.
Feng, Z., Leung, L. R., Hagos, S., Houze, R. A., Burleyson, C. D., and Balaguru, K. (2016). More frequent intense and long-lived storms dominate the springtime trend in central US rainfall. *Nat. Commun.* 7, 13429. doi:10.1038/ncomms13429.
Fiddes, S. L., Pezza, A. B., and Barras, V. (2015). A new perspective on Australian snow. *Atmos. Sci. Lett.* 16, 246–252. doi:10.1002/asl2.549.
Field, R. D., van der Werf, G. R., Fanin, T., Fetzer, E. J., Fuller, R., Jethva, H., et al. (2016). Indonesian fire activity and smoke pollution in 2015 show persistent nonlinear sensitivity to El Niño-induced drought. *Proc. Natl. Acad. Sci.* 113, 9204–9209. doi:10.1073/pnas.1524888113.
Filahi, S., Tanarhte, M., Mouhir, L., El Morhit, M., and Tramblay, Y. (2016). Trends in indices of daily temperature and precipitations extremes in Morocco. *Theor. Appl. Climatol.* 124, 959–972. doi:10.1007/s00704-015-1472-4.
Fioravanti, G., Piervitali, E., and Desiato, F. (2016). Recent changes of temperature extremes over Italy: an index-based analysis. *Theor. Appl. Climatol.* 123, 473–486. doi:10.1007/s00704-014-1362-1.
Fischer, A. M., Keller, D. E., Liniger, M. A., Rajczak, J., Schär, C., and Appenzeller, C. (2015). Projected changes in precipitation intensity and frequency in Switzerland: a multi-model perspective. *Int. J. Climatol.* 35, 3204–3219. doi:10.1002/joc.4162.
Fischer, E. M., and Knutti, R. (2012). Robust projections of combined humidity and temperature extremes. *Nat. Clim. Chang.* 3, 126.
Fischer, E. M., and Knutti, R. (2015). Anthropogenic contribution to global occurrence of heavy-precipitation and high-temperature extremes. *Nat. Clim. Chang.* 5, 560–564. doi:10.1038/nclimate2617.
Fischer, E. M., Sedláček, J., Hawkins, E., and Knutti, R. (2014). Models agree on forced response pattern of precipitation and temperature extremes. *Geophys. Res. Lett.* 41, 8554–8562. doi:10.1002/2014GL062018.
Flach, M., Gans, F., Brenning, A., Denzler, J., Reichstein, M., Rodner, E., et al. (2017). Multivariate anomaly detection for Earth observations: a comparison of algorithms and feature extraction techniques. *Earth Syst. Dyn.* 8, 677–696. doi:10.5194/esd-8-677-2017.
Flach, M., Sippel, S., Gans, F., Bastos, A., Brenning, A., Reichstein, M., et al. (2018). Contrasting biosphere responses to hydrometeorological extremes: revisiting the 2010 western Russian heatwave. *Biogeosciences* 15, 6067–6085. doi:10.5194/bg-15-6067-2018.
Flato, G., Marotzke, J., Abiodun, B., Braconnot, P., Chou, S. C., Collins, W., et al. (2013). Evaluation of Climate Models. *Clim. Chang. 2013 Phys. Sci. Basis. Contrib. Work. Gr. I to Fifth Assess. Rep. Intergov. Panel Clim.*

Chang., 741–866. doi:10.1017/CBO9781107415324.020.
Ford, T. W., and Labosier, C. F. (2017). Meteorological conditions associated with the onset of flash drought in the Eastern United States. *Agric. For. Meteorol.* 247, 414–423. doi:10.1016/j.agrformet.2017.08.031.
Forzieri, G., Feyen, L., Rojas, R., Flörke, M., Wimmer, F., and Bianchi, A. (2014). Ensemble projections of future streamflow droughts in Europe. *Hydrol. Earth Syst. Sci.* 18, 85–108. doi:10.5194/hess-18-85-2014.
Franz, M., Alonso, R., Arneth, A., Büker, P., Elvira, S., Gerosa, G., et al. (2018). Evaluation of simulated biomass damage in forest ecosystems induced by ozone against observation-based estimates. *Biogeosciences*. doi:10.5194/bg-2018-358.
Frei, P., Kotlarski, S., Liniger, M. A., and Schär, C. (2018). Future snowfall in the Alps: projections based on the EURO-CORDEX regional climate models. *Cryosph.* 12, 1–24. doi:10.5194/tc-12-1-2018.
Freund, M., Henley, B. J., Karoly, D. J., Allen, K. J., and Baker, P. J. (2017). Multi-century cool- and warm-season rainfall reconstructions for Australia's major climatic regions. *Clim. Past* 13, 1751–1770. doi:10.5194/cp-13-1751-2017.
Freychet, N., Hsu, H.-H., Chou, C., and Wu, C.-H. (2015). Asian Summer Monsoon in CMIP5 Projections: A Link between the Change in Extreme Precipitation and Monsoon Dynamics. *J. Clim.* 28, 1477–1493. doi:10.1175/JCLI-D-14-00449.1.
Freychet, N., Tett, S. F. B., Hegerl, G. C., and Wang, J. (2018). Central-Eastern China Persistent Heat Waves: Evaluation of the AMIP Models. *J. Clim.* 31, 3609–3624. doi:10.1175/JCLI-D-17-0480.1.
Frölicher, T. L., Fischer, E. M., and Gruber, N. (2018). Marine heatwaves under global warming. *Nature* in press. doi:10.1038/s41586-018-0383-9.
Fu, G., Yu, J., Yu, X., Ouyang, R., Zhang, Y., Wang, P., et al. (2013a). Temporal variation of extreme rainfall events in China, 1961–2009. *J. Hydrol.* 487, 48–59. doi:10.1016/J.JHYDROL.2013.02.021.
Fu, R., Yin, L., Li, W., Arias, P. A., Dickinson, R. E., Huang, L., et al. (2013b). Increased dry-season length over southern Amazonia in recent decades and its implication for future climate projection. *Proc. Natl. Acad. Sci. U. S. A.* 110, 18110–18115. doi:10.1073/pnas.1302584110.
Funk, C., Davenport, F., Harrison, L., Magadzire, T., Galu, G., Artan, G. A., et al. (2018a). Anthropogenic Enhancement of Moderate-to-Strong El Niño Events Likely Contributed to Drought and Poor Harvests in Southern Africa During 2016. *Bull. Am. Meteorol. Soc.* 99, S91–S96. doi:10.1175/BAMS-D-17-0112.1.
Funk, C., Harrison, L., Shukla, S., Korecha, D., Magadzire, T., Husak, G., et al. (2016). Assessing the Contributions of Local and East Pacific Warming to the 2015 Droughts in Ethiopia and Southern Africa. *Bull. Am. Meteorol. Soc.* 97, S75–S80. doi:10.1175/BAMS-D-16-0167.1.
Funk, C., Harrison, L., Shukla, S., Pomposi, C., Galu, G., Korecha, D., et al. (2018b). Examining the role of unusually warm Indo-Pacific sea surface temperatures in recent African droughts. *Q. J. R. Meteorol. Soc.*, 1–20. doi:10.1002/acr.
Funk, C., Nicholson, S. E., Landsfeld, M., Klotter, D., Peterson, P., and Harrison, L. (2015a). The Centennial Trends Greater Horn of Africa precipitation dataset. *Sci. Data* 2, 150050. Available at: http://dx.doi.org/10.1038/sdata.2015.50.
Funk, C., Shukla, S., Hoell, A., and Livneh, B. (2015b). Assessing the contributions of east African and west pacific warming to the 2014 boreal spring east African drought. *Bull. Am. Meteorol. Soc.* 96, S77–S82. doi:10.1175/BAMS-D-15-00106.1.
Fyfe, J. C., and Gillett, N. P. (2014). Recent observed and simulated warming. *Nat. Clim. Chang.* 4, 150–151.
Fyfe, J. C., Meehl, G. A., England, M. H., Mann, M. E., Santer, B. D., Flato, G. M., et al. (2016). Making sense of the early-2000s warming slowdown. *Nat. Clim. Chang.* 6, 224.
Gajić-Čapka, M., Cindrić, K., and Pasarić, Z. (2015). Trends in precipitation indices in Croatia, 1961–2010. *Theor. Appl. Climatol.* 121, 167–177. doi:10.1007/s00704-014-1217-9.
Galanaki, E., Lagouvardos, K., Kotroni, V., Flaounas, E., and Argiriou, A. (2018). Thunderstorm climatology in the Mediterranean using cloud-to-ground lightning observations. *Atmos. Res.* 207, 136–144. doi:https://doi.org/10.1016/j.atmosres.2018.03.004.
Galarneau, T. J., Bosart, L. F., and Schumacher, R. S. (2010). Predecessor rain events ahead of tropical cyclones. *Mon. Weather Rev.* 138, 3272–3297. doi:10.1175/2010MWR3243.1.
Gale, E. L., and Weather, M. A. S. (2013). The 2011 Thailand flood: climate causes and return periods. *Weather* 68, 233–237.
Gallant, A. J. E., Reeder, M. J., Risbey, J. S., and Hennessy, K. J. (2013). The characteristics of seasonal-scale droughts in Australia, 1911-2009. *Int. J. Climatol.* 33, 1658–1672. doi:10.1002/joc.3540.
Ganguli, P., and Ganguly, A. R. (2016). Robustness of meteorological droughts in dynamically downscaled climate simulations. *JAWRA J. Am. Water Resour. Assoc.* 52, 138–167. doi:10.1111/1752-1688.12374.
Gao, X., Shi, Y., Han, Z., Wang, M., Wu, J., Zhang, D., et al. (2017). Performance of RegCM4 over major river basins in China. *Adv. Atmos. Sci.* 34, 441–455. doi:10.1007/s00376-016-6179-7.
Gao, Y., Lu, J., and Leung, L. R. (2016). Uncertainties in projecting future changes in atmospheric rivers and their impacts on heavy precipitation over Europe. *J. Clim.* 29, 6711–6726. doi:10.1175/JCLI-D-16-0088.1.
Gao, Y., Xiao, L., Chen, D., Xu, J., and Zhang, H. (2018). Comparison between past and future extreme precipitations

simulated by global and regional climate models over the Tibetan Plateau. *Int. J. Climatol.* 38, 1285–1297. doi:10.1002/joc.5243.

Gardent, M., Rabatel, A., Dedieu, J.-P., and Deline, P. (2014). Multitemporal glacier inventory of the French Alps from the late 1960s to the late 2000s. *Glob. Planet. Change* 120, 24–37. doi:https://doi.org/10.1016/j.gloplacha.2014.05.004.

Garner, A. J., Mann, M. E., Emanuel, K. A., Kopp, R. E., Lin, N., Alley, R. B., et al. (2017). Impact of climate change on New York City's coastal flood hazard: Increasing flood heights from the preindustrial to 2300 CE. *Proc. Natl. Acad. Sci.* 114, 11861 LP-11866. Available at: http://www.pnas.org/content/114/45/11861.abstract.

Gastineau, G., and Soden, B. J. (2009). Model projected changes of extreme wind events in response to global warming. *Geophys. Res. Lett.* 36. doi:10.1029/2009GL037500.

Gastineau, G., and Soden, B. J. (2011). Evidence for a weakening of tropical surface wind extremes in response to atmospheric warming. *Geophys. Res. Lett.* 38. doi:10.1029/2011GL047138.

Gbobaniyi, E., Sarr, A., Sylla, M. B., Diallo, I., Lennard, C., Dosio, A., et al. (2014). Climatology, annual cycle and interannual variability of precipitation and temperature in CORDEX simulations over West Africa. *Int. J. Climatol.* 34, 2241–2257.

Geng, Q., and Sugi, M. (2003). Possible change of extratropical cyclone activity due to enhanced greenhouse gases and sulfate aerosols - Study with a high-resolution AGCM. *J. Clim.* 16, 2262–2274.

Gervais, M., Tremblay, L. B., Gyakum, J. R., and Atallah, E. (2014). Representing extremes in a daily gridded precipitation analysis over the United States: Impacts of station density, resolution, and gridding methods. *J. Clim.* 27, 5201–5218. doi:10.1175/JCLI-D-13-00319.1.

Ghosh, S., Das, D., Kao, S.-C., and Ganguly, A. R. (2012). Lack of uniform trends but increasing spatial variability in observed Indian rainfall extremes. *Nat. Clim. Chang.* 2. doi:10.1038/nclimate1327.

Giorgi, F., Coppola, E., Raffaele, F., Diro, G. T., Fuentes-Franco, R., Giuliani, G., et al. (2014). Changes in extremes and hydroclimatic regimes in the CREMA ensemble projections. *Clim. Change* 125, 39–51. doi:10.1007/s10584-014-1117-0.

Giorgi, F., Jones, C., and Asrar, G. (2009). Addressing climate information needs at the regional level: the CORDEX framework. *WMO Bull.* 58, 175.

Giuntoli, I., Renard, B., Vidal, J.-P., and Bard, A. (2013). Low flows in France and their relationship to large-scale climate indices. *J. Hydrol.* 482, 105–118. doi:10.1016/j.jhydrol.2012.12.038.

Giuntoli, I., Vidal, J.-P., Prudhomme, C., and Hannah, D. M. (2015). Future hydrological extremes: The uncertainty from multiple global climate and global hydrological models. *Earth Syst. Dyn.* 6, 267–285. doi:10.5194/esd-6-267-2015.

Gobbett, D. L., Nidumolu, U., and Crimp, S. (2018). Modelling frost generates insights for managing risk of minimum temperature extremes. *Weather Clim. Extrem.*, 1–9. doi:10.1016/j.wace.2018.06.003.

Gobiet, A., Kotlarski, S., Beniston, M., Heinrich, G., Rajczak, J., and Stoffel, M. (2014). 21st century climate change in the European Alps—A review. *Sci. Total Environ.* 493, 1138–1151. doi:10.1016/j.scitotenv.2013.07.050.

Goddard, P. B., Yin, J., Griffies, S. M., and Zhang, S. (2015). An extreme event of sea-level rise along the Northeast coast of North America in 2009–2010. *Nat. Commun.* 6, 6346. Available at: https://doi.org/10.1038/ncomms7346.

González-Hidalgo, J. C., Vicente-Serrano, S. M., Peña-Angulo, D., Salinas, C., Tomas-Burguera, M., and Beguería, S. (2018). High-resolution spatio-temporal analyses of drought episodes in the western Mediterranean basin (Spanish mainland, Iberian Peninsula). *Acta Geophys.* 66, 381–392. doi:10.1007/s11600-018-0138-x.

Gosling, S. N., Zaherpour, J., Mount, N. J., Hattermann, F. F., Dankers, R., Arheimer, B., et al. (2017). A comparison of changes in river runoff from multiple global and catchment-scale hydrological models under global warming scenarios of 1 °C, 2 °C and 3 °C. *Clim. Change* 141, 577–595. doi:10.1007/s10584-016-1773-3.

Gou, X., Deng, Y., Gao, L., Chen, F., Cook, E., Yang, M., et al. (2015). Millennium tree-ring reconstruction of drought variability in the eastern Qilian Mountains, northwest China. *Clim. Dyn.* 45, 1761–1770. doi:10.1007/s00382-014-2431-y.

Grams, C. M., Binder, H., Pfahl, S., Piaget, N., and Wernli, H. (2014). Atmospheric processes triggering the central European floods in June 2013. *Nat. Hazards Earth Syst. Sci.* 14, 1691–1702. doi:10.5194/nhess-14-1691-2014.

Greve, P., Gudmundsson, L., and Seneviratne, S. I. (2018). Regional scaling of annual mean precipitation and water availability with global temperature change. *Earth Syst. Dyn.* 9, 227–240. doi:10.3929/ethz-b-000251688.

Greve, P., Orlowsky, B., Mueller, B., Sheffield, J., Reichstein, M., and Seneviratne, S. I. (2014). Global assessment of trends in wetting and drying over land. *Nat. Geosci.* 7, 716–721. doi:10.1038/NGEO2247.

Greve, P., Roderick, M. L., and Seneviratne, S. I. (2017). Simulated changes in aridity from the last glacial maximum to 4xCO2. *Environ. Res. Lett.* 12, 114021. doi:10.1088/1748-9326/aa89a3.

Griffin, D., and Anchukaitis, K. J. (2014). How unusual is the 2012-2014 California drought? *Geophys. Res. Lett.* 41, 9017–9023. doi:10.1002/2014GL062433.

Grise, K. M., and Polvani, L. M. (2014). The response of midlatitude jets to increased CO2: Distinguishing the roles of sea surface temperature and direct radiative forcing. *Geophys. Res. Lett.* 41, 6863–6871. doi:10.1002/2014GL061638.

Grise, K. M., Son, S. W., Correa, G. J. P., and Polvani, L. M. (2014). The response of extratropical cyclones in the

Southern Hemisphere to stratospheric ozone depletion in the 20th century. *Atmos. Sci. Lett.* 15, 29–36. doi:10.1002/asl2.458.

Grose, M. R., Risbey, J. S., Black, M. T., and Karoly, D. J. (2015). Attribution of Exceptional Mean Sea Level Pressure Anomalies South of Australia in August 2014. *Bull. Am. Meteorol. Soc.* 96, S158–S162. doi:10.1175/BAMS-D-15-00116.1.

Grotjahn, R., Black, R., Leung, R., Wehner, M. F., Barlow, M., Bosilovich, M., et al. (2016). *North American extreme temperature events and related large scale meteorological patterns: a review of statistical methods, dynamics, modeling, and trends*. Springer Berlin Heidelberg doi:10.1007/s00382-015-2638-6.

Gu, H., Yu, Z., Wang, G., Wang, J., Ju, Q., Yang, C., et al. (2014). Impact of climate change on hydrological extremes in the Yangtze River Basin, China. *Stoch. Environ. Res. Risk Assess.* 29, 693–707. doi:10.1007/s00477-014-0957-5.

Gudmundsson, L., Leonard, M., Do, H. X., Westra, S., and Seneviratne, S. I. (2019). Observed Trends in Global Indicators of Mean and Extreme Streamflow. *Geophys. Res. Lett.* 46, 756–766. doi:10.1029/2018GL079725.

Gudmundsson, L., and Seneviratne, S. I. (2016). Anthropogenic climate change affects meteorological drought risk in Europe. *Environ. Res. Lett.* 11. doi:10.1088/1748-9326/11/4/044005.

Gudmundsson, L., Seneviratne, S. I., and Zhang, X. (2017). Anthropogenic climate change detected in European renewable freshwater resources. *Nat. Clim. Chang.* 7, 813–816. doi:10.1038/nclimate3416.

Guillod, B. P., Orlowsky, B., Miralles, D. G., Teuling, A. J., and Seneviratne, S. I. (2015). Reconciling spatial and temporal soil moisture effects on afternoon rainfall. *Nat. Commun.* 6, 6443. doi:10.1038/ncomms7443.

Guimberteau, M., Ronchail, J., Espinoza, J. C. C., Lengaigne, M., Sultan, B., Polcher, J., et al. (2013). Future changes in precipitation and impacts on extreme streamflow over Amazonian sub-basins. *Environ. Res. Lett.* 8, 014035. doi:10.1088/1748-9326/8/1/014035.

Guo, J., Huang, G., Wang, X., Li, Y., and Lin, Q. (2018). Dynamically-downscaled projections of changes in temperature extremes over China. *Clim. Dyn.* 50, 1045–1066. doi:10.1007/s00382-017-3660-7.

Gupta, P., and Uniyal, S. (2015). Landslides and flash floods caused by extreme rainfall events/cloudbursts in Uttarkashi District of Uttarakhand. *J. South Asia Disaster Stud.*, 77–92.

Gutmann, E. D., Rasmussen, R. M., Liu, C., Ikeda, K., Bruyere, C. L., Done, J. M., et al. (2018). Changes in hurricanes from a 13-Yr convection-permitting pseudo- global warming simulation. *J. Clim.* 31, 3643–3657. doi:10.1175/JCLI-D-17-0391.1.

Hagos, S. M., Leung, L. R., Yoon, J.-H., Lu, J., and Gao, Y. (2016). A projection of changes in landfalling atmospheric river frequency and extreme precipitation over western North America from the Large Ensemble CESM simulations. *Geophys. Res. Lett.* 43, 1357–1363. doi:10.1002/2015GL067392.

Haig, J., Nott, J., and Reichart, G.-J. (2014). Australian tropical cyclone activity lower than at any time over the past 550-1,500 years. *Nature* 505, 667–671.

Hall, A., and Qu, X. (2006). Using the current seasonal cycle to constrain snow albedo feedback in future climate change. *Geophys. Res. Lett.* 33, L03502. doi:10.1029/2005GL025127.

Hall, J., Arheimer, B., Borga, M., Brázdil, R., Claps, P., Kiss, A., et al. (2014). Understanding flood regime changes in Europe: A state-of-the-art assessment. *Hydrol. Earth Syst. Sci.* 18, 2735–2772. doi:10.5194/hess-18-2735-2014.

Hamada, A., Takayabu, Y. N., Liu, C., and Zipser, E. J. (2015). Weak linkage between the heaviest rainfall and tallest storms. *Nat. Commun.* 6, 1–6. doi:10.1038/ncomms7213.

Han, F., Cook, K. H., and Vizy, E. K. (2019). Changes in intense rainfall events and dry periods across Africa in the twenty-first century. *Clim. Dyn.*, 1–21. doi:10.1007/s00382-019-04653-z.

Han, J.-Y., Baik, J.-J., and Khain, A. P. (2011). A Numerical Study of Urban Aerosol Impacts on Clouds and Precipitation. *J. Atmos. Sci.* 69, 504–520. doi:10.1175/JAS-D-11-071.1.

Han, T., Chen, H., Hao, X., and Wang, H. (2018). Projected changes in temperature and precipitation extremes over the Silk Road Economic Belt regions by the Coupled Model Intercomparison Project Phase 5 multi-model ensembles. *Int. J. Climatol.* 38, 4077–4091. doi:10.1002/joc.5553.

Hannaford, J. (2015). Climate-driven changes in UK river flows: A review of the evidence. *Prog. Phys. Geogr.* 39, 29–48.

Hannart, A., Vera, C., Otto, F. E. L., and Cerne, B. (2015). Causal influence of anthropogenic forcings on the argentinian heat wave of December 2013. *Bull. Am. Meteorol. Soc.* 96, S41–S45. doi:10.1175/BAMS-D-15-00137.1.

Hansen, B. B., Isaksen, K., Benestad, R. E., Kohler, J., Pedersen, Å. Ø., Loe, L. E., et al. (2014). Warmer and wetter winters: characteristics and implications of an extreme weather event in the High Arctic. *Environ. Res. Lett.* 9, 114021. doi:10.1088/1748-9326/9/11/114021.

Hanzer, F., Förster, K., Nemec, J., and Strasser, U. (2018). Projected cryospheric and hydrological impacts of 21st century climate change in the Ötztal Alps (Austria) simulated using a physically based approach. *Hydrol. Earth Syst. Sci.* 22, 1593–1614. doi:10.5194/hess-22-1593-2018.

Hapuarachchi, H. A. P., Wang, Q. J., and Pagano, T. C. (2011). A review of advances in flash flood forecasting. *Hydrol. Process.* 25, 2771–2784. doi:10.1002/hyp.8040.

Harrington, L. J. (2017). Investigating differences between event-as-class and probability density-based attribution

statements with emerging climate change. *Clim. Change* 141, 641–654. doi:10.1007/s10584-017-1906-3.
Harrington, L. J., and Otto, F. E. (2018a). Adapting attribution science to the climate extremes of tomorrow. *Environ. Res. Lett.* Available at: http://iopscience.iop.org/10.1088/1748-9326/aaf4cc.
Harrington, L. J., and Otto, F. E. L. (2018b). Changing population dynamics and uneven temperature emergence combine to exacerbate regional exposure to heat extremes under 1.5 °C and 2 °C of warming. *Environ. Res. Lett.* 13, 034011. doi:10.1088/1748-9326/aaaa99.
Harrington, L., and Renwick, J. (2014). Secular changes in New Zealand rainfall characteristics 1950-2009. *Weather Clim.* 34, 50–59.
Harrington, L., Rosier, S., Dean, S. M., Stuart, S., and Scahill, A. (2014). the Role of Anthropogenic Climate Change in the 2013 Drought Over North Island, New Zealand. *Bull. Am. Meteorol. Soc.* 95, S45–S48. doi:http://dx.doi.org/.
Hartmann, D. J., Klein Tank, A. M. G., Rusticucci, M., Alexander, L. V, Brönnimann, S., Charabi, Y. A.-R., et al. (2013). Observations: Atmosphere and Surface. *Clim. Chang. 2013 Phys. Sci. Basis. Contrib. Work. Gr. I to Fifth Assess. Rep. Intergov. Panel Clim. Chang.*, 159–254. doi:10.1017/CBO9781107415324.008.
Hartmann, F., Merten, J., Fink, M., and Faust, H. (2018). Indonesia's Fire Crisis 2015 A Twofold Perturbation on the Ground. *Pacific Geogr.* 49, 4–11.
Haslinger, K., Schöner, W., and Anders, I. (2016). Future drought probabilities in the Greater Alpine Region based on COSMO-CLM experiments – spatial patterns and driving forces. *Meteorol. Zeitschrift* 25, 137–148. doi:10.1127/metz/2015/0604.
Hauser, M., Gudmundsson, L., Orth, R., Jézéquel, A., Haustein, K., Vautard, R., et al. (2017). Methods and Model Dependency of Extreme Event Attribution: The 2015 European Drought. *Earth's Futur.* 5, 1034–1043. doi:10.1002/2017EF000612.
Hauser, M., Orth, R., and Seneviratne, S. I. (2016). Role of soil moisture versus recent climate change for the 2010 heat wave in western Russia. *Geophys. Res. Lett.* 43, 2819–2826. doi:10.1002/2016GL068036.
Hawcroft, M., Dacre, H., Forbes, R., Hodges, K., Shaffrey, L., and Stein, T. (2017). Using satellite and reanalysis data to evaluate the representation of latent heating in extratropical cyclones in a climate model. *Clim. Dyn.* doi:10.1007/s00382-016-3204-6.
Hawcroft, M. K., Shaffrey, L. C., Hodges, K. I., and Dacre, H. F. (2016). Can climate models represent the precipitation associated with extratropical cyclones? *Clim. Dyn.* doi:10.1007/s00382-015-2863-z.
He, F., and Posselt, D. J. (2015). Impact of Parameterized Physical Processes on Simulated Tropical Cyclone Characteristics in the Community Atmosphere Model. *J. Clim.* 28, 9857–9872.
He, J., and Soden, B. J. (2015). Anthropogenic Weakening of the Tropical Circulation: The Relative Roles of Direct CO2 Forcing and Sea Surface Temperature Change. *J. Clim.* 28, 8728–8742. doi:10.1175/JCLI-D-15-0205.1.
He, X., Wada, Y., Wanders, N., and Sheffield, J. (2017). Intensification of hydrological drought in California by human water management. *Geophys. Res. Lett.* 44, 1777–1785. doi:10.1002/2016GL071665.
Heidinger, H., Carvalho, L., Jones, C., Posadas, A., and Quiroz, R. (2018). A new assessment in total and extreme rainfall trends over central and southern Peruvian Andes during 1965-2010. *Int. J. Climatol.* 38, e998–e1015. doi:10.1002/joc.5427.
Helama, S., Sohar, K., Läänelaid, A., Bijak, S., and Jaagus, J. (2018). Reconstruction of precipitation variability in Estonia since the eighteenth century, inferred from oak and spruce tree rings. *Clim. Dyn.* 50, 4083–4101. doi:10.1007/s00382-017-3862-z.
Held, I. M., and Soden, B. J. (2006). Robust responses of the hydrological cycle to global warming. *J. Clim.* 19, 5686–5699. doi:10.1175/JCLI3990.1.
Held, I. M., and Zhao, M. (2011). The Response of Tropical Cyclone Statistics to an Increase in CO2 with Fixed Sea Surface Temperatures. *J. Clim.* 24, 5353–5364. doi:10.1175/JCLI-D-11-00050.1.
Herbel, I., Croitoru, A. E., Rus, A. V., Roşca, C. F., Harpa, G. V., Ciupertea, A. F., et al. (2018). The impact of heat waves on surface urban heat island and local economy in Cluj-Napoca city, Romania. *Theor. Appl. Climatol.* 133, 681–695. doi:10.1007/s00704-017-2196-4.
Herger, N., Angélil, O., Abramowitz, G., Donat, M., Stone, D., and Lehmann, K. (2018). Calibrating Climate Model Ensembles for Assessing Extremes in a Changing Climate. *J. Geophys. Res. Atmos.* 123, 5988–6004. doi:10.1029/2018JD028549.
Herold, N., Ekström, M., Kala, J., Goldie, J., and Evans, J. P. (2018). Australian climate extremes in the 21st century according to a regional climate model ensemble: Implications for health and agriculture. *Weather Clim. Extrem.* 20, 54–68. doi:10.1016/j.wace.2018.01.001.
Herrera-Estrada, J. E., and Sheffield, J. (2017). Uncertainties in future projections of summer droughts and heat waves over the contiguous United States. *J. Clim.* 30, 6225–6246. doi:10.1175/JCLI-D-16-0491.1.
Herring, S. C., Christidis, N., Hoell, A., Kossin, J. P., Schreck, C. J., and Stott, P. A. (2018). Explaining Extreme Events of 2016 from a Climate Perspective. *Bull. Am. Meteorol. Soc.* 99, S1–S157. doi:10.1175/BAMS-ExplainingExtremeEvents2016.1.
Herring, S. C., Hoell, A., Hoerling, M. P., Kossin, J. P., Schreck, C. J., and Stott, P. A. (2016). Explaining Extreme Events of 2015 from a Climate Perspective. *Bull. Am. Meteorol. Soc.* 97, S1–S145. doi:10.1175/BAMS-ExplainingExtremeEvents2015.1.

Herring, S. C., Hoerling, M. P., Kossin, J. P., Peterson, T. C., and Stott, P. A. (2015). Explaining Extreme Events of 2014 from a Climate Perspective. *Bull. Am. Meteorol. Soc.* 96, S1–S172. doi:10.1175/BAMS-ExplainingExtremeEvents2014.1.
Herring, S. C., Hoerling, M. P., Peterson, T. C., and Stott, P. a. (2014). Explaining Extreme Events of 2013 from a Climate Perspective. *Bull. Am. Meteorol. Soc.* 95, S1–S104. doi:10.1175/1520-0477-95.9.S1.1.
Hidalgo, H. G., Alfaro, E. J., and Quesada-Montano, B. (2017). Observed (1970–1999) climate variability in Central America using a high-resolution meteorological dataset with implication to climate change studies. *Clim. Change* 141, 13–28. doi:10.1007/s10584-016-1786-y.
Hideo, S., Masahiro, W., Yukiko, I., Masato, M., Masayoshi, I., Masahide, K., et al. (2013). An event attribution of the 2010 drought in the South Amazon region using the MIROC5 model. *Atmos. Sci. Lett.* 14, 170–175. doi:10.1002/asl2.435.
Hirabayashi, Y., Mahendran, R., Koirala, S., Konoshima, L., Yamazaki, D., Watanabe, S., et al. (2013). Global flood risk under climate change. *Nat. Clim. Chang.* 3, 816. doi:10.1038/nclimate1911.
Hirsch, A. L., Guillod, B. P., Seneviratne, S. I., Beyerle, U., Boysen, L. R., Brovkin, V., et al. (2018). Biogeophysical Impacts of Land-Use Change on Climate Extremes in Low-Emission Scenarios: Results From HAPPI-Land. *Earth's Futur.* 6, 396–409. doi:10.1002/2017EF000744.
Hirsch, A. L., Pitman, A. J., Seneviratne, S. I., Evans, J. P., and Haverd, V. (2014). Summertime maximum and minimum temperature coupling asymmetry over Australia determined using WRF. *Geophys. Res. Lett.* 41, 1546–1552. doi:10.1002/2013GL059055.
Hirsch, A. L., Wilhelm, M., Davin, E. L., Thiery, W., and Seneviratne, S. I. (2017). Can climate-effective land management reduce regional warming? *J. Geophys. Res. Atmos.* 122, 2269–2288. doi:10.1002/2016JD026125.
Hirschi, M., Seneviratne, S. I., Alexandrov, V., Boberg, F., Boroneant, C., Christensen, O. B., et al. (2011). Observational evidence for soil-moisture impact on hot extremes in southeastern Europe. *Nat. Geosci.* 4, 17–21. doi:10.1038/ngeo1032.
Hoegh-Guldberg, O., Jacob, D., Taylor, M., Bindi, M., Brown, S., Camilloni, I., et al. (2018). “Impacts of 1.5°C Global Warming on Natural and Human Systems. In: Global warming of 1.5°C. An IPCC Special Report on the impacts of global warming of 1.5°C above pre-industrial levels and related global greenhouse gas emission pathways, in the context of ,” in, eds. V. Masson-Delmotte, P. Zhai, H. O. Pörtner, D. Roberts, J. Skea, P. R. Shukla, et al. (Geneva, Switzerland: World Meteorological Organization), in press. Available at: https://www.ipcc.ch/sr15.
Hoerling, M., Eischeid, J., Kumar, A., Leung, R., Mariotti, A., Mo, K., et al. (2014). Causes and predictability of the 2012 great plains drought. *Bull. Am. Meteorol. Soc.* 95, 269–282. doi:10.1175/BAMS-D-13-00055.1.
Hoerling, M., Eischeid, J., Perlwitz, J., Quan, X.-W., Wolter, K., and Cheng, L. (2016). Characterizing Recent Trends in U.S. Heavy Precipitation. *J. Clim.* 29, 2313–2332. doi:10.1175/JCLI-D-15-0441.1.
Hoerling, M., Kumar, A., Dole, R., Nielsen-Gammon, J. W., Eischeid, J., Perlwitz, J., et al. (2013). Anatomy of an extreme event. *J. Clim.* 26, 2811–2832. doi:10.1175/JCLI-D-12-00270.1.
Holland, G., and Bruyère, C. L. (2014). Recent intense hurricane response to global climate change. *Clim. Dyn.* 42, 617–627. doi:10.1007/s00382-013-1713-0.
Holloway, C. E., Wing, A. A., Bony, S., Muller, C., Masunaga, H., L'Ecuyer, T. S., et al. (2017). Observing Convective Aggregation. *Surv. Geophys.* 38, 1199–1236. doi:10.1007/s10712-017-9419-1.
Hong, C.-C., Lee, M.-Y., Hsu, H.-H., and Tseng, W.-L. (2018). Distinct Influences of the ENSO-Like and PMM-Like SST Anomalies on the Mean TC Genesis Location in the Western North Pacific: The 2015 Summer as an Extreme Example. *J. Clim.* 31, 3049–3059. doi:10.1175/JCLI-D-17-0504.1.
Houze, R. A., McMurdie, L. A., Rasmussen, K. L., Kumar, A., and Chaplin, M. M. (2017). Multiscale Aspects of the Storm Producing the June 2013 Flooding in Uttarakhand, India. *Mon. Weather Rev.* 145, 4447–4466. doi:10.1175/MWR-D-17-0004.1.
Hu, Z., Li, Q., Chen, X., Teng, Z., Chen, C., Yin, G., et al. (2016). Climate changes in temperature and precipitation extremes in an alpine grassland of Central Asia. *Theor. Appl. Climatol.* 126, 519–531. doi:10.1007/s00704-015-1568-x.
Huang, H., Winter, J. M., Osterberg, E. C., Horton, R. M., and Beckage, B. (2017a). Total and Extreme Precipitation Changes over the Northeastern United States. *J. Hydrometeorol.* 18, 1783–1798. doi:10.1175/JHM-D-16-0195.1.
Huang, J., Yu, H., Dai, A., Wei, Y., and Kang, L. (2017b). Drylands face potential threat under 2 °C global warming target. *Nat. Clim. Chang.* 7, 417–422. doi:10.1038/nclimate3275.
Huang, S., Kumar, R., Flörke, M., Yang, T., Hundecha, Y., Kraft, P., et al. (2017c). Evaluation of an ensemble of regional hydrological models in 12 large-scale river basins worldwide. *Clim. Change* 141, 381–397. doi:10.1007/s10584-016-1841-8.
Hui, P., Tang, J., Wang, S., Niu, X., Zong, P., and Dong, X. (2018). Climate change projections over China using regional climate models forced by two CMIP5 global models. Part I: evaluation of historical simulations. *Int. J. Climatol.* 38, e57–e77. doi:10.1002/joc.5351.
Huijnen, V., Wooster, M. J., Kaiser, J. W., Gaveau, D. L. A., Flemming, J., Parrington, M., et al. (2016). Fire carbon emissions over maritime southeast Asia in 2015 largest since 1997. *Sci. Rep.* 6, 1–8. doi:10.1038/srep26886.
Hundecha, Y., Sunyer, M. A., Lawrence, D., Madsen, H., Willems, P., Bürger, G., et al. (2016). Inter-comparison of

statistical downscaling methods for projection of extreme flow indices across Europe. *J. Hydrol.* 541, 1273–1286. doi:10.1016/j.jhydrol.2016.08.033.
Hunt, E. D., Svoboda, M., Wardlow, B., Hubbard, K., Hayes, M., and Arkebauer, T. (2014). Monitoring the effects of rapid onset of drought on non-irrigated maize with agronomic data and climate-based drought indices. *Agric. For. Meteorol.* 191, 1–11. doi:10.1016/j.agrformet.2014.02.001.
Hunt, K. M. R., Turner, A. G., and Shaffrey, L. C. (2018). Extreme Daily Rainfall in Pakistan and North India: Scale Interactions, Mechanisms, and Precursors. *Mon. Weather Rev.* 146, 1005–1022. doi:10.1175/MWR-D-17-0258.1.
Hurley, J. V., and Boos, W. R. (2015). A global climatology of monsoon low-pressure systems. *Q. J. R. Meteorol. Soc.* 141, 1049–1064. doi:10.1002/qj.2447.
Hussain, M. S., and Lee, S. (2013). The regional and the seasonal variability of extreme precipitation trends in Pakistan. *Asia-Pacific J. Atmos. Sci.* 49, 421–441. doi:10.1007/s13143-013-0039-5.
Imada, Y., Maeda, S., Watanabe, M., Shiogama, H., Mizuta, R., Ishii, M., et al. (2017). Recent enhanced seasonal temperature contrast in Japan from large ensemble high-resolution climate simulations. *Atmosphere (Basel).* 8. doi:10.3390/atmos8030057.
Imada, Y., Watanabe, M., Mori, M., Kimoto, M., Shiogama, H., and Ishii, M. (2013). Contribution of Atmospheric Circulation Change to the 2012 Heavy Rainfall in Southwestern Japan. *Bull. Am. Meteorol. Soc.* 96, 52–54.
Imbach, P., Chou, S. C., Lyra, A., Rodrigues, D., Rodriguez, D., Latinovic, D., et al. (2018). Future climate change scenarios in Central America at high spatial resolution. *PLoS One* 13, e0193570. doi:10.1371/journal.pone.0193570.
Imhoff, M. L., Zhang, P., Wolfe, R. E., and Bounoua, L. (2010). Remote sensing of the urban heat island effect across biomes in the continental USA. *Remote Sens. Environ.* 114, 504–513. doi:10.1016/j.rse.2009.10.008.
Immerzeel, W. W., Petersen, L., Ragettli, S., and Pellicciotti, F. (2014). The importance of observed gradients of air temperature and precipitation for modeling runoff from a glacierized watershed in the Nepalese Himalayas. *Water Resour. Res.* 50, 2212–2226. doi:doi:10.1002/2013WR014506.
IPCC (2012). *Managing the Risks of Extreme Events and Disasters to Advance Climate Change Adaptation. A Special Report of Working Groups I and II of the Intergovernmental Panel on Climate Change*. Cambridge University Press.
IPCC (2013). *Climate Change 2013 - The Physical Science Basis. Contribution of Working Group I to the Fifth Assessment Report of the Intergovernmental Panel on Climate Change*. , ed. Intergovernmental Panel on Climate Change Cambridge: Cambridge University Press doi:10.1017/CBO9781107415324.
IPCC (2018). Summary for Policymakers. In: Global warming of 1.5°C. An IPCC Special Report on the impacts of global warming of 1.5°C above pre-industrial levels and related global greenhouse gas emission pathways, in the context of strengthening the global response to. , eds. V. Masson-Delmotte, P. Zhai, H.-O. Pörtner, D. Roberts, J. Skea, P. R. Shukla, et al. In Press.
Irannezhad, M., Chen, D., Kløve, B., and Moradkhani, H. (2017). Analysing the variability and trends of precipitation extremes in Finland and their connection to atmospheric circulation patterns. *Int. J. Climatol.* 37, 1053–1066. doi:10.1002/joc.5059.
Ishak, E. H., Rahman, A., Westra, S., Sharma, A., and Kuczera, G. (2013). Evaluating the non-stationarity of australian annual maximum flood. *J. Hydrol.* 494, 134–145. doi:10.1016/j.jhydrol.2013.04.021.
Ishiyama, T., Satoh, M., and Yamada, Y. (2018). Potential differences in North Pacific tropical cyclone activity between the super El Niño years of 1997 and 2015. *J. Meteorol. Soc. Japan*.
Jakob, D., and Walland, D. (2016). Variability and long-term change in Australian temperature and precipitation extremes. *Weather Clim. Extrem.* 14, 36–55. doi:10.1016/j.wace.2016.11.001.
Japan Meteorological Agency (2018). Primary Factors behind the Heavy Rain Event of July 2018 and the Subsequent Heatwave in Japan from Mid-July Onward. Available at: http://ds.data.jma.go.jp/tcc/tcc/news/press_20180822.pdf.
Jeon, S., Paciorek, C. J., and Wehner, M. F. (2016). Quantile-based bias correction and uncertainty quantification of extreme event attribution statements. *Weather Clim. Extrem.* 12, 24–32. doi:https://doi.org/10.1016/j.wace.2016.02.001.
Jeon, S., Prabhat, Byna, S., Gu, J., Collins, W. D., and Wehner, M. F. (2015). Characterization of extreme precipitation within atmospheric river events over California. *Adv. Stat. Climatol. Meteorol. Oceanogr.* 1, 45–57. doi:10.5194/ascmo-1-45-2015.
Jeong, S.-J., Ho, C.-H., Piao, S., Kim, J., Ciais, P., Lee, Y.-B., et al. (2014). Effects of double cropping on summer climate of the North China Plain and neighbouring regions. *Nat. Clim. Chang.* 4, 615–619. doi:10.1038/nclimate2266.
Jézéquel, A., Dépoues, V., Guillemot, H., Trolliet, M., Vanderlinden, J.-P., and Yiou, P. (2018). Behind the veil of extreme event attribution. *Clim. Change*. doi:10.1007/s10584-018-2252-9.
Ji, F., Evans, J. P. J. P., Argueso, D., Fita, L., and Di Luca, A. (2015). Using large-scale diagnostic quantities to investigate change in East Coast Lows. *Clim. Dyn.* 45, 2443–2453. doi:10.1007/s00382-015-2481-9.
Ji, Z., and Kang, S. (2015). Evaluation of extreme climate events using a regional climate model for China. *Int. J. Climatol.* 35, 888–902. doi:10.1002/joc.4024.

Jiang, F., Hu, R.-J., Wang, S.-P., Zhang, Y.-W., and Tong, L. (2013). Trends of precipitation extremes during 1960–2008 in Xinjiang, the Northwest China. *Theor. Appl. Climatol.* 111, 133–148. doi:10.1007/s00704-012-0657-3.
Johnson, N. C., Xie, S. P., Kosaka, Y., and Li, X. (2018). Increasing occurrence of cold and warm extremes during the recent global warming slowdown. *Nat. Commun.* 9, 4–6. doi:10.1038/s41467-018-04040-y.
Jones, C., and Carvalho, L. M. V. (2013). Climate Change in the South American Monsoon System: Present Climate and CMIP5 Projections. *J. Clim.* 26, 6660–6678. doi:10.1175/JCLI-D-12-00412.1.
Jung, T., Vitart, F., Ferranti, L., and Morcrette, J.-J. (2011). Origin and predictability of the extreme negative NAO winter of 2009/10. *Geophys. Res. Lett.* 38. doi:10.1029/2011GL046786.
Kamae, Y., Mei, W., Xie, S. P., Naoi, M., and Ueda, H. (2017a). Atmospheric rivers over the Northwestern Pacific: Climatology and interannual variability. *J. Clim.* 30, 5605–5619. doi:10.1175/JCLI-D-16-0875.1.
Kamae, Y., Shiogama, H., Imada, Y., Mori, M., Arakawa, O., Mizuta, R., et al. (2017b). Forced response and internal variability of summer climate over western North America. *Clim. Dyn.* 49, 403–417. doi:10.1007/s00382-016-3350-x.
Kamae, Y., Shiogama, H., Watanabe, M., and Kimoto, M. (2014). Attributing the increase in Northern Hemisphere hot summers since the late 20th century. *Geophys. Res. Lett.* 41, 5192–5199. doi:10.1002/2014GL061062.
Kanada, S., Takemi, T., Kato, M., Yamasaki, S., Fudeyasu, H., Tsuboki, K., et al. (2017). A multimodel intercomparison of an intense typhoon in future, warmer climates by Four 5-km-Mesh models. *J. Clim.* 30, 6017–6036. doi:10.1175/JCLI-D-16-0715.1.
Kanada, S., and Wada, A. (2016). Sensitivity to Horizontal Resolution of the Simulated Intensifying Rate and Inner-Core Structure of Typhoon Ida, an Extremely Intense Typhoon. *J. Meteorol. Soc. Japan. Ser. II* 94A, 181–190. doi:10.2151/jmsj.2015-037.
Kanada, S., Wada, A., and Sugi, M. (2013). Future changes in structures of extremely intense tropical cyclones using a 2-km mesh nonhydrostatic model. *J. Clim.* 26, 9986–10005. doi:10.1175/JCLI-D-12-00477.1.
Kaniewski, D., Van Campo, E., and Weiss, H. (2012). Drought is a recurring challenge in the Middle East. *Proc. Natl. Acad. Sci. U. S. A.* 109, 3862–3867. doi:10.1073/pnas.1116304109.
Karl, T. R., Arguez, A., Huang, B., Lawrimore, J. H., McMahon, J. R., Menne, M. J., et al. (2015). Possible artifacts of data biases in the recent global surface warming hiatus. *Science (80-.).* 348, 1469 LP-1472. Available at: http://science.sciencemag.org/content/348/6242/1469.abstract.
Katz, R. W. (2010). Statistics of extremes in climate change. *Clim. Change* 100, 71–76. doi:10.1007/s10584-010-9834-5.
Kawase, H., Murata, A., Mizuta, R., Sasaki, H., Nosaka, M., Ishii, M., et al. (2016). Enhancement of heavy daily snowfall in central Japan due to global warming as projected by large ensemble of regional climate simulations. *Clim. Change* 139, 265–278. doi:10.1007/s10584-016-1781-3.
Kay, A. L., Bell, V. A., Guillod, B. P., Jones, R. G., and Rudd, A. C. (2018). National-scale analysis of low flow frequency: historical trends and potential future changes. *Clim. Change* 147, 585–599. doi:10.1007/s10584-018-2145-y.
Kay, J. E., Deser, C., Phillips, A., Mai, A., Hannay, C., Strand, G., et al. (2015a). The Community Earth System Model (CESM) Large Ensemble Project: A Community Resource for Studying Climate Change in the Presence of Internal Climate Variability. *Bull. Am. Meteorol. Soc.* 96, 1333–1349. doi:10.1175/BAMS-D-13-00255.1.
Kay, S., Caesar, J., Wolf, J., Bricheno, L., Nicholls, R. J., Islam, A. K. M. S., et al. (2015b). Modelling the increased frequency of extreme sea levels in the Ganges–Brahmaputra–Meghna delta due to sea level rise and other effects of climate change. *Environ. Sci. Process. Impacts* 17, 1311–1322.
Kelley, C. P., Mohtadi, S., Cane, M. A., Seager, R., and Kushnir, Y. (2015). Climate change in the Fertile Crescent and implications of the recent Syrian drought. *Proc. Natl. Acad. Sci. U. S. A.* 112, 3241–3246. doi:10.1073/pnas.1421533112.
Kendon, E. J., Ban, N., Roberts, N. M., Fowler, H. J., Roberts, M. J., Chan, S. C., et al. (2017). Do Convection-Permitting Regional Climate Models Improve Projections of Future Precipitation Change? *Bull. Am. Meteorol. Soc.* 98, 79–93. doi:10.1175/BAMS-D-15-0004.1.
Kendon, E. J., Roberts, N. M., Fowler, H. J., Roberts, M. J., Chan, S. C., and Senior, C. A. (2014). Heavier summer downpours with climate change revealed by weather forecast resolution model. *Nat. Clim. Chang.* 4, 570–576. doi:10.1038/nclimate2258.
Kendon, M. (2014). Has there been a recent increase in UK weather records? *Weather* 69, 327–332. doi:10.1002/wea.2439.
Kew, S. F., Philip, S., van Oldenborgh, G. J., Otto, F. E. L., Vautard, R., and van der Schrier, G. (2018). The exceptional summer heat wave in souther Europe 2017. *Bull. Am. Meteorol. Soc.* doi:10.1175/BAMS-D-18-0109.1.
Kew, S. F., Selten, F. M., Lenderink, G., and Hazeleger, W. (2013). The simultaneous occurrence of surge and discharge extremes for the Rhine delta. *Nat. Hazards Earth Syst. Sci.* 13, 2017–2029. doi:10.5194/nhess-13-2017-2013.
Kharin, V. V., Flato, G. M., Zhang, X., Gillett, N. P., Zwiers, F., and Anderson, K. J. (2018). Risks from Climate Extremes Change Differently from 1.5°C to 2.0°C Depending on Rarity. *Earth's Futur.* 6, 704–715.

doi:10.1002/2018EF000813.
Kharin, V. V., Zwiers, F. W., Zhang, X., and Wehner, M. (2013). Changes in temperature and precipitation extremes in the CMIP5 ensemble. *Clim. Change* 119, 345–357. doi:10.1007/s10584-013-0705-8.
Kim, B., and Sanders, B. F. (2016). Dam-Break Flood Model Uncertainty Assessment: Case Study of Extreme Flooding with Multiple Dam Failures in Gangneung, South Korea. *J. Hydraul. Eng.* 142, 05016002. doi:10.1061/(ASCE)HY.1943-7900.0001097.
Kim, D., Moon, Y., Camargo, S. J., Wing, A. A., Sobel, A. H., Murakami, H., et al. (2018). Process-Oriented Diagnosis of Tropical Cyclones in High-Resolution GCMs. *J. Clim.* 31, 1685–1702. doi:10.1175/JCLI-D-17-0269.1.
Kim, H. S., Vecchi, G. A., Knutson, T. R., Anderson, W. G., Delworth, T. L., Rosati, A., et al. (2014). Tropical cyclone simulation and response to CO2 doubling in the GFDL CM2.5 high-resolution coupled climate model. *J. Clim.* 27, 8034–8054. doi:10.1175/JCLI-D-13-00475.1.
Kim, Y. H., Min, S. K., Zhang, X., Zwiers, F., Alexander, L. V., Donat, M. G., et al. (2016). Attribution of extreme temperature changes during 1951–2010. *Clim. Dyn.* 46, 1769–1782. doi:10.1007/s00382-015-2674-2.
King, A. D. (2017). Attributing changing rates of temperature record-breaking to anthropogenic influences: Climate change and record-breaking. 1–13.
King, A. D., Black, M. T., Min, S.-K., Fischer, E. M., Mitchell, D. M., Harrington, L. J., et al. (2016a). Emergence of heat extremes attributable to anthropogenic influences. *Geophys. Res. Lett.* 43, 3438–3443. doi:10.1002/2015GL067448.
King, A. D., Jan van Oldenborgh, G., Karoly, D. J., Lewis, S. C., and Cullen, H. (2015). Attribution of the record high Central England temperature of 2014 to anthropogenic influences. *Environ. Res. Lett.* 10, 054002. doi:10.1088/1748-9326/10/5/054002.
King, A. D., Karoly, D. J., Donat, M. G., and Alexander, L. V. (2014). Climate change turns Australia's 2013 big dry into a year of record-breaking heat. *Bull. Am. Meteorol. Soc.* 95, S41–S45. doi:10.1175/1520-0477-95.9.S1.1.
King, A. D., Karoly, D. J., and Henley, B. J. (2017). Australian climate extremes at 1.5 °C and 2 °C of global warming. *Nat. Clim. Chang.* 7, 412–416. doi:10.1038/nclimate3296.
King, A. D., Knutti, R., Uhe, P., Mitchell, D. M., Lewis, S. C., Arblaster, J. M., et al. (2018). On the linearity of local and regional temperature changes from 1.5°C to 2°C of global warming. *J. Clim.*, JCLI-D-17-0649.1. doi:10.1175/JCLI-D-17-0649.1.
King, A. D., Lewis, S. C., Perkins, S. E., Alexander, L. V, Donat, M. G., Karoly, D. J., et al. (2013). Limited evidence of anthropogenic influence on the 2011 - 12 extreme rainfall over Southeast Australia. *Bull. Amer. Meteor. Soc.* 94, 55–58.
King, A. D., Oldenborgh, G. J. van, and Karoly, D. J. (2016b). Climate Change and El NiÑo Increase Likelihood of Indonesain Heat and Drought. *Bull. Am. Meteorol. Soc.* 97, S113–S117. Available at: http://www.ametsoc.net/eee/2015/22_indonesia_heat.pdf.
Kingston, D. G., Stagge, J. H., Tallaksen, L. M., and Hannah, D. M. (2015). European-scale drought: Understanding connections between atmospheric circulation and meteorological drought indices. *J. Clim.* 28, 505–516. doi:10.1175/JCLI-D-14-00001.1.
Kinter, J. L., Cash, B., Achuthavarier, D., Adams, J., Altshuler, E., Dirmeyer, P., et al. (2013). Revolutionizing climate modeling with project athena: A multi-institutional, international collaboration. *Bull. Am. Meteorol. Soc.* 94, 231–245. doi:10.1175/BAMS-D-11-00043.1.
Kitoh, A. (2017). The Asian Monsoon and its Future Change in Climate Models : A Review. 95. doi:10.2151/jmsj.2017-002.
Kitoh, A., and Endo, H. (2019). Future Changes in Precipitation Extremes Associated with Tropical Cyclones Projected by Large-Ensemble Simulations. *J. Meteorol. Soc. Japan. Ser. II* 97, 141–152. doi:10.2151/jmsj.2019-007.
Kjeldsen, T. R., Macdonald, N., Lang, M., Mediero, L., Albuquerque, T., Bogdanowicz, E., et al. (2014). Documentary evidence of past floods in Europe and their utility in flood frequency estimation. *J. Hydrol.* 517, 963–973. doi:10.1016/j.jhydrol.2014.06.038.
Klutse, N. A. B., Sylla, M. B., Diallo, I., Sarr, A., Dosio, A., Diedhiou, A., et al. (2016). Daily characteristics of West African summer monsoon precipitation in CORDEX simulations. *Theor. Appl. Climatol.* 123, 369–386.
Knutson, T., Camargo, S., Chan, J., Emanuel, K., Ho, C.-H., Kossin, J., et al. (2019a). Tropical Cyclones and Climate Change Assessment : Part I . Detection and Attribution. *Bull. Am. Meteorol. Soc.* revised.
Knutson, T., Camargo, S. J., Chan, J. C. L., Emanuel, K., Ho, C., Mohapatra, M., et al. (2019b). Tropical Cyclones and Climate Change Assessment : Part II . Late 21 st Century Projections. *Bull. Am. Meteorol. Soc.* in review.
Knutson, T. R., Sirutis, J. J., Vecchi, G. A., Garner, S., Zhao, M., Kim, H.-S., et al. (2013). Dynamical Downscaling Projections of Twenty-First-Century Atlantic Hurricane Activity: CMIP3 and CMIP5 Model-Based Scenarios. *J. Clim.* 26, 6591–6617. doi:10.1175/JCLI-D-12-00539.1.
Knutson, T. R., Sirutis, J. J., Zhao, M., Tuleya, R. E., Bender, M., Vecchi, G. A., et al. (2015). Global Projections of Intense Tropical Cyclone Activity for the Late Twenty-First Century from Dynamical Downscaling of CMIP5/RCP4.5 Scenarios. *J. Clim.* 28, 7203–7224. doi:10.1175/JCLI-D-15-0129.1.
Knutson, T., Zeng, F., and Wittenberg, A. (2014). Seasonal and annual mean precipitation extremes during during 2013: A U.S. focused analysis. *Bull. Amer. Meteor. Soc.* 95, S19–S23.

Kodama, C., Iga, S., and Satoh, M. (2014). Impact of the sea surface temperature rise on storm-track clouds in global nonhydrostatic aqua planet simulations. *Geophys. Res. Lett.* 41, 3545–3552. doi:10.1002/2014GL059972.
Kolby Smith, W., Reed, S. C., Cleveland, C. C., Ballantyne, A. P., Anderegg, W. R. L., Wieder, W. R., et al. (2015). Large divergence of satellite and Earth system model estimates of global terrestrial CO2 fertilization. *Nat. Clim. Chang.* 6, 306. Available at: http://dx.doi.org/10.1038/nclimate2879.
Konrad, C. P., and Dettinger, M. D. (2017). Flood Runoff in Relation to Water Vapor Transport by Atmospheric Rivers Over the Western United States, 1949–2015. *Geophys. Res. Lett.* 44, 11,411-456,462. doi:10.1002/2017GL075399.
Köplin, N., Schädler, B., Viviroli, D., and Weingartner, R. (2014). Seasonality and magnitude of floods in Switzerland under future climate change. *Hydrol. Process.* 28, 2567–2578. doi:10.1002/hyp.9757.
Kossin, J. P. (2018). A global slowdown of tropical-cyclone translation speed. *Nature* 558, 104–107. doi:10.1038/s41586-018-0158-3.
Kossin, J. P., Emanuel, K. A., and Camargo, S. J. (2016). Past and Projected Changes in Western North Pacific Tropical Cyclone Exposure. *J. Clim.* 29, 5725–5739. doi:10.1175/JCLI-D-16-0076.1.
Kossin, J. P., Emanuel, K. A., and Vecchi, G. A. (2014). The poleward migration of the location of tropical cyclone maximum intensity. *Nature*, 4–7. doi:10.1038/nature13278.
Kossin, J. P., Hall, T., Knutson, T., Kunkel, K. E., Trapp, R. J., Waliser, D. E., et al. (2017). Ch. 9: Extreme Storms. Climate Science Special Report: Fourth National Climate Assessment, Volume I. , eds. D. J. Wuebbles, D. W. Fahey, K. A. Hibbard, D. J. Dokken, B. C. Stewart, and T. K. Maycock Washington, DC doi:10.7930/J07S7KXX.
Kossin, J. P., Olander, T. L., and Knapp, K. R. (2013). Trend analysis with a new global record of tropical cyclone intensity. *J. Clim.* 26, 9960–9976. doi:10.1175/JCLI-D-13-00262.1.
Kotlarski, S., Keuler, K., Christensen, O. B., Colette, A., Déqué, M., Gobiet, A., et al. (2014). Regional climate modeling on European scales: A joint standard evaluation of the EURO-CORDEX RCM ensemble. *Geosci. Model Dev.* 7, 1297–1333. doi:10.5194/gmd-7-1297-2014.
Kropáček, J., Neckel, N., Tyrna, B., Holzer, N., Hovden, A., Gourmelen, N., et al. (2015). Repeated glacial lake outburst flood threatening the oldest Buddhist monastery in north-western Nepal. *Nat. Hazards Earth Syst. Sci.* 15, 2425–2437. doi:10.5194/nhess-15-2425-2015.
Kruger, A. C., and Sekele, S. S. (2013). Trends in extreme temperature indices in South Africa: 1962-2009. *Int. J. Climatol.* 33, 661–676. doi:10.1002/joc.3455.
Kruk, M. C., Hilburn, K., and Marra, J. J. (2015). Using Microwave Satellite Data to Assess Changes in Storminess over the Pacific Ocean. *Mon. Weather Rev.* 143, 3214–3229. doi:10.1175/MWR-D-14-00280.1.
Krysanova, V., Vetter, T., Eisner, S., Huang, S., Pechlivanidis, I., Strauch, M., et al. (2017). Intercomparison of regional-scale hydrological models and climate change impacts projected for 12 large river basins worldwide - A synthesis. *Environ. Res. Lett.* 12. doi:10.1088/1748-9326/aa8359.
Kumar Mishra, B., and Herath, S. (2015). Assessment of Future Floods in the Bagmati River Basin of Nepal Using Bias-Corrected Daily GCM Precipitation Data. *J. Hydrol. Eng.* 20, 05014027. doi:10.1061/(ASCE)HE.1943-5584.0001090.
Kumar, S., Allan, R. P., Zwiers, F., Lawrence, D. M., and Dirmeyer, P. A. (2015). Revisiting trends in wetness and dryness in the presence of internal climate variability and water limitations over land. *Geophys. Res. Lett.* 42, 10,867-10,875. doi:10.1002/2015GL066858.
Kumar, S. P. and R. S. N. and D. N. (2017). Linkage between global sea surface temperature and hydroclimatology of a major river basin of India before and after 1980. *Environ. Res. Lett.* 12, 124002. Available at: http://stacks.iop.org/1748-9326/12/i=12/a=124002.
Kundzewicz, Z. W., Kanae, S., Seneviratne, S. I., Handmer, J., Nicholls, N., Peduzzi, P., et al. (2014). Flood risk and climate change: global and regional perspectives. *Hydrol. Sci. J.* 59, 1–28. doi:10.1080/02626667.2013.857411.
Kundzewicz, Z. W., Krysanova, V., Dankers, R., Hirabayashi, Y., Kanae, S., Hattermann, F. F., et al. (2017). Differences in flood hazard projections in Europe–their causes and consequences for decision making. *Hydrol. Sci. J.* 62, 1–14. doi:10.1080/02626667.2016.1241398.
Kundzewicz, Z. W., Pin'skwar, I., and Brakenridge, G. R. (2018). Changes in river flood hazard in Europe: A review. *Hydrol. Res.* 49, 294–302. doi:10.2166/nh.2017.016.
Kunii, M., Otsuka, M., Shimoji, K., and Seko, H. (2016). Ensemble Data Assimilation and Forecast Experiments for the September 2015 Heavy Rainfall Event in Kanto and Tohoku Regions with Atmospheric Motion Vectors from Himawari-8. *Sola* 12, 209–214. doi:10.2151/sola.2016-042.
Kunkel, K. E., Karl, T. R., Brooks, H., Kossin, J., Lawrimore, J. H., Arndt, D., et al. (2013). Monitoring and understanding trends in extreme storms: State of knowledge. *Bull. Am. Meteorol. Soc.* 94, 499–514. doi:10.1175/BAMS-D-11-00262.1.
Lacerda, F. F., Nobre, P., Sobral, M. C., Lopes, G. M. B., Chou, S. C., Assad, E. D., et al. (2015). Long-term Temperature and Rainfall Trends over Northeast Brazil and Cape Verde. *J. Earth Sci. Clim. Change* 06. doi:10.4172/2157-7617.1000296.
Lackmann, G. M. (2013). The south-central U.S. flood of may 2010: Present and future. *J. Clim.* 26, 4688–4709. doi:10.1175/JCLI-D-12-00392.1.

Lackmann, G. M. (2014). Hurricane Sandy before 1900 and after 2100. *Bull. Am. Meteorol. Soc.* 96, 547–560. doi:10.1175/BAMS-D-14-00123.1.
Laliberté, F., Howell, S. E. L., and Kushner, P. J. (2015). Regional variability of a projected sea ice-free Arctic during the summer months. *Geophys. Res. Lett.* 43, 256–263. doi:10.1002/2015GL066855.
Langerwisch, F., Rost, S., Gerten, D., Poulter, B., Rammig, A., and Cramer, W. (2013). Potential effects of climate change on inundation patterns in the Amazon Basin. *Hydrol. Earth Syst. Sci.* 17, 2247–2262. doi:10.5194/hess-17-2247-2013.
Latif, M., Semenov, V. A., and Park, W. (2015). Super El Niños in response to global warming in a climate model. *Clim. Change* 132, 489–500. doi:10.1007/s10584-015-1439-6.
Lau, N.-C., and Nath, M. J. (2014). Model simulation and projection of European heat waves in present-day and future climates. *J. Clim.* 27, 3713–3730. doi:10.1175/JCLI-D-13-00284.1.
Lavers, D. A., and Villarini, G. (2015). The contribution of atmospheric rivers to precipitation in Europe and the United States. *J. Hydrol.* 522, 382–390. doi:https://doi.org/10.1016/j.jhydrol.2014.12.010.
Lawal, K. A., Abatan, A. A., Angélil, O., Olaniyan, E., Olusoji, V. H., Oguntunde, P. G., et al. (2016). The Late Onset of the 2015 Wet Season in Nigeria. *Bull. Am. Meteorol. Soc.* 97, S63–S69. doi:10.1175/BAMS-D-16-0131.1.
Lee, D., Min, S., Fischer, E., Shiogama, H., and Bethke, I. (2018). Impacts of half a degree additional warming on the Asian summer monsoon rainfall characteristics. *Environ. Res. Lett.* 13. doi:10.1088/1748-9326/aab55d.
Lee, J., Li, S., Lund, R., Lee, J., Li, S., and Lund, R. (2014). Trends in Extreme U.S. Temperatures. *J. Clim.* 27, 4209–4225. doi:10.1175/JCLI-D-13-00283.1.
Lehmann, J., Coumou, D., Frieler, K., Eliseev, A. V., and Levermann, A. (2014). Future changes in extratropical storm tracks and baroclinicity under climate change. *Environ. Res. Lett.* 9. doi:10.1088/1748-9326/9/8/084002.
Lehner, F., Coats, S., Stocker, T. F., Pendergrass, A. G., Sanderson, B. M., Raible, C. C., et al. (2017). Projected drought risk in 1.5°C and 2°C warmer climates. *Geophys. Res. Lett.* 44, 7419–7428. doi:10.1002/2017GL074117.
Lehner, F., and Stocker, T. F. (2015). From local perception to global perspective. *Nat. Clim. Chang.* 5, 731–734. doi:10.1038/nclimate2660.
Lejeune, Q., Davin, E. L., Gudmundsson, L., Winckler, J., and Seneviratne, S. I. (2018). Historical deforestation locally increased the intensity of hot days in northern mid-latitudes. *Nat. Clim. Chang.* 8, 386–390. doi:10.1038/s41558-018-0131-z.
Lejeune, Q., Seneviratne, S. I., and Davin, E. L. (2017). Historical Land-Cover Change Impacts on Climate: Comparative Assessment of LUCID and CMIP5 Multimodel Experiments. *J. Clim.* 30, 1439–1459. doi:10.1175/JCLI-D-16-0213.1.
Lelieveld, J., Proestos, Y., Hadjinicolaou, P., Tanarhte, M., Tyrlis, E., and Zittis, G. (2016). Strongly increasing heat extremes in the Middle East and North Africa (MENA) in the 21st century. *Clim. Change* 137, 245–260. doi:10.1007/s10584-016-1665-6.
Lemordant, L., Gentine, P., Stéfanon, M., Drobinski, P., and Fatichi, S. (2016). Modification of land-atmosphere interactions by CO2 effects: Implications for summer dryness and heat wave amplitude. *Geophys. Res. Lett.* 43, 10,240-10,248. doi:10.1002/2016GL069896.
Lemordant, L., Gentine, P., Swann, A. S., Cook, B. I., and Scheff, J. (2018). Critical impact of vegetation physiology on the continental hydrologic cycle in response to increasing CO 2. *Proc. Natl. Acad. Sci.* 115, 4093–4098. doi:10.1073/pnas.1720712115.
Lenderink, G., Barbero, R., Loriaux, J. M., and Fowler, H. J. (2017). Super-Clausius–Clapeyron Scaling of Extreme Hourly Convective Precipitation and Its Relation to Large-Scale Atmospheric Conditions. *J. Clim.* 30, 6037–6052. doi:10.1175/JCLI-D-16-0808.1.
Leonard, M., Westra, S., Phatak, A., Lambert, M., van den Hurk, B., Mcinnes, K., et al. (2014). A compound event framework for understanding extreme impacts. *Wiley Interdiscip. Rev. Clim. Chang.* 5, 113–128. doi:10.1002/wcc.252.
Lestari, D. O., Sutriyono, E., Sabaruddin, S., and Iskandar, I. (2018). Respective Influences of Indian Ocean Dipole and El Niño-Southern Oscillation on Indonesian Precipitation. *J. Math. Fundam. Sci.* 50, 257–272. doi:10.5614/j.math.fund.sci.2018.50.3.3.
Lewis, S. C., and Karoly, D. J. (2013). Anthropogenic contributions to Australia's record summer temperatures of 2013. *Geophys. Res. Lett.* 40, 3705–3709. doi:10.1002/grl.50673.
Lewis, S. C., and Karoly, D. J. (2014a). Are estimates of anthropogenic and natural influences on Australia's extreme 2010–2012 rainfall model-dependent? *Clim. Dyn.* 45, 679–695. doi:10.1007/s00382-014-2283-5.
Lewis, S. C., and Karoly, D. J. (2014b). The Role of Anthropogenic Forcing in the Record 2013 Australia-Wide Annual and Spring Temperatures [in "Explaining Extremes of 2013 from a Climate Perspective"]. *Bull. Am. Meteorol. Soc.* 95, S31--S34.
Lewis, S. C., and King, A. D. (2015). Dramatically increased rate of observed hot record breaking in recent Australian temperatures. *Geophys. Res. Lett.* 42, 7776–7784. doi:10.1002/2015GL065793.
Lewis, S. C., and King, A. D. (2017). Evolution of mean, variance and extremes in 21st century temperatures. *Weather Clim. Extrem.* 15, 1–10. doi:10.1016/j.wace.2016.11.002.
Lewis, S. C., King, A. D., and Mitchell, D. M. (2017a). Australia's Unprecedented Future Temperature Extremes Under

Paris Limits to Warming. *Geophys. Res. Lett.* 44, 9947–9956.
Lewis, S. C., King, A. D., and Perkins-Kirkpatrick, S. E. (2017b). Defining a New Normal for Extremes in a Warming World. *Bull. Am. Meteorol. Soc.* 98, 1139–1151. doi:10.1175/BAMS-D-16-0183.1.
Lhotka, O., Kyselý, J., and Farda, A. (2018). Climate change scenarios of heat waves in Central Europe and their uncertainties. *Theor. Appl. Climatol.* 131, 1043–1054. doi:10.1007/s00704-016-2031-3.
Li, C., Fang, Y., Caldeira, K., Zhang, X., Diffenbaugh, N. S., and Michalak, A. M. (2018a). Widespread persistent changes to temperature extremes occurred earlier than predicted. *Sci. Rep.* 8, 1007. doi:10.1038/s41598-018-19288-z.
Li, C., Zwiers, F. W., Zhang, X., and Li, G. (2018b). How much information is required to well-constrain local estimates of future precipitation extremes. *Earth's Futur.* (in revisi.
Li, D., Bou-Zeid, E., and Oppenheimer, M. (2014a). The effectiveness of cool and green roofs as urban heat island mitigation strategies. *Environ. Res. Lett.* 9, 055002. doi:10.1088/1748-9326/9/5/055002.
Li, D., Zhou, T., Zou, L., Zhang, W., and Zhang, L. (2018c). Extreme High-Temperature Events Over East Asia in 1.5°C and 2°C Warmer Futures: Analysis of NCAR CESM Low-Warming Experiments. *Geophys. Res. Lett.* 45, 1541–1550. doi:10.1002/2017GL076753.
Li, H., Chen, H., and Wang, H. (2017). Effects of anthropogenic activity emerging as intensified extreme precipitation over China. *J. Geophys. Res. Atmos.* 122, 6899–6914. doi:10.1002/2016JD026251.
Li, M. (2017). Temperature reconstruction and volcanic eruption signal from tree-ring width and maximum latewood density over the past 304 years in the southeastern Tibetan Plateau. 2021–2032. doi:10.1007/s00484-017-1395-0.
Li, M., Woollings, T., Hodges, K., and Masato, G. (2014b). Extratropical cyclones in a warmer, moister climate: A recent Atlantic analogue. *Geophys. Res. Lett.* 41, 8594–8601. doi:10.1002/2014GL062186.
Li, W., Jiang, Z., Zhang, X., and Li, L. (2018d). On the Emergence of Anthropogenic Signal in Extreme Precipitation Change Over China. *Geophys. Res. Lett.* doi:10.1029/2018GL079133.
Li, W., Jiang, Z., Zhang, X., Li, L., and Sun, Y. (2018e). Additional risk in extreme precipitation in China from 1.5 °C to 2.0 °C global warming levels. *Sci. Bull.* 63, 228–234. doi:10.1016/J.SCIB.2017.12.021.
Li, Y., Zhao, M., Motesharrei, S., Mu, Q., Kalnay, E., and Li, S. (2015). Local cooling and warming effects of forests based on satellite observations. *Nat. Commun.* 6, 6603. doi:10.1038/ncomms7603.
Lin, L., Ge, E., Liu, X., Liao, W., and Luo, M. (2018a). Urbanization effects on heat waves in Fujian Province, Southeast China. *Atmos. Res.* 210, 123–132. doi:https://doi.org/10.1016/j.atmosres.2018.04.011.
Lin, L., Wang, Z., Xu, Y., and Fu, Q. (2016). Sensitivity of precipitation extremes to radiative forcing of greenhouse gases and aerosols. *Geophys. Res. Lett.* 43, 9860–9868. doi:10.1002/2016GL070869.
Lin, L., Wang, Z., Xu, Y., Fu, Q., and Dong, W. (2018b). Larger Sensitivity of Precipitation Extremes to Aerosol Than Greenhouse Gas Forcing in CMIP5 Models. *J. Geophys. Res. Atmos.* doi:10.1029/2018JD028821.
Lin, N., and Emanuel, K. (2016). Grey swan tropical cyclones. *Nat. Clim. Chang.* 6, 106–111. doi:10.1038/nclimate2777.
Little, C. M., Horton, R. M., Kopp, R. E., Oppenheimer, M., Vecchi, G. A., and Villarini, G. (2015). Joint projections of US East Coast sea level and storm surge. *Nat. Clim. Chang.* 5, 1114. doi:10.1038/nclimate2801.
Liu, L., Xu, H., Wang, Y., and Jiang, T. (2017a). Impacts of 1.5 and 2 °C global warming on water availability and extreme hydrological events in Yiluo and Beijiang River catchments in China. *Clim. Change* 145, 145–158. doi:10.1007/s10584-017-2072-3.
Liu, T., Huang, C. C., Pang, J., Zhou, Y., Zhang, Y., Ji, L., et al. (2014). Extraordinary hydro-climatic events during 1800 – 1600 yr BP in the Jin – Shaan Gorges along the middle Yellow River , China. *Palaeogeogr. Palaeoclimatol. Palaeoecol.* 410, 143–152. doi:10.1016/j.palaeo.2014.05.039.
Liu, Y., Zhang, X., Song, H., Cai, Q., Li, Q., Zhao, B., et al. (2017b). Tree-ring-width-based PDSI reconstruction for central Inner Mongolia, China over the past 333 years. *Clim. Dyn.* 48, 867–879. doi:10.1007/s00382-016-3115-6.
Ljungqvist, F. C., Krusic, P. J., Sundqvist, H. S., Zorita, E., Brattström, G., and Frank, D. (2016). Northern Hemisphere hydroclimate variability over the past tawelve centuries. *Nature* 532, 94–98. doi:10.1038/nature17418.
Lloyd-Hughes, B. (2014). The impracticality of a universal drought definition. *Theor. Appl. Climatol.* 117, 607–611. doi:10.1007/s00704-013-1025-7.
Lok, C. C. F., and Chan, J. C. L. (2017). Changes of tropical cyclone landfalls in South China throughout the twenty-first century. *Clim. Dyn.* 0, 0. doi:10.1007/s00382-017-4023-0.
López-Franca, N., Zaninelli, P., Carril, A., Menéndez, C., and Sánchez, E. (2016). Changes in temperature extremes for 21st century scenarios over South America derived from a multi-model ensemble of regional climate models. *Clim. Res.* 68, 151–167. doi:10.3354/cr01393.
Lorenz, R., Argüeso, D., Donat, M. G., Pitman, A. J., Hurk, B. Van Den, Berg, A., et al. (2016). Influence of land-atmosphere feedbacks on temperature and precipitation extremes in the GLACE-CMIP5 ensemble. *J. Geophys. Res.* 121, 607–623. doi:10.1002/2015JD024053.
Lorenzo-Lacruz, J., Mořan-Tejeda, E., Vicente-Serrano, S. M., and Ĺopez-Moreno, J. I. (2013). Streamflow droughts in the Iberian Peninsula between 1945 and 2005: Spatial and temporal patterns. *Hydrol. Earth Syst. Sci.* 17. doi:10.5194/hess-17-119-2013.
Lott, F. C., Christidis, N., and Stott, P. A. (2013). Can the 2011 East African drought be attributed to human-induced

climate change? *Geophys. Res. Lett.* 40, 1177–1181. doi:10.1002/grl.50235.
Lott, F. C., and Stott, P. A. (2016). Evaluating Simulated Fraction of Attributable Risk Using Climate Observations. *J. Clim.* 29, 4565–4575. doi:10.1175/JCLI-D-15-0566.1.
Lovino, M. A., Müller, O. V., Berbery, E. H., and Müller, G. V. (2018). How have daily climate extremes changed in the recent past over northeastern Argentina? *Glob. Planet. Change* 168, 78–97. doi:10.1016/J.GLOPLACHA.2018.06.008.
Lu, C., Sun, Y., Wan, H., Zhang, X., and Yin, H. (2016). Anthropogenic influence on the frequency of extreme temperatures in China. *Geophys. Res. Lett.* 43, 6511–6518. doi:10.1002/2016GL069296.
Lu, C., Sun, Y., and Zhang, X. (2018). Multimodel detection and attribution of changes in warm and cold spell durations. *Environ. Res. Lett.* 13, 074013. doi:10.1088/1748-9326/aacb3e.
Lu, C., and Zhou, B. (2018). Influences of the 11-yr Sunspot Cycle and Polar Vortex Oscillation on Observed Winter Temperature Variations in China. *J. Meteorol. Res.* 32, 367–379. doi:10.1007/s13351-018-7101-2.
Lucas, C., Timbal, B., and Nguyen, H. (2014). The expanding tropics: a critical assessment of the observational and modeling studies. *Wiley Interdiscip. Rev. Clim. Chang.* 5, 89–112. doi:10.1002/wcc.251.
Luiz Silva, W., Xavier, L. N. R., Maceira, M. E. P., and Rotunno, O. C. (2018). Climatological and hydrological patterns and verified trends in precipitation and streamflow in the basins of Brazilian hydroelectric plants. *Theor. Appl. Climatol.* doi:10.1007/s00704-018-2600-8.
Luo, M., and Lau, N.-C. (2016). Heat Waves in Southern China: Synoptic Behavior, Long-Term Change, and Urbanization Effects. *J. Clim.* 30, 703–720. doi:10.1175/JCLI-D-16-0269.1.
Luong, T. M., Castro, C. L., Chang, H.-I., Lahmers, T., Adams, D. K., and Ochoa-Moya, C. A. (2017). The More Extreme Nature of North American Monsoon Precipitation in the Southwestern United States as Revealed by a Historical Climatology of Simulated Severe Weather Events. *J. Appl. Meteorol. Climatol.* 56, 2509–2529. doi:10.1175/JAMC-D-16-0358.1.
Luterbacher, J., Werner, J. P., Smerdon, J. E., Fernández-Donado, L., González-Rouco, F. J., Barriopedro, D., et al. (2016). European summer temperatures since Roman times. *Environ. Res. Lett.* 11, 024001. doi:10.1088/1748-9326/11/2/024001.
Lyra, A., Tavares, P., Chou, S. C., Sueiro, G., Dereczynski, C., Sondermann, M., et al. (2018). Climate change projections over three metropolitan regions in Southeast Brazil using the non-hydrostatic Eta regional climate model at 5-km resolution. *Theor. Appl. Climatol.* 132, 663–682. doi:10.1007/s00704-017-2067-z.
Ma, S., Zhou, T., Dai, A., and Han, Z. (2015). Observed Changes in the Distributions of Daily Precipitation Frequency and Amount over China from 1960 to 2013. *J. Clim.* 28, 6960–6978. doi:10.1175/JCLI-D-15-0011.1.
Ma, S., Zhou, T., Stone, D. A., Polson, D., Dai, A., Stott, P. A., et al. (2017). Detectable Anthropogenic Shift toward Heavy Precipitation over Eastern China. *J. Clim.* 30, 1381–1396. doi:10.1175/JCLI-D-16-0311.1.
Macdonald, N., and Sangster, H. (2017). High-magnitude flooding across Britain since AD 1750. *Hydrol. Earth Syst. Sci.* 21, 1631–1650. doi:10.5194/hess-21-1631-2017.
Madhura, R. K., Krishnan, R., Revadekar, J. V, Mujumdar, M., and Goswami, B. N. (2015). Changes in western disturbances over the Western Himalayas in a warming environment. *Clim. Dyn.* 44, 1157–1168. doi:10.1007/s00382-014-2166-9.
Madsen, H., Lawrence, D., Lang, M., Martinkova, M., and Kjeldsen, T. R. (2014). Review of trend analysis and climate change projections of extreme precipitation and floods in Europe. *J. Hydrol.* 519, 3634–3650. doi:10.1016/j.jhydrol.2014.11.003.
Mahony, C. R., and Cannon, A. J. (2018). Wetter summers can intensify departures from natural variability in a warming climate. *Nat. Commun.* 9, 783. doi:10.1038/s41467-018-03132-z.
Maksimović, Č., Prodanović, D., Boonya-Aroonnet, S., Leitão, J. P., Djordjević, S., and Allitt, R. (2009). Overland flow and pathway analysis for modelling of urban pluvial flooding. *J. Hydraul. Res.* 47, 512–523. doi:10.1080/00221686.2009.9522027.
Mallakpour, I., and Villarini, G. (2015). The changing nature of flooding across the central United States. *Nat. Clim. Chang.* 5, 250. Available at: http://dx.doi.org/10.1038/nclimate2516.
Manda, A., Nakamura, H., Asano, N., Iizuka, S., Miyama, T., Moteki, Q., et al. (2014). Impacts of a warming marginal sea on torrential rainfall organized under the Asian summer monsoon. *Sci. Rep.* 4, 1–6. doi:10.1038/srep05741.
Mangini, W., Viglione, A., Hall, J., Hundecha, Y., Ceola, S., Montanari, A., et al. (2018). Detection of trends in magnitude and frequency of flood peaks across Europe. *Hydrol. Sci. J.* 63, 493–512. doi:10.1080/02626667.2018.1444766.
Mann, M. E., and Gleick, P. H. (2015). Climate change and California drought in the 21st century. *Proc. Natl. Acad. Sci. U. S. A.* 112, 3858–3859. doi:10.1073/pnas.1503667112.
Marciano, C. G., Lackmann, G. M., and Robinson, W. A. (2015). Changes in U.S. East Coast cyclone dynamics with climate change. *J. Clim.* 28, 468–484. doi:10.1175/JCLI-D-14-00418.1.
Marengo, J. A., and Bernasconi, M. (2015). Regional differences in aridity/drought conditions over Northeast Brazil: present state and future projections. *Clim. Change* 129, 103–115. doi:10.1007/s10584-014-1310-1.
Marengo, J. A., and Espinoza, J. C. (2016). Extreme seasonal droughts and floods in Amazonia: causes, trends and impacts. *Int. J. Climatol.* 36, 1033–1050. doi:10.1002/joc.4420.

Marengo, J. A., Torres, R. R., and Alves, L. M. (2017). Drought in Northeast Brazil—past, present, and future. *Theor. Appl. Climatol.* 129, 1189–1200. doi:10.1007/s00704-016-1840-8.
Marengo, J., Alves, L., and Torres, R. (2016). Regional climate change scenarios in the Brazilian Pantanal watershed. *Clim. Res.* 68, 201–213. doi:10.3354/cr01324.
Marlier, M. E., Defries, R. S., Voulgarakis, A., Kinney, P. L., Randerson, J. T., Shindell, D. T., et al. (2013). El Niño and health risks from landscape fire emissions in southeast Asia. *Nat. Clim. Chang.* 3, 131–136. doi:10.1038/nclimate1658.
Marthews, T., Otto, F.E.L., Mitchell, D., Dadson, S.J. and Jones, G., Marthews, T. R., Otto, F. E. L., Mitchell, D., Dadson, S. J., Jones, R. G., et al. (2015). The 2014 drought in the Horn of Africa: Attribution of meteorological drivers. *Bull. Am. Meteorol. Soc.* 96, S83–S88. doi:10.1175/BAMS-D-15-00115.1.
Martin, E. R. (2018). Future Projections of Global Pluvial and Drought Event Characteristics. *Geophys. Res. Lett.* doi:10.1029/2018GL079807.
Martins, E.S.P.R., Coelho, C.A.S., Haarsma, R., Otto, F.E.L., King, A.D., van Oldenborgh, G.J., Kew, S., Philip, S., Vasconcelos Junior, F.C. and Cullen, H. (2017). A multimethod attribution analysis of the prolonged Northeast Brazil hydrometeorological drought (2012-16). *Bull. Am. Meteorol. Soc.* 98, 65–68. Available at: http://www.ametsoc.net/eee/2016/ch13.pdf.
Martius, O., Pfahl, S., and Chevalier, C. (2016). A global quantification of compound precipitation and wind extremes. *Geophys. Res. Lett.* 43, 7709–7717. doi:10.1002/2016GL070017.
Marty, C., Schlögl, S., Bavay, M., and Lehning, M. (2017). How much can we save? Impact of different emission scenarios on future snow cover in the Alps. *Cryosph.* 11, 517–529. doi:10.5194/tc-11-517-2017.
Mascioli, N. R., Fiore, A. M., Previdi, M., and Correa, G. (2016). Temperature and Precipitation Extremes in the United States: Quantifying the Responses to Anthropogenic Aerosols and Greenhouse Gases. *J. Clim.* 29, 2689–2701. doi:10.1175/JCLI-D-15-0478.1.
Masood, M., and Takeuchi, K. (2015). Climate Change Impact on the Manageability of Floods and Droughts of the Ganges-Brahmaputra-Meghna Basins Using Flood Duration Curves and Drought Duration Curves, J. *Disaster Res.* 5, 991–1000.
Masood, M., Yeh, P. J. F., Hanasaki, N., and Takeuchi, K. (2014). Model study of the impacts of future climate change on the hydrology of Ganges–Brahmaputra–Meghna (GBM) basin. *Hydrol. Earth Syst. Sci. Discuss* 11, 5747–5791.
Masson-Delmotte, V., M, S., Abe-Ouchi, A., Beer, J., Ganopolski, A., Rouco, J. F. G., et al. (2013). "Information from Paleoclimate Archives. In: Climate Change 2013: The Physical Science Basis. Contribution of Working Group I to the Fifth Assessment Report of the Intergovernmental Panel on Climate Change," in, 383–464. doi:10.1017/CBO9781107415324.013.
Mastrandrea, M., Field, C. B., Stocker, T. F., Edenhofer, O., Ebi, K. L., Frame, D. J., et al. (2010). Guidance Note for Lead Authors of the IPCC Fifth Assessment Report on Consistent Treatment of Uncertainties.
Mateo, C. M. R., Yamazaki, D., Kim, H., Champathong, A., Vaze, J., and Oki, T. (2017). Impacts of spatial resolution and representation of flow connectivity on large-scale simulation of floods. *Hydrol. Earth Syst. Sci.* 21, 5143–5163. doi:10.5194/hess-21-5143-2017.
Mathbout, S., Lopez-Bustins, J. A., Martin-Vide, J., Bech, J., and Rodrigo, F. S. (2018a). Spatial and temporal analysis of drought variability at several time scales in Syria during 1961–2012. *Atmos. Res.* 200, 153–168. doi:10.1016/j.atmosres.2017.09.016.
Mathbout, S., Lopez-Bustins, J. A., Royé, D., Martin-Vide, J., Bech, J., and Rodrigo, F. S. (2018b). Observed Changes in Daily Precipitation Extremes at Annual Timescale Over the Eastern Mediterranean During 1961–2012. *Pure Appl. Geophys.* 175, 3875–3890. doi:10.1007/s00024-017-1695-7.
Matthes, H., Rinke, A., and Dethloff, K. (2015). Recent changes in Arctic temperature extremes: Warm and cold spells during winter and summer. *Environ. Res. Lett.* 10. doi:10.1088/1748-9326/10/11/114020.
Matti, B., Dahlke, H. E., Dieppois, B., Lawler, D. M., and Lyon, S. W. (2017). Flood seasonality across Scandinavia—Evidence of a shifting hydrograph? *Hydrol. Process.* 31, 4354–4370. doi:10.1002/hyp.11365.
Maúre, G., Pinto, I., Ndebele-Murisa, M., Muthige, M., Lennard, C., Nikulin, G., et al. (2018). The southern African climate under 1.5 °C and 2 °C of global warming as simulated by CORDEX regional climate models. *Environ. Res. Lett.* doi:10.1088/1748-9326/aab190.
Mazdiyasni, O., and AghaKouchak, A. (2015). Substantial increase in concurrent droughts and heatwaves in the United States. *Proc. Natl. Acad. Sci. U. S. A.* 112, 11484–11489. doi:10.1073/pnas.1422945112.
Mcbride, J. l., Sahany, S., Hassim, M. E. E., Nguyen, C. M., Lim, S.-Y., Rahmat, R., et al. (2015). The 2014 Record Dry Spell at Singapore: An Intertropical Convergence Zone (ITCZ) Drought. *Bull. Am. Meteorol. Soc.* 96, S126–S130. doi:10.1175/BAMS-D-15-00117.1.
McInnes, K. L., Erwin, T. A., and Bathols, J. M. (2011). Global Climate Model projected changes in 10 m wind speed and direction due to anthropogenic climate change. *Atmos. Sci. Lett.* 12, 325–333. doi:10.1002/asl.341.
McInnes, K. L., Walsh, K. J. E., Hoeke, R. K., O'Grady, J. G., Colberg, F., and Hubbert, G. D. (2014). Quantifying storm tide risk in Fiji due to climate variability and change. *Glob. Planet. Change* 116, 115–129. doi:https://doi.org/10.1016/j.gloplacha.2014.02.004.

McInnes, K. L., White, C. J., Haigh, I. D., Hemer, M. A., Hoeke, R. K., Holbrook, N. J., et al. (2016). Natural hazards in Australia: sea level and coastal extremes. *Clim. Change* 139, 69–83. doi:10.1007/s10584-016-1647-8.
McKenzie, D., and Littell, J. S. (2017). Climate change and the eco-hydrology of fire: Will area burned increase in a warming western USA. *Ecol. Appl.* 27, 26–36. doi:10.1002/eap.1420.
Mcvicar, T. R., Roderick, M. L., Donohue, R. J., and Van Niel, T. G. (2012). Less bluster ahead? ecohydrological implications of global trends of terrestrial near-surface wind speeds. *Ecohydrology* 5, 381–388. doi:10.1002/eco.1298.
Mediero, L., Kjeldsen, T. R., Macdonald, N., Kohnova, S., Merz, B., Vorogushyn, S., et al. (2015). Identification of coherent flood regions across Europe by using the longest streamflow records. *J. Hydrol.* 528, 341–360. doi:10.1016/j.jhydrol.2015.06.016.
Meehl, Gerald A, Hu, A., Arblaster, J. M., Fasullo, J., and Trenberth, K. E. (2013). Externally Forced and Internally Generated Decadal Climate Variability Associated with the Interdecadal Pacific Oscillation. *J. Clim.* 26, 7298–7310.
Mei, W., and Xie, S. P. (2016). Intensification of landfalling typhoons over the northwest Pacific since the late 1970s. *Nat. Geosci.* 9, 753–757. doi:10.1038/ngeo2792.
Meng, F., Liu, T., Huang, Y., Luo, M., Bao, A., and Hou, D. (2016). Quantitative Detection and Attribution of Runoff Variations in the Aksu River Basin. *Water* 8. doi:10.3390/w8080338.
Meseguer-Ruiz, O., Ponce-Philimon, P. I., Quispe-Jofré, A. S., Guijarro, J. A., and Sarricolea, P. (2018). Spatial behaviour of daily observed extreme temperatures in Northern Chile (1966–2015): data quality, warming trends, and its orographic and latitudinal effects. *Stoch. Environ. Res. Risk Assess.* 32, 3503–3523. doi:10.1007/s00477-018-1557-6.
Meyer, J. D. D., and Jin, J. (2017). The response of future projections of the North American monsoon when combining dynamical downscaling and bias correction of CCSM4 output. *Clim. Dyn.* 49, 433–447. doi:10.1007/s00382-016-3352-8.
Milly, P. C. D., and Dunne, K. A. (2016). Potential evapotranspiration and continental drying. *Nat. Clim. Chang.* 6, 946–949. doi:10.1038/nclimate3046.
Min, E., Hazeleger, W., van Oldenborgh, G. J., and Sterl, A. (2013). Evaluation of trends in high temperature extremes in north-western Europe in regional climate models. *Environ. Res. Lett.* 8, 014011. doi:10.1088/1748-9326/8/1/014011.
Min, S.-K., Zhang, X., Zwiers, F. W., and Hegerl, G. C. (2011). Human contribution to more-intense precipitation extremes. *Nature* 470, 378–381. doi:10.1038/nature09763.
Minetti, J. L., Poblete, A. G., Vargas, W. M., and Ovejero, D. P. (2014). Trends of the Drought Indices in Southern Hemisphere Subtropical Regions. *J. Earth Sci. Res.* 2, 36–47. Available at: http://www.labclisud.com.ar/wp-content/uploads/2014/09/Trends-of-the-Drought-Indices-in-Southern-Hemisphere-Subtropical-Regions.pdf [Accessed July 12, 2018].
Miralles, D. G., Gentine, P., Seneviratne, S. I., and Teuling, A. J. (2018). Land-atmospheric feedbacks during droughts and heatwaves: state of the science and current challenges. *Ann. N. Y. Acad. Sci.*
Miralles, D. G., Teuling, A. J., Van Heerwaarden, C. C., and De Arellano, J. V. G. (2014). Mega-heatwave temperatures due to combined soil desiccation and atmospheric heat accumulation. *Nat. Geosci.* 7, 345–349. doi:10.1038/ngeo2141.
Mirza, M. M. Q. (2011). Climate change, flooding in South Asia and implications. *Reg. Environ. Chang.* 11, 95–107.
Mishra, V., Ganguly, A. R., Nijssen, B., and Lettenmaier, D. P. (2015). Changes in observed climate extremes in global urban areas. *Environ. Res. Lett.* 10, 024005. doi:10.1088/1748-9326/10/2/024005.
Mishra, V., Kumar, D., Ganguly, A. R., Sanjay, J., Mujumdar, M., Krishnan, R., et al. (2014a). Reliability of regional and global climate models to simulate precipitation extremes over India. *J. Geophys. Res. Atmos.* 119, 9301–9323. doi:10.1002/2014JD021636.
Mishra, V., Shah, R., and Thrasher, B. (2014b). Soil Moisture Droughts under the Retrospective and Projected Climate in India. *J. Hydrometeorol.* 15, 2267–2292. doi:10.1175/JHM-D-13-0177.1.
Mo, K. C., and Lettenmaier, D. P. (2018). Drought variability and trends over the central United States in the instrumental record. *J. Hydrometeorol.* 19, 1149–1166. doi:10.1175/JHM-D-17-0225.1.
Moftakhari, H. R., Salvadori, G., AghaKouchak, A., Sanders, B. F., and Matthew, R. A. (2017). Compounding effects of sea level rise and fluvial flooding. *Proc. Natl. Acad. Sci.* 114, 9785–9790. doi:10.1073/pnas.1620325114.
Mohammed, K., Islam, A. K. M. S., Islam, G. M. T., Alfieri, L., Khan, M. J. U., Bala, S. K., et al. (2018). Future Floods in Bangladesh under 1.5° C, 2° C, and 4° C Global Warming Scenarios. *J. Hydrol. Eng.* 23, 4018050.
Mohammed, K., Islam, A. S., Islam, G. M. T., Alfieri, L., Bala, S. K., and Khan, M. J. U. (2017). Extreme flows and water availability of the Brahmaputra River under 1.5 and 2 °C global warming scenarios. *Clim. Change* 145, 159–175. doi:10.1007/s10584-017-2073-2.
Möller, I., Kudella, M., Rupprecht, F., Spencer, T., Paul, M., van Wesenbeeck, B. K., et al. (2014). Wave attenuation over coastal salt marshes under storm surge conditions. *Nat. Geosci.* 7, 727. Available at: http://dx.doi.org/10.1038/ngeo2251.
Monjo, R., Gaitán, E., Pórtoles, J., Ribalaygua, J., and Torres, L. (2016). Changes in extreme precipitation over Spain

using statistical downscaling of CMIP5 projections. *Int. J. Climatol.* 36, 757–769. doi:10.1002/joc.4380.
Moon, H., Guillod, B. P., Gudmundsson, L., and Seneviratne, S. I. (2019). Soil Moisture Effects on Afternoon Precipitation Occurrence in Current Climate Models. *Geophys. Res. Lett.* 46, 1861–1869. doi:10.1029/2018GL080879.
Mora, C., Spirandelli, D., Franklin, E. C., Lynham, J., Kantar, M. B., Miles, W., et al. (2018). Broad threat to humanity from cumulative climate hazards intensified by greenhouse gas emissions. *Nat. Clim. Chang.* 8, 1062–1071. doi:10.1038/s41558-018-0315-6.
Moron, V., Oueslati, B., Pohl, B., Rome, S., and Janicot, S. (2016). Trends of mean temperatures and warm extremes in northern tropical Africa (1961-2014) from observed and PPCA-reconstructed time series. *J. Geophys. Res. Atmos.* 121, 5298–5319. doi:10.1002/2015JD024303.
Mote, P. W., Rupp, D. E., Li, S., Sharp, D. J., Otto, F., Uhe, P. F., et al. (2016). Perspectives on the causes of exceptionally low 2015 snowpack in the western United States. *Geophys. Res. Lett.* 43, 10,910-980,988. doi:10.1002/2016GL069965.
Mudersbach, C., Bender, J., and Netzel, F. (2017). An analysis of changes in flood quantiles at the gauge Neu Darchau (Elbe River) from 1875 to 2013. *Stoch. Environ. Res. Risk Assess.* 31, 145–157. doi:10.1007/s00477-015-1173-7.
Mueller, B., and Seneviratne, S. (2014). Systematic land climate and evapotranspiration biases in CMIP5 simulations. *Geophys. Res. Lett.* 41, 128–134. doi:10.1002/2013GL058055.
Mueller, B., and Seneviratne, S. I. (2012). Hot days induced by precipitation deficits at the global scale. *Proc. Natl. Acad. Sci.* 109, 12398–12403. doi:10.1073/pnas.1204330109.
Mueller, B., and Zhang, X. (2016). Causes of drying trends in northern hemispheric land areas in reconstructed soil moisture data. *Clim. Change* 134, 255–267. doi:10.1007/s10584-015-1499-7.
Mueller, B., Zhang, X., and Zwiers, F. W. (2016a). Historically hottest summers projected to be the norm for more than half of the world's population within 20 years. *Environ. Res. Lett.* 11, 1–15. doi:10.1088/1748-9326/11/4/044011.
Mueller, N. D., Butler, E. E., McKinnon, K. A., Rhines, A., Tingley, M., Holbrook, N. M., et al. (2016b). Cooling of US Midwest summer temperature extremes from cropland intensification. *Nat. Clim. Chang.* 6, 317–322. doi:10.1038/nclimate2825.
Muerth, M. J., Gauvin St-Denis, B., Ricard, S., Velázquez, J. A., Schmid, J., Minville, M., et al. (2013). On the need for bias correction in regional climate scenarios to assess climate change impacts on river runoff. *Hydrol. Earth Syst. Sci.* 17, 1189–1204. doi:10.5194/hess-17-1189-2013.
Muis, S., Verlaan, M., Winsemius, H. C., Aerts, J. C. J. H., and Ward, P. J. (2016). A global reanalysis of storm surges and extreme sea levels. *Nat. Commun.* 7, 11969. Available at: http://dx.doi.org/10.1038/ncomms11969.
Mukherjee, S., Mishra, A., and Trenberth, K. E. (2018). Climate Change and Drought: a Perspective on Drought Indices. *Curr. Clim. Chang. Reports* 4, 145–163. doi:10.1007/s40641-018-0098-x.
Muller, J., Collins, J. M., Gibson, S., and Paxton, L. (2017). "Recent Advances in the Emerging Field of Paleotempestology," in *Hurricanes and Climate Change: Volume 3*, eds. J. M. Collins and K. Walsh (Cham: Springer International Publishing), 1–33. doi:10.1007/978-3-319-47594-3_1.
Murakami, H., Levin, E., Delworth, T. L., Gudgel, R., and Hsu, P.-C. (2018). Dominant effect of relative tropical Atlantic warming on major hurricane occurrence. *Science (80-.).* Available at: http://science.sciencemag.org/content/early/2018/09/26/science.aat6711.abstract.
Murakami, H., Li, T., and Hsu, P. C. (2014). Contributing factors to the recent high level of accumulated cyclone energy (ACE) and power dissipation index (PDI) in the North Atlantic. *J. Clim.* 27, 3023–3034. doi:10.1175/JCLI-D-13-00394.1.
Murakami, H., Vecchi, G. A., Delworth, T. L., Wittenberg, A. T., Underwood, S., Gudgel, R., et al. (2017). Dominant Role of Subtropical Pacific Warming in Extreme Eastern Pacific Hurricane Seasons: 2015 and the Future. *J. Clim.* 30, 243–264. doi:10.1175/JCLI-D-16-0424.1.
Muramatsu, T., Kato, T., Nakazato, M., Endo, H., and Kitoh, A. (2016). Future Change of Tornadogenesis-Favorable Environmental Conditions in Japan Estimated by a 20-km-Mesh Atmospheric General Circulation Model. *J. Meteorol. Soc. Japan. Ser. II* 94A, 105–120. doi:10.2151/jmsj.2015-053.
Murari, K. K., Ghosh, S., Patwardhan, A., Daly, E., and Salvi, K. (2015). Intensification of future severe heat waves in India and their effect on heat stress and mortality. *Reg. Environ. Chang.* 15. doi:10.1007/s10113-014-0660-6.
Murata, A., Sasaki, H., Kawase, H., Nosaka, M., Aoyagi, T., Oh'izumi, M., et al. (2017). Projection of Future Climate Change over Japan in Ensemble Simulations Using a Convection-Permitting Regional Climate Model with Urban Canopy. *SOLA* 13, 219–223. doi:10.2151/sola.2017-040.
Murata, A., Sasaki, H., Kawase, H., Nosaka, M., Oh'izumi, M., Kato, T., et al. (2015). Projection of Future Climate Change over Japan in Ensemble Simulations with a High-Resolution Regional Climate Model. *SOLA* 11, 90–94. doi:10.2151/sola.2015-022.
Musselman, K. N., Lehner, F., Ikeda, K., Clark, M. P., Prein, A. F., Liu, C., et al. (2018). Projected increases and shifts in rain-on-snow flood risk over western North America. *Nat. Clim. Chang.* 8, 808–812. doi:10.1038/s41558-018-0236-4.
Najafi, M. R., Zwiers, F. W., and Gillett, N. P. (2017). Attribution of Observed Streamflow Changes in Key British Columbia Drainage Basins. *Geophys. Res. Lett.* 44, 11,11-12,20. doi:10.1002/2017GL075016.

Nakano, M., Wada, A., Sawada, M., Yoshimura, H., Onishi, R., Kawahara, S., et al. (2017). Global 7km mesh nonhydrostatic Model Intercomparison Project for improving TYphoon forecast (TYMIP-G7): Experimental design and preliminary results. *Geosci. Model Dev.* 10, 1368–1381. doi:10.5194/gmd-10-1363-2017.
Nakayama, T., and Shankman, D. (2013). Impact of the Three-Gorges Dam and water transfer project on Changjiang floods. *Glob. Planet. Change* 100, 38–50. doi:10.1016/j.gloplacha.2012.10.004.
Nasim, W., Amin, A., Fahad, S., Awais, M., Khan, N., Mubeen, M., et al. (2018). Future risk assessment by estimating historical heat wave trends with projected heat accumulation using SimCLIM climate model in Pakistan. *Atmos. Res.* 205, 118–133. doi:https://doi.org/10.1016/j.atmosres.2018.01.009.
Nasrollahi, N., Aghakouchak, A., Cheng, L., Damberg, L., Phillips, T. J., Miao, C., et al. (2015). How well do CMIP5 climate simulations replicate historical trends and patterns of meteorological droughts? *Water Resour. Res.* 51, 2847–2864. doi:10.1002/2014WR016318.
Nastos, P. T., and Kapsomenakis, J. (2015). Regional climate model simulations of extreme air temperature in Greece. Abnormal or common records in the future climate? *Atmos. Res.* 152, 43–60. doi:10.1016/j.atmosres.2014.02.005.
National Academies of Sciences, Engineering, and M. (2016). *Attribution of Extreme Weather Events in the Context of Climate Change*. Washington, D.C.: National Academies Press doi:10.17226/21852.
Naumann, G., Alfieri, L., Wyser, K., Mentaschi, L., Betts, R. A., Carrao, H., et al. (2018). Global Changes in Drought Conditions Under Different Levels of Warming. *Geophys. Res. Lett.* 45, 3285–3296. doi:10.1002/2017GL076521.
Nayak, S., Dairaku, K., Takayabu, I., Suzuki-Parker, A., and Ishizaki, N. N. (2017). Extreme precipitation linked to temperature over Japan: current evaluation and projected changes with multi-model ensemble downscaling. *Clim. Dyn.* 51, 1–17. doi:10.1007/s00382-017-3866-8.
Naz, B. S., Kao, S.-C., Ashfaq, M., Rastogi, D., Mei, R., and Bowling, L. C. (2016). Regional hydrologic response to climate change in the conterminous United States using high-resolution hydroclimate simulations. *Glob. Planet. Change* 143, 100–117. doi:10.1016/j.gloplacha.2016.06.003.
Neukom, R., Gergis, J., Karoly, D. J., Wanner, H., Curran, M., Elbert, J., et al. (2014). Inter-hemispheric temperature variability over the past millennium. *Nat. Clim. Chang.* 4, 362–367. doi:10.1038/nclimate2174.
Neumann, B., Vafeidis, A. T., Zimmermann, J., and Nicholls, R. J. (2015). Future coastal population growth and exposure to sea-level rise and coastal flooding - A global assessment. *PLoS One* 10. doi:10.1371/journal.pone.0118571.
Nguyen, H., Lucas, C., Evans, A., Timbal, B., and Hanson, L. (2015). Expansion of the Southern Hemisphere hadley cell in response to greenhouse gas forcing. *J. Clim.* 28, 8067–8077. doi:10.1175/JCLI-D-15-0139.1.
Nicholls, R. J., Brown, S., Goodwin, P., Wahl, T., Lowe, J., Solan, M., et al. (2018). Stabilization of global temperature at 1.5°C and 2.0°C: implications for coastal areas. *Philos. Trans. R. Soc. A Math. Phys. Eng. Sci.* 376, 20160448. doi:10.1098/rsta.2016.0448.
Nicholson, S. E. (2017). Climate and climatic variability of rainfall over eastern Africa. *Rev. Geophys.* 55, 590–635.
Nicolet, G., Eckert, N., Morin, S., and Blanchet, J. (2016). Decreasing spatial dependence in extreme snowfall in the French Alps since 1958 under climate change. *J. Geophys. Res. Atmos.* 121, 8297–8310. doi:10.1002/2016JD025427.
Nie, J., Sobel, A. H., Shaevitz, D. A., and Wang, S. (2018). Dynamic amplification of extreme precipitation sensitivity. *Proc. Natl. Acad. Sci.* 115, 9467 LP-9472. doi:10.1073/pnas.1800357115.
Nied, M., Pardowitz, T., Nissen, K., Ulbrich, U., Hundecha, Y., and Merz, B. (2014). On the relationship between hydro-meteorological patterns and flood types. *J. Hydrol.* 519, 3249–3262. doi:10.1016/j.jhydrol.2014.09.089.
Nikulin, G., Lennard, C., Dosio, A., Kjellström, E., Chen, Y., Hänsler, A., et al. (2018). The effects of 1.5 and 2 degrees of global warming on Africa in the CORDEX ensemble. *Environ. Res. Lett.* 13, 065003. doi:10.1088/1748-9326/aab1b1.
Nilsen, I. B., Stagge, J. H., and Tallaksen, L. M. (2017). A probabilistic approach for attributing temperature changes to synoptic type frequency. *Int. J. Climatol.* 37, 2990–3002. doi:10.1002/joc.4894.
Niranjan Kumar, K., Rajeevan, M., Pai, D. S., Srivastava, A. K., and Preethi, B. (2013). On the observed variability of monsoon droughts over India. *Weather Clim. Extrem.* 1, 42–50. doi:10.1016/J.WACE.2013.07.006.
Nishant, M., Bodo, B., and J., M. P. (2016). Spatiotemporal patterns and trends of Indian monsoonal rainfall extremes. *Geophys. Res. Lett.* 43, 1710–1717. doi:10.1002/2016GL067841.
Niu, X., Wang, S., Tang, J., Lee, D.-K., Gutowski, W., Dairaku, K., et al. (2018). Ensemble evaluation and projection of climate extremes in China using RMIP models. *Int. J. Climatol.* 38, 2039–2055. doi:10.1002/joc.5315.
Nka, B. N., Oudin, L., Karambiri, H., Paturel, J. E., and Ribstein, P. (2015). Trends in floods in West Africa: Analysis based on 11 catchments in the region. *Hydrol. Earth Syst. Sci.* 19, 4707–4719. doi:10.5194/hess-19-4707-2015.
Norris, J., Chen, G., and David Neelin, J. (2019). Thermodynamic versus dynamic controls on extreme precipitation in a warming climate from the Community Earth System Model Large Ensemble. *J. Clim.* 32, 1025–1045. doi:10.1175/JCLI-D-18-0302.1.
Nott, J., Smithers, S., Walsh, K., and Rhodes, E. (2009). Sand beach ridges record 6000 year history of extreme tropical cyclone activity in northeastern Australia. *Quat. Sci. Rev.* 28, 1511–1520. doi:10.1016/j.quascirev.2009.02.014.
O'Gorman, P. A. (2015). Precipitation Extremes Under Climate Change. *Curr. Clim. Chang. Reports* 1, 49–59. doi:10.1007/s40641-015-0009-3.

O'Gorman, P. A., and Schneider, T. (2009). The physical basis for increases in precipitation extremes in simulations of 21st-century climate change. *Proc. Natl. Acad. Sci.* 106, 14773–14777. doi:10.1073/pnas.0907610106.
Oizumi, T., Saito, K., Ito, J., Kuroda, T., Doc, L., DUC, L., et al. (2018). Ultra-High-Resolution Numerical Weather Prediction with a Large Domain Using the K Computer: A Case Study of the Izu Oshima Heavy Rainfall Event on October 15-16, 2013. *J. Meteorol. Soc. Japan. Ser. II* 96, 25–54. doi:10.2151/jmsj.2018-006.
Oleson, K. W., Bonan, G. B., and Feddema, J. (2010). Effects of white roofs on urban temperature in a global climate model. *Geophys. Res. Lett.* 37, n/a-n/a. doi:10.1029/2009GL042194.
Oliver, E. C. J., Lago, V., Hobday, A. J., Holbrook, N. J., Ling, S. D., and Mundy, C. N. (2018a). Marine heatwaves off eastern Tasmania_ Trends, interannual variability, and predictability. *Prog. Oceanogr.* 161, 116–130.
Oliver, R. J., Mercado, L. M., Sitch, S., Simpson, D., Medlyn, B. E., Lin, Y.-S., et al. (2018b). Large but decreasing effect of ozone on the European carbon sink. *Biogeosciences* 15, 4245–4269. doi:10.5194/bg-15-4245-2018.
Olson, R., Evans, J., Di Luca, A., and Argüeso, D. (2016). The NARCliM project: model agreement and significance of climate projections. *Clim. Res.* 69, 209–227. doi:10.3354/cr01403.
Oppenheimer, M., Campos, M., Warren, R., Birkmann, J., Luber, G., and O'Neill, B. (2014). Emergent risks and key vulnerabilities. In: Climate Change 2014: Impacts, Adaptation, and Vulnerability. Part A: Global and Sectoral Aspects. Contribution of Working Group II to the Fifth Assessment Report of the Intergovernmental Panel on Climate Change.
Orlowsky, B., and Seneviratne, S. I. (2012). Global changes in extreme events: regional and seasonal dimension. *Clim. Change* 110, 669–696. doi:10.1007/s10584-011-0122-9.
Orlowsky, B., and Seneviratne, S. I. (2013). Elusive drought: Uncertainty in observed trends and short-and long-term CMIP5 projections. *Hydrol. Earth Syst. Sci.* 17, 1765–1781. doi:10.5194/hess-17-1765-2013.
Orth, R., Staudinger, M., Seneviratne, S. I., Seibert, J., and Zappa, M. (2015). Does model performance improve with complexity? A case study with three hydrological models. *J. Hydrol.* 523, 147–159. doi:10.1016/j.jhydrol.2015.01.044.
Orth, R., Vogel, M. M., Luterbacher, J., Pfister, C., and Seneviratne, S. I. (2016a). Did European temperatures in 1540 exceed present-day records? *Environ. Res. Lett.* 11, 114021. doi:10.1088/1748-9326/11/11/114021.
Orth, R., Zscheischler, J., and Seneviratne, S. I. (2016b). Record dry summer in 2015 challenges precipitation projections in Central Europe. *Sci. Rep.* 6, 28334. Available at: http://dx.doi.org/10.1038/srep28334.
Osakada, Y., and Nakakita, E. (2018). Future Change of Occurrence Frequency of Baiu Heavy Rainfall and Its Linked Atmospheric Patterns by Multiscale Analysis. *Sola* 14, 79–85. doi:10.2151/sola.2018-014.
Osima, S., Indasi, V. S., Zaroug, M., Endris, H. S., Gudoshava, M., Misiani, H. O., et al. (2018). Projected climate over the Greater Horn of Africa under 1.5° C and 2° C global warming. *Environ. Res. Lett.* 13, 65004.
Otkin, J. A., Anderson, M. C., Hain, C., Svoboda, M., Johnson, D., Mueller, R., et al. (2016). Assessing the evolution of soil moisture and vegetation conditions during the 2012 United States flash drought. *Agric. For. Meteorol.* 218–219, 230–242. doi:10.1016/j.agrformet.2015.12.065.
Otkin, J. A., Svoboda, M., Hunt, E. D., Ford, T. W., Anderson, M. C., Hain, C., et al. (2018). Flash droughts: A review and assessment of the challenges imposed by rapid-onset droughts in the United States. *Bull. Am. Meteorol. Soc.* 99, 911–919. doi:10.1175/BAMS-D-17-0149.1.
Otto, F. E. L. (2017). Attribution of Weather and Climate Events. *Annu. Rev. Environ. Resour.* 42, null. doi:10.1146/annurev-environ-102016-060847.
Otto, F. E. L., Boyd, E., Jones, R. G., Cornforth, R. J., James, R., Parker, H. R., et al. (2015a). Attribution of extreme weather events in Africa: a preliminary exploration of the science and policy implications. *Clim. Change* 132, 531–543. doi:10.1007/s10584-015-1432-0.
Otto, F. E. L., Haustein, K., Uhe, P., Coelho, C. A. S., Aravequia, J. A., Almeida, W., et al. (2015b). Factors Other Than Climate Change, Main Drivers of 2014/15 Water Shortage in Southeast Brazil. *Bull. Am. Meteorol. Soc.* 96, S35–S40. doi:10.1175/BAMS-D-15-00120.1.
Otto, F. E. L., Massey, N., van Oldenborgh, G. J., Jones, R. G., and Allen, M. R. (2012). Reconciling two approaches to attribution of the 2010 Russian heat wave. *Geophys. Res.\ Lett.* 39, L04702. doi:10.1029/2011GL050422.
Otto, F. E. L., Philip, S., Kew, S., Li, S., King, A., and Cullen, H. (2018a). Attributing high-impact extreme events across timescales—a case study of four different types of events. *Clim. Change* 149, 399–412. doi:10.1007/s10584-018-2258-3.
Otto, F. E. L., Rosier, S. M., Allen, M. R., Massey, N. R., Rye, C. J., and Quintana, J. I. (2015c). Attribution analysis of high precipitation events in summer in England and Wales over the last decade. *Clim. Change* 132, 77–91. doi:10.1007/s10584-014-1095-2.
Otto, F. E. L., van der Wiel, K., van Oldenborgh, G. J., Philip, S., Kew, S. F., Uhe, P., et al. (2018b). Climate change increases the probability of heavy rains in Northern England/Southern Scotland like those of storm Desmond—a real-time event attribution revisited. *Environ. Res. Lett.* 13, 024006. doi:10.1088/1748-9326/aa9663.
Otto, F. E. L., van Oldenborgh, G. J., Eden, J., Stott, P. A., Karoly, D. J., and Allen, M. R. (2016). The attribution question. *Nat. Clim. Chang.* 6, 813–816. doi:10.1038/nclimate3089.
Otto, F. E. L., Wolski, P., Lehner, F., Tebaldi, C., van Oldenborgh, G. J., Hogesteeger, S., et al. (2018c). Anthropogenic influence on the drivers of the Western Cape drought 2015–2017. *Environ. Res. Lett.* 13, 124010.

doi:10.1088/1748-9326/aae9f9.
Oxford English Dictionary (2019). Oxford English Dictionary. Available at: https://en.oxforddictionaries.com.
Ozturk, T., Ceber, Z. P., Türkeş, M., and Kurnaz, M. L. (2015). Projections of climate change in the Mediterranean Basin by using downscaled global climate model outputs. *Int. J. Climatol.* 35, 4276–4292. doi:10.1002/joc.4285.
Paciorek, C. J., Stone, D. A., and Wehner, M. F. (2018). Quantifying statistical uncertainty in the attribution of human influence on severe weather. *Weather Clim. Extrem.* 20, 69–80. doi:10.1016/j.wace.2018.01.002.
Padrón, R. S., Gudmundsson, L., and Seneviratne, S. I. (2019). Observational Constraints Reduce Likelihood of Extreme Changes in Multidecadal Land Water Availability. *Geophys. Res. Lett.* 46, 736–744. doi:10.1029/2018GL080521.
PaiMazumder, D., and Done, J. M. (2014). Uncertainties in long-term drought characteristics over the Canadian Prairie provinces, as simulated by the Canadian RCM. *Clim. Res.* 58, 209–220. doi:10.3354/cr01196.
Pal, J. S., and Eltahir, E. A. B. (2016). Future temperature in southwest Asia projected to exceed a threshold for human adaptability. *Nat. Clim. Chang.* 6, 197–200. doi:10.1038/nclimate2833.
Pall, P., Patricola, C. M., Wehner, M. F., Stone, D. A., Paciorek, C. J., and Collins, W. D. (2017). Diagnosing conditional anthropogenic contributions to heavy Colorado rainfall in September 2013. *Weather Clim. Extrem.* 17, 1–6. doi:https://doi.org/10.1016/j.wace.2017.03.004.
Paltan, H., Allen, M., Haustein, K., Fuldauer, L., and Dadson, S. (2018). Global implications of 1.5 °C and 2 °C warmer worlds on extreme river flows. *Environ. Res. Lett.* 13, 94003. doi:10.1088/1748-9326/aad985.
Panisset, J. S., Libonati, R., Gouveia, C. M. P., Machado-Silva, F., França, D. A., França, J. R. A., et al. (2018). Contrasting patterns of the extreme drought episodes of 2005, 2010 and 2015 in the Amazon Basin. *Int. J. Climatol.* 38, 1096–1104. doi:10.1002/joc.5224.
Panthou, G., Vischel, T., and Lebel, T. (2014). Recent trends in the regime of extreme rainfall in the Central Sahel. *Int. J. Climatol.* 34, 3998–4006. doi:10.1002/joc.3984.
Park, C., and Min, S.-K. (2018). Multi-RCM near-term projections of summer climate extremes over East Asia. *Clim. Dyn.* 0, 1–16. doi:10.1007/s00382-018-4425-7.
Park, C., Min, S.-K., Lee, D., Cha, D.-H., Suh, M.-S., Kang, H.-S., et al. (2016). Evaluation of multiple regional climate models for summer climate extremes over East Asia. *Clim. Dyn.* 46, 2469–2486. doi:10.1007/s00382-015-2713-z.
Parker, T. J., Berry, G. J., Reeder, M. J., and Nicholls, N. (2014). Modes of climate variability and heat waves in Victoria, southeastern Australia. *Geophys. Res. Lett.* 41, 6926–6934. doi:10.1002/2014GL061736.
Pascale, S., Lucarini, V., Feng, X., Porporato, A., and ul Hasson, S. (2016). Projected changes of rainfall seasonality and dry spells in a high greenhouse gas emissions scenario. *Clim. Dyn.* 46, 1331–1350. doi:10.1007/s00382-015-2648-4.
Paschalis, A., Fatichi, S., Molnar, P., Rimkus, S., and Burlando, P. (2014). On the effects of small scale space-time variability of rainfall on basin flood response. *J. Hydrol.* 514, 313–327. doi:10.1016/j.jhydrol.2014.04.014.
Patarčić, M., Gajić-Čapka, M., Cindrić, K., and Branković, C. (2014). Recent and near-future changes in precipitationextreme indices over the Croatian Adriatic coast. *Clim. Res.* 61, 157–176. doi:10.3354/cr01250.
Patil, N., Venkataraman, C., Muduchuru, K., Ghosh, S., and Mondal, A. (2018). Disentangling sea-surface temperature and anthropogenic aerosol influences on recent trends in South Asian monsoon rainfall. *Clim. Dyn.* doi:10.1007/s00382-018-4251-y.
Patra, P. K., Crisp, D., Kaiser, J. W., Wunch, D., Saeki, T., Ichii, K., et al. (2017). The Orbiting Carbon Observatory (OCO-2) tracks 2-3 peta-gram increase in carbon release to the atmosphere during the 2014-2016 El Niño. *Sci. Rep.* 7, 1–12. doi:10.1038/s41598-017-13459-0.
Patricola, C. M., Saravanan, R., and Chang, P. (2018). The Response of Atlantic Tropical Cyclones to Suppression of African Easterly Waves. *Geophys. Res. Lett.* 45, 471–479. doi:10.1002/2017GL076081.
Patricola, C. M., and Wehner, M. F. (2018). Anthropogenic influences on major tropical cyclone events. *Nature* 563, 339–346. doi:10.1038/s41586-018-0673-2.
Paul, S., Ghosh, S., Mathew, M., Devanand, A., Karmakar, S., and Niyogi, D. (2018). Increased Spatial Variability and Intensification of Extreme Monsoon Rainfall due to Urbanization. *Sci. Rep.* 8, 3918. doi:10.1038/s41598-018-22322-9.
Paxian, A., Hertig, E., Seubert, S., Vogt, G., Jacobeit, J., and Paeth, H. (2014). Present-day and future mediterranean precipitation extremes assessed by different statistical approaches. *Clim. Dyn.* 44, 845–860. doi:10.1007/s00382-014-2428-6.
Pedersen, S. H., Liston, G. E., Tamstorf, M. P., Westergaard-Nielsen, A., and Schmidt, N. M. (2015). Quantifying Episodic Snowmelt Events in Arctic Ecosystems. *Ecosystems* 18, 839–856. doi:10.1007/s10021-015-9867-8.
Pedron, I. T., Silva Dias, M. A. F., de Paula Dias, S., Carvalho, L. M. V., and Freitas, E. D. (2017). Trends and variability in extremes of precipitation in Curitiba - Southern Brazil. *Int. J. Climatol.* 37, 1250–1264. doi:10.1002/joc.4773.
Pendergrass, A. G., Lehner, F., Sanderson, B. M., and Xu, Y. (2015). Does extreme precipitation intensity depend on the emissions scenario? *Geophys. Res. Lett.* 42, 8767–8774. doi:10.1002/2015GL065854.
Peng, S., Piao, S., Ciais, P., Friedlingstein, P., Ottle, C., Bréon, F.-M., et al. (2012). Surface Urban Heat Island Across 419 Global Big Cities. *Environ. Sci. Technol.* 46, 696–703. doi:10.1021/es2030438.

Pepler, A. S., Luca, A. Di, Ji, F., Alexander, L. V, Evans, J. P., and Sherwood, S. C. (2016). Projected changes in east Australian midlatitude cyclones during the 21st century. *Geophys. Res. Lett.* 43, 334–340. doi:10.1002/2015GL067267.Received.
Perkins-Kirkpatrick, S. E., and Gibson, P. B. (2018). Changes in regional heatwave characteristics as a function of increasing global temperature. *Sci. Rep.*, 1–12.
Perkins, S. E. (2015). A review on the scientific understanding of heatwaves their measurement, driving mechanisms, and changes at the global scale. *Atmos. Res.* 164–165, 242–267.
Perkins, S. E., Lewis, S. C., King, A. D., and Alexander, L. V (2014a). Increased simulated risk of the hot Australian summer of 2012-2013 due to anthropogenic activity as measured by heatwave frequency and intensity [in "Explaining Extremes of 2013 from a Climate Perspective"]. *Bull. Am. Meteorol. Soc.* 95, S34--S37.
Perkins, S. E., Moise, A., Whetton, P., and Katzfey, J. (2014b). Regional changes of climate extremes over Australia - A comparison of regional dynamical downscaling and global climate model simulations. *Int. J. Climatol.* 34, 3456–3478. doi:10.1002/joc.3927.
Persad, G. G., and Caldeira, K. (2018). Divergent global-scale temperature effects from identical aerosols emitted in different regions. *Nat. Commun.* 9, 3289. doi:10.1038/s41467-018-05838-6.
Peterson, T. C., Heim, R. R., Hirsch, R., Kaiser, D. P., Brooks, H., Diffenbaugh, N. S., et al. (2013a). Monitoring and Understanding Changes in Heat Waves, Cold Waves, Floods, and Droughts in the United States: State of Knowledge. *Bull. Am. Meteorol. Soc.* 94, 821–834. doi:10.1175/BAMS-D-12-00066.1.
Peterson, T. C., Hoerling, M. P., Stott, P. A., and Herring, S. C. (2013b). Explaining Extreme Events of 2012 from a Climate Perspective. *Bull. Am. Meteorol. Soc.* 94, S1–S74. doi:10.1175/BAMS-D-13-00085.1.
Peterson, T. C., Stott, P. A., and Herring, S. (2012). Explaining Extreme Events of 2011 from a Climate Perspective. *Bull. Am. Meteorol. Soc.* 93, 1041–1067. doi:10.1175/BAMS-D-12-00021.1.
Pfahl, S., O'Gorman, P. A., and Fischer, E. M. (2017). Understanding the regional pattern of projected future changes in extreme precipitation. *Nat. Clim. Chang.* 7, 423. Available at: http://dx.doi.org/10.1038/nclimate3287.
Philip, S., Kew, S. F., Jan van Oldenborgh, G., Otto, F., O'Keefe, S., Haustein, K., et al. (2018a). Attribution Analysis of the Ethiopian Drought of 2015. *J. Clim.* 31, 2465–2486. doi:10.1175/JCLI-D-17-0274.1.
Philip, S., Sparrow, S., Kew, S. F. F., van der Wiel, K., Wanders, N., Singh, R., et al. (2018b). Attributing the 2017 Bangladesh floods from meteorological and hydrological perspectives. *Hydrol. Earth Syst. Sci. Discuss.* 2018, 1–32. doi:10.5194/hess-2018-379.
Piaget, N., Froidevaux, P., Giannakaki, P., Gierth, F., Martius, O., Riemer, M., et al. (2015). Dynamics of a local Alpine flooding event in October 2011: moisture source and large-scale circulation. *Q. J. R. Meteorol. Soc.* 141, 1922–1937. doi:10.1002/qj.2496.
Pinto, I., Lennard, C., Tadross, M., Hewitson, B., Dosio, A., Nikulin, G., et al. (2016). Evaluation and projections of extreme precipitation over southern Africa from two CORDEX models. *Clim. Change* 135. doi:10.1007/s10584-015-1573-1.
Pisaniello, J. D., Tingey-Holyoak, J., and Burritt, R. L. (2012). Appropriate small dam management for minimizing catchment-wide safety threats: International benchmarked guidelines and demonstrative cases studies. *Water Resour. Res.* 48. doi:10.1029/2011WR011155.
Pithan, F., and Mauritsen, T. (2014). Arctic amplification dominated by temperature feedbacks in contemporary climate models. *Nat. Geosci.* 7, 181–184. doi:10.1038/ngeo2071.
Porat, N., Halevi, R., and Dohrenwend, J. (2014). A 2000 year natural record of magnitudes and frequencies for the largest Upper Colorado River floods near Moab, Utah. 5249–5269. doi:10.1002/2013WR014835.Received.
Power, S., Delage, F., Chung, C., Kociuba, G., and Keay, K. (2013). Robust twenty-first-century projections of El Niño and related precipitation variability. *Nature* 502, 541–545. doi:10.1038/nature12580.
Prein, A. F., Gobiet, A., Suklitsch, M., Truhetz, H., Awan, N. K., Keuler, K., et al. (2013). Added value of convection permitting seasonal simulations. *Clim. Dyn.* 41, 2655–2677. doi:10.1007/s00382-013-1744-6.
Prein, A. F., Gobiet, A., Truhetz, H., Keuler, K., Goergen, K., Teichmann, C., et al. (2016a). Precipitation in the EURO-CORDEX 0.11∘ and 0.44∘ simulations: high resolution, high benefits? *Clim. Dyn.* 46, 383–412. doi:10.1007/s00382-015-2589-y.
Prein, A. F., and Holland, G. J. (2018). Global estimates of damaging hail hazard. *Weather Clim. Extrem.* 22, 10–23. doi:10.1016/j.wace.2018.10.004.
Prein, A. F., Langhans, W., Fosser, G., Ferrone, A., Ban, N., Goergen, K., et al. (2015). A review on regional convection-permitting climate modeling: Demonstrations, prospects, and challenges. *Rev. Geophys.* 53, 323–361. doi:10.1002/2014RG000475.
Prein, A. F., Liu, C., Ikeda, K., Bullock, R., Rasmussen, R. M., Holland, G. J., et al. (2017a). Simulating North American mesoscale convective systems with a convection-permitting climate model. *Clim. Dyn.* 0, 1–16. doi:10.1007/s00382-017-3993-2.
Prein, A. F., Liu, C., Ikeda, K., Trier, S. B., Rasmussen, R. M., Holland, G. J., et al. (2017b). Increased rainfall volume from future convective storms in the US. *Nat. Clim. Chang.* 7, 880–884. doi:10.1038/s41558-017-0007-7.
Prein, A. F., Rasmussen, R. M., Ikeda, K., Liu, C., Clark, M. P., and Holland, G. J. (2016b). The future intensification of hourly precipitation extremes. *Nat. Clim. Chang.* 7, 48. doi:10.1038/nclimate3168.

Prein, A. F., Rasmussen, R., and Stephens, G. (2017c). Challenges and Advances in Convection-Permitting Climate Modeling. *Bull. Am. Meteorol. Soc.* 98, 1027–1030. doi:10.1175/BAMS-D-16-0263.1.
Priya, P., Krishnan, R., Mujumdar, M., and Houze, R. A. (2017). Changing monsoon and midlatitude circulation interactions over the Western Himalayas and possible links to occurrences of extreme precipitation. *Clim. Dyn.* 49, 2351–2364. doi:10.1007/s00382-016-3458-z.
Prudhomme, C., Giuntoli, I., Robinson, E. L., Clark, D. B., Arnell, N. W., Dankers, R., et al. (2014). Hydrological droughts in the 21st century, hotspots and uncertainties from a global multimodel ensemble experiment. *Proc. Natl. Acad. Sci. U. S. A.* 111, 3262–3267. doi:10.1073/pnas.1222473110.
Púčik, T., Groenemeijer, P., Rädler, A. T., Tijssen, L., Nikulin, G., Prein, A. F., et al. (2017). Future Changes in European Severe Convection Environments in a Regional Climate Model Ensemble. *J. Clim.* 30, 6771–6794. doi:10.1175/JCLI-D-16-0777.1.
Qian, C., Wang, J., Dong, S., Yin, H., Burke, C., Ciavarella, A., et al. (2018). Human Influence on the Record-breaking Cold Event in January of 2016 in Eastern China. *Bull. Am. Meteorol. Soc.* 99, S118–S122. doi:10.1175/BAMS-D-17-0095.1.
Quan, X.-W., Hoerling, M., Smith, L., Perlwitz, J., Zhang, T., Hoell, A., et al. (2018). Extreme California Rains During Winter 2015/16: A Change in El Niño Teleconnection? *Bull. Am. Meteorol. Soc.* 99, S49–S53. doi:10.1175/BAMS-D-17-0118.1.
Quesada, B., Vautard, R., Yiou, P., Hirschi, M., and Seneviratne, S. I. (2012). Asymmetric European summer heat predictability from wet and dry southern winters and springs. *Nat. Clim. Chang.* 2, 736–741. doi:10.1038/nclimate1536.
Radić, V., Cannon, A. J., Menounos, B., and Gi, N. (2015). Future changes in autumn atmospheric river events in British Columbia, Canada, as projected by CMIP5 global climate models. *J. Geophys. Res. Atmos.* 120, 9279–9302. doi:10.1002/2015JD023279.
Rajczak, J., Pall, P., and Schär, C. (2013). Projections of extreme precipitation events in regional climate simulations for Europe and the Alpine Region. *J. Geophys. Res. Atmos.* 118, 3610–3626. doi:10.1002/jgrd.502972013.
Rajczak, J., and Schär, C. (2017). Projections of Future Precipitation Extremes Over Europe: A Multimodel Assessment of Climate Simulations. *J. Geophys. Res. Atmos.* 122, 10,773-10,800. doi:10.1002/2017JD027176.
Ralph, F. M., and Dettinger, M. D. (2012). Historical and national perspectives on extreme west coast precipitation associated with atmospheric rivers during december 2010. *Bull. Am. Meteorol. Soc.* doi:10.1175/BAMS-D-11-00188.1.
Ralph, F. M., Dettinger, M. D., Cairns, M. M., Galarneau, T. J., and Eylander, J. (2018). Defining “Atmospheric River”: How the Glossary of Meteorology Helped Resolve a Debate. *Bull. Am. Meteorol. Soc.* 99, 837–839. doi:10.1175/BAMS-D-17-0157.1.
Ramos, A. M., Tomé, R., Trigo, R. M., Liberato, M. L. R., and Pinto, J. G. (2016). Projected changes in atmospheric rivers affecting Europe in CMIP5 models. *Geophys. Res. Lett.* 43, 9315–9323. doi:10.1002/2016GL070634.
Ramos, A. M., Trigo, R. M., Liberato, M. L. R., and Tomé, R. (2015). Daily Precipitation Extreme Events in the Iberian Peninsula and Its Association with Atmospheric Rivers. *J. Hydrometeorol.* 16, 579–597. doi:10.1175/JHM-D-14-0103.1.
Rasmijn, L. M., Van Der Schrier, G., Bintanja, R., Barkmeijer, J., Sterl, A., and Hazeleger, W. (2018). Future equivalent of 2010 Russian heatwave intensified by weakening soil moisture constraints. *Nat. Clim. Chang.* 8, 381–385. doi:10.1038/s41558-018-0114-0.
Rasmussen, K. L., and Houze, R. A. (2011). Orogenic Convection in Subtropical South America as Seen by the TRMM Satellite. *Mon. Weather Rev.* 139, 2399–2420. doi:10.1175/MWR-D-10-05006.1.
Rasmussen, K. L., Prein, A. F., Rasmussen, R. M., Ikeda, K., and Liu, C. (2017). Changes in the convective population and thermodynamic environments in convection-permitting regional climate simulations over the United States. *Clim. Dyn.* doi:10.1007/s00382-017-4000-7.
Ratnam, J. V., Behera, S. K., Ratna, S. B., Rajeevan, M., and Yamagata, T. (2016). Anatomy of Indian heatwaves. *Sci. Rep.* 6, 1–11. doi:10.1038/srep24395.
Raymond, F., Ullmann, A., Camberlin, P., Oueslati, B., and Drobinski, P. (2018). Atmospheric conditions and weather regimes associated with extreme winter dry spells over the Mediterranean basin. *Clim. Dyn.* 50, 4437–4453. doi:10.1007/s00382-017-3884-6.
Reed, A. J., Mann, M. E., Emanuel, K. A., Lin, N., Horton, B. P., Kemp, A. C., et al. (2015a). Increased threat of tropical cyclones and coastal flooding to New York City during the anthropogenic era. *Proc. Natl. Acad. Sci.* doi:10.1073/pnas.1513127112.
Reed, K. A., Bacmeister, J. T., Rosenbloom, N. A., Wehner, M. F., Bates, S. C., Lauritzen, P. H., et al. (2015b). Impact of the dynamical core on the direct simulation of tropical cyclones in a high-resolution global model. *Geophys. Res. Lett.* 42, 3603–3608. doi:10.1002/2015GL063974.
Reed, K. A., and Jablonowski, C. (2011). Impact of physical parameterizations on idealized tropical cyclones in the Community Atmosphere Model. *Geophys. Res. Lett.* 38. doi:10.1029/2010GL046297.
Reed, K. A., Stansfield, A. M., Wehner, M. F., and Zarycki, C. M. (2019). Forecasted attribution of the human influence on hurricane florence. *Sci. Adv.*, Submitted.

Rehbein, A., Ambrizzi, T., and Mechoso, C. R. (2018). Mesoscale convective systems over the Amazon basin. Part I: climatological aspects. *Int. J. Climatol.* 38, 215–229. doi:10.1002/joc.5171.

Ribes, A., Thao, S., Vautard, R., Dubuisson, B., Somot, S., Colin, J., et al. (2018). Observed increase in extreme daily rainfall in the French Mediterranean. *Clim. Dyn.*, 1–20. doi:10.1007/s00382-018-4179-2.

Ridley, J., Wiltshire, A., and Mathison, C. (2013). More frequent occurrence of westerly disturbances in Karakoram up to 2100. *Sci. Total Environ.* 468–469, S31–S35. doi:10.1016/J.SCITOTENV.2013.03.074.

Rimi, R. H., Haustein, K., Allen, M. R., and Barbour, E. J. (2019). Risks of Pre-Monsoon Extreme Rainfall Events of Bangladesh: Is Anthropogenic Climate Change Playing a Role? *Bull. Am. Meteorol. Soc.* 100, S61–S65. doi:10.1175/BAMS-D-18-0152.1.

Risser, M. D., and Wehner, M. F. (2017). Attributable Human-Induced Changes in the Likelihood and Magnitude of the Observed Extreme Precipitation during Hurricane Harvey. *Geophys. Res. Lett.* 44, 12,412-457,464. doi:10.1002/2017GL075888.

Rizman, A. M., Dennis, L. Y. C., and Liu, C. (2008). A review on the generation, determination and mitigation of Urban Heat Island. *J. Environ. Sci.* 20, 120–128. doi:10.1016/S1001-0742(08)60019-4.

Roberts, M. J., Vidale, P. L., Senior, C., Hewitt, H. T., Bates, C., Berthou, S., et al. (2018). The Benefits of Global High Resolution for Climate Simulation: Process Understanding and the Enabling of Stakeholder Decisions at the Regional Scale. *Bull. Am. Meteorol. Soc.* 99, 2341–2359. doi:10.1175/BAMS-D-15-00320.1.

Rodell, M., Famiglietti, J. S., Wiese, D. N., Reager, J. T., Beaudoing, H. K., Landerer, F. W., et al. (2018). Emerging trends in global freshwater availability. *Nature* 557, 651–659. doi:10.1038/s41586-018-0123-1.

Roderick, M. L., Greve, P., and Farquhar, G. D. (2015). On the assessment of aridity with changes in atmospheric CO<inf>2</inf> *Water Resour. Res.* 51, 5450–5463. doi:10.1002/2015WR017031.

Rogger, M., Agnoletti, M., Alaoui, A., Bathurst, J. C., Bodner, G., Borga, M., et al. (2017). Land use change impacts on floods at the catchment scale: Challenges and opportunities for future research. *Water Resour. Res.* 53, 5209–5219. doi:10.1002/2017WR020723.

Rohini, P., Rajeevan, M., and Srivastava, A. K. (2016). On the Variability and Increasing Trends of Heat Waves over India. *Sci. Rep.*, 1–9.

Romero, R., and Emanuel, K. (2017). Climate change and hurricane-like extratropical cyclones: Projections for North Atlantic polar lows and medicanes based on CMIP5 models. *J. Clim.* 30, 279–299. doi:10.1175/JCLI-D-16-0255.1.

Roth, M., Buishand, T. A., Jongbloed, G., Klein Tank, A. M. G., and van Zanten, J. H. (2014). Projections of precipitation extremes based on a regional, non-stationary peaks-over-threshold approach: A case study for the Netherlands and north-western Germany. *Weather Clim. Extrem.* 4, 1–10. doi:10.1016/j.wace.2014.01.001.

Roth, M., Jongbloed, G., and Buishand, A. (2018). Monotone trends in the distribution of climate extremes. *Theor. Appl. Climatol.* doi:10.1007/s00704-018-2546-x.

Roudier, P., Andersson, J. C. M., Donnelly, C., Feyen, L., Greuell, W., and Ludwig, F. (2016). Projections of future floods and hydrological droughts in Europe under a +2°C global warming. *Clim. Change* 135, 341–355. doi:10.1007/s10584-015-1570-4.

Rowell, D. P., Booth, B. B. B., Nicholson, S. E., and Good, P. (2015). Reconciling Past and Future Rainfall Trends over East Africa. *J. Clim.* 28, 9768–9788. doi:10.1175/JCLI-D-15-0140.1.

Roxy, M. K. K., Ghosh, S., Pathak, A., Athulya, R., Mujumdar, M., Murtugudde, R., et al. (2017). A threefold rise in widespread extreme rain events over central India. *Nat. Commun.* 8, 708. doi:10.1038/s41467-017-00744-9.

Ruffault, J., Curt, T., Martin-Stpaul, N. K., Moron, V., and Trigo, R. M. (2018). Extreme wildfire events are linked to global-change-type droughts in the northern Mediterranean. *Nat. Hazards Earth Syst. Sci.* 18, 847–856. doi:10.5194/nhess-18-847-2018.

Ruml, M., Gregorić, E., Vujadinović, M., Radovanović, S., Matović, G., Vuković, A., et al. (2017). Observed changes of temperature extremes in Serbia over the period 1961 − 2010. *Atmos. Res.* 183, 26–41. doi:10.1016/j.atmosres.2016.08.013.

Russo, S., Marchese, A. F., Sillmann, J., and Immé, G. (2016). When will unusual heat waves become normal in a warming Africa? *Environ. Res. Lett.* 11, 054016. doi:10.1088/1748-9326/11/5/054016.

Russo, S., Sillmann, J., and Fischer, E. M. (2015). Top ten European heatwaves since 1950 and their occurrence in the coming decades. *Environ. Res. Lett.* 10. doi:10.1088/1748-9326/10/12/124003.

Ruti, P. M., Somot, S., Giorgi, F., Dubois, C., Flaounas, E., Obermann, A., et al. (2016). Med-CORDEX initiative for Mediterranean climate studies. *Bull. Am. Meteorol. Soc.* 97, 1187–1208. doi:10.1175/BAMS-D-14-00176.1.

Rutz, J. J., Steenburgh, W. J., and Ralph, F. M. (2014). Climatological Characteristics of Atmospheric Rivers and Their Inland Penetration over the Western United States. *Mon. Weather Rev.* 142, 905–921. doi:10.1175/MWR-D-13-00168.1.

Salathé, E. P., Hamlet, A. F., Mass, C. F., Lee, S.-Y., Stumbaugh, M., and Steed, R. (2014). Estimates of twenty-first-century flood risk in the Pacific Northwest based on regional climate model simulations. *J. Hydrometeorol.* 15, 1881–1899. doi:10.1175/JHM-D-13-0137.1.

Salinger, J. (2013). New Zealand Climate : Patterns of Drought 1941 - 2013. *New Zeal. Clim. Patterns Drought 1941 - 2013* 32, 2–19.

Salvador, M. de A., and de Brito, J. I. B. (2018). Trend of annual temperature and frequency of extreme events in the MATOPIBA region of Brazil. *Theor. Appl. Climatol.* 133, 253–261. doi:10.1007/s00704-017-2179-5.
Salvi, K., and Ghosh, S. (2016). Projections of Extreme Dry and Wet Spells in the 21st Century India Using Stationary and Non-stationary Standardized Precipitation Indices. *Clim. Change* 139, 667–681. doi:10.1007/s10584-016-1824-9.
Samaniego, L., Kumar, R., Breuer, L., Chamorro, A., Flörke, M., Pechlivanidis, I. G., et al. (2017). Propagation of forcing and model uncertainties on to hydrological drought characteristics in a multi-model century-long experiment in large river basins. *Clim. Change* 141, 435–449. doi:10.1007/s10584-016-1778-y.
Samaniego, L., Thober, S., Kumar, R., Wanders, N., Rakovec, O., Pan, M., et al. (2018). Anthropogenic warming exacerbates European soil moisture droughts. *Nat. Clim. Chang.* 8, 421–426. doi:10.1038/s41558-018-0138-5.
Sanderson, B. M., Xu, Y., Tebaldi, C., Wehner, M., O'Neill, B., Jahn, A., et al. (2017a). Community climate simulations to assess avoided impacts in 1.5 and 2C futures. *Earth Syst. Dyn.* 8, 827–847. doi:10.5194/esd-8-827-2017.
Sanderson, M., Economou, T., Salmon, K., and Jones, S. (2017b). Historical Trends and Variability in Heat Waves in the United Kingdom. *Atmosphere (Basel).* 8, 117–191.
Santer, B. D., Fyfe, J. C., Pallotta, G., Flato, G. M., Meehl, G. A., England, M. H., et al. (2017). Causes of differences in model and satellite tropospheric warming rates. *Nat. Geosci.* 10, 478.
Sarangi, C., Tripathi, S. N., Kanawade, V. P., Koren, I., and Pai, D. S. (2017). Investigation of the aerosol–cloud–rainfall association over the Indian summer monsoon region. *Atmos. Chem. Phys.* 17, 5185–5204. doi:10.5194/acp-17-5185-2017.
Satoh, M., Noda, A. T., Seiki, T., Chen, Y.-W., Kodama, C., Yamada, Y., et al. (2018). Toward reduction of the uncertainties in climate sensitivity due to cloud processes using a global non-hydrostatic atmospheric model. *Prog. Earth Planet. Sci.* 5, 67. doi:10.1186/s40645-018-0226-1.
Satoh, M., Stevens, B., Judt, F., Khairoutdinov, M., Lin, S., and Putman, W. M. (2019). Global Cloud-Resolving Models. *Curr. Clim. Chang. Reports*.
Satoh, M., Tomita, H., Yashiro, H., Kajikawa, Y., Miyamoto, Y., Yamaura, T., et al. (2017). Outcomes and challenges of global high-resolution non-hydrostatic atmospheric simulations using the K computer. *Prog. Earth Planet. Sci.* 4, 13. doi:10.1186/s40645-017-0127-8.
Satoh, M., Yamada, Y., Sugi, M., Komada, C., and Noda, A. T. (2015). Constraint on Future Change in Global Frequency of Tropical Cyclones due to Global Warming. *J. Meteorol. Soc. Japan. Ser. II* 93, 489–500. doi:10.2151/jmsj.2015-025.
Saurral, R. I., Camilloni, I. A., and Barros, V. R. (2017). Low-frequency variability and trends in centennial precipitation stations in southern South America. *Int. J. Climatol.* 37, 1774–1793. doi:10.1002/joc.4810.
Schaaf, B., and Feser, F. (2018). Is there added value of convection-permitting regional climate model simulations for storms over the German Bight and Northern Germany? *Meteorol. Hydrol. Water Manag. Oper. Appl.* 6, 21–37. doi:10.26491/mhwm/85507.
Schaller, N., Kay, A. L., Lamb, R., Massey, N. R., van Oldenborgh, G. J., Otto, F. E. L., et al. (2016). Human influence on climate in the 2014 southern England winter floods and their impacts. *Nat. Clim. Chang.* 6, 627–634. doi:10.1038/nclimate2927.
Schaller, N., Otto, F. E. L., van Oldenborgh, G. J., Massey, N. R., Sparrow, S., and Allen, M. R. (2014). The heavy precipitation event of May-June 2013 in the upper Danube and Elbe basins. *Bull. Amer. Meteor. Soc.* 95, S69–S72.
Schaller, N., Sillmann, J., Anstey, J., Fischer, E. M., Grams, C. M., and Russo, S. (2018). Influence of blocking on Northern European and Western Russian heatwaves in large climate model ensembles. *Environ. Res. Lett.* 13. doi:10.1088/1748-9326/aaba55.
Scheff, J. (2018). Drought Indices, Drought Impacts, CO2, and Warming: a Historical and Geologic Perspective. *Curr. Clim. Chang. Reports* 4, 202–209. doi:10.1007/s40641-018-0094-1.
Scheff, J., and Frierson, D. M. W. (2015). Terrestrial aridity and its response to greenhouse warming across CMIP5 climate models. *J. Clim.* 28, 5583–5600. doi:10.1175/JCLI-D-14-00480.1.
Scheff, J., Seager, R., Liu, H., and Coats, S. (2017). Are glacials dry? Consequences for paleoclimatology and for greenhouse warming. *J. Clim.* 30, 6593–6609. doi:10.1175/JCLI-D-16-0854.1.
Scherrer, S. C., Fischer, E. M., Posselt, R., Liniger, M. A., Croci-Maspoli, M., and Knutti, R. (2016). Emerging trends in heavy precipitation and hot temperature extremes in Switzerland. *J. Geophys. Res. Atmos.* 121, 2626–2637. doi:10.1002/2015JD024634.
Schewe, J., Heinke, J., Gerten, D., Haddeland, I., Arnell, N. W., Clark, D. B., et al. (2014). Multimodel assessment of water scarcity under climate change. *Proc. Natl. Acad. Sci. U. S. A.* 111, 3245–3250. doi:10.1073/pnas.1222460110.
Schoetter, R., Cattiaux, J., and Douville, H. (2015). Changes of western European heat wave characteristics projected by the CMIP5 ensemble. *Clim. Dyn.* 45, 1601–1616. doi:10.1007/s00382-014-2434-8.
Schubert, S. D., Stewart, R. E., Wang, H., Barlow, M., Berbery, E. H., Cai, W., et al. (2016). Global meteorological drought: A synthesis of current understanding with a focus on sst drivers of precipitation deficits. *J. Clim.* 29,

3989–4019. doi:10.1175/JCLI-D-15-0452.1.
Schubert, S. D., Wang, H., Koster, R. D., Suarez, M. J., and Groisman, P. Y. (2014). Northern Eurasian heat waves and droughts. *J. Clim.* 27, 3169–3207. doi:10.1175/JCLI-D-13-00360.1.
Schumacher, R. S., and Johnson, R. H. (2005). Organization and Environmental Properties of Extreme-Rain-Producing Mesoscale Convective Systems. *Mon. Weather Rev.* 133, 961–976. doi:10.1175/MWR2899.1.
Schwanghart, W., Worni, R., Huggel, C., Stoffel, M., and Korup, O. (2016). Uncertainty in the Himalayan energy–water nexus: estimating regional exposure to glacial lake outburst floods. *Environ. Res. Lett.* 11, 074005. doi:10.1088/1748-9326/11/7/074005.
Seager, R., and Hoerling, M. (2014). Atmosphere and ocean origins of North American droughts. *J. Clim.* 27, 4581–4606. doi:10.1175/JCLI-D-13-00329.1.
Sedlmeier, K., Feldmann, H., and Schädler, G. (2018). Compound summer temperature and precipitation extremes over central Europe. *Theor. Appl. Climatol.* 131, 1493–1501. doi:10.1007/s00704-017-2061-5.
Seiler, C., Hutjes, R. W. A., and Kabat, P. (2013). Likely Ranges of Climate Change in Bolivia. *J. Appl. Meteorol. Climatol.* 52, 1303–1317. doi:10.1175/JAMC-D-12-0224.1.
Şen, Z. (2018). *Flood Modeling, Prediction and Mitigation*. Cham: Springer International Publishing doi:10.1007/978-3-319-52356-9.
Senatore, A., Hejabi, S., Mendicino, G., Bazrafshan, J., and Irannejad, P. (2018). Climate conditions and drought assessment with the Palmer Drought Severity Index in Iran: evaluation of CORDEX South Asia climate projections (2070–2099). *Clim. Dyn.*, 1–27. doi:10.1007/s00382-018-4171-x.
Seneviratne, S. I., Corti, T., Davin, E. L., Hirschi, M., Jaeger, E. B., Lehner, I., et al. (2010). Investigating soil moisture-climate interactions in a changing climate: A review. *Earth-Science Rev.* 99, 125–161. doi:10.1016/j.earscirev.2010.02.004.
Seneviratne, S. I., Donat, M. G., Mueller, B., and Alexander, L. V. (2014). No pause in the increase of hot temperature extremes. *Nat. Clim. Chang.* 4, 161–163. doi:10.1038/nclimate2145.
Seneviratne, S. I., Donat, M. G., Pitman, A. J., Knutti, R., and Wilby, R. L. (2016). Allowable CO2emissions based on regional and impact-related climate targets. *Nature* 529, 477–483. doi:10.1038/nature16542.
Seneviratne, S. I., Nicholls, N., Easterling, D., Goodess, C. M., Kanae, S., Kossin, J., et al. (2012). "Changes in Climate Extremes and their Impacts on the Natural Physical Environment," in *Managing the Risks of Extreme Events and Disasters to Advance Climate Change Adaptation*, eds. C. B. Field, V. Barros, T. F. Stocker, and Q. Dahe (Cambridge, UK, and New York, NY, USA: Cambridge University Press), 109–230. doi:10.1017/CBO9781139177245.006.
Seneviratne, S. I., Phipps, S. J., Pitman, A. J., Hirsch, A. L., Davin, E. L., Donat, M. G., et al. (2018a). Land radiative management as contributor to regional-scale climate adaptation and mitigation. *Nat. Geosci.* 11, 88–96. doi:10.1038/s41561-017-0057-5.
Seneviratne, S. I., Wartenburger, R., Guillod, B. P., Hirsch, A. L., Vogel, M. M., Brovkin, V., et al. (2018b). Climate extremes, land–climate feedbacks and land-use forcing at 1.5°C. *Philos. Trans. R. Soc. A Math. Phys. Eng. Sci.* 376, 20160450. doi:10.1098/rsta.2016.0450.
Seneviratne, S. I., Wilhelm, M., Stanelle, T., Van Den Hurk, B., Hagemann, S., Berg, A., et al. (2013). Impact of soil moisture-climate feedbacks on CMIP5 projections: First results from the GLACE-CMIP5 experiment. *Geophys. Res. Lett.* 40, 5212–5217. doi:10.1002/grl.50956.
Seo, Y.-W., Kim, H., Yun, K.-S., Lee, J.-Y., Ha, K.-J., and Moon, J.-Y. (2014). Future change of extreme temperature climate indices over East Asia with uncertainties estimation in the CMIP5. *Asia-Pacific J. Atmos. Sci.* 50, 609–624. doi:10.1007/s13143-014-0050-5.
Seo, Y.-W., Yun, K.-S., Lee, J.-Y., Lee, Y.-W., Ha, K.-J., and Jhun, J.-G. (2018). Future changes due to model biases in probabilities of extreme temperatures over East Asia using CMIP5 data. *Int. J. Climatol.* 38, 1177–1188. doi:10.1002/joc.5233.
Seth, A., Giannini, A., Rojas, M., Rauscher, S. A., Bordoni, S., Singh, D., et al. (2019). Monsoon Responses to Climate Changes—Connecting Past, Present and Future. *Curr. Clim. Chang. Reports*. doi:10.1007/s40641-019-00125-y.
Shaevitz, D. A., Camargo, S. J., Sobel, A. H., Jonas, J. A., Kim, D., Kumar, A., et al. (2014). Characteristics of tropical cyclones in high-resolution models in the present climate. *J. Adv. Model. Earth Syst.* 6, 1154–1172. doi:10.1002/2014MS000372.
Sharma, A., Wasko, C., and Lettenmaier, D. P. (2018). If Precipitation Extremes Are Increasing, Why Aren't Floods? *Water Resour. Res.* 54, 8545–8551. doi:10.1029/2018WR023749.
Sharmila, S., and Walsh, K. J. E. (2018). Recent poleward shift of tropical cyclone formation linked to Hadley cell expansion. *Nat. Clim. Chang.* doi:10.1038/s41558-018-0227-5.
Shastri, H., Paul, S., Ghosh, S., and Karmakar, S. (2015). Impacts of urbanization on Indian summer monsoon rainfall extremes. *J. Geophys. Res. Atmos.* 120, 496–516. doi:10.1002/2014JD022061.
Shaw, T. A. A., Baldwin, M., Barnes, E. A. A., Caballero, R., Garfinkel, C. I. I., Hwang, Y.-T., et al. (2016). Storm track processes and the opposing influences of climate change. *Nat. Geosci.* 9, 656–664. doi:10.1038/ngeo2783.
Sheffield, J., Wood, E. F., and Roderick, M. L. (2012). Little change in global drought over the past 60 years. *Nature* 491, 435–438. doi:10.1038/nature11575.

Sheikh, M. M., Manzoor, N., Ashraf, J., Adnan, M., Collins, D., Hameed, S., et al. (2015). Trends in extreme daily rainfall and temperature indices over South Asia. *Int. J. Climatol.* doi:10.1002/joc.4081.
Shepherd, J. M. (2013). Impacts of Urbanization on Precipitation and Storms: Physical Insights and Vulnerabilities. *Clim. Vulnerability*, 109–125. doi:10.1016/B978-0-12-384703-4.00503-7.
Shepherd, T. G. (2014). Atmospheric circulation as a source of uncertainty in climate change projections. *Nat. Geosci.* 7, 703–708. doi:10.1038/NGEO2253.
Shepherd, T. G. (2016). A Common Framework for Approaches to Extreme Event Attribution. *Curr. Clim. Chang. Reports* 2, 28–38. doi:10.1007/s40641-016-0033-y.
Shepherd, T. G., Boyd, E., Calel, R. A., Chapman, S. C., Dessai, S., Dima-West, I. M., et al. (2018). Storylines: an alternative approach to representing uncertainty in physical aspects of climate change. *Clim. Change* 151, 555–571. doi:10.1007/s10584-018-2317-9.
Sherwood, S. C., and Huber, M. (2010). An adaptability limit to climate change due to heat stress. *Proc. Natl. Acad. Sci.* 107, 9552–9555. doi:10.1073/pnas.0913352107.
Sherwood, S., and Fu, Q. (2014). A Drier Future? *Science (80-.).* 343, 737–739. doi:10.1126/science.1247620.
Shevchenko, O., Lee, H., Snizhko, S., and Mayer, H. (2014). Long-term analysis of heat waves in Ukraine. *Int. J. Climatol.* 34, 1642–1650. doi:10.1002/joc.3792.
Shi, Y., Wang, G., and Gao, X. (2017). Role of resolution in regional climate change projections over China. *Clim. Dyn.* 51, 2375–2396. doi:10.1007/s00382-017-4018-x.
Shiogama, H., Imada, Y., Mori, M., Mizuta, R., Stone, D., Yoshida, K., et al. (2016). Attributing Historical Changes in Probabilities of Record-Breaking Daily Temperature and Precipitation Extreme Events. *SOLA* 12, 225–231. doi:10.2151/sola.2016-045.
Shkolnik, I., Pavlova, T., Efimov, S., and Zhuravlev, S. (2018). Future changes in peak river flows across northern Eurasia as inferred from an ensemble of regional climate projections under the IPCC RCP8.5 scenario. *Clim. Dyn.* 50, 215–230. doi:10.1007/s00382-017-3600-6.
Shukla, S., Safeeq, M., Aghakouchak, A., Guan, K., and Funk, C. (2015). Temperature impacts on the water year 2014 drought in California. *Geophys. Res. Lett.* 42, 4384–4393. doi:10.1002/2015GL063666.
Sigmond, M., Fyfe, J. C., and Swart, N. C. (2018). Ice-free Arctic projections under the Paris Agreement. *Nat. Clim. Chang.* 8, 404–408. doi:10.1038/s41558-018-0124-y.
Sikorska, A. E., Viviroli, D., and Seibert, J. (2015). Flood-type classification in mountainous catchments using crisp and fuzzy decision trees. *Water Resour. Res.* 51, 7959–7976. doi:10.1002/2015WR017326.
Sillmann, J., Donat, M. G., Fyfe, J. C., and Zwiers, F. W. (2014). Observed and simulated temperature extremes during the recent warming hiatus. *Environ. Res. Lett.* 9, 64023–64029.
Sillmann, J., Kharin, V. V., Zhang, X., Zwiers, F. W., and Bronaugh, D. (2013a). Climate extremes indices in the CMIP5 multimodel ensemble: Part 1. Model evaluation in the present climate. *J. Geophys. Res. Atmos.* 118, 1716–1733. doi:10.1002/jgrd.50203.
Sillmann, J., Kharin, V. V, Zwiers, F. W., Zhang, X., and Bronaugh, D. (2013b). Climate extremes indices in the CMIP5 multimodel ensemble: Part 2. Future climate projections. *J. Geophys. Res. Atmos.* 118, 2473–2493. doi:10.1002/jgrd.50188.
Singh, S., Ghosh, S., Sahana, A. S., Vittal, H., and Karmakar, S. (2017). Do dynamic regional models add value to the global model projections of Indian monsoon? *Clim. Dyn.* 48, 1375–1397. doi:10.1007/s00382-016-3147-y.
Singh, V., and Goyal, M. K. (2016). Changes in climate extremes by the use of CMIP5 coupled climate models over eastern Himalayas. *Environ. Earth Sci.* 75, 839. doi:10.1007/s12665-016-5651-0.
Sippel, S., El-Madany, T. S., Migliavacca, M., Mahecha, M. D., Carrara, A., Flach, M., et al. (2018a). Warm Winter, Wet Spring, and an Extreme Response in Ecosystem Functioning on the Iberian Peninsula. *Bull. Am. Meteorol. Soc.* 99, S80–S85. doi:10.1175/BAMS-D-17-0135.1.
Sippel, S., and Otto, F. E. L. (2014). Beyond climatological extremes - assessing how the odds of hydrometeorological extreme events in South-East Europe change in a warming climate. *Clim. Change* 125, 381–398. doi:10.1007/s10584-014-1153-9.
Sippel, S., Otto, F. E. L., Flach, M., and van Oldenborgh, G. J. (2016). The role of anthropogenic warming in 2015 central european heat waves. *Bull. Am. Meteorol. Soc.* 97, S51–S56. doi:10.1175/BAMS-D-16-0150.1.
Sippel, S., Reichstein, M., Ma, X., Mahecha, M. D., Lange, H., Flach, M., et al. (2018b). Drought, Heat, and the Carbon Cycle: a Review. *Curr. Clim. Chang. Reports* 4, 266–286. doi:10.1007/s40641-018-0103-4.
Sippel, S., Zscheischler, J., Heimann, M., Lange, H., Mahecha, M. D., van Oldenborgh, G. J., et al. (2017). Have precipitation extremes and annual totals been increasing in the world's dry regions over the last 60 years? *Hydrol. Earth Syst. Sci.* 21, 441–458. doi:10.5194/hess-21-441-2017.
Siswanto, Jan van Oldenborgh, G., van der Schrier, G., Lenderink, G., and van den Hurk, B. (2015). Trends in High-Daily Precipitation Events in Jakarta and the Flooding of January 2014. *Bull. Am. Meteorol. Soc.* 96, S131–S135. doi:10.1175/BAMS-D-15-00128.1.
Skansi, M. de los M., Brunet, M., Sigró, J., Aguilar, E., Arevalo Groening, J. A., Bentancur, O. J., et al. (2013). Warming and wetting signals emerging from analysis of changes in climate extreme indices over South America. *Glob. Planet. Change* 100, 295–307. doi:10.1016/j.gloplacha.2012.11.004.

Smerdon, J. E., and Pollack, H. N. (2016). Reconstructing Earth's surface temperature over the past 2000 years: the science behind the headlines. *Wiley Interdiscip. Rev. Clim. Chang.* 7, 746–771. doi:10.1002/wcc.418.
Smith, B. K., Smith, J. A., Baeck, M. L., Villarini, G., and Wright, D. B. (2013). Spectrum of storm event hydrologic response in urban watersheds. *Water Resour. Res.* 49, 2649–2663. doi:10.1002/wrcr.20223.
Sohn, B. J., Ryu, G.-H., Song, H.-J., and Ou, M.-L. (2013). Characteristic Features of Warm-Type Rain Producing Heavy Rainfall over the Korean Peninsula Inferred from TRMM Measurements. *Mon. Weather Rev.* 141, 3873–3888. doi:10.1175/MWR-D-13-00075.1.
Sorribas, M. V., Paiva, R. C. D., Melack, J. M., Bravo, J. M., Jones, C., Carvalho, L., et al. (2016). Projections of climate change effects on discharge and inundation in the Amazon basin. *Clim. Change* 136, 555–570. doi:10.1007/s10584-016-1640-2.
Spinoni, J., Barbosa, P., De Jager, A., McCormick, N., Naumann, G., Vogt, J. V., et al. (2019). A new global database of meteorological drought events from 1951 to 2016. *J. Hydrol. Reg. Stud.* 22, 100593. doi:10.1016/J.EJRH.2019.100593.
Spinoni, J., Naumann, G., Carrao, H., Barbosa, P., and Vogt, J. (2014). World drought frequency, duration, and severity for 1951-2010. *Int. J. Climatol.* 34, 2792–2804. doi:10.1002/joc.3875.
Spinoni, J., Naumann, G., and Vogt, J. (2015). Spatial patterns of European droughts under a moderate emission scenario. *Adv. Sci. Res.* 12, 179–186. doi:10.5194/asr-12-179-2015.
Spinoni, J., Naumann, G., and Vogt, J. V. (2017). Pan-European seasonal trends and recent changes of drought frequency and severity. *Glob. Planet. Change* 148, 113–130. doi:10.1016/j.gloplacha.2016.11.013.
Spinoni, J., Vogt, J. V, Barbosa, P., Dosio, A., McCormick, N., Bigano, A., et al. (2018a). Changes of heating and cooling degree-days in Europe from 1981 to 2100. *Int. J. Climatol.* 38, e191–e208. doi:10.1002/joc.5362.
Spinoni, J., Vogt, J. V, Naumann, G., Barbosa, P., and Dosio, A. (2018b). Will drought events become more frequent and severe in Europe? *Int. J. Climatol.* 38, 1718–1736. doi:10.1002/joc.5291.
Stagge, J. H., Kingston, D. G., Tallaksen, L. M., and Hannah, D. M. (2017). Observed drought indices show increasing divergence across Europe. *Sci. Rep.* 7. doi:10.1038/s41598-017-14283-2.
Staten, P. W., Lu, J., Grise, K. M., Davis, S. M., and Birner, T. (2018). Re-examining tropical expansion. *Nat. Clim. Chang.* 8, 768–775. doi:10.1038/s41558-018-0246-2.
Stegall, S. T., and Kunkel, K. E. (2017). Monthly Extreme Temperature Trends in CMIP5 Hindcast/Prediction Simulations, 1981–2010 and 2006–35. *J. Appl. Meteorol. Climatol.* 56, 1141–1154. doi:10.1175/JAMC-D-16-0281.1.
Stegehuis, A. I., Vautard, R., Ciais, P., Teuling, A. J., Jung, M., and Yiou, P. (2013). Summer temperatures in Europe and land heat fluxes in observation-based data and regional climate model simulations. *Clim. Dyn.* 41, 455–477. doi:10.1007/s00382-012-1559-x.
Sterling, S. M., Ducharne, A., and Polcher, J. (2013). The impact of global land-cover change on the terrestrial water cycle. *Nat. Clim. Chang.* 3, 385–390. doi:10.1038/nclimate1690.
Stoffel, M., and Corona, C. (2018). Future winters glimpsed in the Alps. *Nat. Geosci.* 11, 458–460. doi:10.1038/s41561-018-0177-6.
Stott, P. A., Christidis, N., Otto, F. E. L., Sun, Y., Vanderlinden, J.-P., van Oldenborgh, G. J., et al. (2016). Attribution of extreme weather and climate-related events. *Wiley Interdiscip. Rev. Clim. Chang.* 7, 23–41. doi:10.1002/wcc.380.
Strong, J. D. O., Vecchi, G. A., and Ginoux, P. (2018). The Climatological Effect of Saharan Dust on Global Tropical Cyclones in a Fully Coupled GCM. *J. Geophys. Res. Atmos.* 123, 5538–5559. doi:10.1029/2017JD027808.
Studholme, J., and Gulev, S. (2018). Concurrent Changes to Hadley Circulation and the Meridional Distribution of Tropical Cyclones. *J. Clim.* 31, 4367–4389. doi:10.1175/JCLI-D-17-0852.1.
Sugi, M., Murakami, H., and Yoshida, K. (2017). Projection of future changes in the frequency of intense tropical cyclones. *Clim. Dyn.* 49, 619–632. doi:10.1007/s00382-016-3361-7.
Sugi, M., Murakami, H., and Yoshimura, J. (2012). On the Mechanism of Tropical Cyclone Frequency Changes Due to Global Warming. *J. Meteorol. Soc. Japan* 90A, 397–408. doi:10.2151/jmsj.2012-A24.
Sui, Y., Lang, X., and Jiang, D. (2018). Projected signals in climate extremes over China associated with a 2 °C global warming under two RCP scenarios. *Int. J. Climatol.* 38, e678–e697. doi:10.1002/joc.5399.
Sun, Q., and Miao, C. (2018). Extreme Rainfall (R20mm, RX5day) in Yangtze–Huai, China, in June–July 2016: The Role of ENSO and Anthropogenic Climate Change. *Bull. Am. Meteorol. Soc.* 99, S102–S106. doi:10.1175/BAMS-D-17-0091.1.
Sun, Q., Miao, C., and Duan, Q. (2016). Extreme climate events and agricultural climate indices in China: CMIP5 model evaluation and projections. *Int. J. Climatol.* 36, 43–61. doi:10.1002/joc.4328.
Sun, X. B., Ren, G. Y., Shrestha, A. B., Ren, Y. Y., You, Q. L., Zhan, Y. J., et al. (2017). Changes in extreme temperature events over the Hindu Kush Himalaya during 1961–2015. *Adv. Clim. Chang. Res.* 8, 157–165. doi:10.1016/j.accre.2017.07.001.
Sun, Y., Hu, T., and Zhang, X. (2018a). Substantial increase in heatwave risks in China in a future warmer world. *Earth's Futur.*, (in rev.).
Sun, Y., Hu, T., Zhang, X., Wan, H., Stott, P., and Lu, C. (2018b). Anthropogenic Influence on the Eastern China 2016

Super Cold Surge. *Bull. Am. Meteorol. Soc.* 99, S123–S127. doi:10.1175/BAMS-D-17-0092.1.

Sun, Y., Zhang, X., Zwiers, F. W., Song, L., Wan, H., Hu, T., et al. (2014). Rapid increase in the risk of extreme summer heat in Eastern China. *Nat. Clim. Chang.* 4, 1082–1085. doi:10.1038/nclimate2410.

Sunyer, M. A., Hundecha, Y., Lawrence, D., Madsen, H., Willems, P., Martinkova, M., et al. (2015). Inter-comparison of statistical downscaling methods for projection of extreme precipitation in Europe. *Hydrol. Earth Syst. Sci.* 19, 1827–1847. doi:10.5194/hess-19-1827-2015.

Supari, Tangang, F., Juneng, L., and Aldrian, E. (2017). Observed changes in extreme temperature and precipitation over Indonesia. *Int. J. Climatol.* 37, 1979–1997. doi:10.1002/joc.4829.

Swain, S., and Hayhoe, K. (2015). CMIP5 projected changes in spring and summer drought and wet conditions over North America. *Clim. Dyn.* 44, 2737–2750. doi:10.1007/s00382-014-2255-9.

Swann, A. L. S. (2018). Plants and Drought in a Changing Climate. *Curr. Clim. Chang. Reports* 4, 192–201. doi:10.1007/s40641-018-0097-y.

Swann, A. L. S., Hoffman, F. M., Koven, C. D., and Randerson, J. T. (2016). Plant responses to increasing CO2 reduce estimates of climate impacts on drought severity. *Proc. Natl. Acad. Sci.* 113, 10019–10024. doi:10.1073/pnas.1604581113.

Szeto, K., Gysbers, P., Brimelow, J., and Stewart, R. (2015). The 2014 Extreme Flood on the Southeastern Canadian Prairies. *Bull. Am. Meteorol. Soc.* 96, S20–S24. doi:10.1175/BAMS-D-15-00110.1.

Tabari, H., and Aghajanloo, M.-B. (2013). Temporal pattern of aridity index in Iran with considering precipitation and evapotranspiration trends. *Int. J. Climatol.* 33, 396–409. doi:10.1002/joc.3432.

Tai, A. P. K., Martin, M. V., and Heald, C. L. (2014). Threat to future global food security from climate change and ozone air pollution. *Nat. Clim. Chang.* 4, 817–821. doi:10.1038/nclimate2317.

Tai, A. P. K., and Val Martin, M. (2017). Impacts of ozone air pollution and temperature extremes on crop yields: Spatial variability, adaptation and implications for future food security. *Atmos. Environ.* 169, 11–21. doi:10.1016/j.atmosenv.2017.09.002.

Takahashi, C., Watanabe, M., and Mori, M. (2017). Significant Aerosol Influence on the Recent Decadal Decrease in Tropical Cyclone Activity Over the Western North Pacific. *Geophys. Res. Lett.* 44, 9496–9504. doi:10.1002/2017GL075369.

Takemi, I. T. and K. H. and H. S. and H. S. and N. M. and Y. S. and T., Takayabu, I., Hibino, K., Sasaki, H., Shiogama, H., Mori, N., et al. (2015). Climate change effects on the worst-case storm surge : a case study of Typhoon Haiyan. *Environ. Res. Lett.* 10, 64011. doi:10.1088/1748-9326/10/6/064011.

Talchabhadel, R., Karki, R., Thapa, B. R., Maharjan, M., and Parajuli, B. (2018). Spatio-temporal variability of extreme precipitation in Nepal. *Int. J. Climatol.* 38, 4296–4313. doi:10.1002/joc.5669.

Tamarin-Brodsky, T., and Kaspi, Y. (2017). Enhanced poleward propagation of storms under climate change. *Nat. Geosci.* 10, 908–913. doi:10.1038/s41561-017-0001-8.

Tamarin, T., and Kaspi, Y. (2017). The poleward shift of storm tracks under global warming: A Lagrangian perspective. *Geophys. Res. Lett.* 44, 10,666-10,674. doi:10.1002/2017GL073633.

Tamura, T., Nicholas, W. A., Oliver, T. S. N., and Brooke, B. P. (2018). Coarse-sand beach ridges at Cowley Beach, north-eastern Australia: Their formative processes and potential as records of tropical cyclone history. *Sedimentology* 65, 721–744. doi:10.1111/sed.12402.

Tandon, N. F., Zhang, X., and Sobel, A. H. (2018). Understanding the Dynamics of Future Changes in Extreme Precipitation Intensity. *Geophys. Res. Lett.* 45, 2870–2878. doi:10.1002/2017GL076361.

Taylor, C. M., Belusic, D., Guichard, F., Parker, D. J., Vischel, T., Bock, O., et al. (2017). Frequency of extreme Sahelian storms tripled since 1982 in satellite observations. *Nature* 544, 475–478. doi:10.1038/nature22069.

Taylor, C. M., de Jeu, R. A. M., Guichard, F., Harris, P. P., and Dorigo, W. A. (2012). Afternoon rain more likely over drier soils. *Nature* 489, 423–426. doi:10.1038/nature11377.

Tebaldi, C., and Wehner, M. F. (2018). Benefits of mitigation for future heat extremes under RCP4.5 compared to RCP8.5. *Clim. Change* 146, 349–361. doi:10.1007/s10584-016-1605-5.

Teuling, A. J. (2018). A hot future for European droughts. *Nat. Clim. Chang.* 8, 364–365. doi:10.1038/s41558-018-0154-5.

Thiery, W., Davin, E. L., Lawrence, D. M., Hirsch, A. L., Hauser, M., and Seneviratne, S. I. (2017). Present-day irrigation mitigates heat extremes. *J. Geophys. Res. Atmos.* 122, 1403–1422. doi:10.1002/2016JD025740.

Thiery, W., Davin, E. L., Seneviratne, S. I., Bedka, K., Lhermitte, S., and van Lipzig, N. P. M. (2016). Hazardous thunderstorm intensification over Lake Victoria. *Nat. Commun.* 7, 12786. doi:10.1038/ncomms12786.

Thober, S., Kumar, R., Wanders, N., Marx, A., Pan, M., Rakovec, O., et al. (2018). Multi-model ensemble projections of European river floods and high flows at 1.5, 2, and 3 degrees global warming. *Environ. Res. Lett.* 13, 014003. doi:10.1088/1748-9326/aa9e35.

Thornalley, D. J. R., Oppo, D. W., Ortega, P., Robson, J. I., Brierley, C. M., Davis, R., et al. (2018). Anomalously weak Labrador Sea convection and Atlantic overturning during the past 150 years. *Nature* 556, 227–230. doi:10.1038/s41586-018-0007-4.

Tian, X., Shu, L., Wang, M., and Zhao, F. (2017). The impact of climate change on fire risk in Daxing'anling, China. *J. For. Res.* 28, 997–1006. doi:10.1007/s11676-017-0383-x.

Tijdeman, E., Hannaford, J., and Stahl, K. (2018). Human influences on streamflow drought characteristics in England and Wales. *Hydrol. Earth Syst. Sci.* 22, 1051–1064. doi:10.5194/hess-22-1051-2018.

Tilinina, N., Gulev, S. K., Rudeva, I., and Koltermann, P. (2013). Comparing cyclone life cycle characteristics and their interannual variability in different reanalyses. *J. Clim.* doi:10.1175/JCLI-D-12-00777.1.

Timmermans, B., Wehner, M., Cooley, D., O'Brien, T., and Krishnan, H. (2019). An evaluation of the consistency of extremes in gridded precipitation data sets. *Clim. Dyn.* doi:10.1007/s00382-018-4537-0.

Timmermans, B., Wehner, M., Cooley, D., O'Brien, T., Thibaud, E., and Krishnan, H. (2018). Consistency of extremes in gridded precipitation data. *Rev. Clim. Dyn.*

Tochimoto, E., and Niino, H. (2018). Structure and Environment of Tornado-Spawning Extratropical Cyclones around Japan. *J. Meteorol. Soc. Japan* 96, 355–380. doi:10.2151/jmsj.2018-043.

Tokinaga, H., and Xie, S.-P. (2010). Wave- and Anemometer-Based Sea Surface Wind (WASWind) for Climate Change Analysis. *J. Clim.* 24, 267–285. doi:10.1175/2010JCLI3789.1.

Tramblay, Y., Badi, W., Driouech, F., El Adlouni, S., Neppel, L., and Servat, E. (2012). Climate change impacts on extreme precipitation in Morocco. *Glob. Planet. Change* 82–83, 104–114. doi:10.1016/J.GLOPLACHA.2011.12.002.

Trancoso, R., Larsen, J. R., McVicar, T. R., Phinn, S. R., and McAlpine, C. A. (2017). CO2 -vegetation feedbacks and other climate changes implicated in reducing base flow. *Geophys. Res. Lett.* 44, 2310–2318. doi:10.1002/2017GL072759.

Trenary, L., DelSole, T., Doty, B., and Tippett, M. K. (2015). Was the Cold Eastern US Winter of 2014 Due to Increased Variability? *Bull. Am. Meteorol. Soc.* 96, S15–S19. doi:10.1175/BAMS-D-15-00138.1.

Trenary, L., DelSole, T., Tippett, M. K., and Doty, B. (2016). Extreme Eastern U.S. Winter of 2015 Not Symptomatic of Climate Change. *Bull. Am. Meteorol. Soc.* 97, S31–S35. doi:10.1175/BAMS-D-16-0156.1.

Trenberth, K. E. (1999). Conceptual Framework for Changes of Extremes of the Hydrological Cycle with Climate Change. *Clim. Change* 42, 327–339. doi:10.1023/A:1005488920935.

Trenberth, K. E., Dai, A., van der Schrier, G., Jones, P. D., Barichivich, J., Briffa, K. R., et al. (2014). Global warming and changes in drought. *Nat. Clim. Chang.* 4, 17. Available at: http://dx.doi.org/10.1038/nclimate2067.

Trenberth, K. E., Fasullo, J. T., and Shepherd, T. G. (2015). Attribution of climate extreme events. *Nat. Clim. Chang.* 5, 725–730. doi:10.1038/nclimate2657.

Trenberth, K., Lijing, C., Peter, J., Yongxin, Z., and John, F. (2018). Hurricane Harvey Links to Ocean Heat Content and Climate Change Adaptation. *Earth's Futur.* 6, 730–744. doi:10.1029/2018EF000825.

Trigo, R. M., Añel, J. A., Barriopedro, D., García-Herrera, R., Gimeno, L., Nieto, R., et al. (2013). The Record Winter Drought of 2011 – 12 in the Iberian Peninsula. *Bull. Am. Meteorol. Soc.*, S41–S45.

Trismidianto, and Satyawardhana, H. (2018). Mesoscale Convective Complexes (MCCs) over the Indonesian Maritime Continent during the ENSO events. *IOP Conf. Ser. Earth Environ. Sci.* 149, 12025. Available at: http://stacks.iop.org/1755-1315/149/i=1/a=012025.

Tsuguti, H., Seino, N., Kawase, H., Imada, Y., Nakaegawa, T., and Takayabu, I. (2018). Meteorological overview and mesoscale characteristics of the Heavy Rain Event of July 2018 in Japan. *Landslides* 16, 363–371. doi:10.1007/s10346-018-1098-6.

Türkeş, M., and Erlat, E. (2018). Variability and trends in record air temperature events of Turkey and their associations with atmospheric oscillations and anomalous circulation patterns. *Int. J. Climatol.* 38, 5182–5204. doi:10.1002/joc.5720.

Twardosz, R., and Kossowska-Cezak, U. (2013). Exceptionally hot summers in Central and Eastern Europe (1951-2010). *Theor. Appl. Climatol.* 112, 617–628. doi:10.1007/s00704-012-0757-0.

U.S. Department of Agriculture Economic Research Service (2016). Bulletin of the American Meteorological Society. Available at: http://hdl.handle.net/10261/110100 [Accessed August 21, 2018].

Udall, B., and Overpeck, J. (2017). The twenty-first century Colorado River hot drought and implications for the future. *Water Resour. Res.* 53, 2404–2418. doi:10.1002/2016WR019638.

Uhe, P., Otto, F. E. L., Haustein, K., van Oldenborgh, G. J., King, A. D., Wallom, D. C. H., et al. (2016). Comparison of methods: Attributing the 2014 record European temperatures to human influences. *Geophys. Res. Lett.* 43, 8685–8693. doi:10.1002/2016GL069568.

Uhe, P., Sjoukje, P., Sarah, K., Kasturi, S., Joyce, K., Emmah, M., et al. (2017). Attributing drivers of the 2016 Kenyan drought. *Int. J. Climatol.* 38, e554–e568. doi:10.1002/joc.5389.

Ukkola, A. M., Pitman, A. J., De Kauwe, M. G., Abramowitz, G., Herger, N., Evans, J. P., et al. (2018). Evaluating CMIP5 model agreement for multiple drought metrics. *J. Hydrometeorol.* 19, 969–988. doi:10.1175/JHM-D-17-0099.1.

Ukkola, A. M., Prentice, I. C., Keenan, T. F., Van Dijk, A. I. J. M., Viney, N. R., Myneni, R. B., et al. (2016). Reduced streamflow in water-stressed climates consistent with CO<inf>2</inf>effects on vegetation. *Nat. Clim. Chang.* 6, 75–78. doi:10.1038/nclimate2831.

Um, M.-J., Kim, Y., and Kim, J. (2017). Evaluating historical drought characteristics simulated in CORDEX East Asia against observations. *Int. J. Climatol.* 37, 4643–4655. doi:10.1002/joc.5112.

van den Besselaar, E. J. M., Klein Tank, A. M. G., and Buishand, T. A. (2013). Trends in European precipitation

extremes over 1951–2010. *Int. J. Climatol.* 33, 2682–2689. doi:10.1002/joc.3619.
van den Hurk, B., Meijgaard, E. van, Valk, P. de, Heeringen, K.-J. van, and Gooijer, J. (2015). Analysis of a compounding surge and precipitation event in the Netherlands. *Environ. Res. Lett.* 10. Available at: http://iopscience.iop.org/article/10.1088/1748-9326/10/3/035001/meta.
van der Ent, R. J., Savenije, H. H. G., Schaefli, B., and Steele-Dunne, S. C. (2010). Origin and fate of atmospheric moisture over continents. *Water Resour. Res.* 46. doi:10.1029/2010WR009127.
van der Wiel, K., Kapnick, S. B., van Oldenborgh, G. J., Whan, K., Philip, S., Vecchi, G. A., et al. (2017). Rapid attribution of the August 2016 flood-inducing extreme precipitation in south Louisiana to climate change. *Hydrol. Earth Syst. Sci.* 21, 897–921. doi:10.5194/hess-21-897-2017.
van Dijk, A. I. J. M., Beck, H. E., Crosbie, R. S., de Jeu, R. A. M., Liu, Y. Y., Podger, G. M., et al. (2013). The Millennium Drought in southeast Australia (2001-2009): Natural and human causes and implications for water resources, ecosystems, economy, and society. *Water Resour. Res.* 49, 1040–1057. doi:10.1002/wrcr.20123.
Van Huijgevoort, M. H. J., Hazenberg, P., Van Lanen, H. A. J., Teuling, A. J., Clark, D. B., Folwell, S., et al. (2013). Global multimodel analysis of drought in runofffor the second half of the twentieth century. *J. Hydrometeorol.* 14, 1535–1552. doi:10.1175/JHM-D-12-0186.1.
Van Lanen, H. A. J., Wanders, N., Tallaksen, L. M., and Van Loon, A. F. (2013). Hydrological drought across the world: Impact of climate and physical catchment structure. *Hydrol. Earth Syst. Sci.* 17, 1715–1732. doi:10.5194/hess-17-1715-2013.
Van Loon, A. F., and Laaha, G. (2015). Hydrological drought severity explained by climate and catchment characteristics. *J. Hydrol.* 526, 3–14. doi:10.1016/j.jhydrol.2014.10.059.
van Oldenborgh, G. J., Otto, F. E. L., Haustein, K., and AchutaRao, K. (2016). The Heavy Precipitation Event of December 2015 in Chennai, India. *Bull. Am. Meteorol. Soc.* 97, S87–S91. doi:10.1175/BAMS-D-16-0129.1.
van Oldenborgh, G. J., Philip, S., Kew, S., van Weele, M., Uhe, P., Otto, F., et al. (2018). Extreme heat in India and anthropogenic climate change. *Nat. Hazards Earth Syst. Sci.* 18, 365–381. doi:10.5194/nhess-18-365-2018.
van Oldenborgh, G. J., van der Wiel, K., Sebastian, A., Singh, R., Arrighi, J., Otto, F., et al. (2017). Attribution of extreme rainfall from Hurricane Harvey, August 2017. *Environ. Res. Lett.* 12, 124009. Available at: http://stacks.iop.org/1748-9326/12/i=12/a=124009.
van Oldenborgh, G. J., van Urk, A., and Allen, M. R. (2012). The absence of a role of climate change in the 2011 Thailand floods. *Bull. Amer. Meteor. Soc.* 9, 1047–1049. doi:10.1175/BAMS-D-12-00021.1.
Vautard, R., Yiou, P., Otto, F., Stott, P., Christidis, N., Oldenborgh, G. J. van, et al. (2016). Attribution of human-induced dynamical and thermodynamical contributions in extreme weather events. *Environ. Res. Lett.* 11, 114009. doi:10.1088/1748-9326/11/11/114009.
Veale, L., and Endfield, G. H. (2016). Situating 1816, the 'year without summer', in the UK. *Geogr. J.* 182, 318–330. doi:10.1111/geoj.12191.
Veldkamp, T. I. E., Wada, Y., Aerts, J. C. J. H., Döll, P., Gosling, S. N. N., Liu, J., et al. (2017). Water scarcity hotspots travel downstream due to human interventions in the 20th and 21st century. *Nat. Commun.* 8, 15697. doi:10.1038/ncomms15697.
Vera, C. S., and Díaz, L. (2015). Anthropogenic influence on summer precipitation trends over South America in CMIP5 models. *Int. J. Climatol.* 35, 3172–3177. doi:10.1002/joc.4153.
Vicente-Serrano, S. M. (2016). Foreword: Drought complexity and assessment under climate change conditions. *Cuad. Investig. Geogr.* 42. doi:10.18172/cig.2961.
Vicente-Serrano, S. M., Beguería, S., and Camarero, J. J. (2017a). *Handbook of Drought and Water Scarcity*. , eds. S. Eslamian and F. Eslamian CRC Press doi:10.1201/9781315404219.
Vicente-Serrano, S. M., Lopez-Moreno, J.-I., Beguería, S., Lorenzo-Lacruz, J., Sanchez-Lorenzo, A., García-Ruiz, J. M., et al. (2014). Evidence of increasing drought severity caused by temperature rise in southern Europe. *Environ. Res. Lett.* 9, 044001. doi:10.1088/1748-9326/9/4/044001.
Vicente-Serrano, S. M., López-Moreno, J. I., Correa, K., Avalos, G., Bazo, J., Azorin-Molina, C., et al. (2018). Recent changes in monthly surface air temperature over Peru, 1964-2014. *Int. J. Climatol.* 38, 283–306. doi:10.1002/joc.5176.
Vicente-Serrano, S. M., Zabalza-Martínez, J., Borràs, G., López-Moreno, J. I., Pla, E., Pascual, D., et al. (2017b). Extreme hydrological events and the influence of reservoirs in a highly regulated river basin of northeastern Spain. *J. Hydrol. Reg. Stud.* 12, 13–32. doi:10.1016/j.ejrh.2017.01.004.
Vikhamar-Schuler, D., Isaksen, K., Haugen, J. E., Tømmervik, H., Luks, B., Schuler, T. V., et al. (2016). Changes in Winter Warming Events in the Nordic Arctic Region. *J. Clim.* 29, 6223–6244. doi:10.1175/JCLI-D-15-0763.1.
Villafuerte, M. Q., and Matsumoto, J. (2015). Significant Influences of Global Mean Temperature and ENSO on Extreme Rainfall in Southeast Asia. *J. Clim.* 28, 1905–1919. doi:10.1175/JCLI-D-14-00531.1.
Villarini, G., Smith, J. A., and Vecchi, G. A. (2012). Changing Frequency of Heavy Rainfall over the Central United States. *J. Clim.* 26, 351–357. doi:10.1175/JCLI-D-12-00043.1.
Vogel, M. M., Orth, R., Cheruy, F., Hagemann, S., Lorenz, R., van den Hurk, B. J. J. M., et al. (2017). Regional amplification of projected changes in extreme temperatures strongly controlled by soil moisture-temperature feedbacks. *Geophys. Res. Lett.* 44, 1511–1519. doi:10.1002/2016GL071235.

Vogel, M. M., Zscheischler, J., and Seneviratne, S. I. (2018). Varying soil moisture–atmosphere feedbacks explain divergent temperature extremes and precipitation projections in central Europe. *Earth Syst. Dyn.* 9, 1107–1125. doi:10.5194/esd-9-1107-2018.

Volosciuk, C., Maraun, D., Semenov, V. A., Tilinina, N., Gulev, S. K., and Latif, M. (2016). Rising Mediterranean Sea Surface Temperatures Amplify Extreme Summer Precipitation in Central Europe. *Sci. Rep.* 6, 32450. Available at: https://doi.org/10.1038/srep32450.

von Buttlar, J., Zscheischler, J., Rammig, A., Sippel, S., Reichstein, M., Knohl, A., et al. (2018). Impacts of droughts and extreme-temperature events on gross primary production and ecosystem respiration: a systematic assessment across ecosystems and climate zones. *Biogeosciences* 15, 1293–1318. doi:10.5194/bg-15-1293-2018.

von Storch, H. (2005). "Models of Global and Regional Climate," in *Encyclopedia of Hydrological Sciences* doi:10.1002/0470848944.hsa035.

Vormoor, K., Lawrence, D., Heistermann, M., and Bronstert, A. (2015). Climate change impacts on the seasonality and generation processes of floods – projections and uncertainties for catchments with mixed snowmelt/rainfall regimes. *Hydrol. Earth Syst. Sci.* 19, 913–931. doi:10.5194/hess-19-913-2015.

Vormoor, K., Lawrence, D., Schlichting, L., Wilson, D., and Wong, W. K. (2016). Evidence for changes in the magnitude and frequency of observed rainfall vs. snowmelt driven floods in Norway. *J. Hydrol.* 538, 33–48. doi:10.1016/J.JHYDROL.2016.03.066.

Vose, R. S., Easterling, D. R., Kunkel, K. E., LeGrande, A. N., and Wehner, M. F. (2017). Ch. 6: Temperature Changes in the United States. Climate Science Special Report: Fourth National Climate Assessment, Volume I. , eds. D. J. Wuebbles, D. W. Fahey, K. A. Hibbard, D. J. Dokken, B. C. Stewart, and T. K. Maycock Washington, DC, DC, USA: U.S. Global Change Research Program doi:10.7930/J0N29V45.

Vries, H., Lenderink, G., and Meijgaard, E. (2014). Future snowfall in western and central Europe projected with a high-resolution regional climate model ensemble. *Geophys. Res. Lett.* 41, 4294–4299. doi:10.1002/2014GL059724.

Wada, Y., van Beek, L. P. H., Wanders, N., and Bierkens, M. F. P. (2013). Human water consumption intensifies hydrological drought worldwide. *Environ. Res. Lett.* 8, 034036. doi:10.1088/1748-9326/8/3/034036.

Wahl, T., Jain, S., Bender, J., Meyers, S. D., and Luther, M. E. (2015). Increasing risk of compound flooding from storm surge and rainfall for major US cities. *Nat. Clim. Chang.* 5, 1093. Available at: http://dx.doi.org/10.1038/nclimate2736.

Waliser, D., and Guan, B. (2017). Extreme winds and precipitation during landfall of atmospheric rivers. *Nat. Geosci.* 10, 179. Available at: http://dx.doi.org/10.1038/ngeo2894.

Walsh, K. J. E. E., Camargo, S. J., Vecchi, G. A., Daloz, A. S., Elsner, J., Emanuel, K., et al. (2015). Hurricanes and climate: The U.S. Clivar working group on hurricanes. *Bull. Am. Meteorol. Soc.* 96, 997–1017. doi:10.1175/BAMS-D-13-00242.1.

Walsh, K. J. E., McBride, J. L., Klotzbach, P. J., Balachandran, S., Camargo, S. J., Holland, G., et al. (2016a). Tropical cyclones and climate change. *Wiley Interdiscip. Rev. Clim. Chang.* 7, 65–89. doi:10.1002/wcc.371.

Walsh, K., White, C. J., McInnes, K., Holmes, J., Schuster, S., Richter, H., et al. (2016b). Natural hazards in Australia: storms, wind and hail. *Clim. Change* 139, 55–67. doi:10.1007/s10584-016-1737-7.

Wan, H., Zhang, X., and Zwiers, F. (2018). Human influence on Canadian temperatures. *Clim. Dyn.* doi:10.1007/s00382-018-4145-z.

Wanders, N., and Van Lanen, H. A. J. (2015). Future discharge drought across climate regions around the world modelled with a synthetic hydrological modelling approach forced by three general circulation models. *Nat. Hazards Earth Syst. Sci.* 15, 487–504. doi:10.5194/nhess-15-487-2015.

Wanders, N., and Wada, Y. (2015). Human and climate impacts on the 21st century hydrological drought. *J. Hydrol.* 526, 208–220. doi:10.1016/j.jhydrol.2014.10.047.

Wang, P., Tang, J., Sun, X., Liu, J., and Juan, F. (2018a). Spatiotemporal characteristics of heat waves over China in regional climate simulations within the CORDEX-EA project. *Clim. Dyn.* doi:10.1007/s00382-018-4167-6.

Wang, S.-Y. S., Zhao, L., Yoon, J.-H., Klotzbach, P., and Gillies, R. R. (2018b). Quantitative attribution of climate effects on Hurricane Harvey's extreme rainfall in Texas. *Environ. Res. Lett.* 13, 54014.

Wang, X., Jiang, D., and Lang, X. (2017a). Future extreme climate changes linked to global warming intensity. *Sci. Bull.* 62, 1673–1680. doi:10.1016/j.scib.2017.11.004.

Wang, X. L., Feng, Y., Chan, R., and Isaac, V. (2016). Inter-comparison of extra-tropical cyclone activity in nine reanalysis datasets. *Atmos. Res.* doi:10.1016/j.atmosres.2016.06.010.

Wang, X. L., Trewin, B., Feng, Y., and Jones, D. (2013). Historical changes in Australian temperature extremes as inferred from extreme value distribution analysis. *Geophys. Res. Lett.* 40, 573–578. doi:10.1002/grl.50132.

Wang, Y., Lee, K.-H., Lin, Y., Levy, M., and Zhang, R. (2014). Distinct effects of anthropogenic aerosols on tropical cyclones. *Nat. Clim. Chang.* 4, 368.

Wang, Y., Xie, Y., Dong, W., Ming, Y., Wang, J., and Shen, L. (2017b). Adverse effects of increasing drought on air quality via natural processes. *Atmos. Chem. Phys.* 17, 12827–12843. doi:10.5194/acp-17-12827-2017.

Wang, Y., Zhou, B., Qin, D., Wu, J., Gao, R., and Song, L. (2017c). Changes in mean and extreme temperature and precipitation over the arid region of northwestern China: Observation and projection. *Adv. Atmos. Sci.* 34, 289–

305. doi:10.1007/s00376-016-6160-5.
Wang, Z., Jiang, Y., Wan, H., Yan, J., and Zhang, X. (2017d). Detection and Attribution of Changes in Extreme Temperatures at Regional Scale. *J. Clim.* 30, 7035–7047. doi:10.1175/JCLI-D-15-0835.1.
Wang, Z., Lin, L., Zhang, X., Zhang, H., Liu, L., and Xu, Y. (2017e). Scenario dependence of future changes in climate extremes under 1.5 °C and 2 °C global warming. *Sci. Rep.* 7, 46432. doi:10.1038/srep46432.
Wartenburger, R., Hirschi, M., Donat, M. G., Greve, P., Pitman, A. J., and Seneviratne, S. I. (2017). Changes in regional climate extremes as a function of global mean temperature: an interactive plotting framework. *Geosci. Model Dev. Discuss.*, 1–30. doi:10.5194/gmd-2017-33.
Wasko, C., and Sharma, A. (2017). Global assessment of flood and storm extremes with increased temperatures. *Sci. Rep.* 7, 7945. doi:10.1038/s41598-017-08481-1.
Wasko, C., Sharma, A., and Westra, S. (2016). Reduced spatial extent of extreme storms at higher temperatures. *Geophys. Res. Lett.* 43, 4026–4032. doi:10.1002/2016GL068509.
Watanabe, M., Kamae, Y., and Kimoto, M. (2014). Robust increase of the equatorial Pacific rainfall and its variability in a warmed climate. *Geophys. Res. Lett.* 41, 3227–3232. doi:10.1002/2014GL059692.
Watterson, I. G., J. Bathols, and Heady, C. (2014). What influences the skill of climate models over the continents? *Bull. Amer. Meteor. Soc.* 95, 689–700. doi:http://dx.doi.org/10.1175/BAMS-D-12-00136.1.
Webster, P. J., Toma, V. E., and Kim, H.-M. (2011). Were the 2010 Pakistan floods predictable? *Geophys. Res. Lett.* 38. doi:10.1029/2010GL046346.
Wehner, M. F., Arnold, J. R., Knutson, T., Kunkel, K. E., and LeGrande, A. N. (2017). “Droughts, floods, and wildfires,” in *Climate Science Special Report: Fourth National Climate Assessment, Volume I*, eds. D. J. Wuebbles, D. W. Fahey, K. A. Hibbard, D. J. Dokken, B. C. Stewart, and T. K. Maycock (Washington, DC, USA: U.S. Global Change Research Program), 231–256. doi:10.7930/J0CJ8BNN.
Wehner, M. F., Reed, K. A., Li, F., Prabhat, Bacmeister, J., Chen, C.-T., et al. (2014). The effect of horizontal resolution on simulation quality in the Community Atmospheric Model, CAM5.1. *J. Adv. Model. Earth Syst.* 6, 980–997. doi:10.1002/2013MS000276.
Wehner, M. F., Reed, K. A., Loring, B., Stone, D., and Krishnan, H. (2018a). Changes in tropical cyclones under stabilized 1.5 and 2.0 °C global warming scenarios as simulated by the Community Atmospheric Model under the HAPPI protocols. *Earth Syst. Dyn.* 9, 187–195. doi:10.5194/esd-9-187-2018.
Wehner, M., Prabhat, Reed, K. A., Stone, D., Collins, W. D., and Bacmeister, J. (2015). Resolution Dependence of Future Tropical Cyclone Projections of CAM5.1 in the U.S. CLIVAR Hurricane Working Group Idealized Configurations. *J. Clim.* 28, 3905–3925. doi:10.1175/JCLI-D-14-00311.1.
Wehner, M., Stone, D., Krishnan, H., AchutaRao, K., and Castillo, F. (2016). The Deadly Combination of Heat and Humidity in India and Pakistan in Summer 2015. *Bull. Am. Meteorol. Soc.* 97, S81–S86. doi:10.1175/BAMS-D-16-0145.1.
Wehner, M., Stone, D., Mitchell, D., Shiogama, H., Fischer, E., Graff, L. S., et al. (2018b). Changes in extremely hot days under stabilized 1.5 and 2.0°C global warming scenarios as simulated by the HAPPI multi-model ensemble. *Earth Syst. Dyn.* 9, 299–311. doi:10.5194/esd-9-299-2018.
Wehner, M., Stone, D., Shiogama, H., Wolski, P., Ciavarella, A., Christidis, N., et al. (2018c). Early 21st century anthropogenic changes in extremely hot days as simulated by the C20C+ detection and attribution multi-model ensemble. *Weather Clim. Extrem.* 20, 1–8. doi:10.1016/J.WACE.2018.03.001.
Wehner, M., Zarzycki, C. M., and Patricola, C. (2018d). “Estimating the human influence on tropical cyclone intensity as the climate changes.,” in *Hurricanes and climate change, volume 4*, ed. J. Collins.
Wei, D., Chi, Z., Yong, P., Ruijie, Z., Huicheng, Z., and Ximing, C. (2015). An analytical framework for flood water conservation considering forecast uncertainty and acceptable risk. *Water Resour. Res.* 51, 4702–4726. doi:10.1002/2015WR017127.
Wen, Q. H., Zhang, X., Xu, Y., and Wang, B. (2013). Detecting human influence on extreme temperatures in China. *Geophys. Res. Lett.* 40, 1171–1176. doi:10.1002/grl.50285.
Wesselink, A., Warner, J., Syed, M. A., Chan, F., Tran, D. D., Huq, H., et al. (2015). Trends in flood risk management in deltas around the world: Are we going ‘soft.’ *Int. J. Water Gov.* 4, 25–46.
Westra, S., Alexander, L. V., and Zwiers, F. W. (2013). Global increasing trends in annual maximum daily precipitation. *J. Clim.* 26, 3904–3918. doi:10.1175/JCLI-D-12-00502.1.
Westra, S., Fowler, H. J., Evans, J. P., Alexander, L. V, Berg, P., Johnson, F., et al. (2014). Future changes to the intensity and frequency of short-duration extreme rainfall. *Rev. Geophys.* 52, 522–555. doi:10.1002/2014RG000464.
Westra, S., White, C. J., and Kiem, A. S. (2016). Introduction to the special issue: historical and projected climatic changes to Australian natural hazards. *Clim. Change* 139, 1–19. doi:10.1007/s10584-016-1826-7.
Wetter, O., and Pfister, C. (2013). An underestimated record breaking event – why summer 1540 was likely warmer than 2003. 41–56. doi:10.5194/cp-9-41-2013.
Wetter, O., Pfister, C., Werner, J. P., Zorita, E., Wagner, S., Seneviratne, S. I., et al. (2014). The year-long unprecedented European heat and drought of 1540 - a worst case. *Clim. Change* 125, 349–363. doi:10.1007/s10584-014-1184-2.

Whan, K., Alexander, L. V., Imielska, A., Mcgree, S., Jones, D., Ene, E., et al. (2014). Trends and variability of temperature extremes in the tropical Western Pacific. *Int. J. Climatol.* 34, 2585–2603. doi:10.1002/joc.3861.
Whan, K., Zscheischler, J., Orth, R., Shongwe, M., Rahimi, M., Asare, E. O., et al. (2015). Impact of soil moisture on extreme maximum temperatures in Europe. *Weather Clim. Extrem.* 9, 57–67. doi:10.1016/j.wace.2015.05.001.
Whan, K., and Zwiers, F. (2016). Evaluation of extreme rainfall and temperature over North America in CanRCM4 and CRCM5. *Clim. Dyn.* 46, 3821–3843. doi:10.1007/s00382-015-2807-7.
Wilcox, L. J., Yiou, P., Hauser, M., Lott, F. C., van Oldenborgh, G. J., Colfescu, I., et al. (2018). Multiple perspectives on the attribution of the extreme European summer of 2012 to climate change. *Clim. Dyn.* 50, 3537–3555. doi:10.1007/s00382-017-3822-7.
Wild, M., Gilgen, H., Roesch, A., Ohmura, A., Long, C. N., Dutton, E. G., et al. (2005). From Dimming to Brightening: Decadal Changes in Solar Radiation at Earth's Surface. *Science (80-.).* 308, 847–850. doi:10.1126/science.1103215.
Wilhelm, M., Davin, E. L., and Seneviratne, S. I. (2015). Climate engineering of vegetated land for hot extremes mitigation: An Earth system model sensitivity study. *J. Geophys. Res. Atmos.* 120, 2612–2623. doi:10.1002/2014JD022293.
Willems, P. (2013). Multidecadal oscillatory behaviour of rainfall extremes in Europe. *Clim. Change* 120, 931–944. doi:10.1007/s10584-013-0837-x.
Willett, K. M., Dunn, R. J. H., Thorne, P. W., Bell, S., de Podesta, M., Parker, D. E., et al. (2014). HadISDH land surface multi-variable humidity and temperature record for climate monitoring. *Clim. Past* 10, 1983–2006.
Willison, J., Robinson, W. A., and Lackmann, G. M. (2013). The Importance of Resolving Mesoscale Latent Heating in the North Atlantic Storm Track. *J. Atmos. Sci.* 70, 2234–2250. doi:10.1175/JAS-D-12-0226.1.
Wirth, S. B., Gilli, A., Simonneau, A., Ariztegui, D., Vannière, B., Glur, L., et al. (2013). A 2000 year long seasonal record of floods in the southern European Alps. *Geophys. Res. Lett.* 40, 4025–4029. doi:10.1002/grl.50741.
Wobus, C., Gutmann, E., Jones, R., Rissing, M., Mizukami, N., Lorie, M., et al. (2017). Climate change impacts on flood risk and asset damages within mapped 100-year floodplains of the contiguous United States. *Nat. Hazards Earth Syst. Sci.* 17, 2199–2211. doi:10.5194/nhess-17-2199-2017.
Woldemichael , Abel, T., Hossain, F., Pielke, R., and Beltrán-Przekurat, A. (2012). Understanding the impact of dam-triggered land use/land cover change on the modification of extreme precipitation. *Water Resour. Res.* 48. doi:10.1029/2011WR011684.
Wolski, P., Stone, D., Tadross, M., Wehner, M., and Hewitson, B. (2014). Attribution of floods in the Okavango basin, Southern Africa. *J. Hydrol.* 511, 350–358. doi:10.1016/j.jhydrol.2014.01.055.
Wolter, K., Eischeid, J. K., Quan, X.-W., Chase, T. n., Hoerling, M., Dole, R. M., et al. (2015). How Unusual was the Cold Winter of 2013/14 in the Upper Midwest? *Bull. Am. Meteorol. Soc.* 96, S10–S14. doi:10.1175/BAMS-D-15-00126.1.
Woodruff, J. D., Irish, J. L., and Camargo, S. J. (2013). Coastal flooding by tropical cyclones and sea-level rise. *Nature* 504, 44. Available at: https://doi.org/10.1038/nature12855.
Woodward, C., Shulmeister, J., Larsen, J., Jacobsen, G. E., and Zawadzki, A. (2014). The hydrological legacy of deforestation on global wetlands. *Science (80-.).* 346, 844–847. doi:10.1126/science.1260510.
Woollings, T., Barriopedro, D., Methven, J., Son, S. W., Martius, O., Harvey, B., et al. (2018). Blocking and its Response to Climate Change. *Curr. Clim. Chang. Reports* 4, 287–300. doi:10.1007/s40641-018-0108-z.
Wooster, M. J., Perry, G. L. W., and Zoumas, A. (2012). Fire, drought and El Niño relationships on Borneo (Southeast Asia) in the pre-MODIS era (1980-2000). *Biogeosciences* 9, 317–340. doi:10.5194/bg-9-317-2012.
Wu, S.-Y. (2015). Changing characteristics of precipitation for the contiguous United States. *Clim. Change* 132, 677–692. doi:10.1007/s10584-015-1453-8.
Wu, W., McInnes, K., O'Grady, J., Hoeke, R., Leonard, M., and Westra, S. (2018). Mapping Dependence Between Extreme Rainfall and Storm Surge. *J. Geophys. Res. Ocean.* 123, 2461–2474. doi:10.1002/2017JC013472.
Wu, Y., and Polvani, L. M. (2017). Recent Trends in Extreme Precipitation and Temperature over Southeastern South America: The Dominant Role of Stratospheric Ozone Depletion in the CESM Large Ensemble. *J. Clim.* 30, 6433–6441. doi:10.1175/JCLI-D-17-0124.1.
Xu, Y., Wu, J., Shi, Y., Zhou, B., Li, R., and Wu, J. (2016). Change in Extreme Climate Events over China Based on CMIP5 Change in Extreme Climate Events over China Based on CMIP5. *Atmos. Ocean. Sci. Lett.* 8, 185–192. doi:10.3878/AOSL20150006.
Xu, Y., Zhou, B. T., Wu, J., Han, Z. Y., Zhang, Y. X., and Wu, J. (2017). Asian climate change under 1.5–4 °C warming targets. *Adv. Clim. Chang. Res.* 8, 99–107. doi:10.1016/j.accre.2017.05.004.
Xue, M., Schleif, J., Kong, F., Thomas, K. W., Wang, Y., and Zhu, K. (2013). Track and Intensity Forecasting of Hurricanes: Impact of Convection-Permitting Resolution and Global Ensemble Kalman Filter Analysis on 2010 Atlantic Season Forecasts. *Weather Forecast.* 28, 1366–1384. doi:10.1175/WAF-D-12-00063.1.
Yamada, Y., Kodama, C., Satoh, M., Nakano, M., Nasuno, T., and Sugi, M. (2019). High-resolution Ensemble Simulations of Intense Tropical Cyclones and Their Internal Variability During the El Ninos of 1997 and 2015. *Geophys. Res. Lett. Rev.* in review.
Yamada, Y., Oouchi, K., Satoh, M., Tomita, H., and Yanase, W. (2010). Projection of changes in tropical cyclone

activity and cloud height due to greenhouse warming: global cloud-system-resolving approach. *Geophys Res Lett* 37.
Yamada, Y., Satoh, M., Sugi, M., Kodama, C., Noda, A. T., Nakano, M., et al. (2017). Response of Tropical Cyclone Activity and Structure to Global Warming in a High-Resolution Global Nonhydrostatic Model. *J. Clim.* 30, 9703–9724. doi:10.1175/JCLI-D-17-0068.1.
Yang, C., Li, L., and Xu, J. (2018a). Changing temperature extremes based on CMIP5 output via semi-parametric quantile regression approach. *Int. J. Climatol.* 38, 3736–3748. doi:10.1002/joc.5524.
Yang, S.-H., Kang, N.-Y., Elsner, J. B., and Chun, Y. (2018b). Influence of Global Warming on Western North Pacific Tropical Cyclone Intensities during 2015. *J. Clim.* 31, 919–925. doi:10.1175/JCLI-D-17-0143.1.
Yang, S., Feng, J., Dong, W., and Chou, J. (2014). Analyses of extreme climate events over china based on CMIP5 historical and future simulations. *Adv. Atmos. Sci.* 31, 1209–1220. doi:10.1007/s00376-014-3119-2.
Yang, Y., Roderick, M. L., Zhang, S., McVicar, T. R., and Donohue, R. J. (2019). Hydrologic implications of vegetation response to elevated CO2 in climate projections. *Nat. Clim. Chang.* 9, 44–48. doi:10.1038/s41558-018-0361-0.
Yang, Y., Zhang, S., McVicar, T. R., Beck, H. E., Zhang, Y., and Liu, B. (2018c). Disconnection Between Trends of Atmospheric Drying and Continental Runoff. *Water Resour. Res.* 54, 4700–4713. doi:10.1029/2018WR022593.
Ye, S., Li, H.-Y., Leung, L. R., Guo, J., Ran, Q., Demissie, Y., et al. (2017). Understanding flood seasonality and its temporal shifts within the contiguous United States. *J. Hydrometeorol.* 18, 1997–2009. doi:10.1175/JHM-D-16-0207.1.
Yettella, V., and Kay, J. E. (2017). How will precipitation change in extratropical cyclones as the planet warms? Insights from a large initial condition climate model ensemble. *Clim. Dyn.* 49, 1765–1781. doi:10.1007/s00382-016-3410-2.
Yin, H., Donat, M. G., Alexander, L. V, and Sun, Y. (2015). Multi-dataset comparison of gridded observed temperature and precipitation extremes over China. *Int. J. Climatol.* 35, 2809–2827. doi:10.1002/joc.4174.
Yin, H., and Sun, Y. (2018). Detection of Anthropogenic Influence on Fixed Threshold Indices of Extreme Temperature. *J. Clim.* 31, 6341–6352. doi:10.1175/JCLI-D-17-0853.1.
Yin, H., Sun, Y., Wan, H., Zhang, X., and Lu, C. (2017). Detection of anthropogenic influence on the intensity of extreme temperatures in China. *Int. J. Climatol.* 37, 1229–1237. doi:10.1002/joc.4771.
Yiou, P., Jézéquel, A., Naveau, P., Otto, F. E. L., Vautard, R., and Vrac, M. (2017). A statistical framework for conditional extreme event attribution. *Adv. Stat. Climatol. Meteorol. Oceanogr.* 3, 17–31. doi:10.5194/ascmo-3-17-2017.
Yoshida, K., Sugi, M., Mizuta, R., Murakami, H., and Ishii, M. (2017). Future Changes in Tropical Cyclone Activity in High-Resolution Large-Ensemble Simulations. *Geophys. Res. Lett.* 44, 9910–9917. doi:10.1002/2017GL075058.
You, Q.-L., Ren, G.-Y., Zhang, Y.-Q., Ren, Y.-Y., Sun, X.-B., Zhan, Y.-J., et al. (2017). An overview of studies of observed climate change in the Hindu Kush Himalayan (HKH) region. *Adv. Clim. Chang. Res.* 8, 141–147. doi:10.1016/J.ACCRE.2017.04.001.
You, Q., Kang, S., Aguilar, E., and Yan, Y. (2008). Changes in daily climate extremes in the eastern and central Tibetan Plateau during 1961-2005. *J. Geophys. Res. Atmos.* 113, 1–17. doi:10.1029/2007JD009389.
Yu, E., Sun, J., Chen, H., and Xiang, W. (2015). Evaluation of a high-resolution historical simulation over China: climatology and extremes. *Clim. Dyn.* 45, 2013–2031. doi:10.1007/s00382-014-2452-6.
Yu, L., Zhong, S., Heilman, W. E., and Bian, X. (2018). Trends in seasonal warm anomalies across the contiguous United States: Contributions from natural climate variability. *Sci. Rep.* 8, 1–13. doi:10.1038/s41598-018-21817-9.
Yu, M., Li, Q., Hayes, M. J., Svoboda, M. D., and Heim, R. R. (2014). Are droughts becoming more frequent or severe in China based on the Standardized Precipitation Evapotranspiration Index: 1951-2010? *Int. J. Climatol.* 34, 545–558. doi:10.1002/joc.3701.
Yuan, X., Wang, L., and Wood, E. F. (2018a). Anthropogenic Intensification of Southern African Flash Droughts as Exemplified by the 2015/16 Season. *Bull. Am. Meteorol. Soc.* 99, S86–S90. doi:10.1175/BAMS-D-17-0077.1.
Yuan, X., Wang, S., and Hu, Z.-Z. (2018b). Do Climate Change and El Niño Increase Likelihood of Yangtze River Extreme Rainfall? *Bull. Am. Meteorol. Soc.* 99, S113–S117. doi:10.1175/BAMS-D-17-0089.1.
Zahid, M., and Rasul, G. (2012). Changing trends of thermal extremes in Pakistan. *Clim. Change*. doi:10.1007/s10584-011-0390-4.
Zappa, G., Shaffrey, L. C., Hodges, K. I., Sansom, P. G., and Stephenson, D. B. (2013a). A multimodel assessment of future projections of north atlantic and european extratropical cyclones in the CMIP5 climate models. *J. Clim.* 26, 5846–5862. doi:10.1175/JCLI-D-12-00573.1.
Zappa, G., Shaffrey, L., and Hodges, K. (2013b). The ability of CMIP5 models to simulate North Atlantic extratropical cyclones. *J. Clim.* doi:10.1175/JCLI-D-12-00501.1.
Zappa, G., and Shepherd, T. G. (2017). Storylines of Atmospheric Circulation Change for European Regional Climate Impact Assessment. *J. Clim.* 30, 6561–6577. doi:10.1175/JCLI-D-16-0807.1.
Zhan, R., Chen, B., and Ding, Y. (2018). Impacts of SST anomalies in the Indian-Pacific basin on Northwest Pacific tropical cyclone activities during three super El Niño years. *J. Oceanol. Limnol.* 36, 20–32. doi:10.1007/s00343-018-6321-8.

Zhang, D., Zhang, Q., Qiu, J., Bai, P., Liang, K., and Li, X. (2018a). Intensification of hydrological drought due to human activity in the middle reaches of the Yangtze River, China. *Sci. Total Environ.* 637–638, 1432–1442. doi:10.1016/j.scitotenv.2018.05.121.

Zhang, J., Gao, Y., Luo, K., Leung, L. R., Zhang, Y., Wang, K., et al. (2018b). Impacts of compound extreme weather events on ozone in the present and future. *Atmos. Chem. Phys.* 18, 9861–9877. doi:10.5194/acp-18-9861-2018.

Zhang, L., Rechtman, T., Karnauskas , Kristopher, B., Li, L., Donnelly, Jeffrey, P., and Kossin , James, P. (2017a). Longwave emission trends over Africa and implications for Atlantic hurricanes. *Geophys. Res. Lett.* 44, 9075–9083. doi:10.1002/2017GL073869.

Zhang, Q., Gu, X., Singh, V. P., Xiao, M., and Xu, C.-Y. (2015a). Flood frequency under the influence of trends in the Pearl River basin, China: Changing patterns, causes and implications. *Hydrol. Process.* 29, 1406–1417. doi:10.1002/hyp.10278.

Zhang, R., Su, F., Jiang, Z., Gao, X., Guo, D., Ni, J., et al. (2015b). An overview of projected climate and environmental changes across the Tibetan Plateau in the 21st century. *Chinese Sci. Bull.* doi:10.1360/N972014-01296.

Zhang, W., Vecchi, G. A., Murakami, H., Delworth, T. L., Paffendorf, K., Jia, L., et al. (2016a). Influences of Natural Variability and Anthropogenic Forcing on the Extreme 2015 Accumulated Cyclone Energy in the Western North Pacific. *Bull. Am. Meteorol. Soc.* 97, S131–S135. doi:10.1175/BAMS-D-16-0146.1.

Zhang, W., Vecchi, G. A., Murakami, H., Villarini, G., and Jia, L. (2016b). The Pacific meridional mode and the occurrence of tropical Cyclones in the western North Pacific. *J. Clim.* 29, 381–398. doi:10.1175/JCLI-D-15-0282.1.

Zhang, W., Villarini, G., Vecchi, G. A., and Smith, J. A. (2018c). Urbanization exacerbated the rainfall and flooding caused by hurricane Harvey in Houston. *Nature* 563, 384–388. doi:10.1038/s41586-018-0676-z.

Zhang, X., Wan, H., Zwiers, F. W., Hegerl, G. C., and Min, S.-K. (2013). Attributing intensification of precipitation extremes to human influence. *Geophys. Res. Lett.* 40, 5252–5257. doi:10.1002/grl.51010.

Zhang, X., Zwiers, F. W., Li, G., Wan, H., and Cannon, A. J. (2017b). Complexity in estimating past and future extreme short-duration rainfall. *Nat. Geosci.* 10, 255. Available at: http://dx.doi.org/10.1038/ngeo2911.

Zhang, Y., Peña-Arancibia, J. L., McVicar, T. R., Chiew, F. H. S., Vaze, J., Liu, C., et al. (2016c). Multi-decadal trends in global terrestrial evapotranspiration and its components. *Sci. Rep.* 6, 19124. doi:10.1038/srep19124.

Zhang, Y., Wang, H., Sun, J., and Drange, H. (2010). Changes in the tropical cyclone genesis potential index over the western north pacific in the SRES A2 scenario. *Adv. Atmos. Sci.* 27, 1246–1258. doi:10.1007/s00376-010-9096-1.

Zhang, Y., You, Q., Chen, C., and Li, X. (2017c). Flash droughts in a typical humid and subtropical basin: A case study in the Gan River Basin, China. *J. Hydrol.* 551, 162–176. doi:10.1016/j.jhydrol.2017.05.044.

Zhao, L., Lee, X., Smith, R. B., and Oleson, K. (2014). Strong contributions of local background climate to urban heat islands. *Nature* 511, 216–219. doi:10.1038/nature13462.

Zhao, M., and Held, I. M. (2011). TC-Permitting GCM Simulations of Hurricane Frequency Response to Sea Surface Temperature Anomalies Projected for the Late-Twenty-First Century. *J. Clim.* 25, 2995–3009. doi:10.1175/JCLI-D-11-00313.1.

Zhao, M., Held, I. M., Lin, S. J., and Vecchi, G. A. (2009). Simulations of global hurricane climatology, interannual variability, and response to global warming using a 50-km resolution GCM. *J. Clim.* 22, 6653–6678. doi:10.1175/2009JCLI3049.1.

Zhao, T., and Dai, A. (2015). The magnitude and causes of global drought changes in the twenty-first century under a low-moderate emissions scenario. *J. Clim.* 28, 4490–4512. doi:10.1175/JCLI-D-14-00363.1.

Zhao, T., and Dai, A. (2017). Uncertainties in historical changes and future projections of drought. Part II: model-simulated historical and future drought changes. *Clim. Change* 144, 535–548. doi:10.1007/s10584-016-1742-x.

Zheng, F., Westra, S., and Sisson, S. A. (2013). Quantifying the dependence between extreme rainfall and storm surge in the coastal zone. *J. Hydrol.* 505, 172–187. doi:10.1016/j.jhydrol.2013.09.054.

Zhou, B., Wen, Q. H., Xu, Y., Song, L., and Zhang, X. (2014a). Projected changes in temperature and precipitation extremes in China by the CMIP5 multimodel ensembles. *J. Clim.* 27, 6591–6611. doi:10.1175/JCLI-D-13-00761.1.

Zhou, B., Xu, Y., Wu, J., Dong, S., and Shi, Y. (2016). Changes in temperature and precipitation extreme indices over China: Analysis of a high-resolution grid dataset. *Int. J. Climatol.* 36, 1051–1066. doi:10.1002/joc.4400.

Zhou, C., Wang, K., and Qi, D. (2017). 21. Attribution of the July 2016 Extreme Precipitation Event Over China's Wuhang. *Bull. Am. Meteorol. Soc.* 99, 107–111. doi:10.1175/BAMS-D-17-0090.1.

Zhou, D., Zhao, S., Liu, S., Zhang, L., and Zhu, C. (2014b). Surface urban heat island in China's 32 major cities: Spatial patterns and drivers. *Remote Sens. Environ.* 152, 51–61. doi:10.1016/j.rse.2014.05.017.

Zhu, J., Huang, G., Wang, X., Cheng, G., and Wu, Y. (2018). High-resolution projections of mean and extreme precipitations over China through PRECIS under RCPs. *Clim. Dyn.* 50, 4037–4060. doi:10.1007/s00382-017-3860-1.

Zilli, M. T., Carvalho, L. M. V., Liebmann, B., and Silva Dias, M. A. (2017). A comprehensive analysis of trends in extreme precipitation over southeastern coast of Brazil. *Int. J. Climatol.* 37, 2269–2279. doi:10.1002/joc.4840.

Zipser, E. J., Cecil, D. J., Liu, C., Nesbitt, S. W., and Yorty, D. P. (2006). Where are the most: Intense thunderstorms on

Earth? *Bull. Am. Meteorol. Soc.* 87, 1057–1071. doi:10.1175/BAMS-87-8-1057.
Zolina, O., Simmer, C., Belyaev, K., Gulev, S. K., and Koltermann, P. (2013). Changes in the duration of European wet and dry spells during the last 60 years. *J. Clim.* 26, 2022–2047. doi:10.1175/JCLI-D-11-00498.1.
Zscheischler, J., Fischer, E. M., and Lange, S. (2018a). The effect of bias adjustment on impact modeling. *Earth Syst. Dyn. Discuss.*, 1–17. doi:10.5194/esd-2018-68.
Zscheischler, J., Fischer, E. M., and Lange, S. (2019). The effect of univariate bias adjustment on multivariate hazard estimates. *Earth Syst. Dyn.* 10, 31–43. doi:10.5194/esd-10-31-2019.
Zscheischler, J., Michalak, A. M., Schwalm, C., Mahecha, M. D., Huntzinger, D. N., Reichstein, M., et al. (2014). Impact of large-scale climate extremes on biospheric carbon fluxes: An intercomparison based on MsTMIP data. *Global Biogeochem. Cycles* 28, 585–600. doi:10.1002/2014GB004826.
Zscheischler, J., and Seneviratne, S. I. (2017). Dependence of drivers affects risks associated with compound events. *Sci. Adv.* 3. Available at: http://advances.sciencemag.org/content/3/6/e1700263.abstract.
Zscheischler, J., Westra, S., van den Hurk, B. J. J. M., Seneviratne, S. I., Ward, P. J., Pitman, A., et al. (2018b). Future climate risk from compound events. *Nat. Clim. Chang.* 8, 469–477. doi:10.1038/s41558-018-0156-3.
Zulkafli, Z., Buytaert, W., Manz, B., Rosas, C. V., Willems, P., Lavado-Casimiro, W., et al. (2016). Projected increases in the annual flood pulse of the Western Amazon. *Environ. Res. Lett.* 11, 014013. doi:10.1088/1748-9326/11/1/014013.

Figures

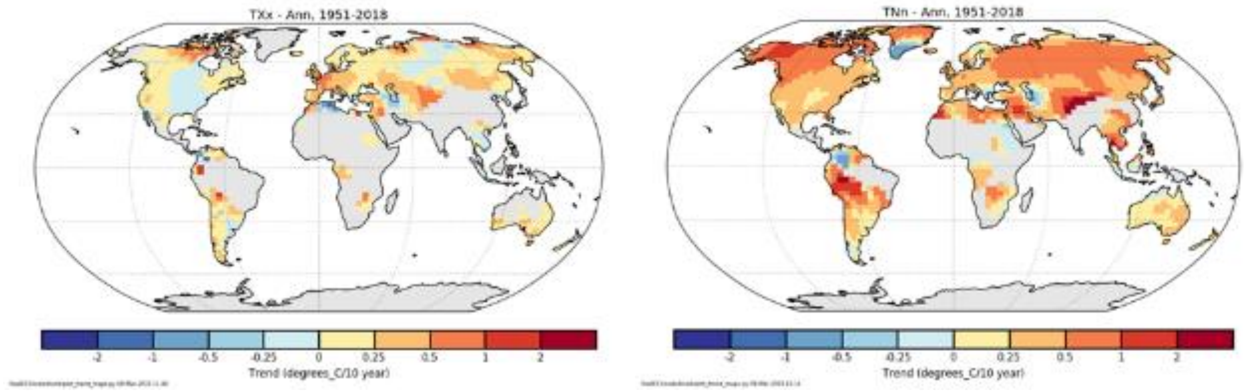

Figure 11.1: Linear trends over 1951-2018 in the annual maximum daily maximum temperature (TXx, 11.1a (left)) and the annual minimum daily minimum temperature (TNn, 11.1b (right)) from the beta version of the most recent HadEX3 data set. Units: °C/decade.

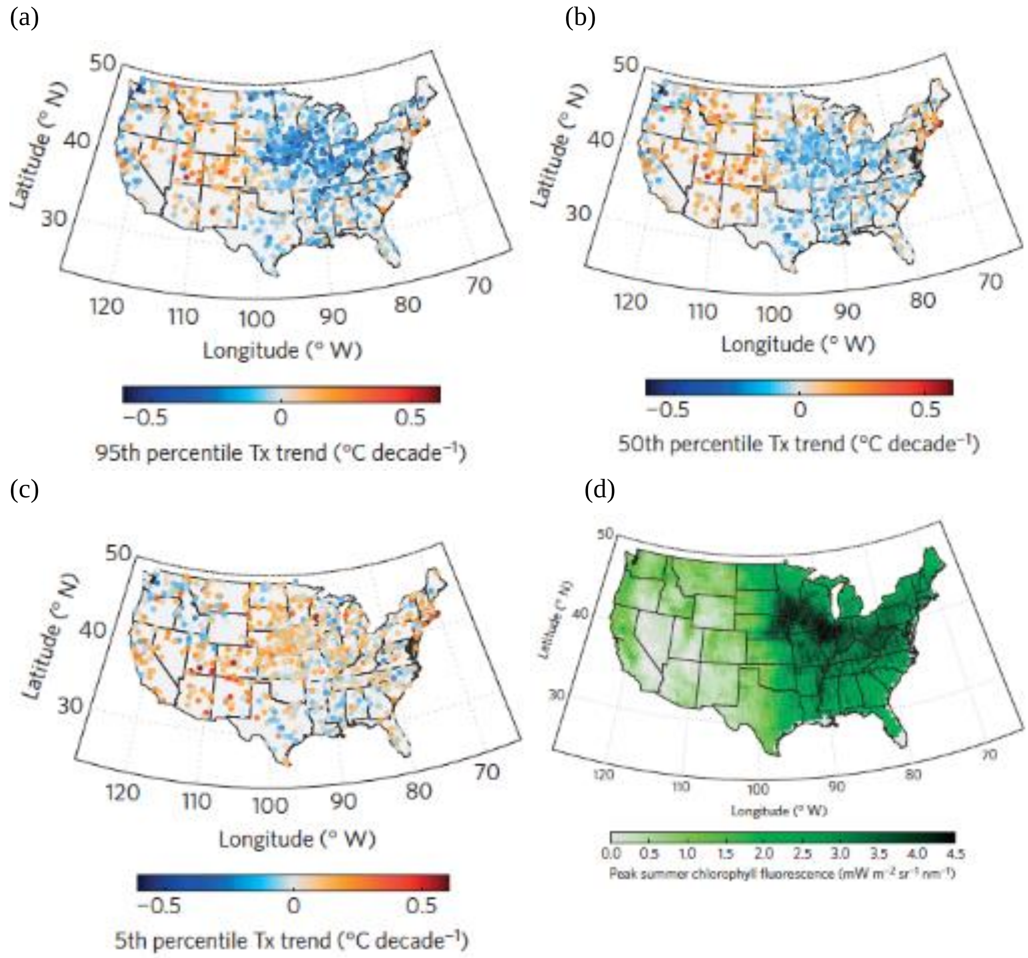

Figure 11.2: Centennial trend towards cooler daily maximum temperatures during the summer in the US Midwest: a) 95th percentile Tx trends (C°/decade), b) 50th percentile Tx trend (°C/decade), c) 5th percentile Tx trend (°C/decade); d) peak rates of summer chlorophyll fluorescence, a measure of plant activity. (from (Mueller et al., 2016).

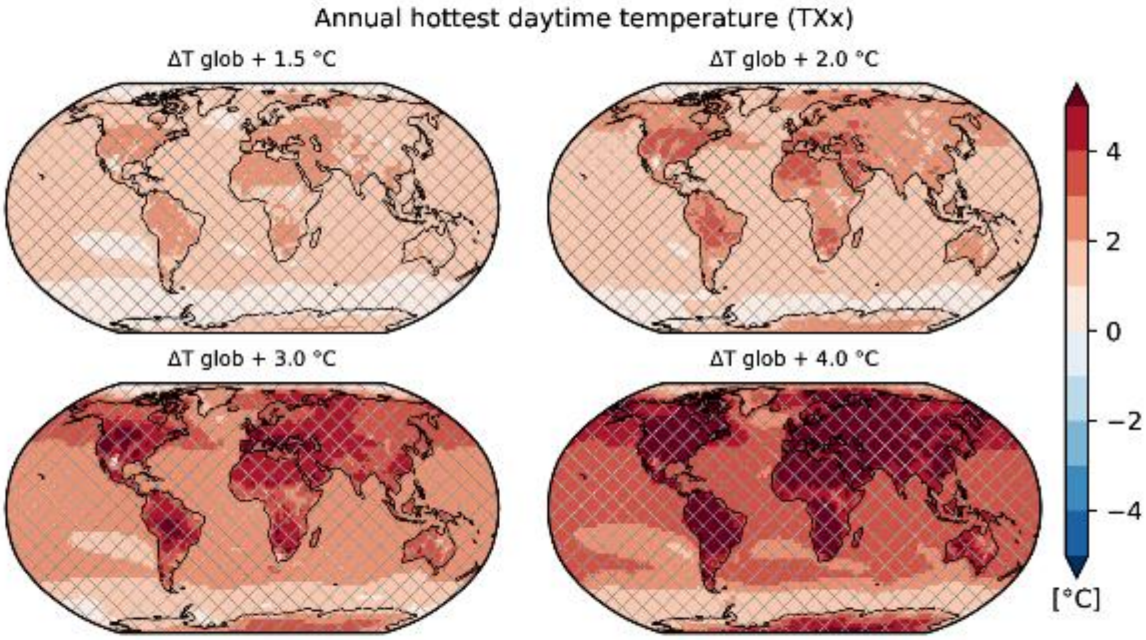

Figure 11.3: Projected changes in temperature of annual hottest daytime temperature (TXx) for projections at 1.5°C, 2°C, 3°C and 4°C of global warming compared to pre-industrial conditions (1851-1900), using empirical scaling relationship based on transient CMIP5 simulations.Cross-hatching highlights areas where at least two-thirds of the models agree on the sign of change as a measure of robustness.

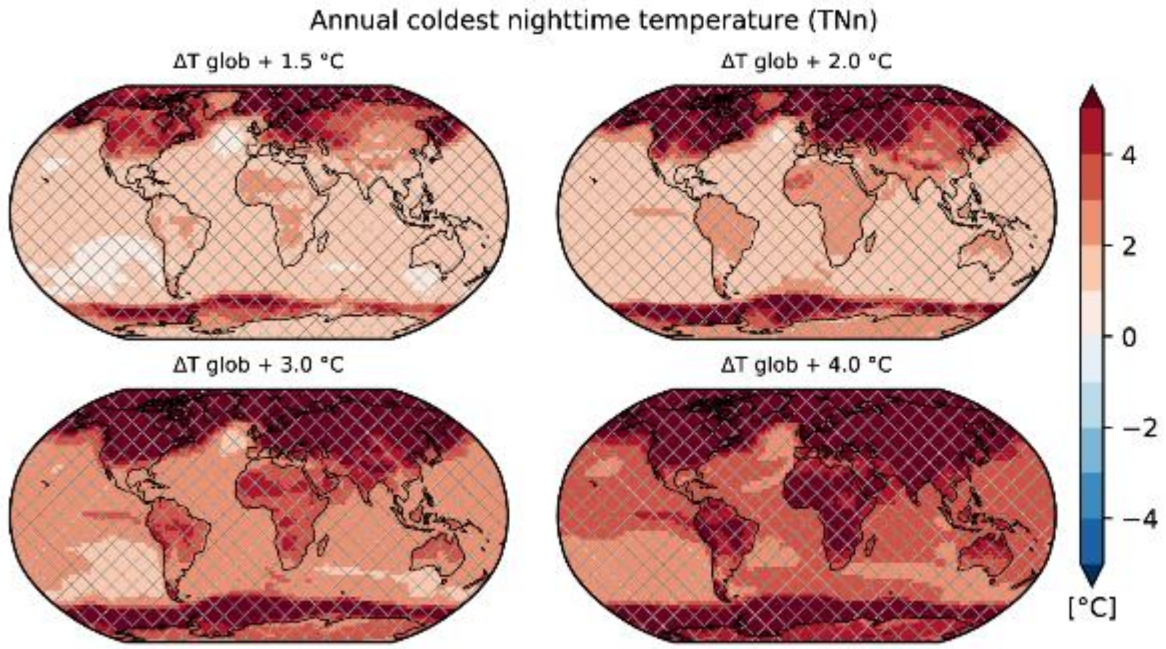

Figure 11.4: Projected changes in temperature of annual coldest night-time temperature (TNn) for projections at 1.5°C, 2°C, 3°C and 4°C of global warming compared to pre-industrial conditions (1851-1900), using empirical scaling relationship based on transient CMIP5 simulations.Cross-hatching highlights areas where at least two-thirds of the models agree on the sign of change as a measure of robustness.

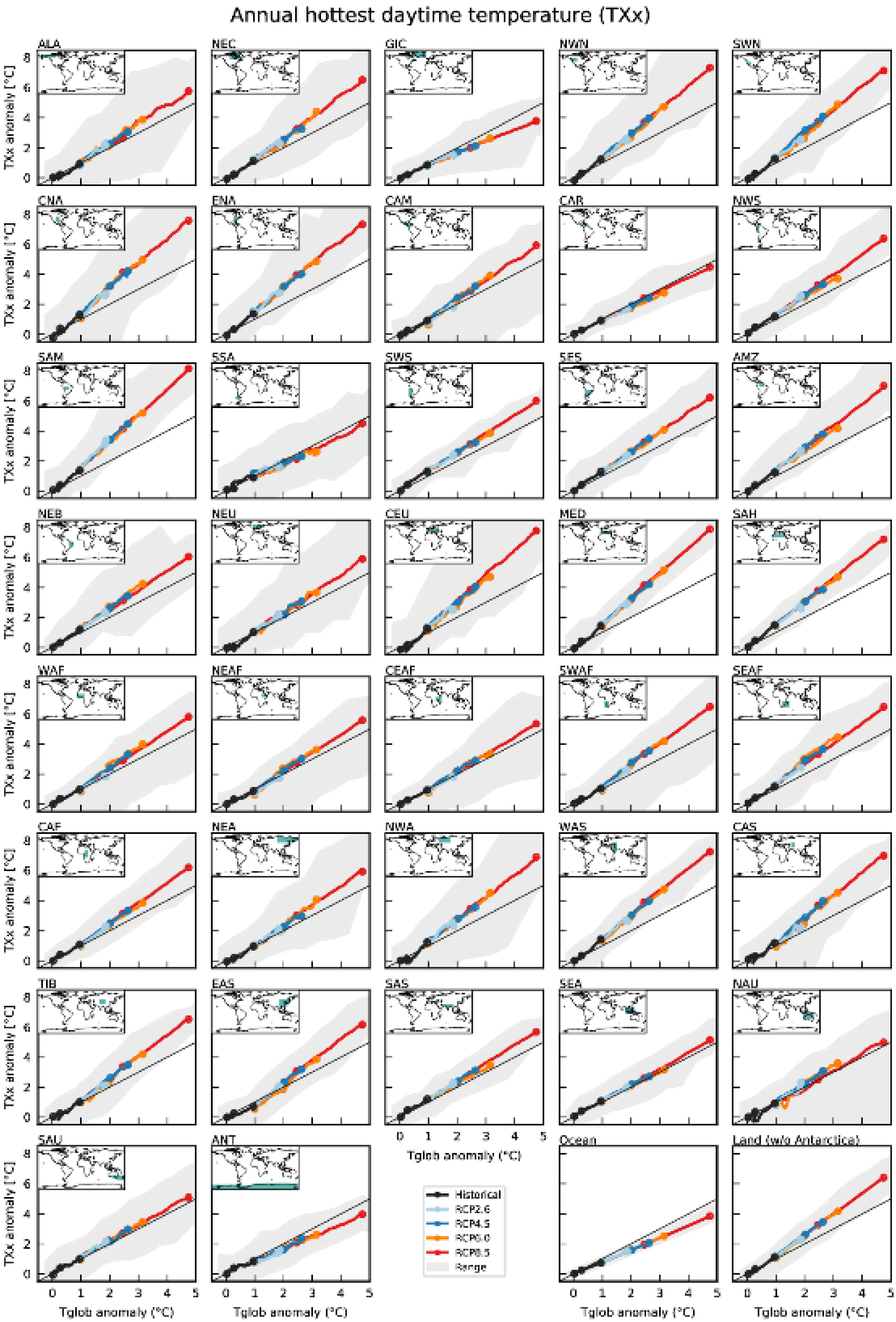

Figure 11.5: Projected regional changes in temperature of annual hottest daytime temperature (TXx) compared to pre-industrial conditions (1851-1900) as function of mean global warming, using empirical scaling relationship based on transient CMIP5 simulations. Analyses for 37 AR6 regions, the global ocean and the global land.

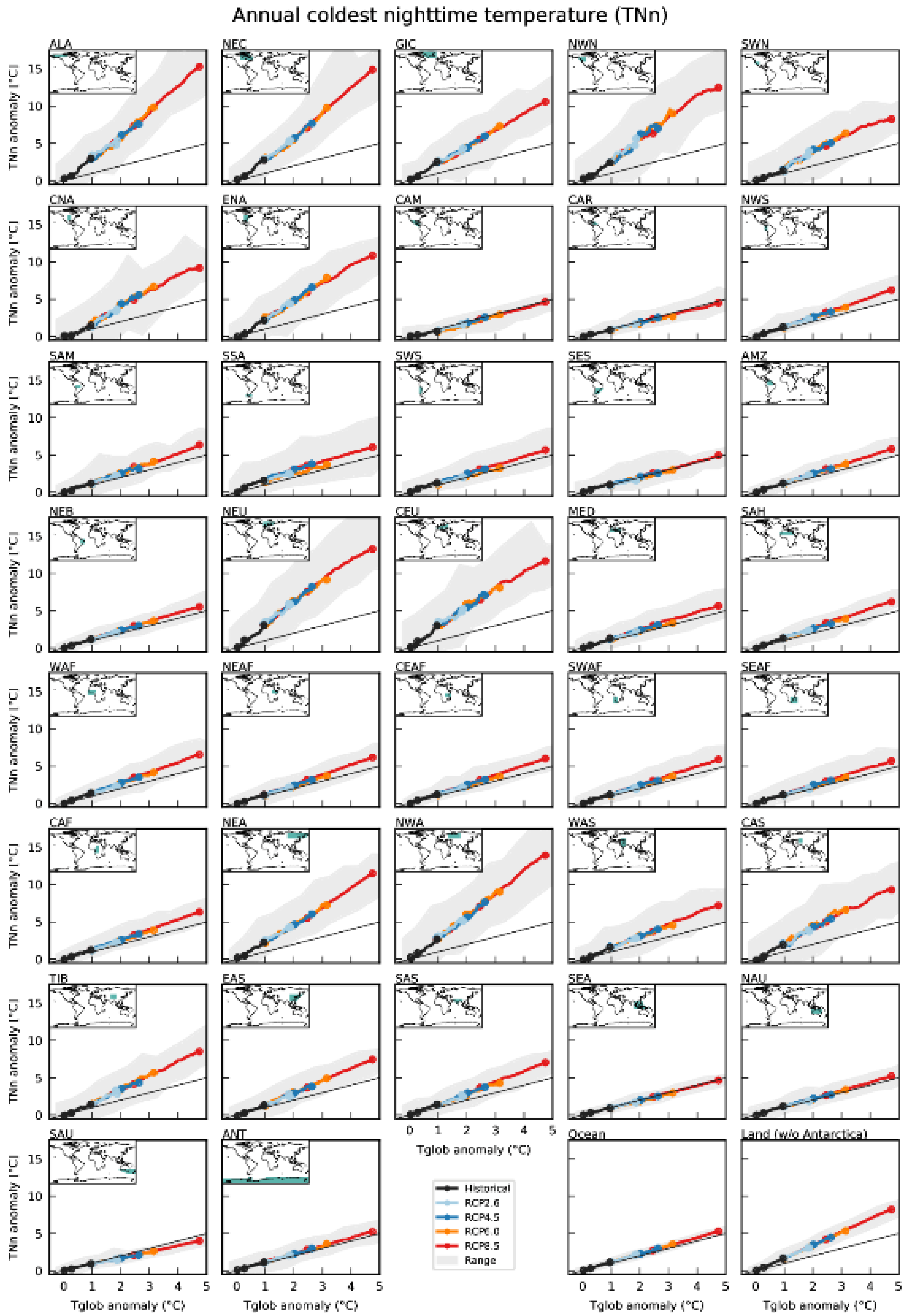

Figure 11.6: Projected regional changes in temperature of annual coldest nighttime temperature (TNn) compared to pre-industrial conditions (1851-1900) as function of mean global warming, using empirical scaling relationship based on transient CMIP5 simulations. Analyses for 37 AR6 regions, the global ocean and the global land.

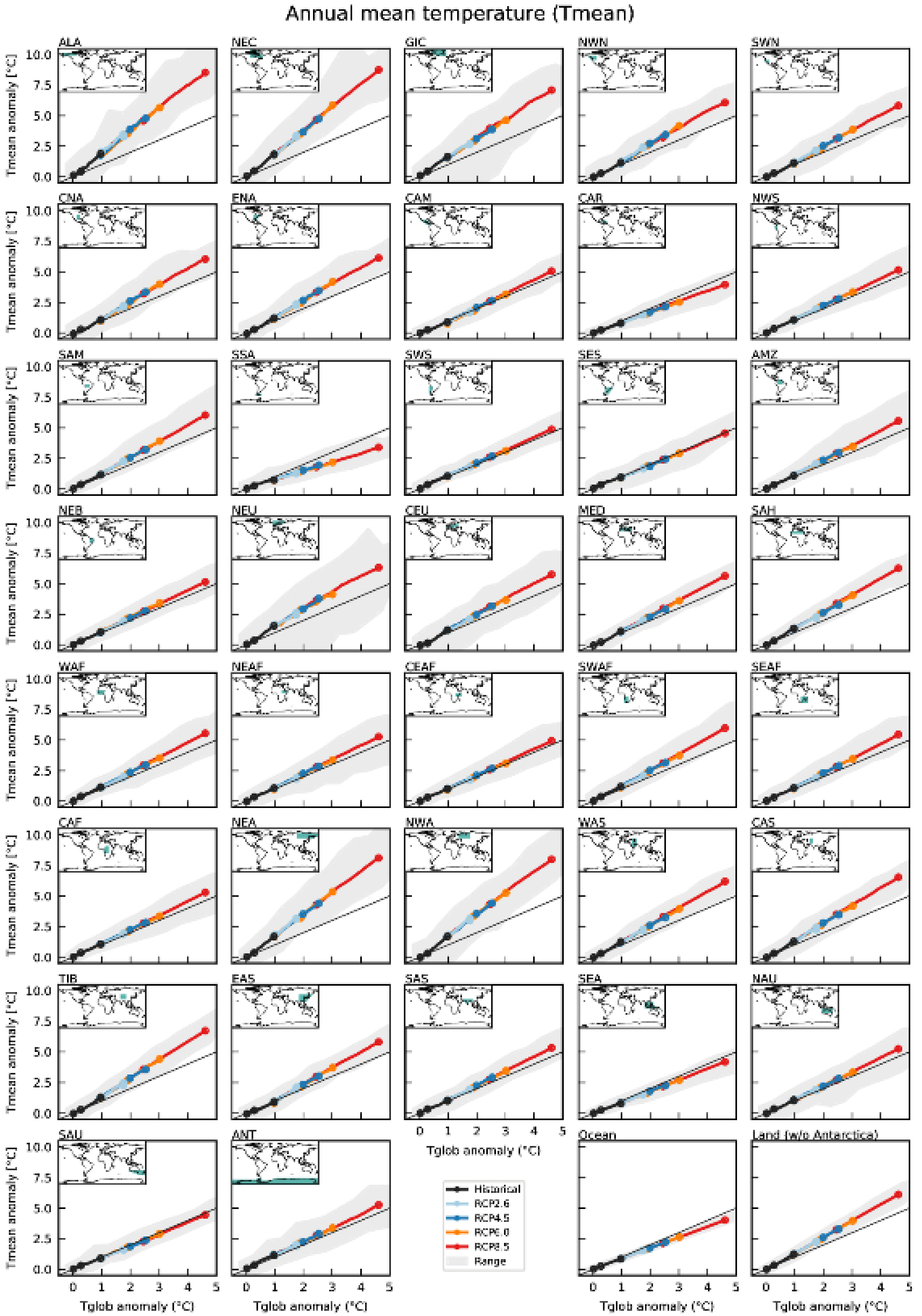

Figure 11.7: Projected changes in regional mean warming (Tmean) compared to pre-industrial conditions (1851-1900) as function of mean global warming, using empirical scaling relationship based on transient CMIP5 simulations. Analyses for 37 AR6 regions, the global ocean and the global land.

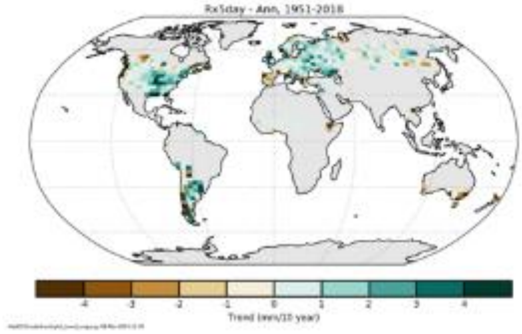

Figure 11.8: Observed linear trend over 1951-2018 in the annual maximum pentadal (5-day) precipitation from the beta version of the most recent HadEX3 data set. Units: °C/decade.

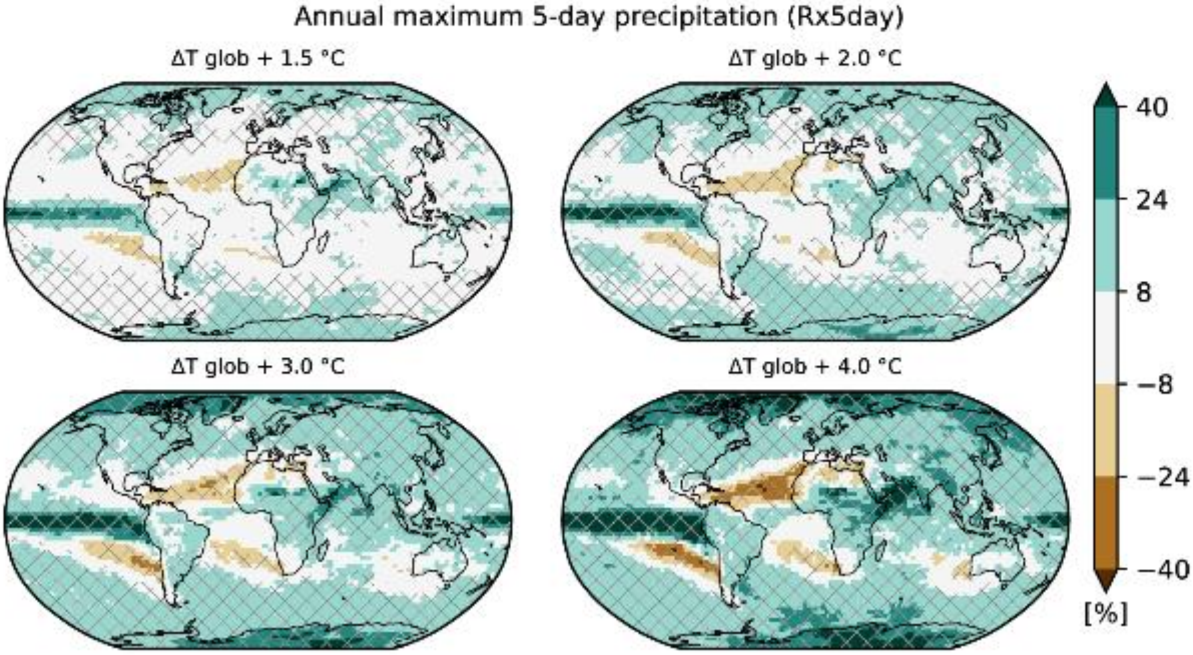

Figure 11.9: Projected changes in annual maximum 5-day precipitation for projections at 1.5°C, 2°C, 3°C and 4°C of global warming compared to pre-industrial conditions (1851-1900), using empirical scaling relationship based on transient CMIP5 simulations. Cross-hatching highlights areas where at least two-thirds of the models agree on the sign of change as a measure of robustness.

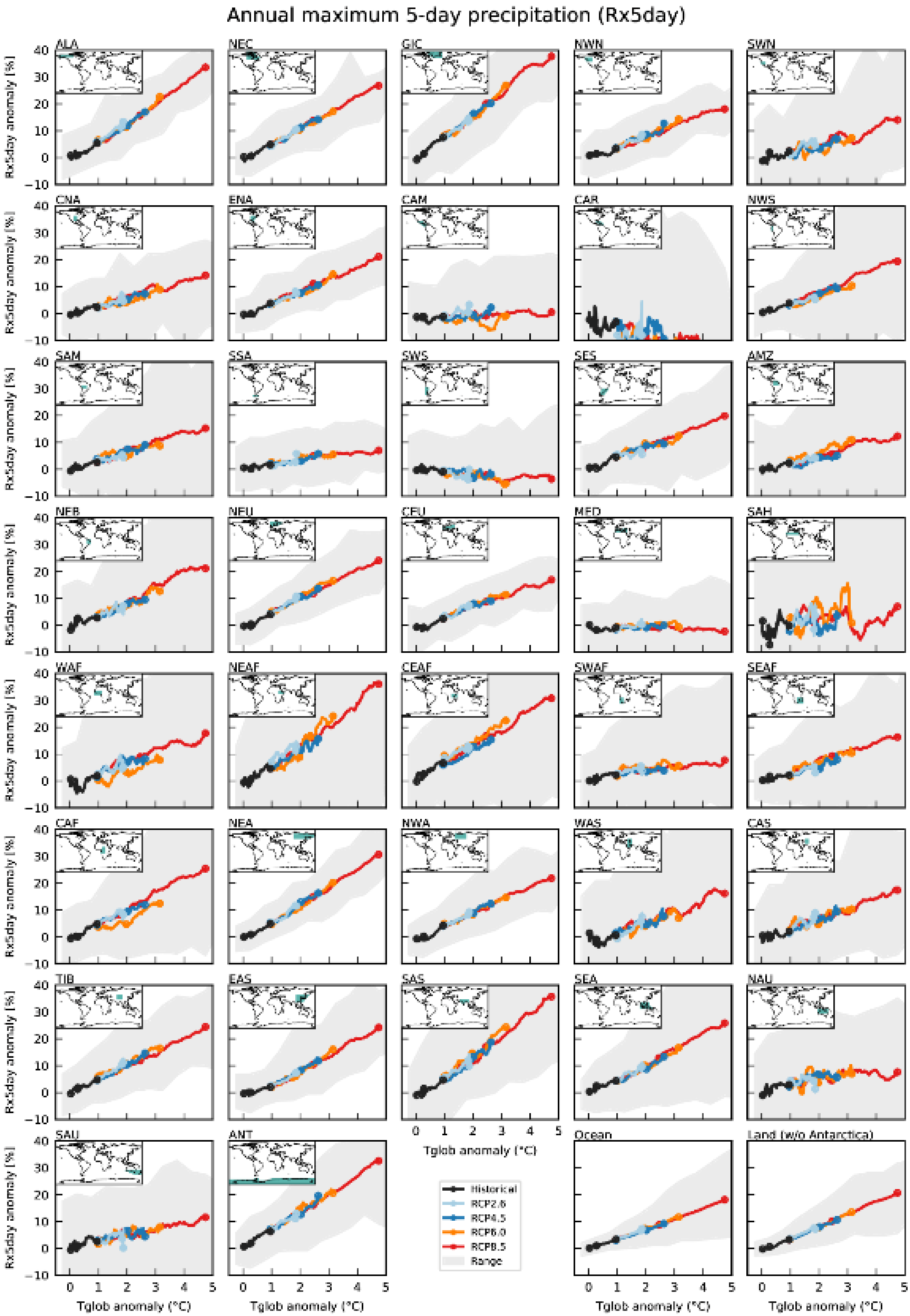

Figure 11.10: Projected changes in annual maximum 5-day precipitation (Rx5day) compared to pre-industrial conditions (1851-1900) as function of mean global warming, using empirical scaling relationship based on transient CMIP5 simulations. Analyses for 37 AR6 regions, the global ocean and the global land.

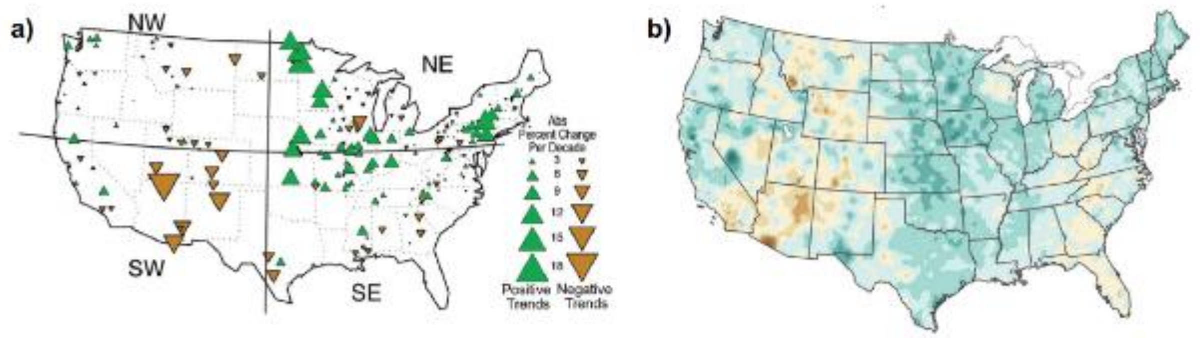

Figure 11.11: Geographic distribution of century-scale changes in (a) flooding and (b) precipitation. In (a), the triangles are located at 200 stream gauges, which have record lengths of 85–127 years. The color and size of the triangles are determined by the trend slope of a regression of the logarithm of the annual flood magnitude vs time for the entire period of record at the site, ending with water year 2008. In (b), trends in total annual precipitation as percentages for a 100-yr period end the same year as the flood data (2008) shown in (a). There are regional similarities between the figures, such as increases in floods and precipitation in the northeastern Great Plains and drying in the Southwest, but not a one-to-one correspondence. From (Peterson et al., 2013)

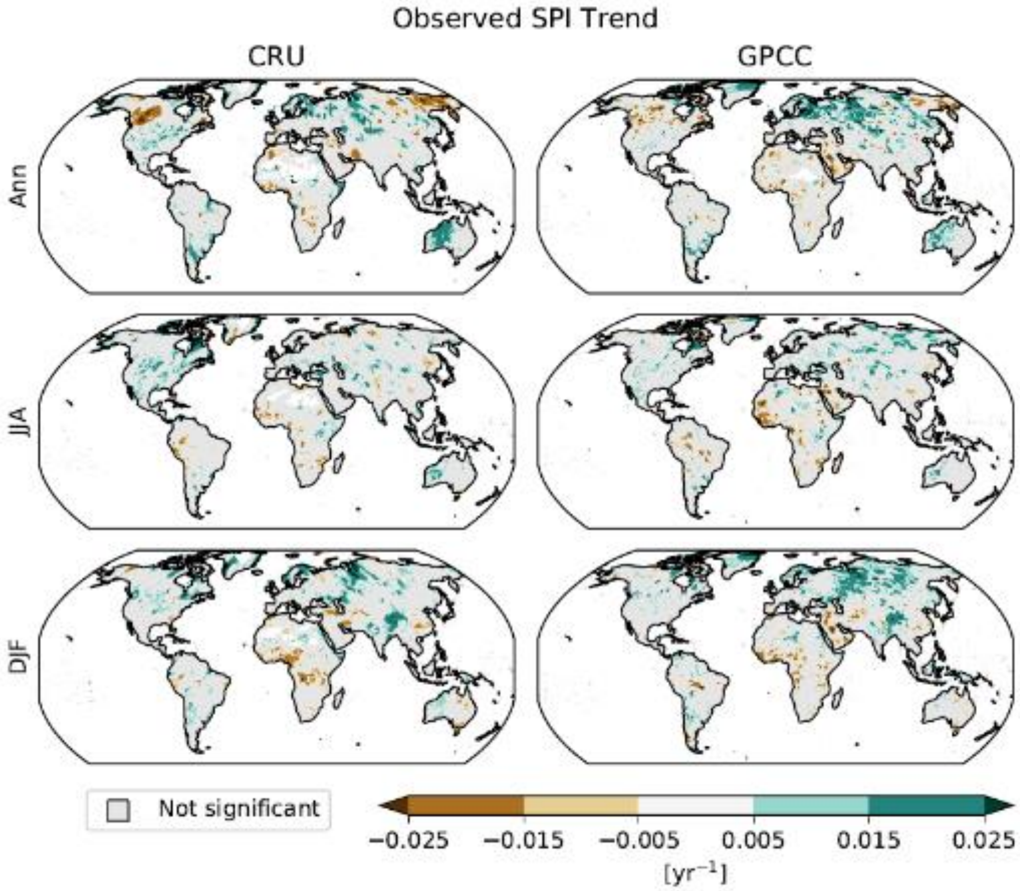

Figure 11.12: Observed Standardized Precipitation Index (SPI) for 12-month (Ann) and 3-month (JJA and DJF) time scales using the Climate Research Unit (CRU) and Global Precipitation Climatology Centre (GPCC) precipitation datasets from 1950 to 2016.

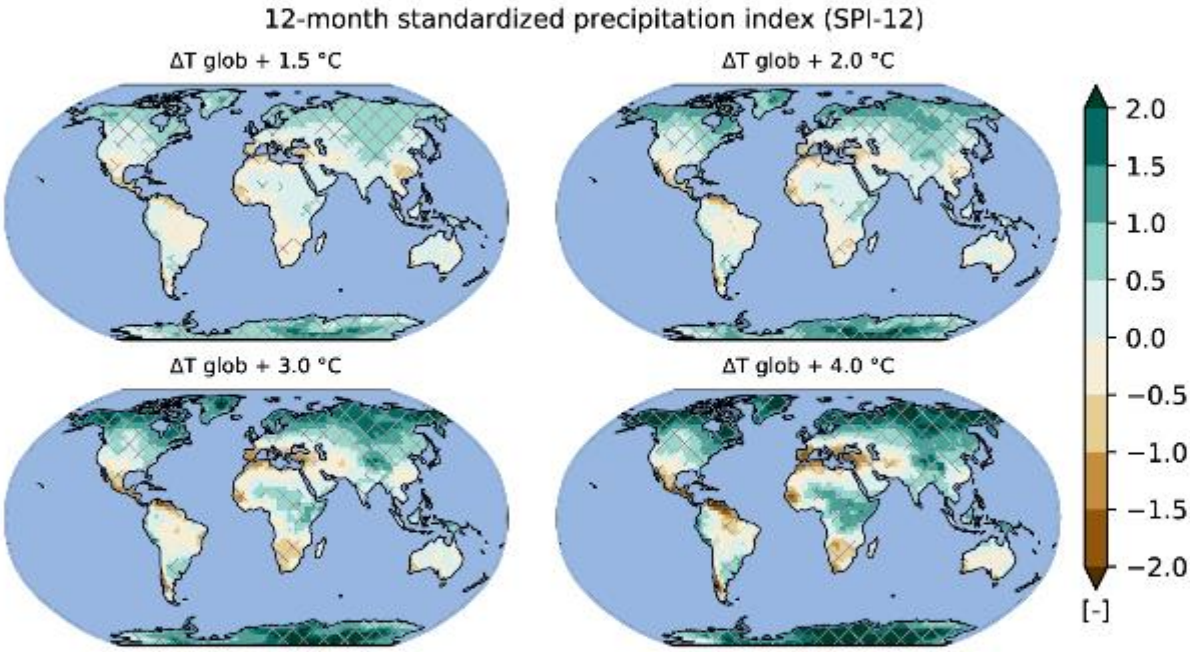

Figure 11.13: Projected changes in 12-month Standardized Precipitation Index for projections at 1.5°C, 2°C, 3°C and 4°C of global warming compared to pre-industrial conditions (1851-1900), using empirical scaling relationship based on transient CMIP5 simulations. Cross-hatching highlights areas where at least two-thirds of the models agree on the sign of change as a measure of robustness.

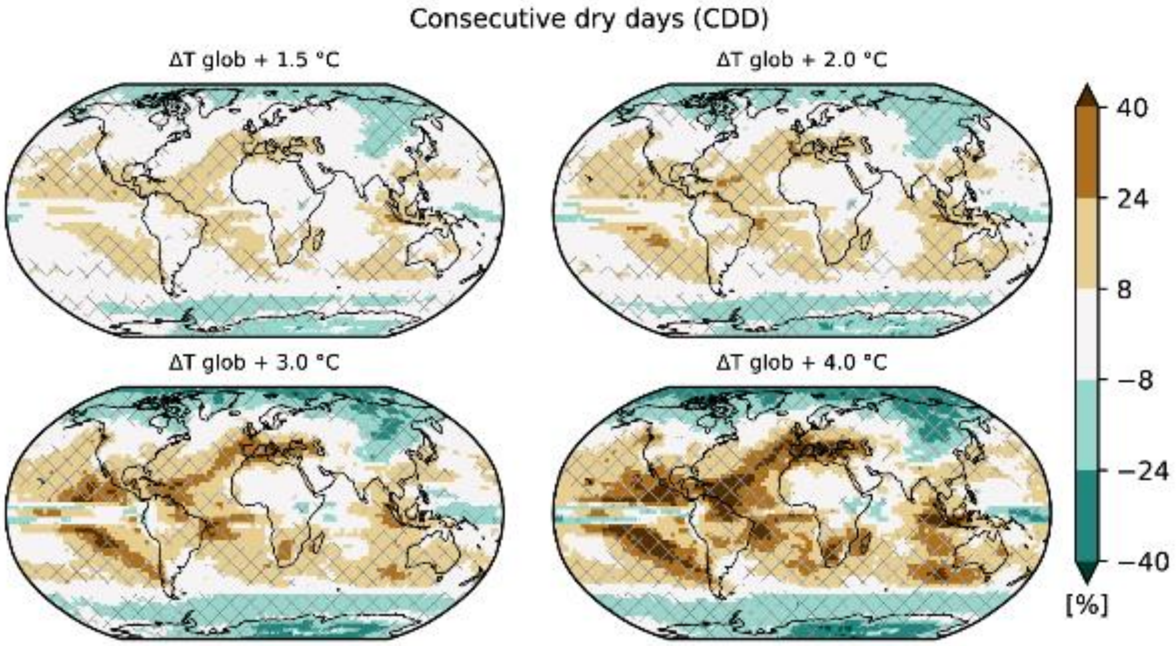

Figure 11.14: Projected changes in consecutive dry days for projections at 1.5°C, 2°C, 3°C and 4°C of global warming compared to pre-industrial conditions (1851-1900), using empirical scaling relationship based on transient CMIP5 simulations. Cross-hatching highlights areas where at least two-thirds of the models agree on the sign of change as a measure of robustness.

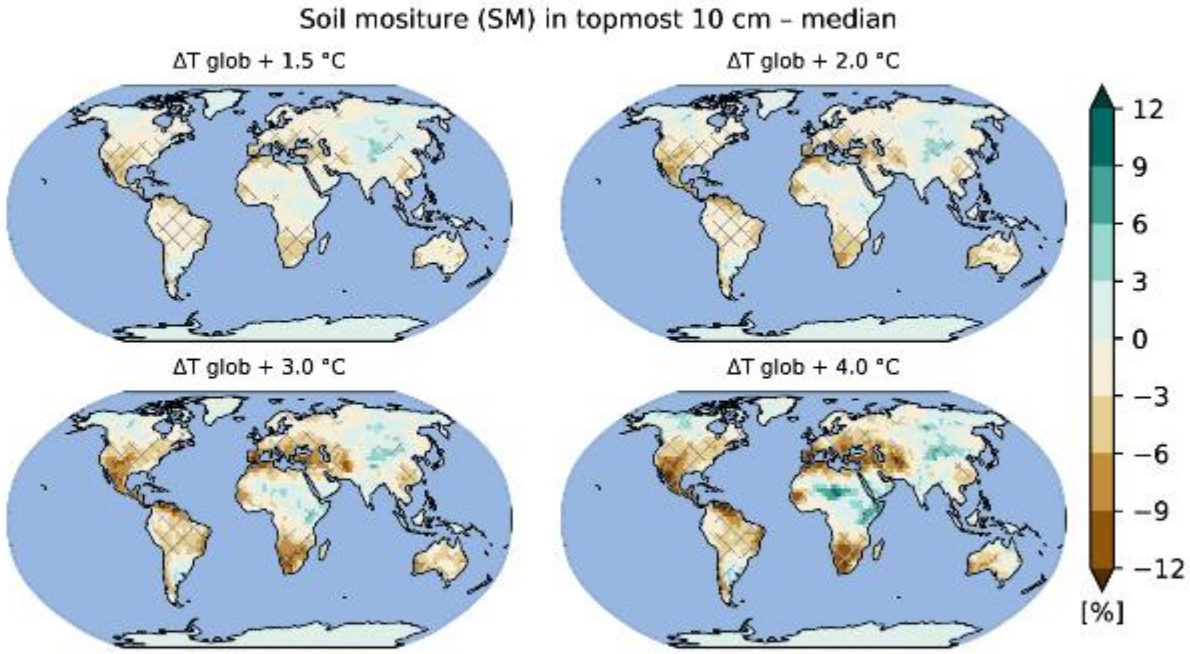

Figure 11.15: Projected changes in surface soil moisture for projections at 1.5°C, 2°C, 3°C and 4°C of global warming compared to pre-industrial conditions (1851-1900), using empirical scaling relationship based on transient CMIP5 simulations. Cross-hatching highlights areas where at least two-thirds of the models agree on the sign of change as a measure of robustness.

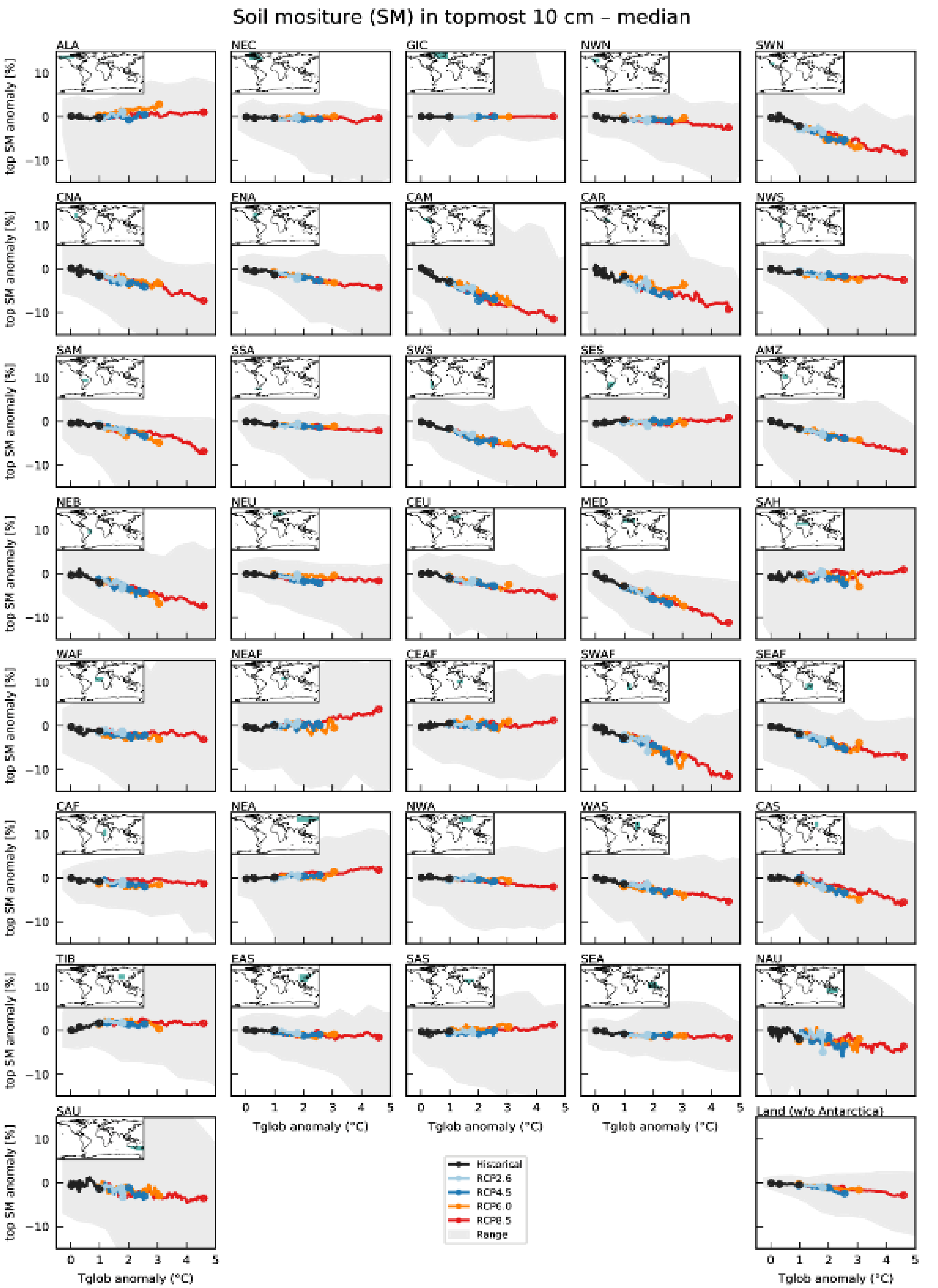

Figure 11.16: Projected changes in surface soil moisture compared to pre-industrial conditions (1851-1900) as function of mean global warming, using empirical scaling relationship based on transient CMIP5 simulations. Analyses for 36 AR6 regions, and the global land.

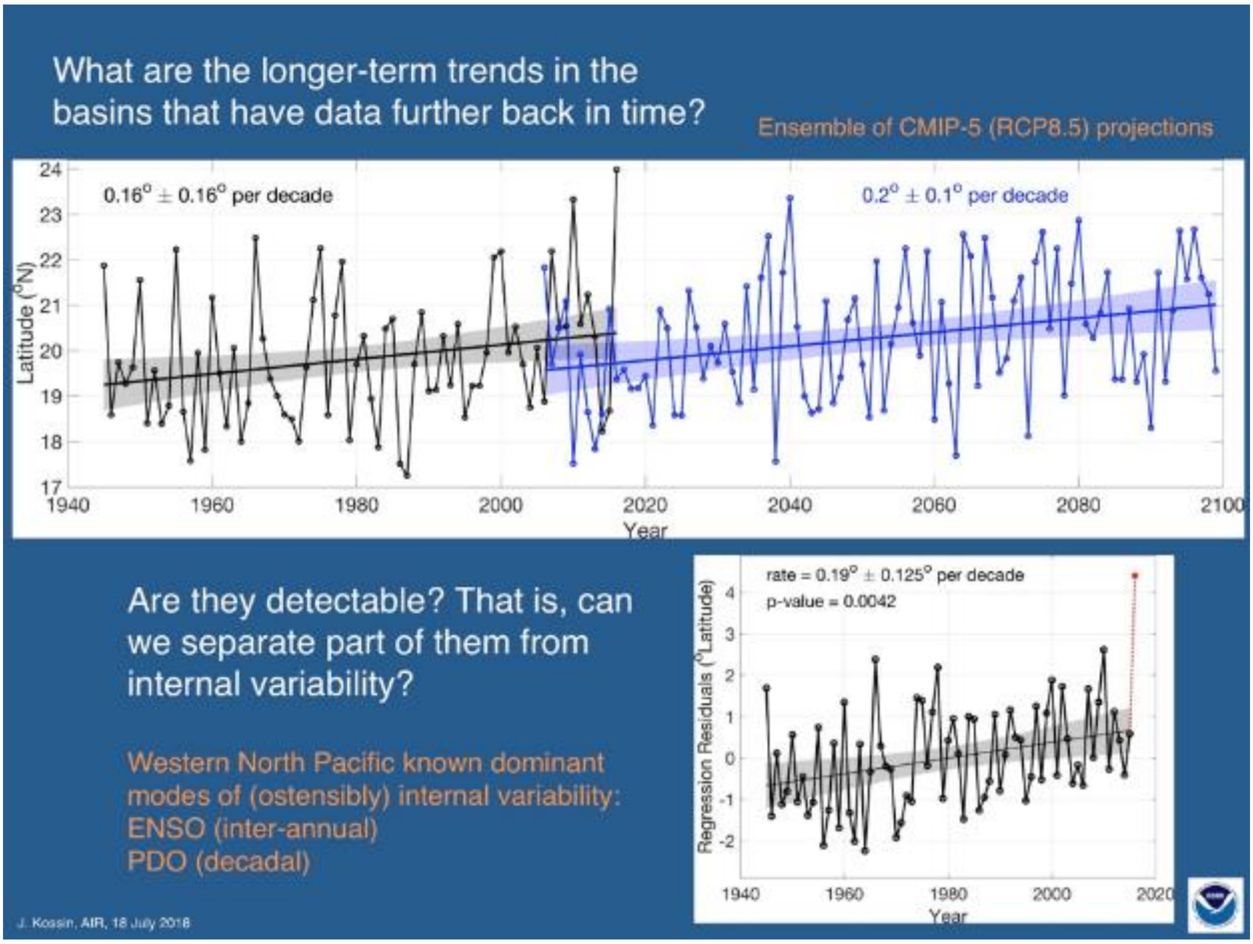

Figure 11.17: A multipanel figure showing polar migration of tropical cyclones in Atlantic and Pacific basins in the observations and CMIP5 simulations. [THIS IS A PLACEHOLDER, WILL BE UPDATED IN THE SOD.]

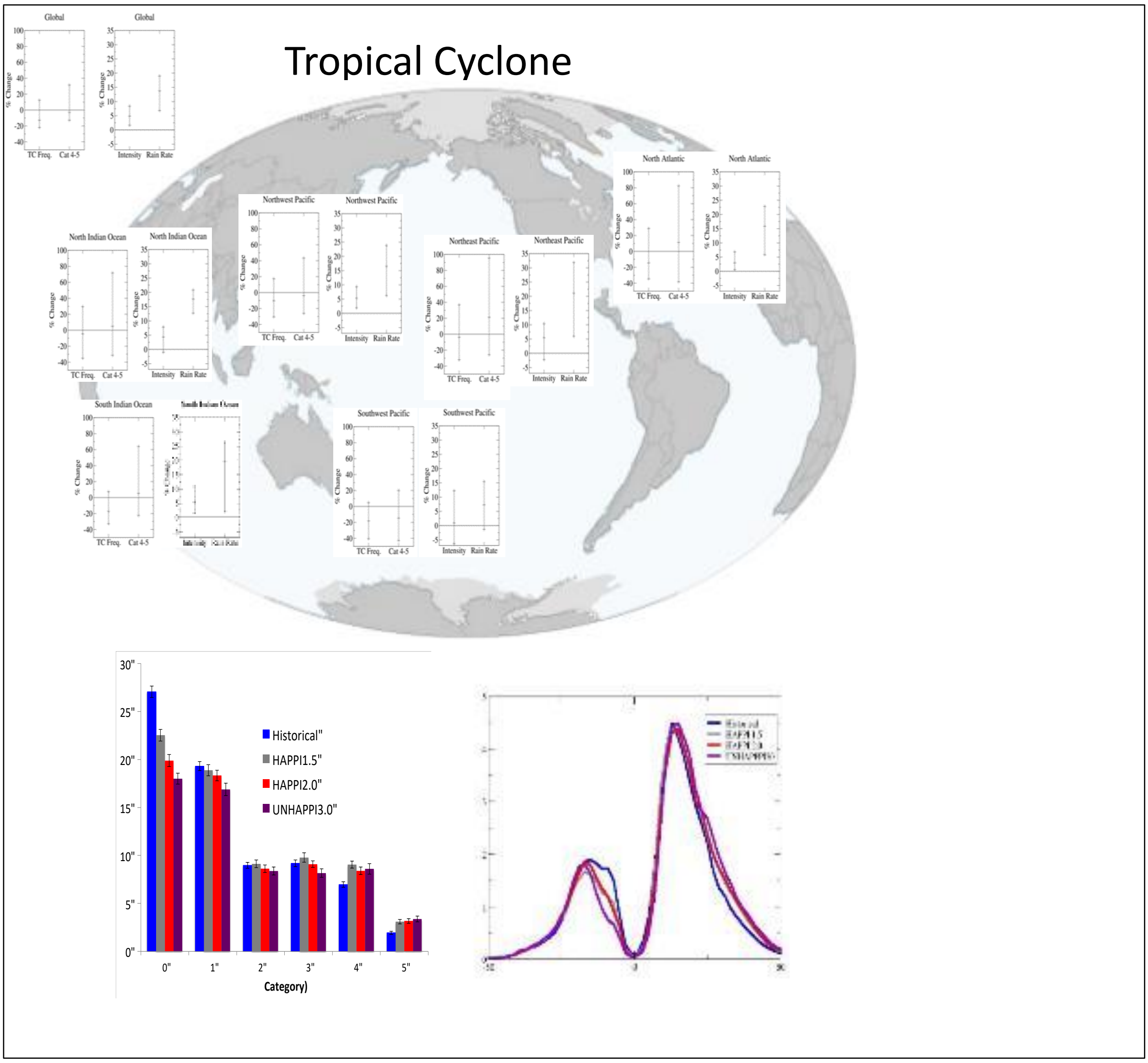

Figure 11.18: Global view of basin level TC changes. [After (Knutson et al., 2019), as an update of Fig. TS. 26 of AR5. (Waiting for HighResMIP results) with additional metrics such as ACE.] Bottom two panels show (left) projected global TC annual frequency by Saffir-Simpson scales from the high-resolution version of CAM5 under present day, 1.5, 2.0 and 3.0C above stabilized preindustrial temperatures warming scenarios and (right) zonal mean TC track density for the same model and warming levels. Updated from (Wehner et al., 2018)

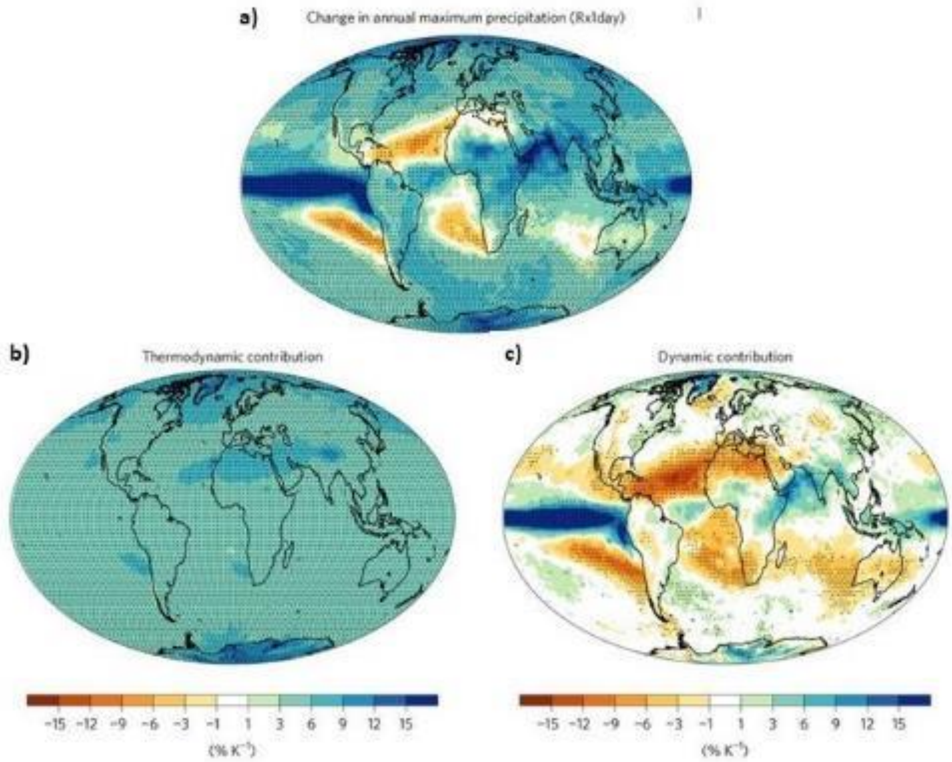

Box 11.1, Figure 1: Multi-model mean fractional changes in thermodynamic scaling in which the vertical velocity ωe is kept constant (it is replaced with its mean value over the period 1950–2100). b, Difference between changes in full scaling and changes in thermodynamic scaling (full minus thermodynamic). Note that the maxima in the Pacific are above 60% K^{-1}. Stippling indicates that at least 80% of the models agree on the sign of signal. (From Pfahl et al., 2017)

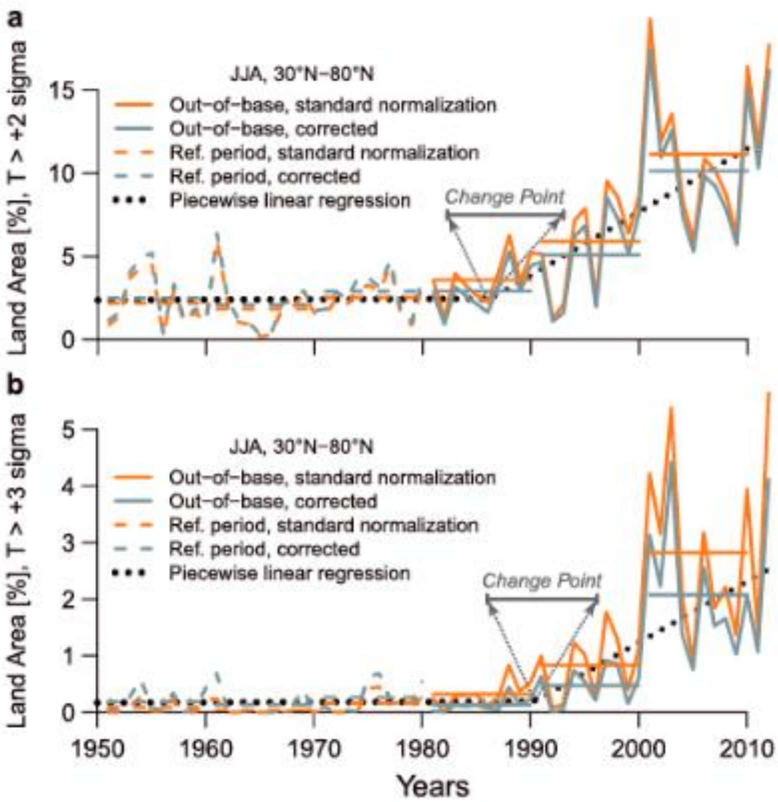

Box 11.3, Figure 1: Analysis of the percentage of land area affected by temperature extremes larger than a) two or b) three standard deviations in June-July-August (JJA) between 30°N and 80°N using an approach using a standard normalization (orange) and a corrected normalization (grey). The more appropriate estimate is the corrected normalization. These panels show for both estimates a substantial increase in the overal land area affected by very high hot extremes since 1990 onward. From Sippel et al. 2015. [THIS FIGURE WILL BE UPDATED UP TO 2018 FOR THE SOD]

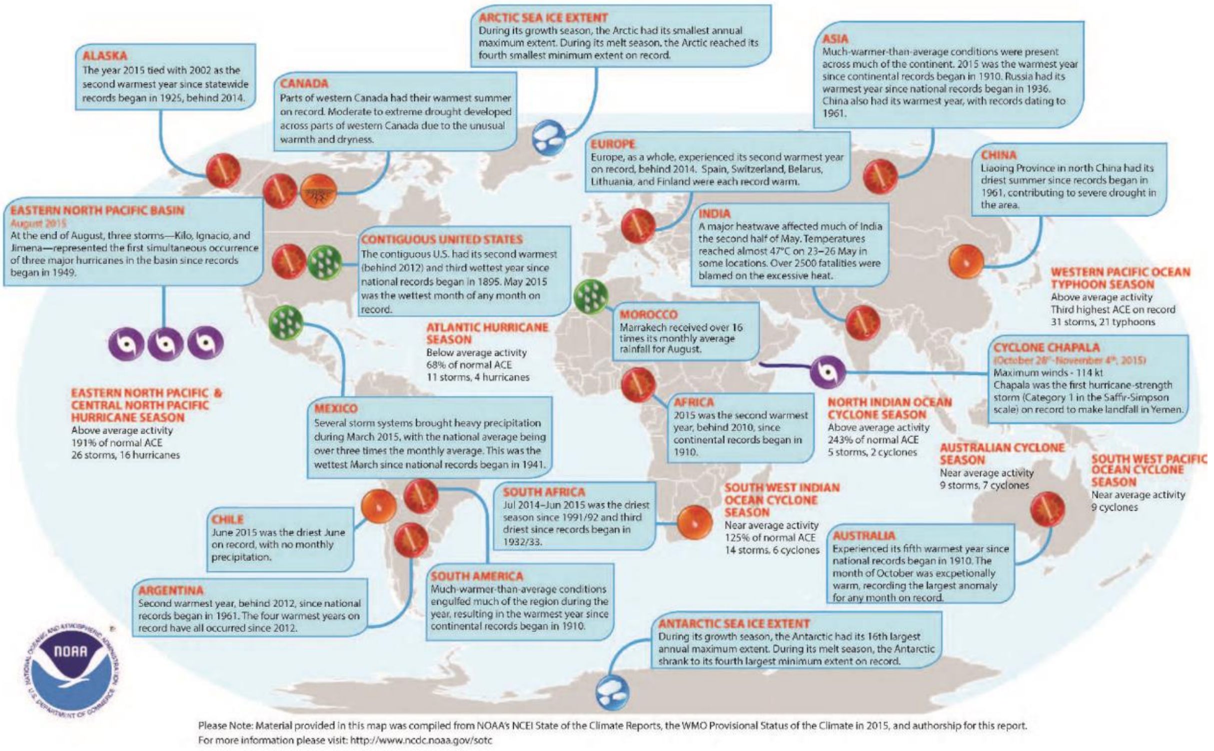

Box 11.3, Figure 2: Geographical distribution of notable climate anomalies and events occurring around the world in 2015 (Adopted from Fig. 1.1 of (Blunden and Arndt, 2016) and to be updated).

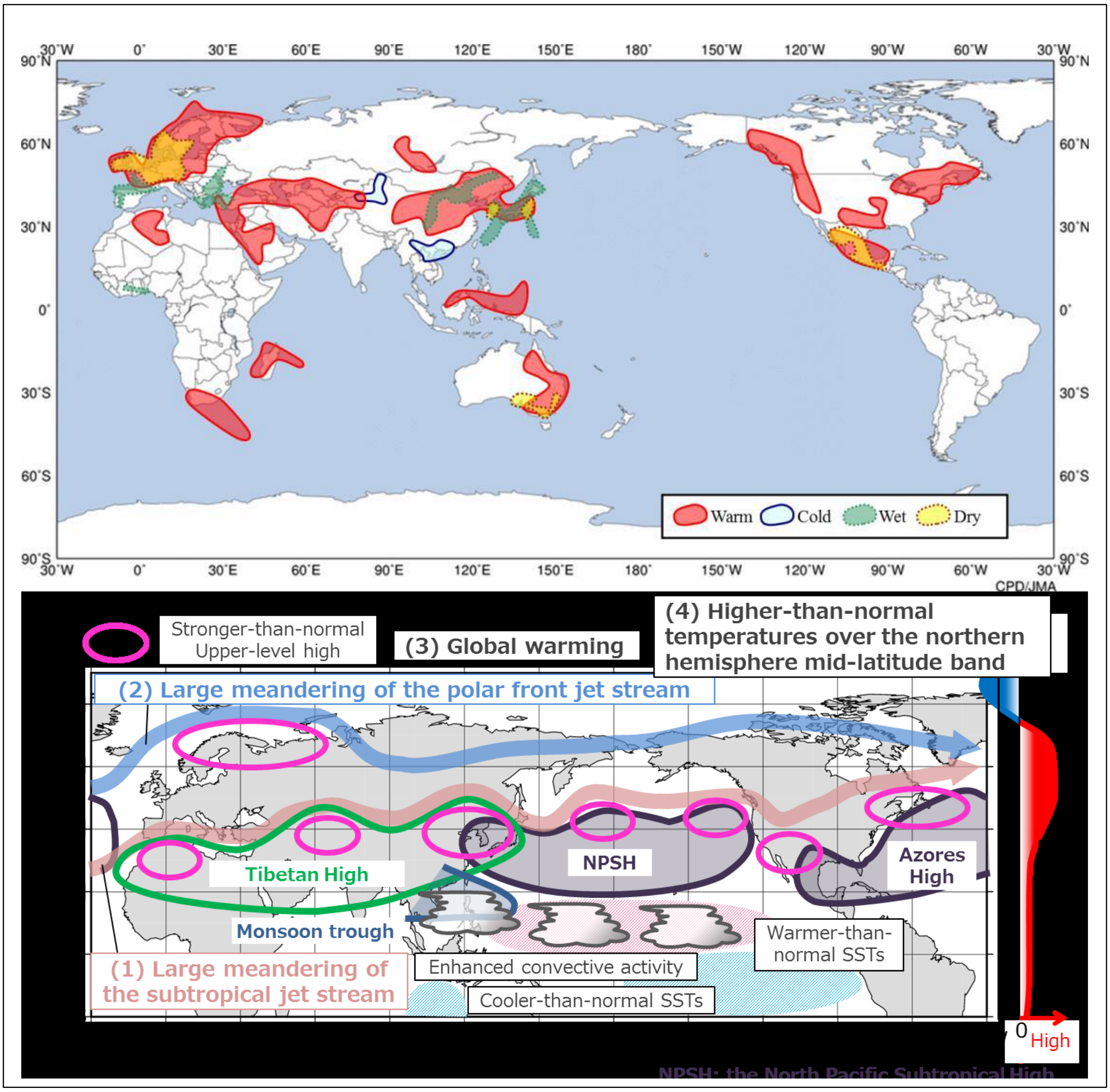

Box 11.3, Figure 3: Global extreme climate events in July 2018 (Japan Meteorological Agency, 2018). This figure shows overlaid climate extremes (warm, cold, wet and dry) from weekly reports for July 2018.

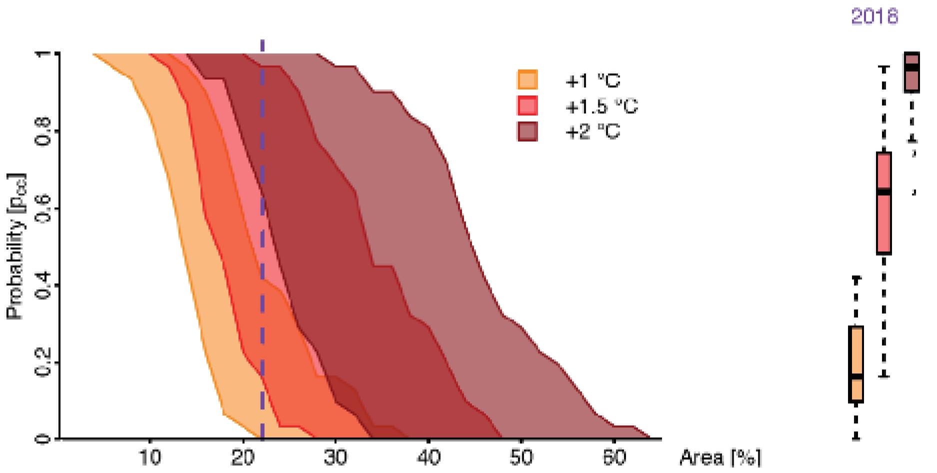

Box 11.3, Figure 4: CMIP5-based multi-model range of probabilities for exceeding concurrent hot days areas for global warming of +1°C (orange), +1.5°C (red) and +2°C (dark red) with respect to 1870-1900, with area experienced in 2018 May-July indicated with dashed blue line. Corresponding box plots for the probabilities of occurrence of the 2018 area at +1°C, +1.5° and +2°C global warming are shown on the right. From Vogel et al. (submitted).

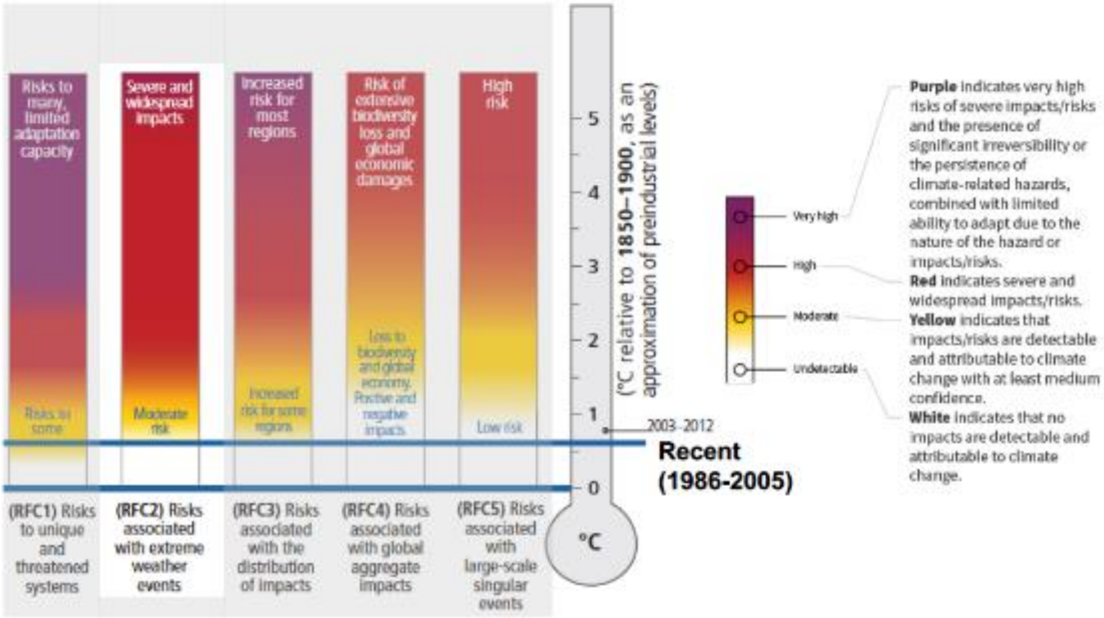

Box 11.5, Figure 1: "Reasons for concerns" (RFCs), highlighting RFC2 on "Risks associated with extreme weather events. From (Oppenheimer et al., 2014, IPCC AR5 WG2).

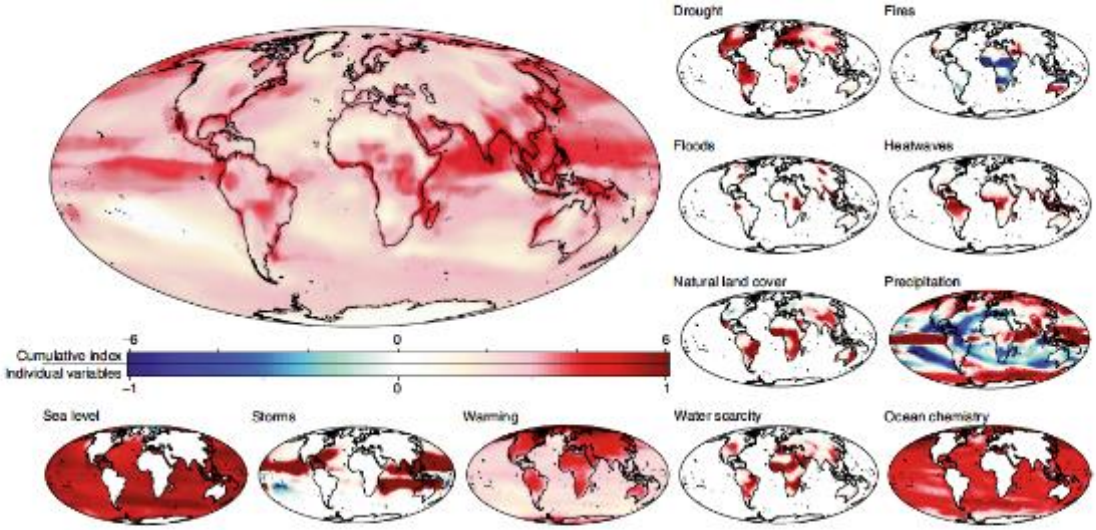

Box 11.5, Figure 2: Cumulative climate hazards within RCP 8.5 scenario, which reaches ca. 4°C of global warming in 2100. The main map shows the cumulative index of climate hazards, which is the summation of the rescaled change in all hazards between 1955 and 2095. Most of the considered hazards are associated with weather and climate extremes. From Mora et al., (2018).

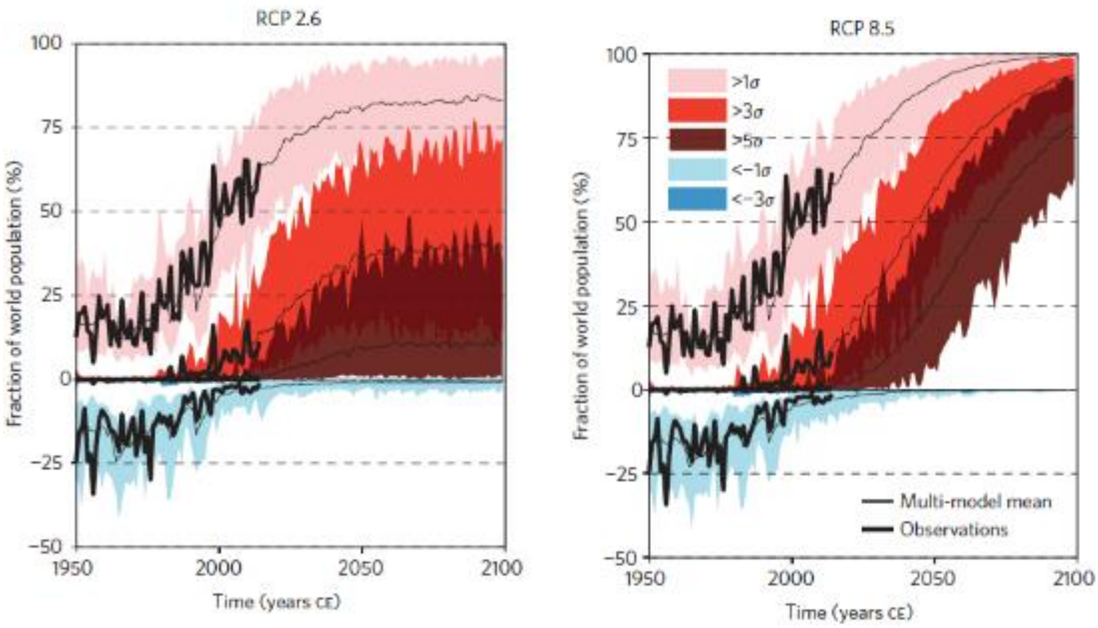

Box 11.5, Figure 3:(Lehner and Stocker, 2015)

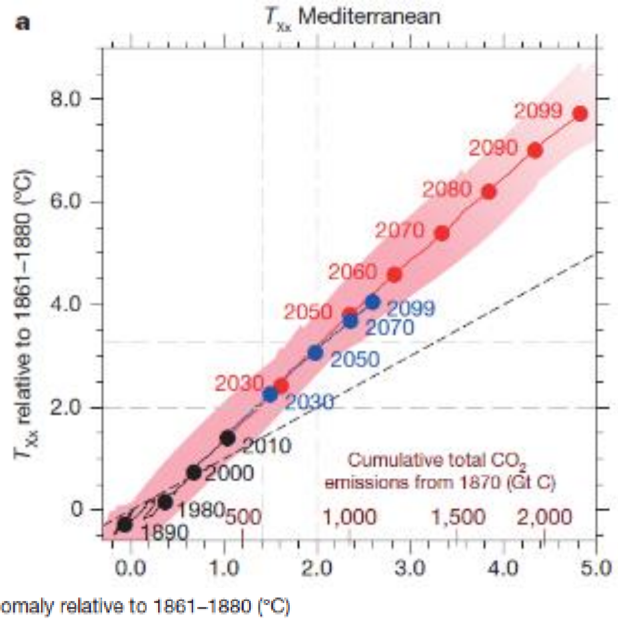

FAQ 11.1, Figure 1: In the Mediterranean, warming of hot extremes is consistently larger than the rise in global mean temperature.

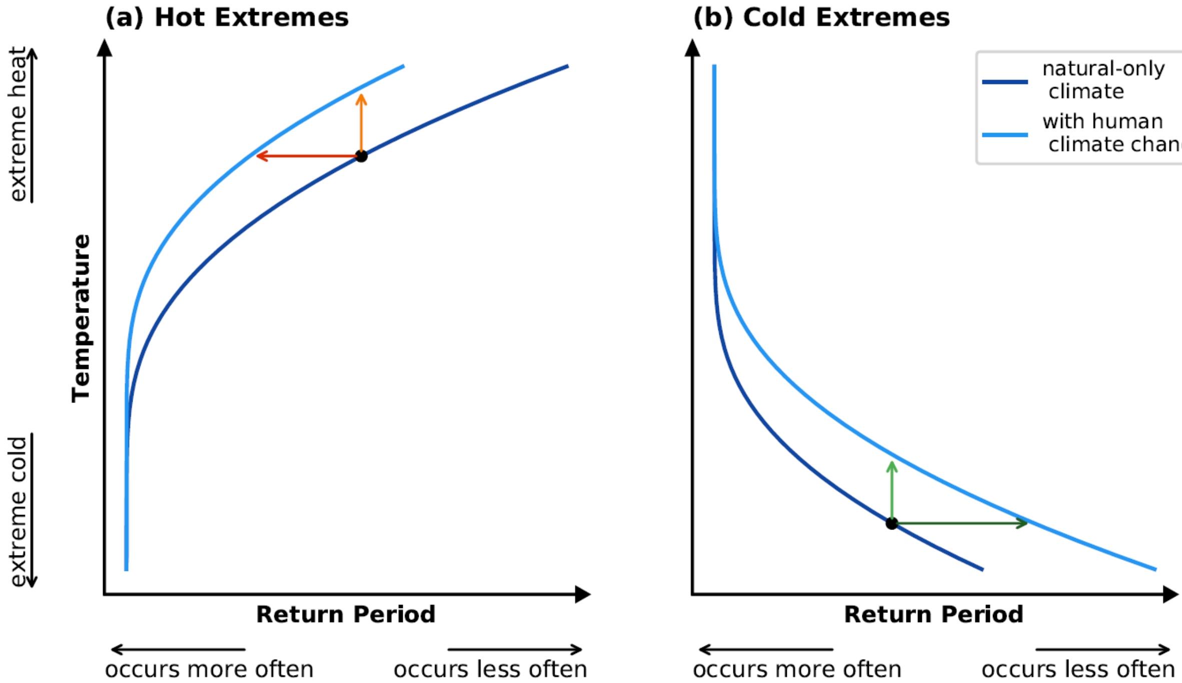

FAQ 11.3, Figure 1: Demonstration of changing temperature extremes with a warming climate. Return periods for hot (a) and cold (b) extremes are shown with a log scale for a natural only climate (dark blue) and a climate that includes human-driven climate change (light blue). A return period describes the average time between events of a certain magnitude; shorter return periods indicate more frequent occurrence. An extreme hot temperature in the natural climate increases in both frequency (red arrow) and magnitude (orange arrow) under climate change. Similarly, an extreme cold temperature in the natural climate decreases in frequency (dark green arrow) and increases in magnitude (light green arrow) withclimate change.

Supplementary Material

11.SM - Chapter 11 Supplementary Material

Coordinating Lead Authors:
Sonia I. Seneviratne (Switzerland), Xuebin Zhang (Canada)

Lead Authors:
Muhammad Adnan (Pakistan), Wafae Badi (Morocco), Claudine Dereczynski (Brazil), Alejandro Di Luca (Australia/Argentina), Subimal Ghosh (India), Iskhaq Iskandar (Indonesia), James Kossin (USA), Sophie Lewis (Australia), Friederike Otto (UK/Germany), Izidine Pinto (Mozambique), Masaki Satoh (Japan), Sergio M. Vicente-Serrano (Spain), Michael Wehner (USA), Botao Zhou (China)

Contributing Authors:
Richard Allan (UK), Markus Donat (Germany/Spain), Robert Dunn (UK), Nathan Gillett (Canada), Peter Greve (Germany/Austria), Lofti Halimi (Algeria), Mathias Hauser (Switzerland), Megan Kirchmeier-Young (Canada/USA), Tim R. McVicar (Australia), Seung-Ki Min (Korea), Jonathan Spinoni (Italy), Ying Sun (China), Wim Thiery (Belgium), Claudia Tebaldi (USA/Italy), Seth Westra (Australia), Jakob Zscheischler (Germany/Switzerland)

Review Editors:
Johnny Chan (China), Asgeir Sorteberg (Norway), Carolina Vera (Argentina)

Chapter Scientists:
Mathias Hauser (Switzerland), Hui Wan (Canada)

Date of Draft: 29 April 2019

Note: TSU Compiled Version

Table of Contents

Supplementary Text

11.SM.1 Computation of projected changes in climate indices

11.SM.1.1 Overview

We produced figures of future projections for a number of climate indices. Currently, the analyzed climate indices are: annual hottest daytime temperature (TXx), coldest night-time temperature (TNn), annual mean warming (Tmean), annual maximum 5-day precipitation (Rx5day), surface soil moisture (SM), consecutive dry days (CDD), 12-month Standardized Precipitation Index (SPI-12). Additionally, annual-mean global-mean temperature (Tglob) is used. All data are shown relative to pre-industrial conditions (1851-1900). A number of climate indices used were defined by the expert group on Climate Change Detection and Indices (ETCCDI) (Karl et al., 1999; Peterson et al., 2001), namely TXx, TNn, Rx5day, CDD.
Two types of figures are provided. First, global maps of the indices for projections at 1.5°C, 2°C, 3°C and 4°C of global warming ("warming-level maps"). The second type of figure shows projected changes in the indices as function of mean global warming, using empirical scaling relationship based on transient CMIP5 simulations ("scaling plots"). For both types of figures, we use the historical scenario, and all four representative concentration pathway (RCP) (Meinshausen et al., 2011) projections (RCP26, RCP45, RCP60, RCP85) .

11.SM.1.2 Data

All data used stems from the CMIP5 archive (Taylor et al., 2012). For the ETCCDI indices used we make use of the "climate extremes indices in the CMIP5 multimodel ensemble" computed and provided by Sillmann et al., 2013. SPI (Mckee et al., 1993) is calculated following the method outlined in Lloyd-Hughes and Saunders (2002) from monthly precipitation data. SPI-12 shows values for December, i.e. for the accumulation period January to December.
All CMIP5 models that pass very basic checks are used and weighted equally. Only the first ensemble member of each model is used. In order to be used, models must (i) provide the corresponding variable, (ii) run from 1851 (or 1850 for SPI) to 2099, and (iii) must not have duplicate time steps or missing time steps.
The annual mean global mean temperature (Tglob) is derived from monthly mean near-surface air temperature (tas in the CMIP5 archive). First, the temperature field is area-averaged using the cosine of the latitude as weight. Then, annual means are computed.

11.SM.1.3 Warming-level maps

We calculate the response of the climate indices at four different global warming levels: 1.5°C, 2°C, 3°C and 4°C (Wartenburger et al., 2017). For each model and RCP combination we determine the year with the smallest difference of Tglob to the desired warming level. However, the temperature difference must be smaller than 0.1°C, else the model is not used. This ensures that the model actually reaches the warming level. Then, the climate index of the corresponding year is read and accumulated in a list. Note that this is done for all RCPs. This means that each model can contribute more than one data point for a given warming level. Finally, the mean (or median) is calculated at each grid point over the list. As a measure of robustness ross-hatching highlights areas where at least two-thirds of the models agree on the sign of change.

11.SM.1.4 Scaling Plots

For the scaling plots we follow a similar procedure as in (Seneviratne et al., 2016). First, regional means are calculated for 37 AR6 regions, the global ocean and the global land. Then, we calculate a centered 10-year running mean and the mean (median) over all available models for each year. This is done for Tglob and the climate index, which are subsequently plotted against each other. This is done for each RCP individually. For the uncertainty we bin the index according to Tglob (over all RCPs), using a bin width of 0.5°C. We show the full range, i.e. the minimum and maximum of the climate index in each bin.

References

Karl, T. R., Nicholls, N., and Ghazi, A. (1999). CLIVAR/GCOS/WMO Workshop on Indices and Indicators for Climate Extremes - Workshop summary. in *Climatic Change* doi:10.1023/A:1005491526870.

Lloyd-Hughes, B., and Saunders, M. A. (2002). A drought climatology for Europe. *Int. J. Climatol.* doi:10.1002/joc.846.

Mckee, T. B., Doesken, N., and Kleist, J. (1993). The relationship of drought frequency and duration to time scales. *AMS 8th Conf. Appl. Climatol.* doi:citeulike-article-id:10490403.

Meinshausen, M., Smith, S. J., Calvin, K., Daniel, J. S., Kainuma, M. L. T., Lamarque, J.-F., et al. (2011). The RCP greenhouse gas concentrations and their extensions from 1765 to 2300. *Clim. Chang.* 109, 213–241. doi:10.1007/s10584-011-0156-z.

Peterson, T. C., Folland, C., Gruza, G., Hogg, W., Mokssit, A., and Plummer, N. (2001). Report on the activities of the Working Group on Climate Change Detection and Related Rapporteurs 1998–2001.

Seneviratne, S. I., Donat, M. G., Pitman, A. J., Knutti, R., and Wilby, R. L. (2016). Allowable CO2emissions based on regional and impact-related climate targets. *Nature* 529, 477–483. doi:10.1038/nature16542.

Sillmann, J., Kharin, V. V., Zhang, X., Zwiers, F. W., and Bronaugh, D. (2013). Climate extremes indices in the CMIP5 multimodel ensemble: Part 1. Model evaluation in the present climate. *J. Geophys. Res. Atmos.* 118, 1716–1733. doi:10.1002/jgrd.50203.

Taylor, K. E., Stouffer, R. J., and Meehl, G. A. (2012). An overview of CMIP5 and the experiment design. *Bull. Am. Meteorol. Soc.* 93, 485–498. doi:10.1175/BAMS-D-11-00094.1.

Wartenburger, R., Hirschi, M., Donat, M. G., Greve, P., Pitman, A. J., and Seneviratne, S. I. (2017). Changes in regional climate extremes as a function of global mean temperature: an interactive plotting framework. *Geosci. Model Dev. Discuss.*, 1–30. doi:10.5194/gmd-2017-33.

Supplementary Figures

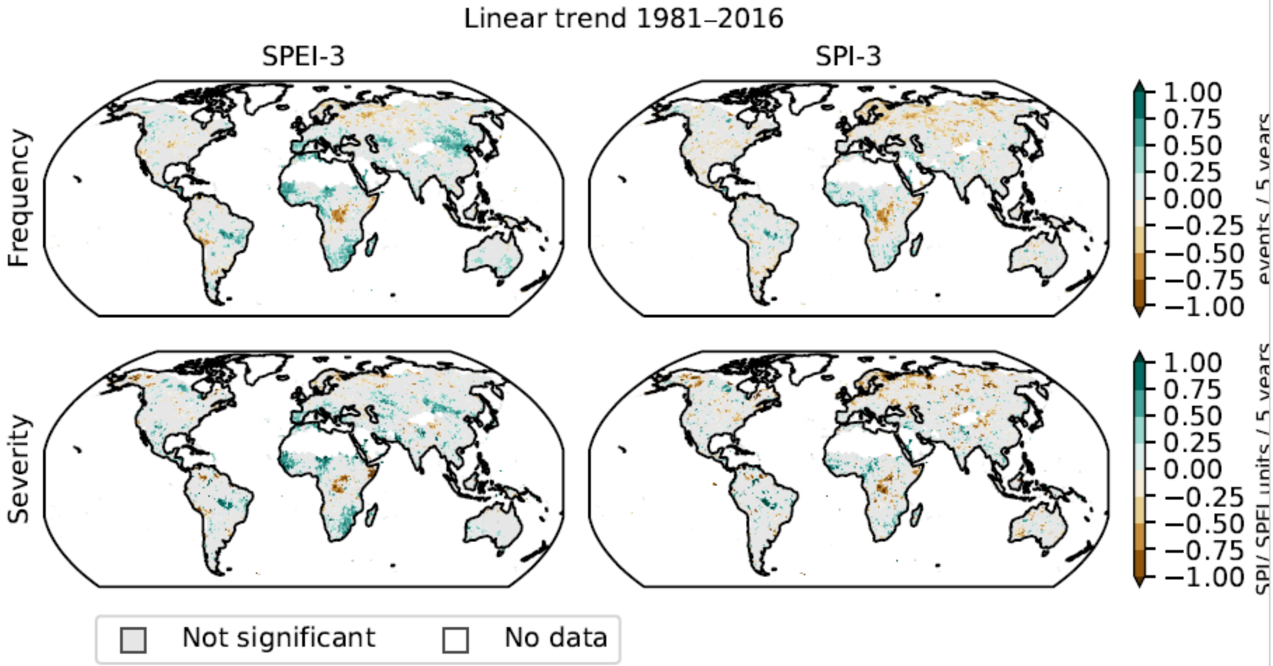

Figure 11.SM.1: Observed trends in drought severity and frequency obtained from 3-month Standardized Precipitation Index (SPI) and Standardized Precipitation Evapotranspiration Index (SPEI) Global Precipitation Climatology Centre (GPCC) precipitation using the Climate Research Unit (CRU) Epot datasets from 1950 to 2016. The threshold to identify drought episodes was set at -1 SPI/SPEI units, which represent 20% of probability (1 event in 5 years).

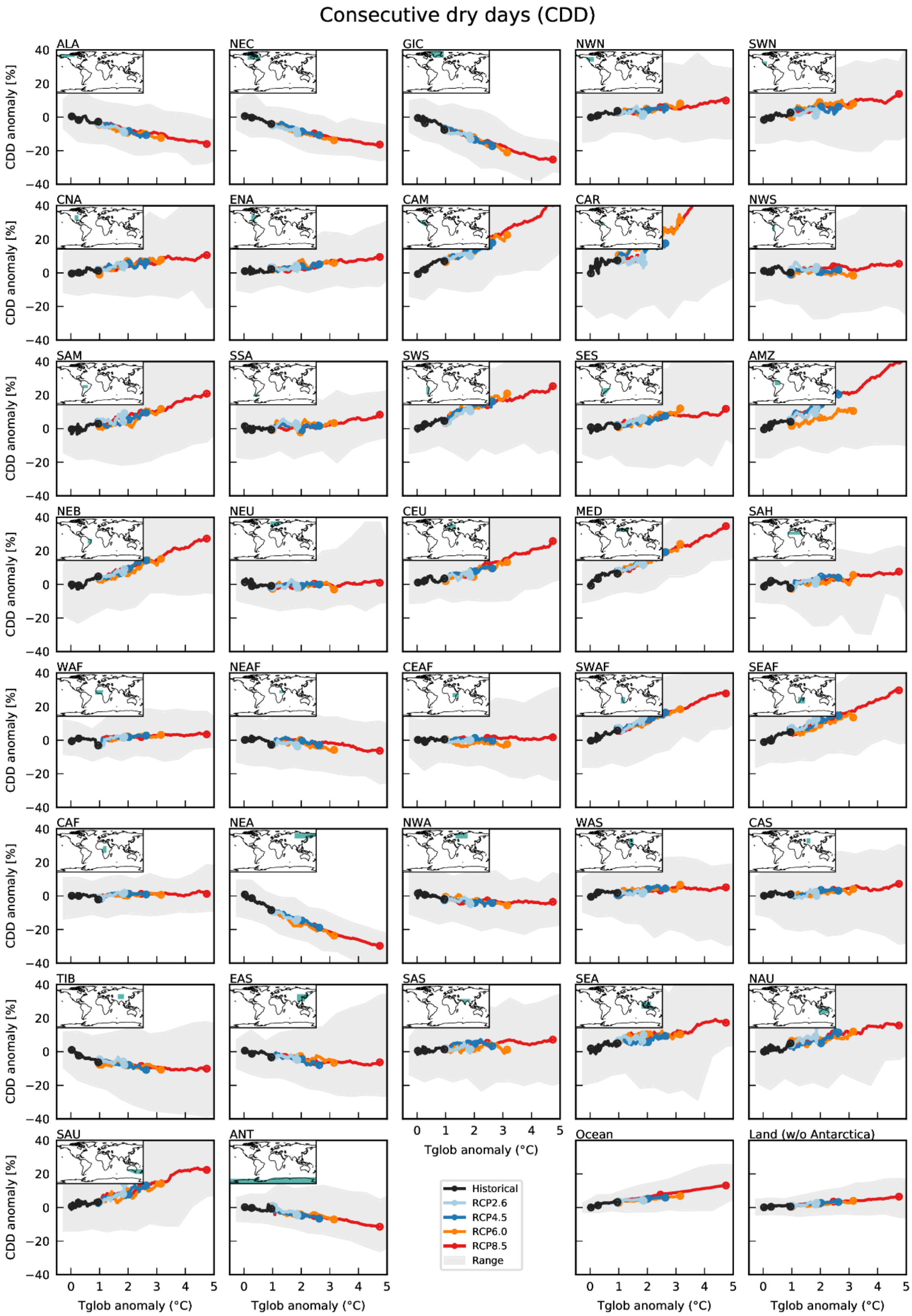

Figure 11.SM.2 : Projected changes in consecutive dry days (CDD) compared to pre-industrial conditions (1851-1900) as function of mean global warming, using empirical scaling relationship based on transient CMIP5 simulations. Analyses for 37 AR6 regions, the global ocean and the global land.

Supplementary Tables

Table 11.SM.1: Most widely used meteorological-based drought and aridity metrics, variables used and relevant references

Climate based indices	**Name**	**Variables needed**	**Relevant references**
PDSI	Palmer Drought Severity Index	P, AED	(Cook *et al.*, 2014; Dai, 2013; Trenberth *et al.*, 2014; Ukkola *et al.*, 2018; Zhao and Dai, 2015, 2017)
SPI	Standardized Precipitation Index	P	(Kingston *et al.*, 2015; Orlowsky and Seneviratne, 2013; Spinoni *et al.*, 2014; Stagge *et al.*, 2017; Vicente-Serrano *et al.*, 2014)
SPEI	Standardized Precipitation Evapotranspiration Index	P, AED	(Beguería *et al.*, 2014; Cook *et al.*, 2014; Kingston *et al.*, 2015; Naumann *et al.*, 2018; Stagge *et al.*, 2017; Vicente-Serrano *et al.*, 2014)
SPDI	Standardized Palmer Drought Index	P, AED	(Ma *et al.*, 2014; Vicente-Serrano *et al.*, 2015)
EDDI	Evaporative Demand Drought Index	AED	(Hobbins *et al.*, 2016; McEvoy *et al.*, 2016)
SEDI	Standardized Evapotranspiration Deficit Index	E, AED	(Kim and Rhee, 2016; Vicente-Serrano *et al.*, 2018)
CDD	Consecutive Dry Days	P	(Donat *et al.*, 2013; Sillmann *et al.*, 2013)

Impact based indices			
SMA	soil moisture anomalies	SM	(Berg and Sheffield, 2018; Orlowsky and Seneviratne, 2013; Samaniego *et al.*, 2018; Seneviratne *et al.*, 2013; Sohrabi *et al.*, 2015; Zhao and Dai, 2015)
low flows	Daily drought flow	Streamflow	(Forzieri *et al.*, 2014; Gosling *et al.*, 2017; Prudhomme *et al.*, 2014; Schewe *et al.*, 2014; Van Lanen *et al.*, 2013; Van Loon and Laaha, 2015; Wada *et al.*, 2013)
SGI	Standardized Groundwater Index	Groundwater	(Bloomfield and Marchant, 2013; Lorenzo-Lacruz *et al.*, 2017; Marchant and Bloomfield, 2018)
SRI, SSI	Standardized Runoff Index, Standardized Streamflow Index	Runoff, Streamflow	(Barker *et al.*, 2016; Kug *et al.*, 2015; Peña-Gallardo *et al.*, 2019)
Vegetation-based	Agro-ecological drought	e.g. GPP, NPP, NDVI, VCI, VHI	(Greve *et al.*, 2017; Roderick *et al.*, 2015; Scheff *et al.*, 2017; Swann, 2018)

Table 11.SM.2: Summary recent attribution studies of drought (Wehner *et al.*, (n.d.)) The '+' symbol indicates that an attributable human-induced increase in frequency and/or magnitude was found, '-' that an attributable decrease in frequency and/or magnitude was found and '0' that no attributable signal was determined. Where two studies examined the same event, both results are provided.

Authors	Event Year and Duration	Multi-model (MM) and/or multi-approach (MA)	Region or State	Type	Attribution Statement
(King, 2017)	2006		southeast Australia	Hot and dry co-occurence	+
(Hideo *et al.*, 2013)	2010		South Amazon region	Meteorological	0
(Lott *et al.*, 2013)	2010		East African	Meteorological	0
(Lott *et al.*, 2013)	2011		East African	Meteorological	1
(Uhe *et al.*, 2017)	2016		Kenya	Meteorological	0
(Rupp and Mote, 2012)/ (Angélil *et al.*, 2016)	MAMJJA 2011		Texas	Meteorological	+/+
(Trigo *et al.*, 2013) / (Angélil *et al.*, 2016)	DJFM 2011/2012		Iberian Peninsula	Meteorological	+/+
Dong et al 2013 /	JJA 2012		Spain	Meteorological	0/+
(Hoerling *et al.*, 2013)	2012		Texas	Meteorological	+
(Rupp and Mote, 2012)/ (Angélil *et al.*, 2016)	MAMJJA 2012		CO, NE, KS, OK, IA, MO, AR & IL	Meteorological	0/0
(Rupp *et al.*, 2013)/ (Angélil *et al.*, 2016)	MAM 2012		CO, NE, KS, OK, IA, MO, AR & IL	Meteorological	0/0
(Rupp *et al.*, 2013) / (Angélil *et al.*, 2016)	JJA 2012		CO, NE, KS, OK, IA, MO, AR & IL	Meteorological	0/+
(Hoerling *et al.*, 2014)	MJJA 2012		Great Plains/Midwest	Meteorological	0
(Harrington *et al.*, 2014) / (Angélil *et al.*, 2016)	JFM 2013		New Zealand	Meteorological	+/0
(Swain *et al.*, 2014)/ (Angélil *et al.*, 2016)	ANN 2013		California	Meteorological	+/+
(Wang and	JS 2013		California	Meteorological	0/+

Schubert, 2014)/ (Angélil *et al.*, 2016)					
(Knutson *et al.*, 2014) / (Angélil *et al.*, 2016)	ANN 2013		California	Meteorological	0/+
(Knutson *et al.*, 2014) / (Angélil *et al.*, 2016)	MAM 2013		U.S. Southern Plains region	Meteorological	0/+
(Barlow and Hoell, 2015)	2013-2014		central southwest Asia	Meteorological	0
(Diffenbaugh *et al.*, 2015)	2012-2014		California	Agricultural	+
(Seager *et al.*, 2015)	2012-2014		California	Agricultural	+
(Cheng *et al.*, 2016)	2011-2015		California	Agricultural	-
(McBride *et al.*, 2015)	2014		Singapore-Malaysia	Meteorological	0
(Marthews, et al. 2015)	2014		East Africa	Meteorological	0
(Funk *et al.*, 2016)	2014		East Africa	Meteorological	+
(Bergaoui *et al.*, 2015)	2015		Southern Levant	Meteorological	+
(Philip *et al.*, 2017)	2015		Ethiopia	Meteorological	+
(Mote *et al.*, 2016)	2015		Washington, Oregon, California	Hydrological (snow water equivalent)	+
(Yuan *et al.*, 2018)	2016		southern Africa	Meteorological (flash)	+
(Funk *et al.*, 2018a)	2016		southern Africa	Meteorological	+
(Otto, F.E.L., et al. 2015)	2014		Brazil	Meteorological	0
(Quan *et al.*, 2018)	2016		Northeast Brazil	Meteorological	0
(Hauser *et al.*, 2017)	2015		Central Europe	Meteorological	0/+